Photobioreactor production of microalgae for potential fuel oils

A thesis presented in partial fulfilment of the

requirements for the degree of

Doctor of Philosophy

in

Biotechnology

at Massey University, Palmerston North, New Zealand

Tiyaporn Luangpipat

2013

Abstract

This work focussed on a detailed characterization of the freshwater microalga *Chlorella vulgaris* as a producer of potential fuel oils. Uniquely, growth and oil production of *C. vulgaris* were characterized in full strength seawater-based media, something that has not been previously reported. *C. vulgaris* was selected for a detailed study after a screening of six potential oil producing microalgae. For photoautotrophic growth, always under carbon sufficiency and at normal growth temperature, the characterization study covered: the biomass growth rate; lipid content in the biomass; productivities of the lipids and the biomass; the biomass loss in the dark; the lipid/biomass yields on macronutrients; and the energy content of the biomass. The above key production parameters were characterized in a purpose-built tubular photobioreactor (~80 L) and in stirred tank photobioreactors (~7.5 L) under conditions of nitrogen sufficiency and at various levels of nitrogen limitation. Production was evaluated in both batch and continuous cultures at various dilution rates using indoor light to mimic sunlight. The production temperature mimicked the relatively warm conditions that would be encountered in a potential production system located outdoors in a tropical climate.

In seawater media at 25–27 °C, *C. vulgaris* was shown to have a crude oil productivity of >37 mg L^{-1} d^{-1} and the energy content of the biomass could exceed 25 kJ g^{-1}, depending on the culture conditions. Both these values were high compared with the reported data for this alga in freshwater media. Compared with continuously illuminated culture, day–night cycling of irradiance reduced oil productivity by ~31%, but the energy content of the biomass were reduced by only about 8%. In seawater, the alga could be grown as rapidly and stably as in freshwater. The lipid content of the biomass commonly exceeded 30% by dry weight and in exceptional cases a lipid content of more than 50% (by weight)

was achieved. Biomass calorific values of ≥27 kJ g^{-1} could be attained in some cases. Nitrogen starvation enhanced the lipid contents of the biomass by >3-fold relative to the lipid contents for the nonstarved case. Steady-state continuous cultures were shown to be possible. Both batch and continuous operations were feasible, especially in stirred tanks, but the culture was more failure prone, or relatively less productive, in the tubular photobioreactor.

Acknowledgements

My doctoral study and this thesis would not have been possible without the support of many individuals. My Thai friends and everyone I shared an office with always helped. The other students I shared the laboratory facilities with were immensely helpful. I would specially like to thank Tawan and his family and Pittiporn who were always supportive.

I am thankful to the Laboratory Manager Ann-Marie Jackson, the other laboratory technicians and the Mechanical Workshop personnel who were consistently helpful.

Encounters with Professors Clive Davies and Tony Paterson were always cheerful and motivating.

A scholarship from my university, Nakhon Sawan Rajabhat University, facilitated my work and Massey University provided me with an excellent environment to work in. I am especially grateful to Neste Oil Corporation, Porvoo, Finland, for funding this research and allowing it to be published.

My supervisor, Professor Yusuf Chisti, supported me academically as well as financially. You are an awesome supervisor ever! I very much enjoyed working with you and your kindness.

I am greatly thankful to my family for everything. Papa, without your inspiration and love, my PhD could not have begun. Thank you for your love; you will always be in my heart.

Table of Contents

List of Figures

List of Tables

Abbreviations

A	Area illuminated by light (m^2)
A_{xxx}	Spectrophotometric absorbance at a wavelength of xxx nm
BR n	Corning stirred photobioreactor run n
C	Biomass concentration at time t ($g\ L^{-1}$)
C_0	Biomass concentration at time zero ($g\ L^{-1}$)
D	Dilution rate (d^{-1})
DCW	Dry cell weight ($g\ L^{-1}$)
DHA	Docosahexaenoic acid
DNA	Deoxyribonucleic acid
DO	Dissolved oxygen
d	Diameter (m)
EPA	Eicosapentaenoic acid
F	Flow rate of the feed ($mL\ d^{-1}$)
I	Irradiance ($\mu mol\ m^{-2}\ s^{-1}$)
k	First-order rate constant for biomass loss (h^{-1})
LED	Light emission diodes
ND	Not determined
N_f	Final concentration of nitrate ($mg\ L^{-1}$)
N_i	Initial concentration of nitrate ($mg\ L^{-1}$)
PAR	Photosynthetically active radiation
PBR n	Tubular photobioreactor run n
P_f	Final concentration of phosphate ($mg\ L^{-1}$)
P_i	Initial concentration of phosphate ($mg\ L^{-1}$)

PTFE	Poly (tetrafluoroethylene), or Teflon
Q_L	Final lipid productivity (g $L^{-1}d^{-1}$)
Q_X	Final biomass productivity (g $L^{-1}d^{-1}$)
q_L	Specific lipid production rate (d^{-1})
q_N	Specific nitrate consumption rate (mg $g^{-1}d^{-1}$)
q_P	Specific phosphate consumption rate (mg $g^{-1}d^{-1}$)
RNA	Ribonucleic acid
RTD	Resistance temperature detector, a type of temperature sensor
RUBISCO	Ribulose-1,5-bisphosphate carboxylase/oxygenase
RuBPCase	Ribulose-1,5-bisphosphate carboxylase/oxygenase
SARDI	South Australia Research and Development Institute
STR n	Stirred tank bioreactor (BioFlo) run n
TL	Total lipids
t	Duration of a batch (d)
t_f	Time at the end of a batch (d)
t_i	Time at the beginning of a batch (d)
V	Working volume of the reactor, or volume (L)
X_f	Final concentration of biomass (g L^{-1})
X_i	Initial concentration of biomass (g L^{-1})
$Y_{L/Light}$	Lipid yield on light (g μmol^{-1})
$Y_{L/N}$	Lipid yield coefficients on nitrate (g mg^{-1})
$Y_{L/P}$	Lipid yield coefficients on phosphate (g mg^{-1})
$Y_{X/Light}$	Biomass yield coefficient on light (g μmol^{-1})
$Y_{X/N}$	Biomass yield coefficient on nitrate (g mg^{-1})
$Y_{X/P}$	Biomass yield coefficient on phosphate (g mg^{-1})

y	Weight fraction of lipids in the biomass
ICP-MS	Inductively coupled plasma mass spectrometry
ICP-OES	Inductively coupled plasma optical emission spectrometry

Chapter 1

Introduction

Microalgae are attracting much attention as potential sources of sustainably produced renewable oils as feedstock for making liquid transport fuels such as diesel and gasoline (Chisti, 2007, 2008; Hu *et al.*, 2008; Rittmann, 2008; Greenwell *et al.*, 2010; Mata *et al.*, 2010; Chisti & Yan, 2011; Chisti, 2012; Jones & Mayfield, 2012). Potentially, microalgae can convert freely available sunlight and carbon dioxide to biochemical energy via photosynthesis. If fuels derived from algal oil are used to displace petroleum fuels so that there is a net reduction in the amount of petroleum consumed, there is the potential to reduce the emissions of climate altering carbon dioxide (Baum *et al.*, 2012). Therefore, algae provide an opportunity for preventing some of the global warming associated with the use of petroleum fuels if these fuels are replaced with algal fuels.

Microalgae are grown commercially (Becker, 1994; Spolaore *et al.*, 2006), but only for relatively high value applications. They are used as aquaculture feeds (Duerr *et al.*, 1998; Hemaiswarya *et al.*, 2011) and nutraceuticals (Kay, 1991; Becker, 1994; Raja *et al.*, 2008). Commercial production of β-carotene (Del Campo *et al.*, 2007; Guedes *et al.*, 2011) and astaxanthin (Lorenz & Cysewski, 2000; Guerin *et al.*, 2003) rely on microalgae. Production of other high-value products is being developed from microalgae (Borowitzka, 1995; Cardozo *et al.*, 2007; Posten & Walter, 2012; Raposo *et al.*, 2013). Unfortunately, fuels are low-value commodity products and are not currently made using algae. Nonetheless, the potential of microalgae as a source of fuels is widely recognized (Chisti, 2007, 2008; Rittmann, 2008; Greenwell *et al.*, 2010; Mata *et al.*, 2010; Chisti & Yan, 2011; Chisti, 2012; Jones & Mayfield, 2012) and many start-up companies (Table 1.1) are attempting to

commercialize such fuels. Whether algal fuels can be produced commercially in the near future is questionable (Wijffels & Barbosa, 2010; Hall & Benemann, 2011; Pate *et al.*, 2011) in view of the many unresolved problems. These include the need to screen for suitable producer species (Griffiths & Harrison, 2009) that are amenable to low-cost large-scale culture (Chisti, 2007; Acién *et al.*, 2012; Chisti, 2012). The cost of production of the algal biomass is affected primarily by the productivity of the algal species, the cost of the production system itself, the cost of separating the biomass from the culture medium (Molina Grima *et al.*, 2003; Uduman *et al.*, 2010; Christenson & Sims, 2011) and the expense associated with the extraction of the oil from the biomass (Cooney *et al.*, 2009; Mercer & Armenta, 2011; Sheng *et al.*, 2011; Chisti, 2012; de Boer *et al.*, 2012; Halim *et al.*, 2012; Araujo *et al.*, 2013). Extensive research is underway in all these areas to develop low-cost technologies that could be used in the context of large scale operations. Notwithstanding the difficulties and the magnitude of the problem, achieving economically viable and environmentally sustainable production of algal fuels is of strategic importance and demands sustained research to ensure that algal fuels are eventually commercialized (Chisti, 2010; Wijffels & Barbosa, 2010; Pate *et al.*, 2011). Fuels that can be produced sustainably and are renewable are necessary to reduce the climatic impact associated with burning fossil fuels.

Table 1.1 Some companies engaged in commercializing algal fuels[a]

Company	Location	Web site
Algenol Biofuels	Bonita Springs, FL, USA	www.algenolbiofuels.com
Aquaflow	Nelson, New Zealand	www.aquaflowgroup.com
Aurora Algae, Inc.	Hayward, CA, USA	www.aurorainc.com
Bioalgene	Seattle, WA, USA	www.bioalgene.com
Bionavitas, Inc.	Redmond, WA, USA	www.bionavitas.com
Bodega Algae, LLC	Boston, MA, USA	www.bodegaalgae.com
LiveFuels, Inc.	San Carlos, CA, USA	www.livefuels.com
Parabel, Inc.	Melbourne, FL, USA	www.parabel.com
Phyco Biosciences	Chandler, AZ, USA	www.phyco.net
Sapphire Energy, Inc.	San Diego, CA, USA	www.sapphireenergy.com
Seambiotic Ltd.	Tel Aviv, Israel	www.seambiotic.com
Solazyme, Inc.	South San Francisco, CA, USA	www.solazyme.com
Solix Biofuels, Inc.	Fort Collins, CO, USA	www.solixbiofuels.com
Synthetic Genomics Inc.	La Jolla, CA, USA	www.syntheticgenomics.com

[a] All the listed companies are focused on photoautotrophic production of algal oil, except Solazyme and Algenol Biofuels. Solazyme produces algal oils via heterotrophic culture whereas Algenol Biofuels uses genetically modified algae to produce ethanol directly through photosynthesis. Source: Chisti & Yan (2011).

This work is concerned with production of high-energy algal biomass that is rich in crude oil for potential use in making transport fuels. Several microalgal species are initially screened for their ability to produce oil in marine culture media. One of the high producers is then examined in detail in terms of its oil productivity; biomass productivity; oil content in the biomass; the ability to grow in two different kinds of photobioreactor systems; survival in the dark; performance in batch and continuous culture operations; and response to nitrogen limitation that is known to improve oil productivity of some microalgae (Illman *et al.*, 2000; Scragg *et al.*, 2002; Courchesne *et al.*, 2009; Stephenson *et al.*, 2010; Yeh & Chang, 2011; Breuer *et al.*, 2012; Přibyl *et al.*, 2012). The total biochemical energy content of the algal biomass obtained under various culture conditions is quantified. The nature of the crude oil produced is preliminary characterized.

Inexplicably, most of the ongoing effort for producing algal oils is focussed on freshwater culture media, but there is a general global shortage of freshwater (Gleick, 1998). This work is concerned with only the seawater-based culture systems as only these are likely to be used commercially. Considering the amount of transport fuels consumed, any likely future production of algal fuels will be a massive operation (Pate *et al.*, 2011) that would be totally unsustainable if freshwater is used as the production medium (Chisti, 2012). The aim of this study is to quantify the oil productivity under the various growth scenarios and gain some insight into factors that influence productivity of an alga that is safe to use and has not been previously characterized in seawater-based media. The relevant literature is reviewed in Chapter 2. The objectives of the study are enunciated in Section 2.7 (Chapter 2). The experimental methods are detailed in Chapter 3. Chapter 4 is concerned with the results and discussion. The key findings and conclusions are summarized in Chapter 5.

Chapter 2

Literature Review

2.1 Microalgae and their culture

Microalgae are eukaryotic primitive microscopic plants that use sunlight for photosynthesis. Microalgae occur widely in freshwaters, marine environments and brackish waters. Some microalgae do not survive without light, but others can use organic carbon (e.g. glucose) as an energy source to grow in the absence of light. Growth exclusively on light as the energy source is known as photoautotrophic. Growth exclusively on organic carbon as an energy source is known as heterotrophic. Growth in which both light and organic carbon are used simultaneously is known as mixotrophic. The basic techniques of microalgal culture are well documented in textbooks (Becker, 1994; Richmond, 2004; Anderson, 2005).

2.2 Attributes of a commercial alga for production of fuel oils

Oils (lipids) are energy-rich and carbon-rich molecules that can be readily used to make fuels such as diesel, gasoline and kerosene (jet fuel). For an alga to be useful for fuel production, it must achieve a high productivity of total lipids in an inexpensive culture medium. Commercial production of algal fuel oils is likely to be feasible only in photoautotrophic growth relying on freely available sunlight and inexpensive carbon dioxide. The latter is expected to be sourced from fossil fuel burning power plants and cement factories (Chen *et al.*, 2012; Chisti, 2012; Van Den Hende *et al.*, 2012), for example. Although, some companies are developing algal oil production based on heterotrophic growth on sugars (Huang *et al.*, 2010; Bumbak *et al.*, 2011; Tabernero *et al.*, 2012), this approach is unlikely to be economically viable or environmentally sustainable. This is because sugars are a

relatively expensive feedstock for producing fuels that are low value commodity products (Tabernero *et al.*, 2012). Furthermore, the use of sugars for producing algal fuels is inefficient as the sugars must be inevitably produced via photosynthesis in plants and then fed to algae to produce biomass and oil.

A microalga for fuel production must grow in a dispersed cell morphology (Figure 2.1) so that the culture broth can be easily mixed and pumped during cultivation. Good mixing is required to facilitate: supply of carbon dioxide to the culture; removal of the photosynthetically generated oxygen that can easily build up to toxic levels; temperature control; and bulk movement of algal cells so that the cells deeper in the fluid are periodically brought to the better illuminated peripheral parts of a culture vessel. Colonial and filamentous morphologies (Figure 2.2) are unsatisfactory as they make mixing difficult and interfere with good light penetration in the culture broth.

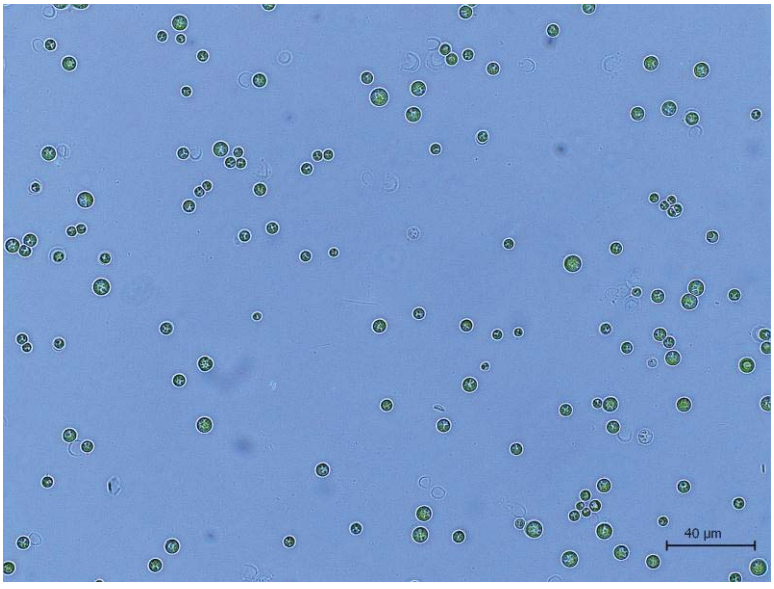

Figure 2.1 A microalga (*Chlorella vulgaris*) with a dispersed cell morphology.

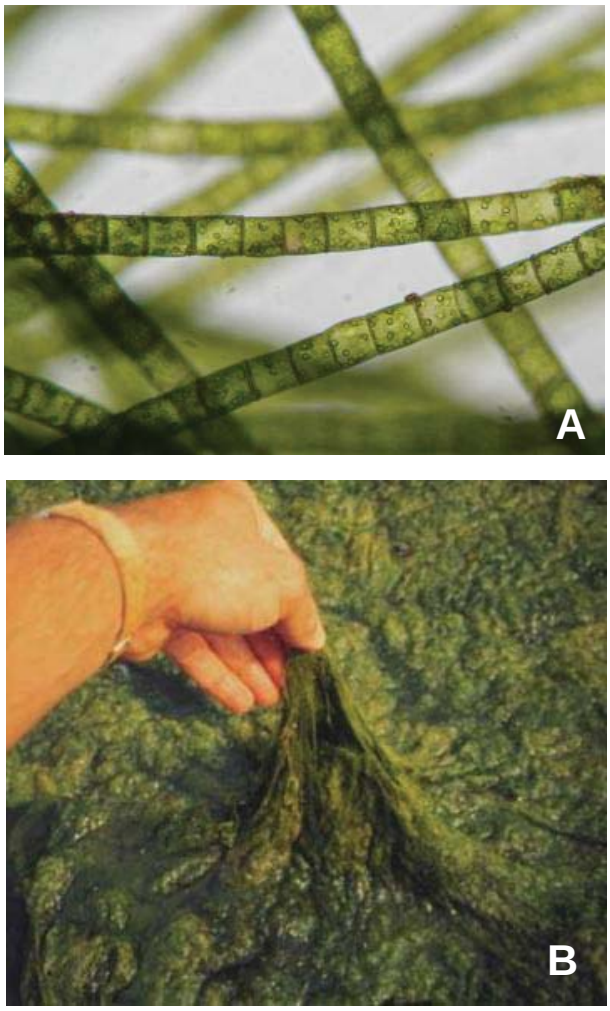

Figure 2.2 Microalgae with filamentous morphologies. Sources:

(A) www.amuraquatics.com/problemweeds1.html; and

(B) www.lifeinfreshwater.org.uk/Species%20Pages/filamentous%20Alga.jpg.html.

Algae genera have not been rigorously compared for their ability to produce lipids; nevertheless, evidence suggests that many green microalgae and diatoms can attain high lipid productivities (Sheehan *et al.*, 1998; Chisti, 2007; Griffiths & Harrison, 2009; Rodolfi *et al.*, 2009). Both marine and freshwater species attain high productivities. In practice, only marine algae are viewed as acceptable for production of fuel oils (Chisti, 2012), although

most of the companies (see Table 1.1) involved in attempts to commercialize algal fuels appear to be focused on freshwater algae. Unfortunately, there is a general global shortage of freshwater (Gleick, 1998) and freshwater supplies are best reserved for use in agriculture and human consumption. The scale of fossil fuel use is such that any replacement algal fuel will need to be produced in huge quantities (Pate *et al.*, 2011) and sustainable production may be possible only if marine algae grown in seawater media are used (Chisti, 2010).

An alga for commercial use in producing fuels must be easy to grow and physically robust. Some algae are too fragile to survive in high levels of turbulence, mixing and pumping (Mazzuca Sobczuk *et al.*, 2006; García Camacho *et al.*, 2007; Gallardo Rodríguez *et al.*, 2009; Chisti, 2010*b;* Gallardo Rodríguez *et al.*, 2011; García Camacho *et al.*, 2011) that are inevitably required for attaining a good productivity in artificial culture devices. In addition, an alga for commercial production of fuels must be capable of rapid growth so that it can outcompete other unwanted microalgae that could easily contaminate a large-scale cultivation process.

The freshwater microalgae *Chlorella vulgaris* is often considered for biodiesel production (Debska *et al.*, 2010; Heredia-Arroyo *et al.*, 2011; Kong *et al.*, 2011; Hempel *et al.*, 2012; Kong *et al.*, 2012) as it has the attributes of rapid growth and the desired morphology (Figure 2.1). *C. vulgaris* is known to accumulate good quantity of oil (e.g. ≥30% w/w in the biomass) and can grow both photoautotrophically and heterotrophically. However, most strains of *C. vulgaris* thrive only in freshwater. In most cases achieving a combination of a high growth and a high lipid content in the biomass, is a challenging task (Csavina *et al.*, 2011). This is because the synthesis of high-energy compounds such as lipids diverts energy and other metabolic resources from growth.

2.3 Microalgae versus plants

Many crop plants can provide oils that are quite suitable for making biodiesel (Banković-Ilić *et al.*, 2012; Borugadda & Goud, 2012). Why then the interest in developing algal fuels? This is because algae offer important potential advantages (Chisti, 2007) over plants: (1) algae can be grown on nonarable land, leaving arable land to existing uses in production of food and fodder; (2) algae can be grown using seawater, leaving most of the globally scarce freshwater (Gleick, 1998) available for other uses; (3) oil productivity of microalgae greatly exceeds that of higher plants; (4) if algal fuel is used to displace fossil fuel, a potential exists for reducing the net emission of carbon dioxide that is contributing to global warming (Baum *et al.*, 2012); and unlike plant seeds and fruits, oil-containing algal biomass can be produced year round in a suitable climate.

A higher oil productivity of algae compared to oil palm, one of the most productive oil crops, has been mentioned in the literature (Chisti, 2007). For example, in laboratory studies, the freshwater microalgae *Choricystis minor* has been shown to achieve a lipid productivity of nearly 4-fold relative to oil palm (Mazzuca Sobczuk & Chisti, 2010). Unfortunately, *C. minor* fails to thrive in seawater.

Estimates of the theoretical maximum oil productivity of microalgae have been as high as 354,000 L $ha^{-1}year^{-1}$ (Weyer *et al.*, 2010) although the more plausible best case estimates have ranged from 40,700 to 53,200 L $ha^{-1}year^{-1}$, depending on local climate (Weyer *et al.*, 2010). For an alga with an oil content of 40% by weight, Cooney *et al.* (2011) estimated a theoretical maximum oil productivity of nearly 159,000 L $ha^{-1}year^{-1}$. For comparison, oil productivity of oil palm is only 5,950 L $ha^{-1}year^{-1}$ (Chisti, 2007). In Figure 2.3, the various estimates of oil productivities of microalgae are compared with those of the other crops. The expected high productivities of algae are the reason for the interest in them.

High productivities have been confirmed in laboratory studies (Mazzuca Sobczuk & Chisti, 2010).

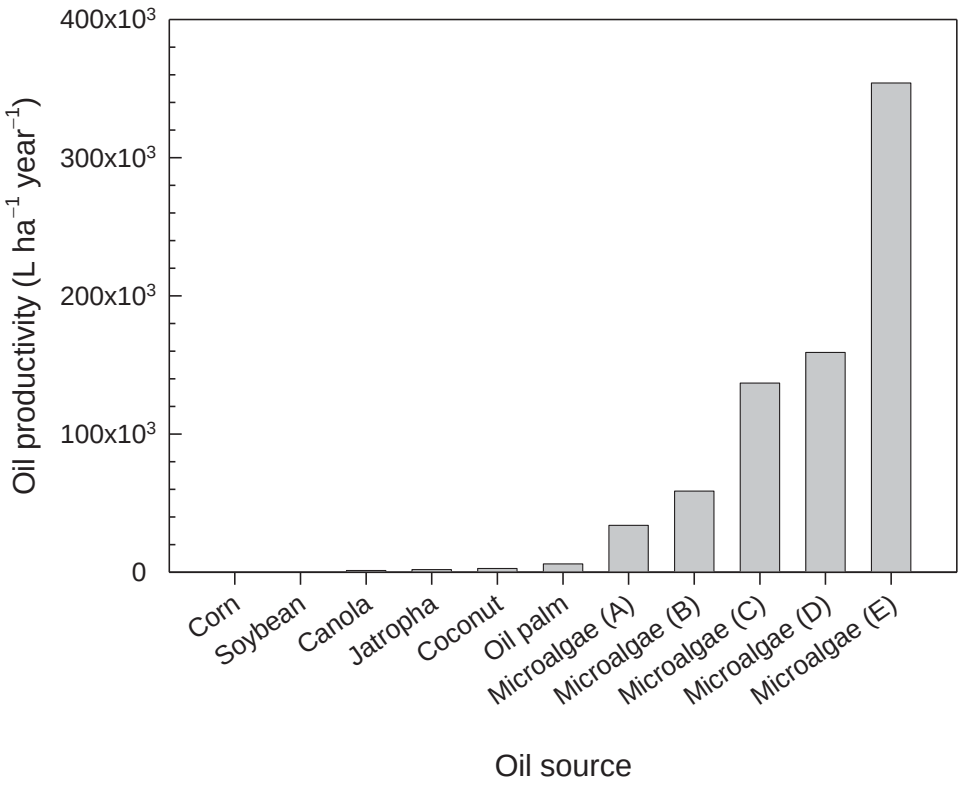

Figure 2.3 Oil productivity of various sources. Productivity of soybean and corn is 172 and 446 L·ha^{-1} year^{-1}, respectively. Microalgae A based on measured biomass productivity in an outdoor tubular photobioreactor and an assumed oil content of 30% (w/w) in the biomass (Chisti, 2007); Microalgae B based on average biomass productivity of a typical outdoor raceway pond in the tropics and an assumed oil content of 40% (w/w) in the biomass (Chisti, 2012); Microalgae C based on measured biomass productivity in an outdoor tubular photobioreactor and an assumed oil content of 70% (w/w) in the biomass (Chisti, 2007); Microalgae D based on the theoretical maximum oil productivity estimated by Cooney *et al.* (2011); Microalgae E based on the theoretical maximum oil productivity estimated by Weyer *et al.* (2010). Sources: Chisti (2007); Chisti (2012); Weyer *et al.* (2010); Cooney *et al.* (2011).

A better productivity of algae relative to plants is partly explained by their higher photosynthetic efficiency. Photosynthetic efficiency is the fraction of the incident sunlight energy that is converted to biochemical energy. The theoretical upper limit of photosynthetic efficiency is 13% (Bolton & Hall, 1991), but a practical upper limit is about 8.3% (Bolton & Hall, 1991). The maximum observed photosynthetic efficiency of plants is only 2.4% (Zhu *et al.*, 2008), but for microalgae, the average annual photosynthetic efficiency during pilot scale field operations has exceeded 5.0% (Chisti, 2012).

Several reasons have been cited for a higher productivity of microalgae compared to plants (Chisti, 2010; Chisti, 2012). Unlike in vascular plants, each algal cell is photosynthetically active. In plants, the tissue not contributing to photosynthesis does consume metabolic energy. For example, up to 52% of the carbon dioxide produced by plants has been attributed to root respiration (Atkin *et al.*, 2000; Chisti, 2012). Roots respire all the time, both during the day and night. Unlike plants, algal cells can directly take up nutrients from the surrounding fluid, without having to rely on energy consuming long-distance transport via roots and stem (Chisti, 2010). In plants, ion uptake by roots consumes up to 70% of the energy produced by root respiration (Poorter *et al.*, 1991; Chisti, 2012). Furthermore, ≤2.7% of a leaf's surface is available for absorption of carbon dioxide (Chisti, 2012) which is required for photosynthesis. Carbon dioxide is absorbed through micropores known as stomata. The total area of these pores is small relative to the total surface area of a leaf. To reach a chloroplast where photosynthesis occurs, carbon dioxide entering the leaf via stomata must diffuse a significant distance that is much longer in a leaf (Parkhurst, 1986; Nielsen *et al.*, 1996) than in a cell of a microalga. Diffusion coefficients of carbon dioxide within a leaf are low (Morison *et al.*, 2005) and insufficient to support appreciable photosynthesis over distances of more than 0.3 mm from the stomata (Morison *et al.*, 2005). This limitation does not exist in microalgae. As a consequence of some of the above

limitations, the median value of the maximum specific growth rate for higher plants is 0.1 day^{-1} or less, but for microalgal species it is about 1 day^{-1} (Nielsen *et al.*, 1996). An extensive review of the literature suggests that the average doubling time for green microalgae is 24 h, corresponding to a specific growth rate of 0.69 d^{-1} (Griffiths & Harrison, 2009), under optimal growing conditions. For microalgae, the specific growth rate is of course always much less than the maximum possible specific growth rate because a typical culture is always light limited because of mutual shading by cells. The maximum specific growth rate, on the other hand, is attained in a highly dilute culture that is not light limited.

A few microalgae are grown commercially for use as aquaculture feeds and production of relatively high-value products (Becker, 1994; Lorenz & Cysewski, 2000; Guerin *et al.*, 2003; Richmond, 2004; Spolaore *et al.*, 2006; Posten & Walter, 2012), but they are not used for producing fuels although they are being extensively researched for this purpose (Scragg *et al.*, 2002; Tsukahara & Sawayama, 2005; Chisti, 2007; Williams, 2007; Dismukes *et al.*, 2008; Hu *et al.*, 2008; Li *et al.*, 2008; Rittmann, 2008; Rosenberg *et al.*, 2008; Schenk *et al.*, 2008; Vasudevan & Briggs, 2008; Rodolfi *et al.*, 2009; Chisti, 2010; Chisti & Yan, 2011). Much of the work focused on production of algal oils for making biofuels concerns freshwater species (Banerjee *et al.*, 2002; Mazzuca Sobczuk & Chisti, 2010; Přibyl *et al.*, 2012; Li *et al.*, 2013).

2.4 Algae culture requirements

Phototrophic growth of microalgae requires the following: light as an energy source; a nutrient medium that contains the inorganic macronutrients (a nitrogen source; a phosphorous source), the essential trace elements and has the required salinity (Bisson &

Kirst, 1995; Ferroni *et al.*, 2007; Affenzeller *et al.*, 2009); a suitable temperature (typically 20–28 °C); and carbon dioxide as a source of inorganic carbon.

2.4.1 Culture media

Various suitable nutrient sufficient media have been developed for algal culture (Becker, 1994; Sánchez *et al.*, 2000; Richmond, 2004; Anderson, 2005). Most media are designed to maximize the production of biomass. Laboratory media are often supplemented with vitamins (Anderson, 2005).

Anderson (2005) lists more than 30 media compositions, for example. Nutritionally complete existing media are quite satisfactory for growing most microalgae to a high biomass concentration, so long as there is sufficient light and carbon dioxide. A medium must of course be selected with consideration of the specific needs of certain types of algae. For example, a medium intended for diatoms must provide silicon to allow the cell to build its exoskeleton. In culture media, phosphorus is always supplied as inorganic phosphate (PO_4^{3-}) that is known to be readily assimilated by algae. Nitrogen may be supplied as nitrate (NO_3^-), ammonium (NH_4^+) and urea ($(NH_2)_2C=O$). The latter is considered to be an organic form of nitrogen and is not commonly used. Algae more readily metabolize ammonium compared to nitrate as ammonium can be directly used in the synthesis of amino acids. Generally, algae will use nitrate nearly as readily as ammonium, but nitrate must be reduced within the cell for metabolic purposes. Ammonium nitrate (NH_4NO_3) is a commonly used source of nitrogen in controlled culture, but the use of $NaNO_3$ is preferred. This is because salts containing ammonium ion tend to release ammonia (NH_3) if the culture becomes alkaline and ammonia is highly toxic to microalgae.

An inexpensive medium that is intended for eventual commercial use should not contain anything other than cheap inorganic salts. Nitrogen and phosphorous are commonly supplied using commercial agricultural fertilizers (Sheehan *et al.*, 1998; Chisti, 2007). Typically, the culture pH must be controlled at an appropriate value as too much CO_2 will make the medium acidic and depletion of CO_2 will rapidly raise pH towards alkaline values. An insufficiency of CO_2 will limit photosynthesis. Typically, algal biomass contains 50% of its dry weight as carbon (Chisti, 2007). This translates to a minimum CO_2 requirement of 1.83 kg per kg of biomass produced (Chisti, 2007). Photosynthesis produces oxygen. One mole of oxygen is produced for each mole of CO_2 consumed. Accumulation of oxygen in the culture medium can inhibit photosynthesis (Molina *et al.*, 2001; He & Häder, 2002) and therefore oxygen must be removed periodically to maintain the concentration near the air saturation level (Molina Grima *et al.*, 1999; Chisti, 2007). Oxygen is typically removed by sparging the culture broth with air. Sparging with a gas such as nitrogen is considered too expensive.

The microalgae biomass grown under normal nutrient sufficient conditions has an approximate elemental composition by number of atoms of C:N:P of 106:16:1 (Weber & Deutsch, 2010). This is the well-known Redfield ratio. It translates to a composition by weight of around 83% C, 14.7% N and 2% P, if only C, N and P are considered. The biomass of course has other elements (e.g. oxygen, sulfur, hydrogen). The total carbon content of the biomass is about 50% by weight (Chisti, 2007) and, therefore, using the above Redfield ratio, the N and P content are around 8.8% (w/w) and 1.2% (w/w), respectively. Other trace elements are present in low amounts. Apart from carbon, all elements are drawn from the dissolved nutrients and water. Actually, carbon is also taken up as dissolved carbon dioxide. Other forms of dissolved inorganic carbon (CO_3^{2-}; HCO_3^-) may be taken up by the

cell. Bicarbonate produced from carbon dioxide may be a future source of carbon for algal culture (Chi *et al.*, 2011).

Outdoor commercial cultures of microalgae often become alkaline (Becker, 1994) during peak sunlight because carbon dioxide is consumed rapidly and may not be replenished sufficiently fast in a large pond. Use of $NaNO_3$ as a nitrogen source avoids the risk of killing the culture, even though ammonium may be a metabolically preferred nitrogen source. In addition to macronutrients, various micronutrients are required for satisfactory growth and metabolic functioning of the algal cell. The key micronutrients are Mg^{2+}, Ca^{2+}, Mn^{2+}, Fe^{3+}, Zn^{2+}, Co^{2+}, Mo^{6+}, Cu^{2+}, and sulfur. Magnesium is needed for making chlorophyll, for example. Algal nutrition and culture media are discussed in depth by Anderson (2005) and Grobbelaar (2004).

2.4.2 Temperature

Temperature is an important factor in influencing the biomass productivity. Micoralgal species capable of growing in extreme conditions exist (Ciniglia *et al.*, 2004; Novis, 2007), but for most commercially useful algae the optimal growth temperature is generally in the range of 24-30 °C (Hanagata *et al.*, 1992; Chisti, 2012). Within limits, the maximum specific growth rate (μ_{max}, d^{-1}) generally increases with growth temperature (Goldman & Carpenter, 1974). This applies to both freshwater and marine species. Effects of temperature on growth are further discussed by Raven & Geider (1988).

For *Chlorella vulgaris* that is of specific interest here, a temperature of >30 °C appears to adversely affect growth of at least some strains (Chinnasamy *et al.*, 2009), but an optimal temperature of 29 °C has been reported for photoautotrophic growth in a freshwater medium (Potvin *et al.*, 2011). The optimal growth temperature may depend on the way the

alga is grown. For example, for *C. vulgaris* growing heterotrophically on glucose, the optimal growth temperature has been found to be 32 °C (Mayo, 1997). A lower optimal growth temperature in phototrophic culture suggests that the photosynthetic apparatus of the cell may be more sensitive to a high temperature compared to the rest of the metabolic machinery.

As the efficiency of photosynthesis is ≤13% (Bolton & Hall, 1991), ≥87% of the sunlight energy received at the photosynthetic apparatus must be dissipated in other ways. The excess energy is dissipated as heat and fluorescence (Szabó *et al.*, 2005). Some of the light absorbed by chlorophyll is emitted as low energy radiation. This is fluorescence. Chlorophyll a, the main form of chlorophyll in green algae, absorbs visible light mainly of wavelengths of 420 nm and 660 nm. Some of this light is reemitted at longer wavelengths of 750-800 nm. The wavelength and energy content of radiation are inversely related. Thus, light of longer wavelength has less energy relative to photons of a shorter wavelength. Chlorophyll fluorescence is further discussed by Krause & Weis (1991) and Maxwell & Johnson (2000). Heat must be removed from the photosynthetic apparatus and the cell by conduction into the culture fluid. A lower culture temperature in phototrophic growth likely helps with the removal of the excess heat. In contrast, during growth on glucose in the dark, this dissipation of light-derived heat does not need to occur.

Interactive effects of temperature and copper on the photochemistry of the photosynthetic apparatus have been reported in *C. vulgaris* (Oukarroum *et al.*, 2012), but appear to be of no concern in a copper-sufficient environment. Temperature may affect metabolic processes also in the dark (at night). For example, the rate of starch degradation is known to be affected by temperature (Nakamura & Miyachi, 1982), being generally faster at a higher temperature, so long as the temperature does not reach a damaging level.

2.4.3 pH

Microalgae generally tolerate well a broad range of pH, for example, pH values ranging from 6.5 to 8.5. Extremophilic microalgae, depending on species, will tolerate higher or lower pHs (Ciniglia *et al.*, 2004; Novis, 2007). In view of a broad range of pH tolerance, pH is not controlled during most algal cultures. The culture is continuously sparged with a mixture of air and carbon dioxide. The latter commonly constitutes 3-6% of the mixture by volume (Chinnasamy *et al.*, 2009; Potvin *et al.*, 2011). This generally keeps the pH in the range of 6.5-7.5 and ensures a sufficiency of carbon dioxide. Continuous sparging also help to remove the photosynthetically produced oxygen. The rate of consumption of CO_2 increases with light level, as within limits, the rate of photosynthesis increases with increasing irradiance (Section 2.4.2). In heterotrophic growth of *C. vulgaris* on glucose, the optimal pH has been reported to be ~6.5 (Mayo, 1997).

2.4.4 Light

Photosynthesis requires light as an energy source. Only sunlight that is in the 400–700 nm wavelength range is effective for photosynthesis. This range constitutes the "photosynthetically active radiation", or PAR. Only about 45% of the incident solar energy is in the PAR range (Goldman, 1979; González & Calbó, 2002). The ability of an alga to obtain sufficient light in a culture system depends on the amount of incident radiation at the light receiving surface, the concentration of the cells in the broth and the surface-to-volume ratio of the photobioreactor (Gordon & Polle, 2007). The surface-to-volume ratio is a function primarily of the channel depth (Gordon & Polle, 2007).

The relationship between the rate of photosynthesis and the incident PAR constitutes the photosynthesis response curve. A typical such curve is shown in Figure 2.4. At PAR value that is below the "light compensation point" (Figure 2.4), the cells consume oxygen to

oxidize cell mass (carbohydrates) to generate energy for maintenance. At light compensation point, the oxygen generation by photosynthesis just matches the oxygen consumption by respiration and there is no net growth. Growth occurs only above the light compensation point. Shade-adapted algae such as those found within or under ice have relatively low compensation points. For such algae compensation point may range from 0.18 to 21 $\mu E \cdot m^{-2} s^{-1}$ (Hsiao, 1988).

Above the light compensation point, the rate of photosynthesis increases linearly with increasing irradiance up to a point. Eventually, the maximum rate of photosynthesis is obtained at the saturating irradiance (Figure 2.4). Increase in irradiance above the saturation level actually reduces the rate of photosynthesis, a phenomenon known as photoinhibition (Figure 2.4). Photoinhibition in shade-adapted algae occurs at light intensities ranging from 10 to 231 $\mu E \cdot m^{-2} s^{-1}$ (Hsiao, 1988). More commonly, a PAR value of around 200–400 $\mu E \cdot m^{-2} s^{-1}$ is needed for photoinhibition. In comparison, the peak PAR level (i.e. at solar noon) at the equator (i.e. a latitude of 0°) on a clear day, is about 2,000 $\mu E \cdot m^{-2} s^{-1}$. Therefore, photosynthesis typically saturates at 10–20% of the peak irradiance, depending on the algal species. Photosynthesis response curve has been further reviewed by Henley (1993).

Because of self-shading by cells, local light level declines rapidly with depth in a high density algal culture (Molina Grima *et al.*, 1999; Chisti, 2006) even when subjected to a saturating light intensity at its surface. As a consequence, under typically used concentration of cells ($\geq$0.5 g L^{-1}), a photobioreactor tube unavoidably contains a well illuminated peripheral zone and an unproductive dark zone (Molina Grima *et al.*, 2000; Molina *et al.*, 2001). Turbulence in the culture broth causes the cells to cyclically move between the light and dark zones. Under conditions of constant external irradiance, the cells therefore experience light–dark cycling (Molina Grima *et al.*, 2000; Molina *et al.*, 2001). Ideally, for a given cell, the mean residence time in uninterrupted darkness must be kept to a minimum to

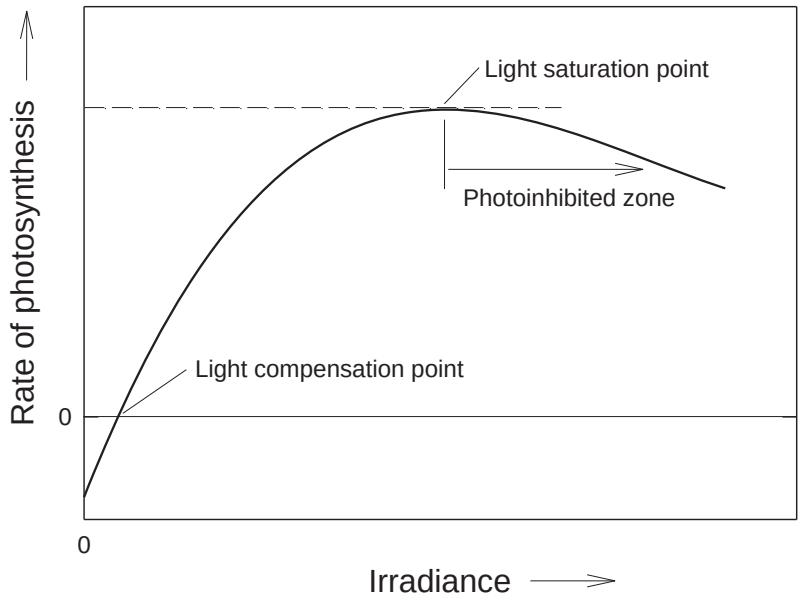

Figure 2.4 A typical photosynthesis response curve.

prevent loss of productivity. Unfortunately, brief periods of continuous darkness reduce culture productivity and in most practicable culture systems the continuous residence time in the dark zone cannot be reduced to the order of milliseconds (Camacho Rubio *et al.*, 2003; Gordon & Polle, 2007) that is necessary for preventing biomass starvation in the dark. A medium duration light–dark cycle of about 12 s (i.e. a 6 s light saturation period followed by 6 s of total darkness) is sufficient to reduce productivity relative to uninterrupted illumination (Janssen *et al.*, 1999).

Although intensely turbulent flow in a photobioreactor ensures that the cells are continually moved from the dark zones to better lit zones, too intense a turbulence can damage at least some algae (Chisti, 1999; García Camacho *et al.*, 2001; Sánchez Mirón *et al.*, 2003; Mazzuca Sobczuk *et al.*, 2006; García Camacho *et al.*, 2007). Nevertheless, some mixing is widely acknowledged to enhance productivity relative to a poorly mixed culture

(Terry & Raymond, 1985; Molina Grima *et al.*, 1999; Pruvost *et al.*, 2002; Camacho Rubio *et al.*, 2003). Use of static mixers in photobioreactor tubes has been found to enhance biomass productivity and reduce the influence of photoinhibition (Ugwu *et al.*, 2005), but static mixers pose problems with the cleaning of photobioreactor tubes.

Indoor photobioreactors require illumination with an artificial light source capable of emitting visible light, i.e. light in the wavelength range of 400–700 nm. Fluorescent lights, red light emitting diodes (LED) and LEDs emitting white light are frequently used (Tang *et al.*, 2011a). Red light emitting diodes (LEDs) of 660 nm wavelength output have been used as the sole light source for photosynthesis in microalgae (Matthijs *et al.*, 1996) and plants (Tennessen *et al.*, 1994; Tennessen *et al.*, 1995). Chlorophyll, the principal light capture pigment in most microalgae, has an absorption maximum at a wavelength of around 660 nm. In addition to being an effective and compact light source, LEDs consume less electricity compared with the other light sources for a given output of light. Consequently, LEDs generate much less heat compared with the other light sources and have a long life. During culture of the cyanobacterium *Spirulina platensis* (synonym *Arthrospira platensis*), highest values of specific growth rates were attained when grown using red LEDs (Wang *et al.*, 2007). Use of LED illumination in a photobioreactor has been found to maximize the growth rate and culture density of *C. vulgaris* (Fu *et al.*, 2012). The nature of the light source may affect photosynthetic efficiency of the alga. For example, Tang (2012) reported that *Chlorella minutissima* grown using fluorescent light had a higher photosynthetic efficiency compared to growth on either the red or white LEDs. Different light sources compared on the basis of the same PAR output, generally provide comparable growth performance. Growth dependence on light is discussed further in the literature (Yokota *et al.*, 1994; Molina Grima *et al.*, 1999; Yun & Park, 2003; Martínez *et al.*, 2012).

2.5 Algal oils

Lipids are substances that are soluble in nonpolar organic solvents such as chloroform and hexane, but not in water. Total lipids include hydrocarbons, chlorophylls, carotenoids, triglycerides, mono- and diglycerides, phospholipids, sulfolipids, glycolipids, waxes, and sterols. All these materials are potentially useful for making liquid hydrocarbon fuels such as gasoline, jet fuel and diesel. Only triglycerides are generally useful for making biodiesel. Microalgae commonly accumulate lipids (Banerjee *et al.*, 2002; Griffiths & Harrison, 2009; Mata *et al.*, 2010). Lipids and lipid metabolism of eukaryotic microalgae has been reviewed recently (Guschina & Harwood, 2006; Courchesne *et al.*, 2009; Harwood & Guschina, 2009; Huang *et al.*, 2010; Khozin-Goldberg & Cohen, 2011). Neutral lipids within an algal cell can be seen in situ by staining with Nile red fluorescent dye (Huang *et al.*, 2009; Doan & Obbard, 2011). Neutral lipid quantification methods based on Nile red staining have been developed (Chen *et al.*, 2009; Bertozzini *et al.*, 2011), but the total lipids in the cell are best quantified by extraction and gravimetric measurements. Various other methods of estimating the lipids have been proposed (Su *et al.*, 2008), but have not gained general acceptance.

Plant oils such as palm oil, soybean oil and corn oil are predominantly triglycerides that can be readily converted to biodiesel by reaction with an alcohol such as methanol. Unlike plant oils, microalgal oils are generally more complex (Banerjee *et al.*, 2002; Guschina & Harwood, 2006; Harwood & Guschina, 2009). Many algal oils contain triglycerides that are rich in long-chain highly polyunsaturated fatty acids (e.g. eicosapentaenoic acid, EPA, 20:5(n-3); docosahexaenoic acid, DHA, 22:6(n-3)) (Belarbi *et al.*, 2000; Guschina & Harwood, 2006). In addition, algal oils contain nontriglyceride compounds such as β-carotene, lycopene, astaxanthin, zeaxanthin and chlorophylls (Figure 2.5). Nontriglyceride oils cannot be converted to biodiesel, but they can be used to make diesel, kerosene (jet fuel) and gasoline. Algal crude oil can be viewed as a crude petroleum

equivalent and can be transformed to usable fuels using some of the same technologies as used in refining petroleum (Chisti, 2012). The long-chain highly unsaturated fatty acids of algal oils do not make good biodiesel (Knothe, 2011; Stansell *et al.*, 2012). This is because these fatty acids are highly susceptible to oxidative degradation during storage, have a high viscosity and high flash points. Algal crude oil has an energy content of around 35,800 kJ kg^{-1} (as measured in this work), or nearly 80% of the average energy content of crude petroleum (Chisti, 2012). Algal oils can be a potential feedstock for making many of the products now derived from petroleum. Fuels derived from algal oils have performed well in internal combustion engines (Haik *et al.*, 2010; Haik *et al.*, 2011).

Extraction of algal oils from the biomass in the context of scalable processes is not the focus of this work. Methods for extraction of algal oils in potential large scale operations have been reviewed in the literature (Cooney *et al.*, 2009; Mercer & Armenta, 2011; Halim *et al.*, 2012), but are of no direct relevance here. For analytical purposes, the Bligh and Dyer (1959) method (Section 3.10.5) is the most widely used (Mazzuca Sobczuk & Chisti, 2010; Sheng *et al.*, 2011; Kanda *et al.*, 2012; Araujo *et al.*, 2013) for lipid extraction and subsequent gravimetric quantification. Bligh and Dyer (1959) method is able to quantitatively extract the oils.

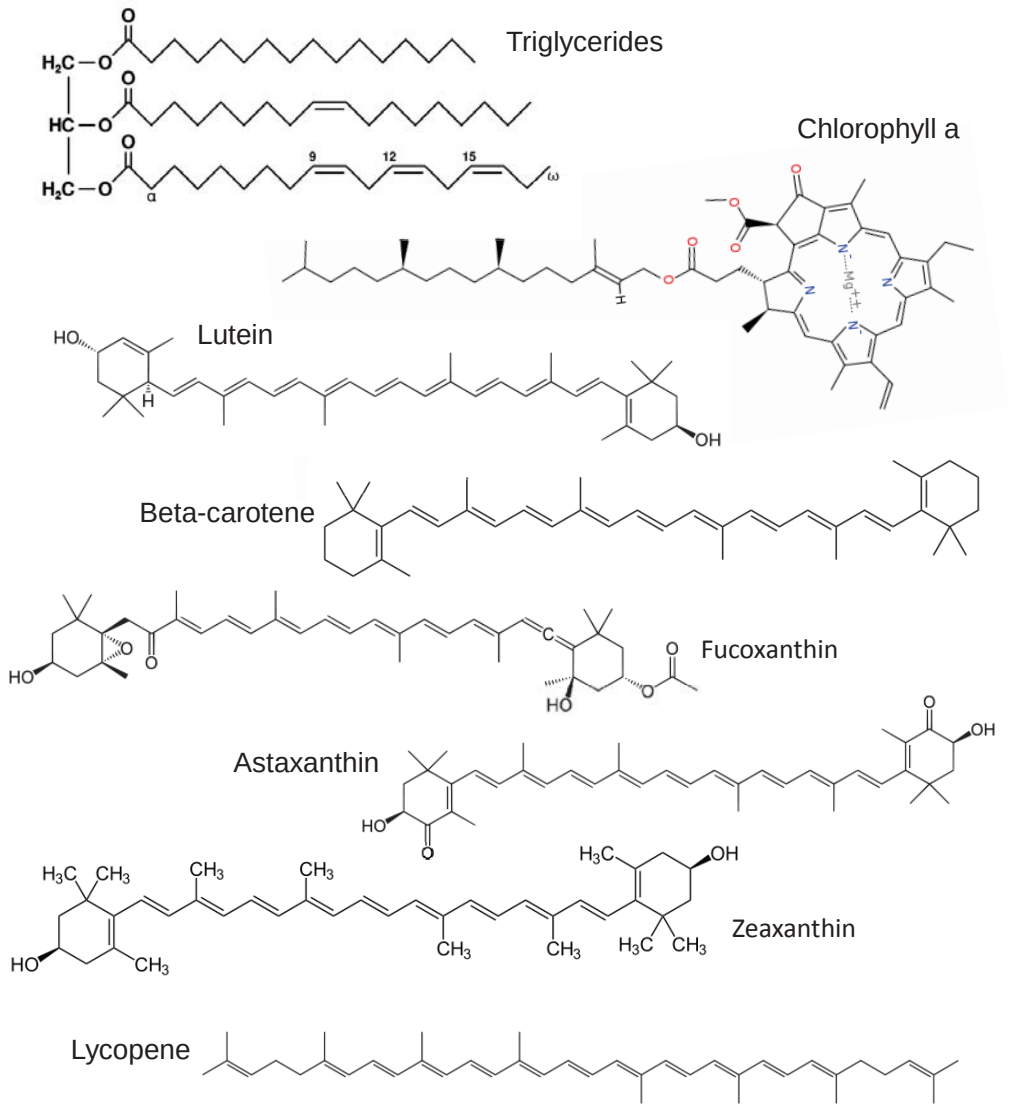

Figure 2.5 Some components of algal crude oil. Structures of individual compounds were obtained from Wikipedia.

Optimal conditions for lipid accumulation in algae are almost never the same as the optimal conditions for biomass growth. Under optimal growth conditions, lipid productivities that have been reported for some microalgae are as follows: 160 $mg \cdot L^{-1}d^{-1}$ for the marine diatom *Amphora* sp.; 99 $mg \cdot L^{-1}d^{-1}$ for the marine green alga *Tetraselmis suecica*; and 97 $mg \cdot L^{-1}d^{-1}$ for the freshwater green alga *Chlorella sorokiniana* (Griffiths & Harrison,

2009). A peak lipid productivity of 32 $mg{\cdot}L^{-1}d^{-1}$ for freshwater *C. vulgaris* has been reported (Potvin *et al.*, 2011). Depending on growth conditions, the lipid contents of freshwater *C. vulgaris* have ranged from 18% (Lam & Lee, 2012) to 55% (Mallick *et al.*, 2012). Under optimal culture conditions, the lipid content of a freshwater *C. vulgaris* was reported to be 21% of biomass dry weight (Bhola *et al.*, 2011), but the biomass had an unusually low calorific value of 17.4 kJ g^{-1} (Bhola *et al.*, 2011). The fatty acid profile of the oil of course depends on the algal species and the culture conditions (Rasoul-Amini *et al.*, 2011; Tang *et al.*, 2011a; Yeh & Chang, 2012). Certain highly productive algae can be difficult to culture consistently. This has been the author's experience with *Tetraselmis subcordiformis*, for example.

In a study spanning 38 microalgae, 4 *Chlorella* strains (*Chlorella* sp., *Chlorella sacchatophila*, *Chlorella minutissima*, *Chlorella vulgaris*) were found to have the highest productivity of fatty acids (not total lipids) for use in transesterification to biodiesel (Hempel *et al.*, 2012). All *Chlorellas* were grown in freshwater media. Productivity of fatty acids was found to be influenced by the culture temperature and irradiance (Hempel *et al.*, 2012). The total lipid productivity of a *C. vulgaris* strain ranged from 80.5 to 88.5 $mg{\cdot}L^{-1}d^{-1}$, but the fatty acid productivity was in the range between 12.6 and 15.6 $mg{\cdot}L^{-1}d^{-1}$ (Hempel *et al.*, 2012). Thus, the fatty acids constituted at most 19% by weight of the total lipids produced. The maximum lipid content in any *Chlorella* biomass was ≤30.2% (w/w) (Hempel *et al.*, 2012).

Lipid productivity can be substantially enhanced under nutritional or other stress (Illman *et al.*, 2000; Courchesne *et al.*, 2009; Griffiths & Harrison, 2009; Rodolfi *et al.*, 2009; Mazzuca Sobczuk & Chisti, 2010; Breuer *et al.*, 2012; Campenni' *et al.*, 2013; James *et al.*, 2013; Ördög *et al.*, 2013). A strategy for maximizing lipid production may therefore involve a two stage operation in which the first stage attempts to grow the biomass as rapidly

as possible and the second stage induces lipid accumulation by imposing nutritional or other stresses. Whether stress conditions and a given type of stress influence lipid accumulation appears to depend to some extent on the algal species. For example, compared to controls, growth at low nitrogen levels has elevated lipid contents of the green algae *C. vulgaris* and *Scenedesmus obliquus*, but not the lipid contents of four species of cyanobacteria (Piorreck *et al.*, 1984; Přibyl *et al.*, 2012).

Culture temperature is known to influence the biochemical composition and lipid contents of algal biomass (Zhu *et al.*, 1997; Converti *et al.*, 2009; James *et al.*, 2013). The lipid content of the biomass respond differently to changes in culture temperature in different microalgae. For example, an increase in temperature from 20 °C to 25 °C led to a doubling of the lipids content of *Nannochloropsis oculata* (Converti *et al.*, 2009). In contrast, an increase in growth temperature from 25 °C to 30 °C reduced the lipid content of *C. vulgaris* grown in freshwater from 14.7% to 5.9% (Converti *et al.*, 2009). In both algae, a 75% decrease in the initial nitrogen concentration in the medium relative to the optimal growth medium, increased the lipid content. In *C. vulgaris* the lipid contents increased 2.8-fold to ~16% (Converti *et al.*, 2009). Zhu *et al*. (1997) found that an increasing of the culture temperature from 15 to 30 °C reduced the neutral lipid proportion in the total lipid fraction of *Isochrysis galbana*. Furthermore, the lipid contents were affected by the growth status (e.g. stationary phase) of the culture. The proportion of the neutral lipid in the total lipid fraction was greater in the stationary phase than in the exponential phase (Zhu *et al.*, 1997). Culture age may affect the number of triglyceride and lipid classes present in the oil (Alonso *et al.*, 2000). Levels of the other cellular constituents – carbohydrates and proteins, for example – are influenced by the nutritional status of growth. For example, the level of carbohydrates may increase under nitrogen deficiency but the level of proteins may decrease (Lynn *et al.*, 2000). In nutrient sufficient growth, different species of microalgae may have

different levels of proteins, carbohydrates and lipids in the biomass (Becker, 1994; González López *et al.*, 2010).

Lipid accumulation has been frequently associated with deprivation of nitrogen and phosphorus (Piorreck *et al.*, 1984; Illman *et al.*, 2000; Scragg *et al.*, 2002; Courchesne *et al.*, 2009; Mazzuca Sobczuk & Chisti, 2010; Scarsella *et al.*, 2010; Breuer *et al.*, 2012; Griffiths *et al.*, 2012; Ördög *et al.*, 2013). The lipid level in different *Chlorella* species responds differently to nitrogen starvation. Of the five *Chlorella* species tested by Illman *et al*. (2000) in freshwater media, all showed an increase in lipid level as a consequence of nitrogen starvation, but the magnitude of the response depended on the species. For example, the total lipids in *C. vulgaris* were increased by >2.2-fold by nitrogen starvation, but the increase was only 10% for *Chlorella sorokiniana* (Illman *et al.*, 2000).

In a pumped tubular photobioreactor, *C. vulgaris* grown in a nonlimited freshwater medium had a biomass productivity of 40 mg $L^{-1}d^{-1}$ and a lipid content in the biomass of 28% (w/w) (Scragg *et al.*, 2002). This was equivalent to a lipid productivity of 11.2 mg $L^{-1}d^{-1}$. The same strain of *C. vulgaris* grown in a nitrogen limited medium had a much lower biomass productivity of 24 mg $L^{-1}d^{-1}$ and the biomass contained 58% lipids (Scragg *et al.*, 2002). The lipid productivity was, therefore, 13.9 mg $L^{-1}d^{-1}$, or about 24% greater than for the same alga grown in a nutrient sufficient medium. The triglycerides in *C. vulgaris* were increased when cultured in nitrogen limited conditions (Stephenson *et al.*, 2010). In diatoms, lipid levels may be elevated by growth limitation induced by deficiency of nitrogen, phosphorous and silicon (Lynn *et al.*, 2000). In some cases, nitrogen deficient media may influence only the profile of the lipids produced (Breuer *et al.*, 2012) and not the lipid content in the biomass. This has been reported for the marine alga *Nannochloris* sp. (Yamaberi *et al.*, 1998), for example. In some algae, increased lipid levels have been observed in biomass grown in a nitrogen sufficient medium after several days of transfer to a

nitrogen free medium (Dempster & Sommerfeld, 1998; Mazzuca Sobczuk & Chisti, 2010). Phosphorus limited conditions have increased the lipid content and lipid productivity in some *Chlorella* sp. (Liang *et al.*, 2013). Compared to controls, increasing the extent of phosphorous limitation has elevated lipid contents in some algae but has decreased the lipid contents of others (Reitan *et al.*, 1994).

Elevated salinity is known to influence lipid accumulation and profiles in numerous marine and freshwater algae (Dempster & Sommerfeld, 1998; Takagi & Yoshida, 2006; Alyabyev *et al.*, 2007; Rao *et al.*, 2007; Gu *et al.*, 2012; Campenni' *et al.*, 2013), although the exact mechanisms for this do not appear to be understood. Whether salt is added at the beginning of the culture, or at some later stage of growth, can also influence lipid accumulation (Takagi & Yoshida, 2006).

Certain micronutrients can influence lipid accumulation. One such nutrient is Fe^{3+}. In *C. vulgaris*, provision of excess $FeCl_3$ has been reported to enhance lipid contents of the biomass by up to 7-fold relative to control (Liu *et al.*, 2008). A maximum lipid level of nearly 57% by dry weight was attained by $FeCl_3$ supplementation at the level of 1.2×10^{-5} M (Liu *et al.*, 2008). In addition, the light level can affect lipid composition in *C. vulgaris* (Nichols, 1965).

The various factors that have been found to affect the lipid content and the lipid composition in different microalgae are summarized in Table 2.1. In conclusion, almost every aspects of a culture environment can be manipulated to impose a physiological stress with the potential to influence lipid accumulation. In practice, certain types of stresses can be imposibly difficult to achieve in a large scale operation. For example, the sunlight level varies naturally and is not amenable to control in most cases. Similarly, a change in temperature of a large volume of culture broth in a reasonable period of time can be expensive and impractical to achieve if thousands of cubic meters of the broth are involved.

Potentially, the productivity of microalgae may be substantially enhanced by genetic engineering. For example, strategies have been identified for molecular level modification of microalgae for enhancing the photosynthetic efficiency (Stephenson *et al.*, 2011) and, therefore, the metabolic productivity. Genetic and metabolic engineering strategies not focussed on improving the photosynthetic efficiency, but other aspects of metabolism provide other opportunities for enhancing the oil productivity of microalgae and modifying the character of the oil produced (Courchesne *et al.*, 2009; Radakovits *et al.*, 2010; Lü *et al.*, 2011; Radakovits *et al.*, 2011; Qin *et al.*, 2012). However, concern has been expressed about the potential ecological risks associated with the use of genetically modified microalgae (Snow & Smith, 2012).

Table 2.1 Various factors that affect lipid content and composition

Factor	Algae	Reference
C/N ratio, aeration	*Chlorella sorokiniana*	Chen & Johns (1991)
Phosphate limitation	*Phaeodactylum tricornutum*, *Chaetoceros* sp., *Isochrysis galbana*, *Pavlova lutheri*, *Nannochloris atomus*, *Tetraselmis* sp., *Gymnodinum* sp.	Reitan *et al.* (1994)
Temperature, growth phase	*Isochrysis galbana*	Zhu *et al.* (1997)
Media composition, light intensity	*Nitzschia communis*	Dempster & Sommerfeld (1998)
Nitrogen concentration	*Phaeodactylum tricornutum*	Alonso *et al.* (2000)
N, P, Si limitation	*Stephanodiscus minutulus*	Lynn *et al.* (2000)
Medium composition	*Isochrysis galbana*	Sánchez *et al.* (2000)
Temperature	*Dunaliella tertiolecta*	Renaud *et al.* (2002)
Salinity	*Dunaliella bardawil*, *Chlorella ellipsoidea*	Gómez *et al.* (2003)
CO_2, light intensity	*Pavlova lutheri*	Carvalho & Malcata (2005)

Table 2.1 Various factors that affect lipid content and composition (Cont.)

Factor	Algae	Reference
Agitation	*Phaeodactylum tricornutum*, *Porphyridium cruentum*	Mazzuca Sobczuk *et al.* (2006)
pH, temperature	*Chlorella protothecoides*	Shi *et al.* (2006)
Salt concentration	*Dunaliella salina*, *Dunaliella bardawil*	Takagi & Yoshida (2006)
Temperature, salinity	*Chlorella ellipsoide, Nannochloris oculata*	Cho *et al.* (2007)
Salinity	*Botryococcus braunii*	Rao *et al.* (2007)
Irradiance, dissolved oxygen concentration, temperature	*Chlorella sorokiniana*	Ugwu *et al.* (2007)
Salinity	*Chlorella vulgaris*, *Chlorella gracilis*	Araújo *et al.* (2008)
Salinity, irradiance	*Dunaliella salina*	Araújo *et al.* (2008)
CO_2	*Chlorella minutissima*	Papazi *et al.* (2008)
Light cycles	*Aphanothece microscopica*	Jacob-Lopes *et al.* (2009)
pH	*Phaeodactylum tricorautum*, *Porphyridium cruentum*	Khalil *et al.* (2010)

Table 2.1 Various factors that affect lipid content and composition (Cont.)

Factor	Algae	Reference
N, P limitation	*Scenedesmus* sp.	Xin *et al.* (2010)
Salinity, nitrogen depletion	*Chlorella saccharophila*	Herrera-Valencia *et al.* (2011)
Light intensity, period of light	*Chlorella minutissima*	Tang *et al.* (2011b)
Temperature	*Scenedesmus* sp.	Xin *et al.* (2011)
Nitrogen starvation	*Chlorella vulgaris, Chlorella zofingiensis, Neochloris oleoabundans, Scenedesmus obliquus*	Breuer *et al*. (2012)
Salinity	*Nannochloropsis oculata*	Gu *et al*. (2012)
Nitrogen source	*Chlorella vulgaris*, *Dunaliella tertiolecta*	(Hulatt *et al.*, 2012)
Nutrition, salinity, luminosity	*Chlorella protothecoides*	Campenni *et al*. (2013)
Nitrogen supplemention	*Tetraselmis subcordiformis*, *Nannochloropsis oculata*, *Pavlova viridis*	Huang *et al.* (2013)

Table 2.1 Various factors that affect lipid content and composition (Cont.)

Factor	Algae	Reference
Temperature, nitrogen starvation	*Chlamydomonas reinhardtii*	James *et al*. (2013)
Nitrogen-stressed condition	*Chlorella* and *Scenedesmus* strains	Ördög *et al*. (2013)

2.6 Culture systems for microalgae

Large-scale systems for phototrophic culture of microalgae can be classified as either open types, or closed. In open systems, the microalgal broth is in contact with the atmosphere. In contrast, in closed culture systems, commonly referred to as photobioreactors, the broth is completely isolated from the external environment.

2.6.1 Open culture systems

Open culture systems are most widely used for large-scale commercial operations (Becker, 1994; Spolaore *et al.*, 2006). They consist of shallow ponds and lagoons (Figure 2.6). The depth of the fluid in a typical open system is in the range of 0.25 to 0.30 m (Becker, 1994; Chisti, 2012). The depth is kept small, as sunlight does not penetrate too deeply in a broth of dark coloured algal cells and a dark volume of fluid is photosynthetically unproductive. In fact, permanently dark regions of a pond or lagoon reduce overall productivity as the biomass residing in these regions consumes stored starch to generate energy for metabolism (Chisti, 2012). Use of unmixed ponds, commonly known as lagoons (Figure 2.6 B) is relatively rare and is viable only for algae that do not settle. For example, the motile marine alga *Dunaliella salina* is commercially cultured in lagoons to produce β-carotene (Figure 2.6 B). This is the only example of the use of unmixed lagoons for large scale algae culture. Mixed ponds, may be circular (Figure 2.6 A), or more often they are shaped like a continuous flow loop, or a racetrack (Figure 2.6 C). Such ponds are known as raceways (Becker, 1994; Chisti, 2007, 2012; Sompech *et al.*, 2012). Raceway ponds are the most widely used system for large scale production of algae. The fluid in the pond is continuously circulated by means of a paddlewheel (Figure 2.6 D) to prevent sedimentation of the biomass

and ensure that the biomass from the deeper darker zones is periodically brought to the better illuminated surface zones.

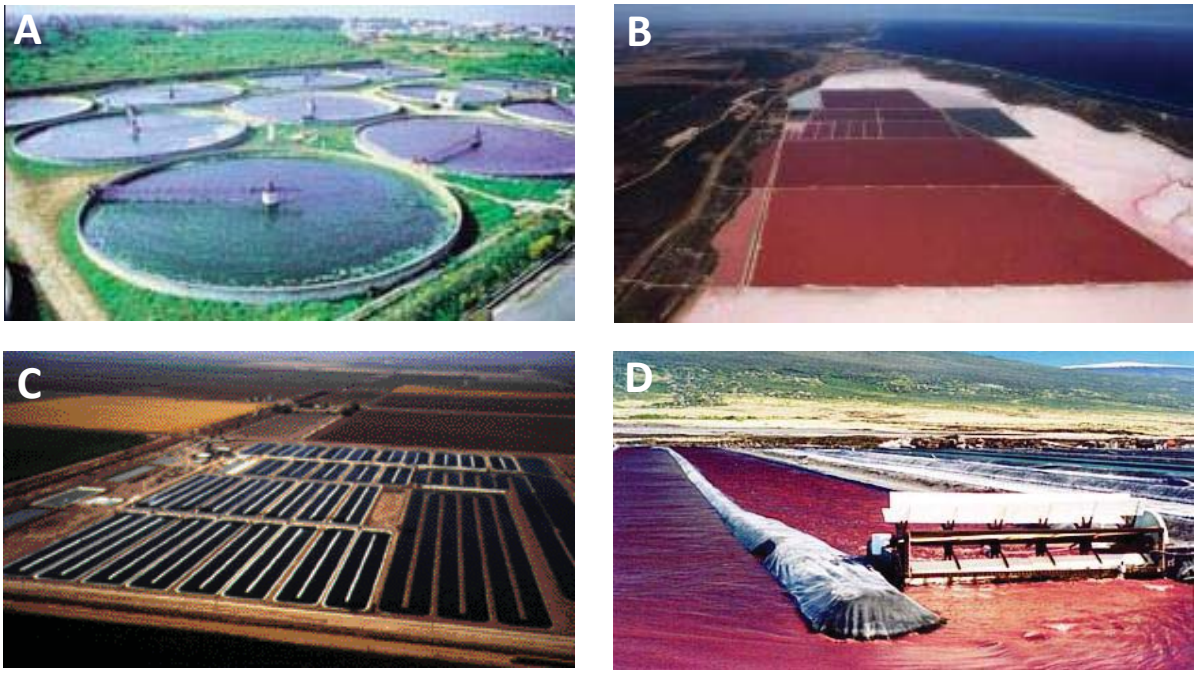

Figure 2.6 Open systems for growing microalgae. (A) Circular ponds of Yaeyama Shokusan Co. Ltd., Japan, for producing *Chlorella* for food and nutraceuticals (www.yaeyamachlorella.com); (B) BASF facility for growing *Dunaliella salina* in static lagoons for the production of β-carotene (Hutt Lagoon, Western Australia, Australia); (C) raceway ponds in California, USA, for producing the cyanobacterium *Spirulina* for nutraceutical purposes (Earthrise® Nutritionals, CA, USA; www.earthrise.com); (D) a paddlewheel for circulating the culture in a raceway pond (Chisti, 2012).

Potentially, ponds shallower than the currently used 0.25 m depth may be desirable to reduce the volume of the dark zone within the fluid. Unfortunately, a pond covering a large area cannot be made much shallower than 0.25 m (Dodd, 1986; Chisti, 2012) because an absolutely flat construction occupying a large surface area is difficult to achieve. Also, the

hydraulics of a pond require a higher depth of the fluid in front of the paddlewheel, where the circulatory flow begins, compared to the depth behind the paddlewheel. This hydrostatic pressure difference generated by the paddlewheel is needed to drive the flow (Dodd, 1986; Chisti, 2012). If the pond is too shallow, a sufficient difference in depth along a long pond would be impossible to achieve.

Open culture systems have other problems: they are susceptible to contamination by unwanted algae, algal pathogens and rotifers that feed on algae (Chisti, 2012); they experience evaporative loss of water in hot dry climates where algae are commonly grown and this requires freshwater to be added to make up the loss on a periodic basis, or the salinity in the pond would rise to an unacceptable level (Chisti, 2012). Often, the freshwater needed to make up for evaporation is in short supply in arid tropical regions. Open ponds are susceptible to factors such as rain and dust storms. Although open ponds are widely used, only a few algae are commercially produced in them. These are algae that either thrive in extremophilic conditions where few other potentially contaminating algae could grow, or they are fast growing algae that would generally outcompete a potential contaminant. For example, *Chlorella vulgaris*, a fast growing freshwater alga is grown in open ponds as it can outgrow most potential contaminants. Similarly, *D. salina* thrives in open ponds because few other algae tolerate the hypersaline conditions that are used to grow it. (*D. salina* culture lagoons are often saturated with salt.) The cyanobacterium *Arthrospira platensis* (previously known as *Spirulina platensis*) is widely cultured in open raceways as it requires highly alkaline growth conditions that do not suit most potential contaminants.

The other major problem with open culture raceways is their low productivity. Typically, a raceway located in the best climatic conditions would achieve a maximum biomass concentration of about 1 g L^{-1}. This is low compared with 4–6 g L^{-1} that can be achieved in some photobioreactors, for example. Similarly, the annual averaged biomass

productivity of a raceway pond does not exceed about 0.025 kg $m^{-2}d^{-1}$, or 82 tons ha^{-1} $year^{-1}$ assuming an operational factor of 90% of the calendar year (Chisti, 2008, 2012). This is about as high as the biomass productivity of sugarcane, a highly productive crop, but much less than the productivity allowed by algal biology (Weyer *et al.*, 2010; Cooney *et al.*, 2011; Chisti, 2012). The main reason for the low productivity of open ponds is their depth (Chisti, 2012): as much as 84% of the culture volume is permanently in the dark once the alga has attained a concentration of around 0.5 kg m^{-3} (Chisti, 2007, 2012). Raceway culture of algae is further reviewed in the literature (Terry & Raymond, 1985; Dodd, 1986; Becker, 1994; Pulz, 2001; Borowitzka, 2005; Spolaore *et al.*, 2006; Chisti, 2012).

In contrast to open ponds, closed photobioreactors tend to be relatively expensive to build and operate, but offer important advantages: a better controlled culture environment; reduced potential for contamination; an ability to grow a diverse range of nonextremophilic algae; a higher biomass productivity due to a high surface-to-volume ratio; and a significantly higher final biomass concentration in the broth compared to a raceway (Chisti, 2007, 2008). A controlled culture environment of a photobioreactor can be used to beneficially affect algal metabolism to obtain products that may not be produced in a less controlled open culture (Moreno *et al.*, 2003).

2.6.2 Closed photobioreactors

Photobioreactors are devices for fully enclosed contained culture of microalgae using natural or artificial light (Molina Grima *et al.*, 1999; Trecidi, 1999). Photobioreactors are widely used for producing many different algae for aquaculture purposes (Becker, 1994; Trecidi, 1999), but tend to be more limited in scale compared to open raceways. Photobioreactors are generally made of either clear glass or plastics that allow penetration of sunlight. The common types of photobioreactors are shown in Figure 2.7. These include the various kinds

of bubble columns (Figure 2.7 A, B) (Sánchez Mirón *et al.*, 1999; Trecidi, 1999; Sánchez Mirón *et al.*, 2000; Sánchez Mirón *et al.*, 2002); bubble columns that have been internally divided by transparent draft tubes or baffles to form airlift photobioreactors (Sánchez Mirón *et al.*, 2000; Sánchez Mirón *et al.*, 2002); tubular photobioreactors (Figure 2.7 D) (Acién Fernández *et al.*, 2001; Molina *et al.*, 2001; Chisti, 2007; Fernández *et al.*, 2012; Wongluang *et al.*, 2013); stirred tanks with transparent walls (Figure 2.7 E) (Huang & Rorrer, 2003; Franco-Lara *et al.*, 2006); and thin rectangular channel configurations (Figure 2.7 F) (Ratchford & Fallowfield, 1992; Trecidi, 1999; Slegers *et al.*, 2011; Quinn *et al.*, 2012). Occasionally, other less conventional configurations may be found. For example, a helical tube configuration in which a flexible transparent plastic tubing is wound around a metal frame in the shape of a coil (Trecidi, 1999; Chisti, 2007) and the culture broth is made to flow through it. Internally illuminated vessels made of steel have been used as photobioreactors (Ogbonna *et al.*, 1996), but have not gained much acceptance in view of their high cost. In fact, steam sterilizable internally illuminated photobioreactors have not been used in any large scale operation.

A bubble column (Figure 2.7 A) is made of a clear glass or plastic tube that typically does not exceed 0.25 m in diameter. The height of the column is generally <4 m (Sánchez Mirón *et al.*, 1999). The column is gently agitated by bubbling with a mixture of air and carbon dioxide. The air has the additional function of removing the oxygen produced by photosynthesis. Temperature is controlled either by installing a metallic water jacket in the bottom region of the column (Sánchez Mirón *et al.*, 1999), or by installation of a cooling coil within the pool of liquid. A production facility based on bubble columns can in principle be scaled up by multiplying the number of columns. The columns would be arranged as trees in a forest (Sánchez Mirón *et al.*, 1999) and spaced to minimize mutual shading. Sometimes, equivalents of a bubble column are obtained by using flexible plastic bags (Becker, 1994;

Trecidi, 1999) supported within metal frames (Figure 2.7 B) or hanging a long sleeve of flexible plastic like an accordion as in Figure 2.7 C. A bubble column configuration of a photobioreactor is sometimes modified to an airlift configuration to improve mixing. This is done by installing a transparent draft-tube, or a straight baffle within the column (Sánchez Mirón *et al.*, 2000; Sánchez Mirón *et al.*, 2002).

Stirred tanks (Figure 2.7 E) are commonly used as photobioreactors to grow algae (Li *et al.*, 2003; Giannelli *et al.*, 2009; Sirisansaneeyakul *et al.*, 2011), but mostly for research purposes and at a scale of less than about 50 L. (Much larger stainless steel fermenters are of course used to grow certain algae heterotrophically in the dark.) Like bubble columns, stirred tanks cannot be scaled up for sunlight driven photosynthetic cultivation, except possibly by increasing the number of individual units. This can be expensive. Nevertheless, for research purposes, laboratory stirred fermenters made of glass are readily used as photobioreactors for highly controlled culture.

Tubular photobioreactors (Molina Grima *et al.*, 1999; Trecidi, 1999; Acién Fernández *et al.*, 2001; Molina *et al.*, 2001) are one of the most commonly used types of photobioreactors. Typically, the culture broth from a reservoir is recirculated through one continuous looped transparent tube (Figure 2.8), or multiple parallel tubes (Figure 2.7 D), back to the reservoir. The recirculation may be achieved either by an airlift pump (Figure 2.8) or a mechanical pump. The array of tubes constitutes the solar collector, or solar loop, where most of the sunlight is captured. Each tube in the solar collector is generally less than 0.1 m in diameter, as increasing the diameter reduces the surface-to-volume ratio and hence the light available for photosynthesis. (The surface-to-volume ratio of a tube is $4/d$ where d is tube diameter.) Tubes much smaller than 0.1 m in diameter are impractical to use in a large photobioreactor as the pressure drop for achieving circulation increases with a reducing diameter and the flow velocity needed to obtain turbulent flow increases.

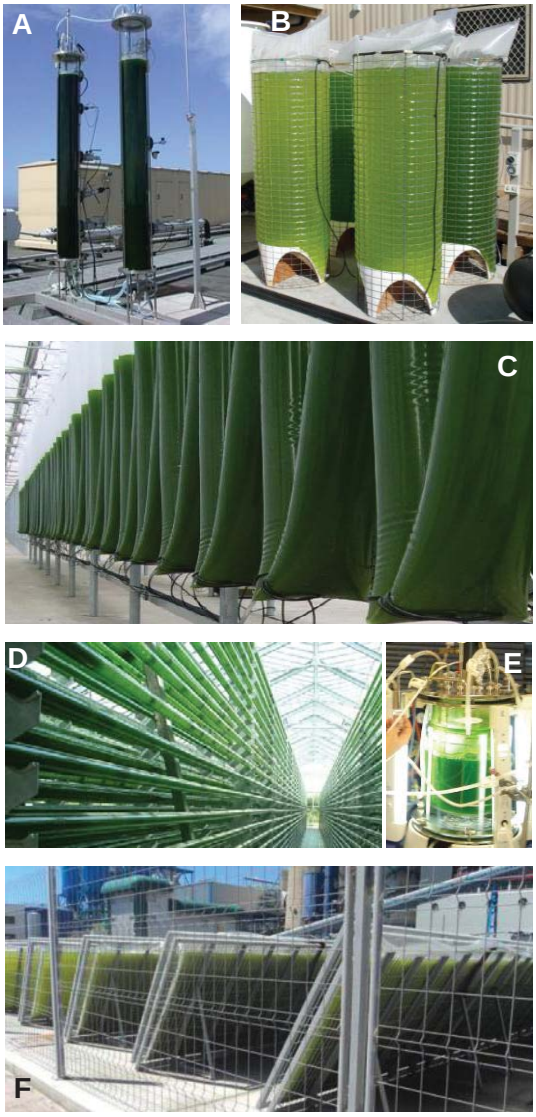

Figure 2.7 Closed systems for growing microalgae. (A) Bubble columns (www.bioenergy-noe.org); (B) bubble column like plastic bags at South Australia Research and Development Institute (SARDI), Henley Beach, Australia (www.sardi.sa.gov.au); (C) bubble column like continuous sleeve of flexible plastic (Novagreen GmbH, Germany); (D) a tubular photobioreactor facility for production of *Chlorella* for food and nutraceutical applications (Roquette Klötze GmbH & Co. KG, Klötze, Germany; www.algomed.de); (E) a stirred tank photobioreactor at Massey University; (F) rectangular channel flexible-walled photobioreactors at the electricity company Endesa, Spain (www.endesa.com).

The tubes of a solar collector may be placed flat on the ground (Figure 2.8), or they may be arranged like multiple parallel fences (Figure 2.7 D) in attempts to accommodate a large number of tubes within a given area. The spacing between adjacent 'fences' is determined by the height of the fence as the adjacent fences must be spaced to minimize mutual shading during the peak sunlight period (Sánchez Mirón *et al.*, 1999).

Thin channel flat plate bioreactors (Hu *et al.*, 1998; Trecidi, 1999; Sierra *et al.*, 2008; Slegers *et al.*, 2011; Bergmann *et al.*, 2013) consist of parallel flat plates made of a transparent material that are spaced 0.10 to 0.15 m apart to form a rectangular channel. The objective is to maximize the surface area relative to volume so that more light can be captured for a given volume of the broth. Thin channel photobioreactors produced using flexible plastic sheets supported in a metal frame (Figure 2.7 F) have been developed to reduce the cost associated with using ridged transparent materials. Thin channel photobioreactors may be mixed simply by sparging with a gas, as in a bubble column, or they may have internal baffles for mixing by an airlift action produced via gas injection. Disposable flat panel airlift photobioreactors have been described (Bergmann *et al.*, 2013). Bubble columns, tubular arrays and thin channels may be oriented at various angles relative to the horizon in attempts to maximize the capture of sunlight.

For production of fuels, only operation with natural sunlight is generally relevant (Chisti, 2007, 2008); nevertheless, for research photobioreactors can be operated indoors using artificial illumination regimens that mimic natural light. In a well-designed algal culture system, light is the sole factor that controls growth as the supply of the other nutrients and carbon dioxide are managed to ensure sufficiency. Unlike the open culture systems, the culture conditions in a photobioreactor are generally well controlled. The temperature is controlled by passing the culture broth through some sort of a heat exchanger.

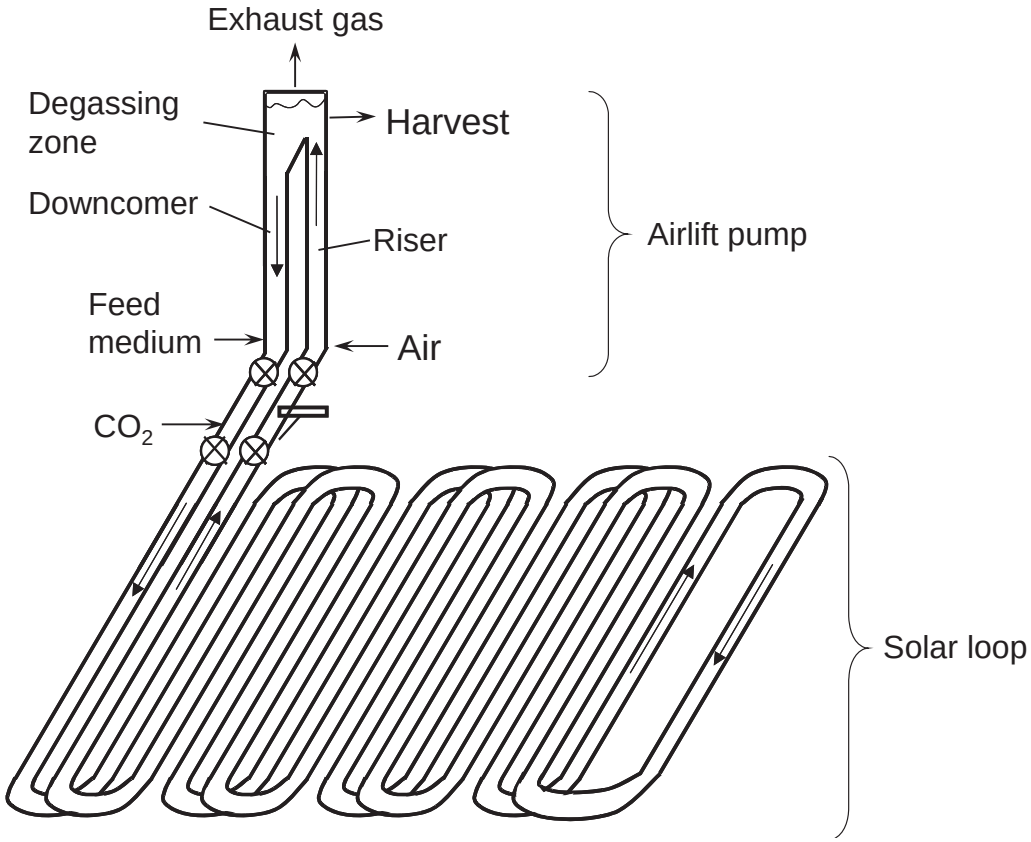

Figure 2.8 A tubular photobioreactor with a single continuous looped tube. The air sparged at the bottom of the riser tube of the airlift pump drives the circulatory flow. The air disengages from the broth in the degassing zone and the gas-free broth returns to the solar loop via the downcomer. The fresh feed medium and carbon dioxide are injected close to the entrance of the fluid in the solar loop. The broth volume in the bioreactor does not change as the rate of harvesting of the broth equals the rate of feeding. The oxygen rich exhaust gas leaves from the top of the airlift pump. The solar loop is immersed in a pool of cooling water to control temperature. Adapted from Acién Fernández *et al.* (2001) and Molina *et al.* (2001).

Outdoor photobioreactors inevitably require temperature control, or they would quickly overheat in intense sunlight (Sánchez Mirón *et al.*, 1999). This is because they generally have a large surface area to capture sunlight compared to the volume of the broth and are not cooled by evaporation as happens in an open culture system. The dissolved oxygen level in a photobioreactor is typically controlled by sparging with air. The oxygen produced by photosynthesis transfers from the broth to the gas phase and leaves the photobioreactor in the exhaust (Sánchez Mirón *et al.*, 1999). Dissolved oxygen levels that are too high (e.g. 300–400% of air saturation; (Acién Fernández *et al.*, 2001; Chisti, 2012) are toxic and suppress photosynthesis. Oxygen generation rate in a photobioreactor can be much higher than in an open culture system as typically a photobioreactor has a higher biomass concentration (e.g. 4–6 g L^{-1}) than an open pond and captures more light per unit volume. The culture is prevented from being carbon limited, by bubbling carbon dioxide typically in response to a signal from a pH sensor (Molina Grima *et al.*, 1999).

During daylight, the outdoor photobioreactors commonly operate as constant volume continuous cultures which are continuously fed with the fresh medium (Molina Grima *et al.*, 1999). The volume in the reactor is kept constant by harvesting the culture broth at the same rate at which it is fed. Feeding and harvest cease at night to prevent washout, as biomass does not grow during the night. Dilution rate is often controlled to control the biomass concentration in the photobioreactor.

Flat panel photobioreactors have been used to grow many algae (Hu *et al.*, 1998; Slegers *et al.*, 2011). Tubular photobioreactors have been used quite widely (Molina Grima *et al.*, 1999; Acién Fernández *et al.*, 2001; Scragg *et al.*, 2002; Ugwu & Aoyagi, 2008; Sasi *et al.*, 2011). Use of bubble columns is common (Sánchez Mirón *et al.*, 1999; Sánchez Mirón *et al.*, 2000; Sánchez Mirón *et al.*, 2002; Sánchez Mirón *et al.*, 2003; Kojima & Lin, 2004), but mostly in small scale operations. *C. vulgaris* has generally been found to be easy to grow

at least in freshwater based media. It has been grown in tubular photobioreactors (Scragg *et al.*, 2002; Sasi *et al.*, 2011), bubble columns (Najafabady *et al.*, 2010; Feng *et al.*, 2011; Rasoul-Amini *et al.*, 2011; Yeh & Chang, 2011; Hulatt *et al.*, 2012) and stirred tanks (Ratchford & Fallowfield, 1992; Illman *et al.*, 2000; Sirisansaneeyakul *et al.*, 2011).

The different types of photobioreactors and the principles of their operation are further discussed in the literature (Molina Grima *et al.*, 1999; Sánchez Mirón *et al.*, 1999; Trecidi, 1999; Acién Fernández *et al.*, 2001; Molina *et al.*, 2001; Pulz, 2001; Janssen *et al.*, 2003; Carvalho *et al.*, 2006; Vasumathi *et al.*, 2012; Bergmann *et al.*, 2013; Wongluang *et al.*, 2013).

2.7 Objectives

The key objectives of this study were as follows:

1. To identify through preliminary screening of several readily accessible microalgae, an alga that would grow easily, rapidly and stably to produce a biomass with a high level (≥20% by weight) of algal crude oil and a high productivity (≥20 mg L^{-1} d^{-1}) of the oil under photoautotrophic growth on artificial light to mimic sunlight. The other constraints were: (a) the need to use an inexpensive seawater-based medium; (b) the requirement for an alga that was safe for possible future commercial use in oil production (some algae are known to produce potent toxins (Garcia Camacho *et al.*, 2007)); (c) a need to limit the choice to either a novel species that had not been previously investigated in detail, or to one that had not been previously studied in seawater media; and (d) the requirement for a consistently good growth in relatively warm water (25–30 °C) as would be encountered in an outdoor algae culture system located in a tropical region with a high level of irradiance year round.

2. A detailed characterization of growth and crude oil production of a preferred algal species identified in Objective 1. Specifically, a characterization of the following at the normal culture temperature and with a sufficiency of carbon dioxide: (a) the specific growth rate; (b) the biomass and lipid yields on macronutrients; (c) the lipid level in the biomass; (d) the lipid and biomass productivities; (e) the biomass loss in the dark due to respiration; and (f) the total energy content of the biomass.
3. An assessment of operational strategies (batch and continuous culture operations) and nitrogen limitation on some of the key productivity parameters noted under Objective 2, in two types of culture systems, a tubular photobioreactor and a stirred tank photobioreactor, as potential devices for biomass production.

4. Although only the algal crude oil was of interest as a potential feedstock for making biofuels, a preliminary characterization of the nature of the oils was carried out for some samples.

The aim was to establish for the target alga, the maximum attainable oil productivity and oil content in the biomass in phototrophic growth in various regimens of operation and nitrogen limitation, always under carbon sufficiency and at the normal culture temperature.

Chapter 3

Materials and Methods

3.1 General methodology

Six microalgae were screened for rapid growth and lipid production capabilities in seawater-based media in 1–2 L culture bottles (Duran bottles) under carbon dioxide supplemented conditions. A selection of both freshwater and marine algae were used in the screening as some freshwater microalgae can grow in seawater and because of the stressed conditions actually produce more lipids than they would in normal freshwater growth. One alga that demonstrated rapid growth and a high lipid productivity (total lipids), was focused on for more detailed studies in a 7.5 L stirred tank photobioreactor and a pilot scale (~80 L) purpose-built tubular photobioreactor. Growth and lipid production were characterized under various operational conditions (e.g. irradiance, culture media compositions). Effect of nitrogen limitation on lipid and biomass productivity was assessed. Batch and continuous operations at various dilution rates were characterized. In selected cases, the composition of the lipids was characterized. The energy content of the biomass produced under various conditions were determined in terms of the calorific value. The objectives were a general culture characterization, identification of the operational factors that might influence lipid productivity and an attempt to maximize lipid productivity.

The relevant microalgae, equipment and the measurement methods are discussed in detail in the following sections.

3.2 Microalgae

Six microalgae were preliminarily assessed for growth in seawater-based media. These were the following freshwater microalgae:

Chlorella vulgaris (green alga, Chlorophyta);

Choricystis minor (green alga, Chlorophyta);

Neochloris sp. (green alga, Chlorophyta);

Pseudococcomyxa simplex (green alga, Chlorophyta);

Scenedesmus sp. (green alga, Chlorophyta);

and an unidentified green marine alga MGA-1-NZ.

MGA-1-NZ and *Scenedesmus* sp. had been isolated by Dr. T. Mazzuca Sobczuk at Massey University, New Zealand. The other algae had been purchased from Landcare Research, Lincoln, New Zealand.

The identity of *C. vulgaris* had been confirmed by *rbc*L gene sequencing (Dr. P. Novis, Landcare Research, Lincoln, New Zealand, personal communication; 19 November 2007). The plastid-encoded single copy *rbcL* gene is the most common gene used to provide sequence data for phylogenetic analyses of plants (Donoghue *et al.*, 1992; Chase *et al.*, 1993; Gielly & Taberlet, 1994). The *rbcL* gene codes for the large subunit of ribulose-1,5-bisphosphate carboxylase/oxygenase (RUBISCO or RuBPCase) (Gielly & Taberlet, 1994). For the other microalgae, the identity was as determined by the relevant phycological culture collections.

Cultures were maintained on agar slants and Petri dishes. BG11 medium (Section 3.3.1) made with distilled water was used for the freshwater algae. The same medium made with artificial seawater (40 g L^{-1} sea salt in distilled water; Section 3.3.2) was used for the marine alga. Freshly inoculated Petri dishes were grown at room temperature (22–25 °C) for 10–15 days, under daylight fluorescent light (15–20 $\mu mol \cdot m^{-2} s^{-1}$ at the surface of the dishes)

and stored at 4 °C (2–8 μmol· $m^{-2}s^{-1}$ light at the surface of the dishes) until needed. Algae were subcultured every 6–8 weeks. Photographs of the six algae are shown in Figures 3.1-3.6.

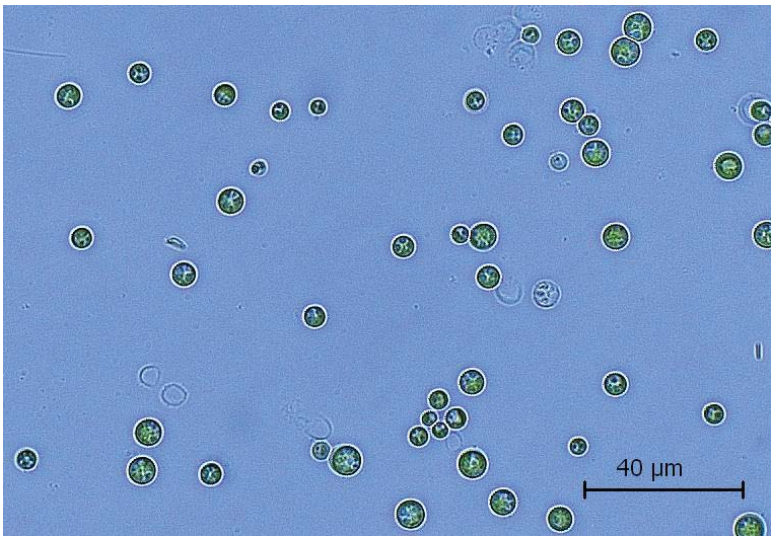

Figure 3.1 *Chlorella vulgaris* in BG-11 made in freshwater.

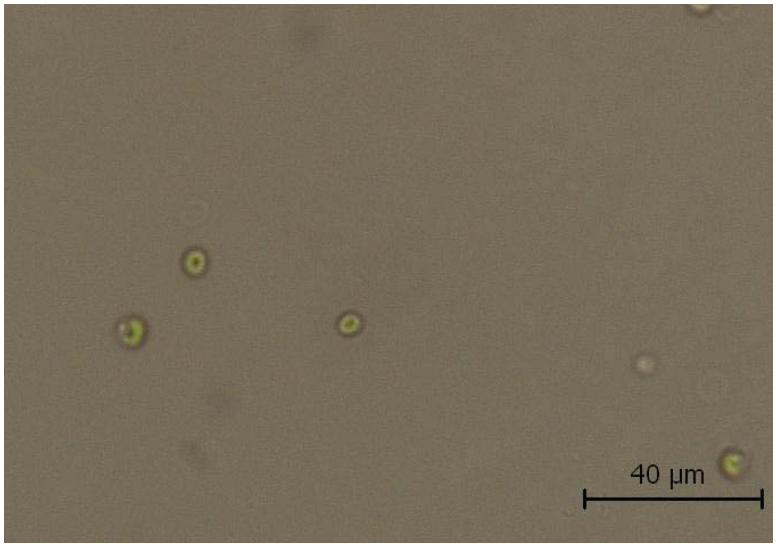

Figure 3.2 *Choricystis minor* in BG-11 made in freshwater.

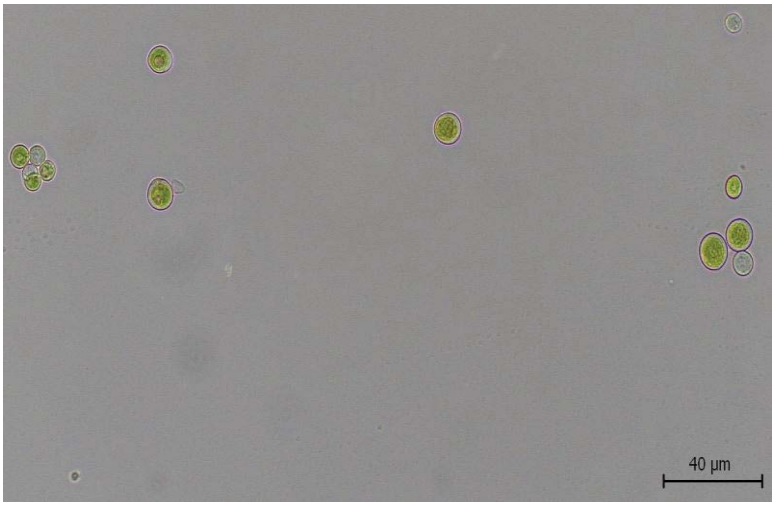

Figure 3.3 *Neochloris* sp. in BG-11 made in freshwater.

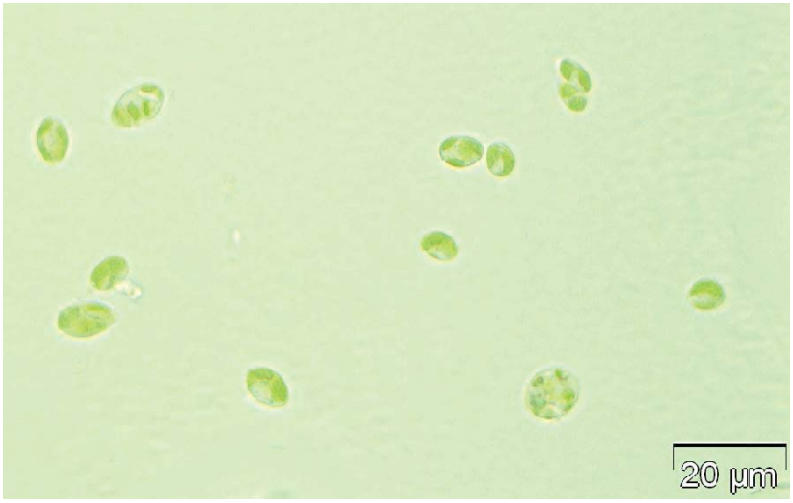

Figure 3.4 *Pseudococcomyxa simplex* in BG-11 made in freshwater.

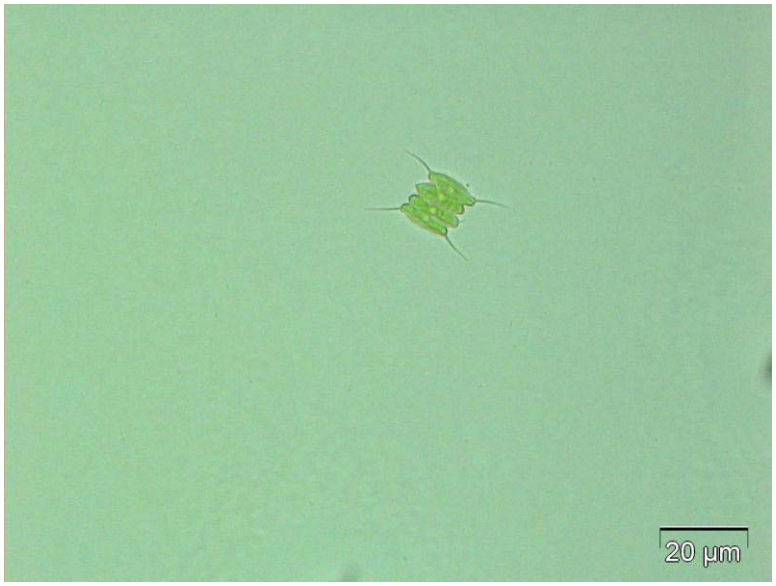

Figure 3.5 *Scenedesmus* sp. in BG-11 made in freshwater.

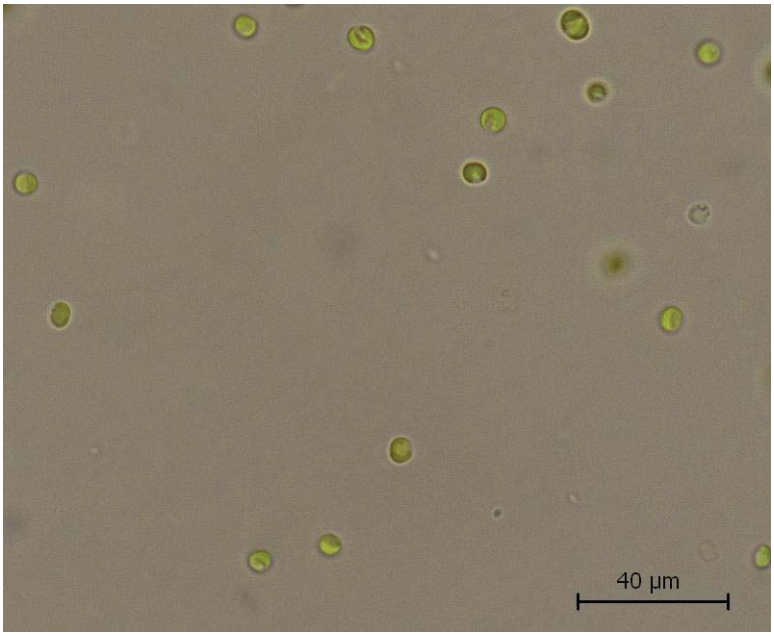

Figure 3.6 MGA-1-NZ in BG-11 made in seawater.

3.3 Growth media

The BG11 medium (Section 3.3.1) was used as the basal medium. All media used in maintenance of cultures and preparation of inocula and Duran bottle (borosilicate glass 3.3, LabSerV, Biolab, Auckland, New Zealand) cultures and stirred tank photobioreactor cultures were sterilized by autoclaving (121 °C, 15 min).

In view of the large volumes (70–80 L) involved, autoclaving of the water used in the tubular photobioreactor operations was not feasible. For use in the tubular photobioreactor, all media components except tap water were autoclaved (121 °C, 15 min) and added to nonsterile tap water from the laboratory potable water supply. The pH of the final medium was adjusted to 7.5 by adding 1 M HCl.

3.3.1 BG 11 culture medium

Stock solutions 1–4 were prepared separately by mixing the components specified in Tables 3.1–3.4. These solutions were autoclaved (121 °C, 15 min) separately, cooled, and kept at 4 °C until needed. For making BG11, specified volumes of the Stocks 1–4 and the specified salts were mixed in the following sequence:

- Stock 1 (10 mL)
- Stock 2 (10 mL)
- Stock 3 (10 mL)
- Na_2CO_3 (0.02 g)
- Stock 4 (1 mL)
- $NaNO_3$ (1.5 g)

and made up with distilled water (or other specified water) to 1 liter. (For solid media, 10 g agar (Difco™, Agar Noble, France) was added prior to making up with distilled water.) The

pH was adjusted to 7.5 using 1 M HCl. For solid media, the vitamins in Table 3.5 were added.

Table 3.1 BG11 stock 1

Component	Quantity
$CaCl_2 \cdot 2H_2O$, LabServ, Biolab (Australia) Ltd.	3.6 g
Citric acid monohydrate ($C_6H_8O_7$), LabServ, Biolab (Australia) Ltd.	0.6 g
Ferric ammonium citrate ($C_6H_{11}FeNO_7 \cdot H_2O$), BDH GPR, BDH Limited, Poole, England	0.6 g
Na_2EDTA ($C_{10}H_{14}N_2Na_2O_8,2H_2O$), BDH GPR, BDH Limited, Poole, England	0.1 g
Distilled water	1.0 L

Table 3.2 BG11 stock 2

Component	Quantity
$MgSO_4 \cdot 7H_2O$, LabServ, Biolab (Australia) Ltd.	7.5 g
Distilled water	1.0 L

Table 3.3 BG11 stock 3

Component	Quantity
$K_2HPO_4 \cdot 3H_2O$, AnalaR, BDH, VWR International Ltd., England	4.0 g
Distilled water	1.0 L

Table 3.4 BG11 stock 4

Component	Quantity
H_3BO_3, AnalaR, BDH Laboratory Supplies, England	2.86 g
$MnCl_2 \cdot 4H_2O$, AnaR, The British Drug Houses Ltd., England	1.81 g
$ZnSO_4 \cdot 7H_2O$, AnalaR, BDH, VWR International Ltd., England	0.222 g
$NaMoO_4 \cdot 2H_2O$, AnalaR, BDH Chemicals Ltd., Poole, England	0.390 g
$CuSO_4 \cdot 5H_2O$, MERCK, Merck KGaH, Germany	0.079 g
$CoCl_2 \cdot 6H_2O$, AnalaR, BDH Chemicals Ltd., Poole, England	0.050 g
Distilled water	1.0 L

Table 3.5 Vitamins solution

Component	Quantity
Thiamine-HCL (vitamin B1), Sigma-Aldrich, USA	0.1 g
Biotin (vitamin H), Sigma-Aldrich, USA	0.0005 g
Cyanocobalamin (vitamin B12), Sigma-Aldrich, USA	0.0005 g
Distilled water	1.0 L

3.3.2 Seawater

Artificial seawater was prepared by dissolving 40 g L^{-1} of sea salt in distilled water or tap water. The sea salt used was either Sigma product no. S9883 (Sigma Chemical Company, St Louis, MO, USA) or natural unrefined Southern Pacific Ocean salt (Pacific Natural Fine Salt; Dominion Salt Ltd., Marlborough, New Zealand). A 40 g L^{-1} solution of sea salt had a calculated salinity of 38.5 ppt. The exact salinity of the media was measured using a

conductivity/salinity meter (EcoSense® EC300; YSI Inc., Yellow Springs, OH, USA) that had been calibrated with a 1.0 molal aqueous solution of KCl (conductivity at 25 °C = 108,621 μS cm^{-1}; Pratt et al., 2001; Shreiner and Pratt, 2004).

Seawater was sterilized by autoclaving (121 °C, 15 min) for use in culture maintenance, inoculum development, Duran bottle cultures and stirred tank photobioreactor studies. Seawater for the tubular photobioreactor was prepared concentrated in 10 L batches and filter sterilized (0.22 μm membrane filter; Millipak-60, catalog number MPHL10CA3, Millipore Corporation, Billerica, MA, USA) to remove any marine microorganisms that may be present in the natural seasalt. Nonsterile potable tap water was then added to the desired concentration.

3.4 Inoculum preparation and Duran bottle cultures

All culture studies carried out at a scale of ≤2 L were conducted in aseptically grown Duran bottles (1 or 2 L total volume per bottle) at 22–25 °C and 126-173 μE· $m^{-2}s^{-1}$ daylight fluorescent light level at the surface of the bottles. The bottles were bubbled (2–5 L min^{-1} at NTP, normal temperature and pressure) with air mixed with 5% (v/v) carbon dioxide. The inlet and exhaust gases were filter sterilized (0.2 μm Teflon membrane filter; Midisart® 2000; Sartorius AG, Goettingen, Germany). The gas mixture used to sparge the bottles was pre-humidified by passing through deionized water at room temperature. The bottles were inoculated from shake flasks that had been grown for 7-days. (The shake flask inocula were started from agar slants or Petri dishes.) The volume of the inoculum was generally 20% (v/v) of the initial volume of the inoculated broth in the bottle. The bottles were sampled immediately after inoculation and subsequently once or twice daily, depending on the experiment. A typical culture arrangement is shown in Figure 3.7.

Figure 3.7 A typical set up for algae growth in gas sparged culture bottles.

3.5 Tubular photobioreactor

A tubular photobioreactor was built by Massey University technical staff specifically for this project (Figures 3.8–3.10). The reactor had a working volume of 75–78 L. It consisted of a vertical bubble column (152 mm internal diameter, 6.3 mm wall thickness, 1.5 m tall) made of clear Plexiglas (the 'degassing column' in Figure 3.8) as the broth reservoir and a serpentine continuous loop of borosilicate glass as the light harvester ('tubular loop' in Figure 3.8). The bubble column had a stainless steel bottom zone that was supported on a stand bolted to the floor. The steel zone included a stainless steel cooling coil, a carbon dioxide sparging frit (200 μm; GKN Filters GmbH, Radevormwald, Germany), a perforated pipe ring sparger (12 holes, 1.5 mm in diameter) for air, and a drain valve. On its side, the bubble column had a valve for sampling. The top of the bubble column was covered by a bolted-on PVC headplate that had ports for a dissolved oxygen sensor, a pH sensor, gas exhaust, addition of media components, feed and harvest. Near the top of the bubble column,

close to the operating level of the culture broth, a connection was provided for the broth returning from the light harvest loop (Figure 3.8). Close to the top of the bubble column, a Pt100 temperature sensor (Omega Engineering Inc., Stamford, CT, USA; platinum RTD Sensor PRTF19-2-100-1/8-6-E) was installed ('temperature sensor' in Figure 3.8).

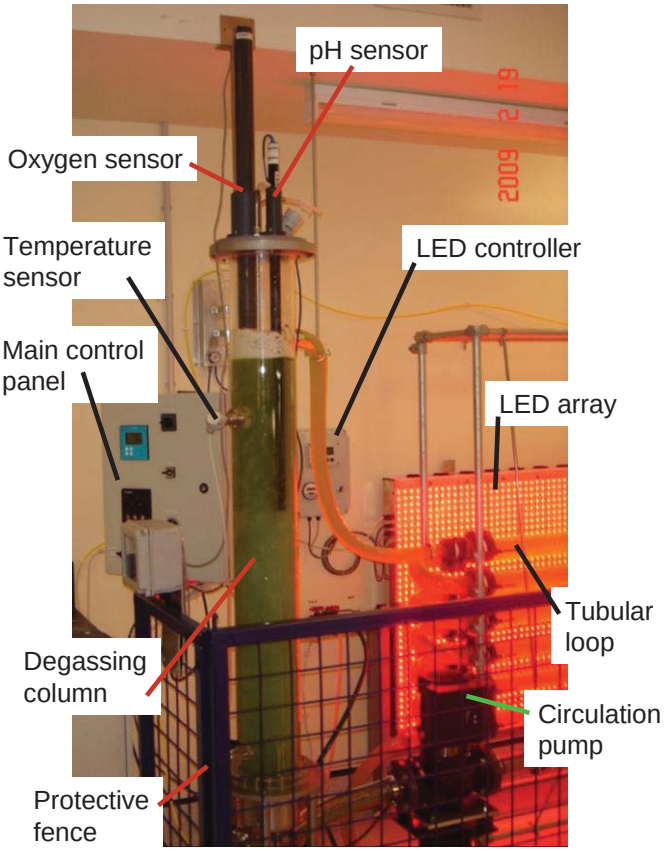

Figure 3.8 Tubular photobioreactor.

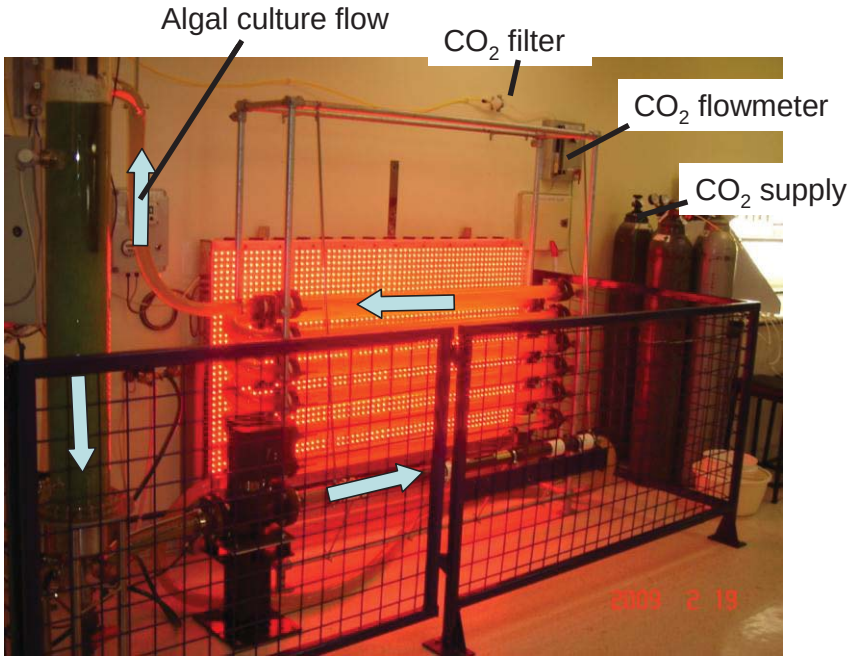

Figure 3.9 Broth recirculation in the tubular loop photobioreactor.

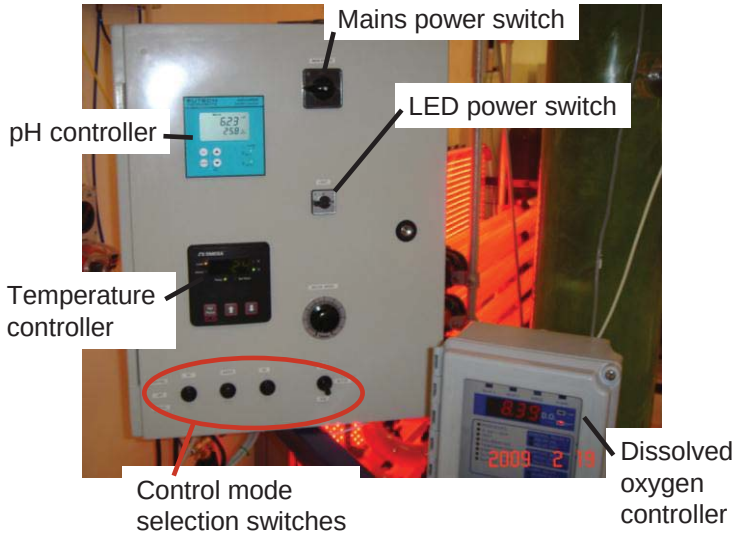

Figure 3.10 Main control panel of the tubular photobioreactor.

The light capture loop was constructed of QVF borosilicate glass 3.3 fittings (QVF Engineering GmbH, Mainz, Germany). At thicknesses in the range of 2–5 mm, borosilicate glass 3.3 has negligible absorption (≤10%) of light in the visible range (i.e. 400–800 nm) (QVF, 2002), or photosynthetically active range (i.e. 400–700 nm). All glass tubes were horizontal to the ground (Figure 3.8 and Figure 3.9). The tubes were arranged in two parallel arrays, mounted perpendicular to the ground (Figure 3.9). Each array had six tubes (50 mm internal diameter, 1500 mm long). The wall-to-wall distance between adjacent tubes in an array was the same as the outer diameter of a tube. The two parallel arrays were offset vertically by a distance equal to the outer diameter of the solar tubes. Thus, each tube was fully exposed to light coming horizontally from a wall-mounted panel located parallel to the tubular array ('LED array' in Figure 3.8). The open ends of the tubes were connected using U-bends of borosilicate glass to obtain a single continuous serpentine flow channel. The various joints were sealed with PTFE (poly (tetrafluoroethylene), or Teflon) gaskets that were flush with the internal walls and GMP-compliant (GMP – good manufacturing practices).

The light collection loop of the photobioreactor was placed parallel to a wall ~0.3 m from the face of a light emission diode (LED) array that was supported on the said wall (Figure 3.9). The lighting array illuminated the entire projected area of the light collection loop with monochromatic light of 660 nm. The LED array (Figure 3.9) could be adjusted to provide a photosynthetically active radiation (PAR) level of up to ~1540 $\mu mol \cdot m^{-2} s^{-1}$, or nearly full tropical sunlight.

The flow entered the light collector loop at the bottom and exited at the top (Figure 3.9). The bottom exit of the bubble column was connected to the entrance of the glass loop via a centrifugal pump ('circulation pump' in Figure 3.8) and paddlewheel flow meter. The flow exiting the top of the light collection loop was returned to the bubble column via a clear

polymer tubing (Figure 3.9). The recirculation flow rate through the light loop was set at the pump and measured by the flow meter.

Temperature, dissolved oxygen concentration and pH were controlled in the bubble column. The main control panel is shown in Figure 3.10. Temperature was controlled automatically (Omega Engineering Inc., Stamford, CT, USA; 1/4 DIN Compact Temperature Controller model CN2110-R20) by on/off switching (solenoid valve) of the mains cooling water. The water flowed through the cooling coil at a preset rate. The temperature measured by the above mentioned sensor provided the control information. Only a cooling capability was provided in the photobioreactor to compensate for the heat absorbed in the light capture loop. The photobioreactor was placed within a temperature controlled room.

Concentration of dissolved oxygen (DO) was controlled automatically using the signal from the DO sensor (Omega Engineering Inc., Stamford, CT, USA; DOE-601 dissolved oxygen sensor, DOE-601-SC sensor cartridge, and DOE-600-SMK submersion mounting kit) ('Oxygen Sensor' in Figure 3.8). The controller used was the model DOCN602 (Omega Engineering Inc., Stamford, CT, USA). Control was achieved by sparging air at a preset flow rate of 5 L min^{-1} through the bubble column to strip out the oxygen produced by photosynthesis. The air sparging was switched on (solenoid valve) once the measured oxygen concentration rose above the setpoint concentration. Air injected into the photobioreactor had passed through a humidifier and been prefiltered through a sterilizing grade filter (0.2 μm Acropak 1500 SuPar® membrane; Pall Corporation, Portsmouth, UK). Prehumidification eliminated evaporative loss of water from the photobioreactor.

pH was controlled by injecting carbon dioxide in response to a signal from a pH sensor (Cole-Parmer 3-ft submersible double-junction pH electrode incorporating a

temperature sensor (100 ohm RTD) for automatic temperature compensation; KH-27001-83) ('pH sensor' in Figure 3.8). Carbon dioxide was injected at a preset flow rate of 1 L min^{-1} whenever the pH value rose above a specified value and injection was continued until the set point pH had been re-established. Control of pH ensured that carbon dioxide was provided as needed so that the rate of photosynthesis would not be limited by a lack of carbon dioxide. An on/off controller was used (Eutech Instruments 1/4-DIN pH 800 on/off controller KH-56705-05; Cole-Parmer Corp., Vernon Hills, IL, USA) to switch on the carbon dioxide supply. Carbon dioxide injected into the photobioreactor had passed through a sterilizing grade filter (0.2 μm Acropak 800 PTFE membrane; Pall Corporation, Portsmouth, UK). The pH sensor was calibrated every 6-months, or prior to commencing a continuous culture run, using standard buffers of pH 7.0 and 4.0.

The photobioreactor that had been filled with the medium was inoculated using cultures that had been grown in Duran bottles (Section 3.4) to a density of around 2–3 g L^{-1}. The volume of the inoculum was generally 10% (v/v) of the initial working volume of the photobioreactor.

3.6 Stirred tank photobioreactor

3.6.1 Batch culture

The 7.5 L stirred tank bioreactor (BIOFLO 110, New Brunswick Scientific, John Morris Scientific Ltd., NZ) with a working volume of 4 L was used. The reactor vessel was made of borosilicate glass and was jacketed. It had an internal diameter of 0.18 m. The vessel had 4 vertical baffles (19 mm width) placed equidistance around its periphery. Two identical 6-bladed Rushton disc turbine agitators, 59.6 mm in diameter, were used for mixing at an agitation speed of 200 rpm. The agitators were mounted on a central shaft with a vertical

distance of 0.15 m between them. The lower agitator was positioned 59.6 mm above the base of the bioreactor vessel. The bioreactor was bubbled with 5% (vol/vol) mixture of carbon dioxide in air at a flow rate of 1 L min^{-1}. The gas sparger consisted of a single hole with a diameter of 4.3 mm, located directly below the lower agitator, about 30 mm above the base of the vessel. The pH and the concentration of dissolved oxygen (DO) in the broth were monitored by using a pre-calibrated Ingold gel-filled pH electrode (model no. 465-35-SC-P-K9/270/9848, Mettler-Toledo) and a pre-calibrated DO electrode (model In Pro 6800 sensor 12/25 mm, Mettler-Toledo), respectively, but both were not controlled.

The temperature was monitored by using a temperature probe and automatically controlled at 25 °C by a solenoid valve that controlled the flow of cold water from a re-circulating cooler (FL300, Julabo, Germany). A heater plate under the reactor was automatically used to raise the temperature if it fell below the set point.

The bioreactor was continuously illuminated by using either 16 vertical fluorescent lamps (NEC FL10EX-N-HG, TRI-PHOSPHOR T5, 26×330 mm, 10 W each) or two sets of adjustable-intensity light emission diodes (LED, two 90 W lamps) that were placed around the bioreactor (Figure 3.11). The bioreactor was operated aseptically.

3.6.2 Continuous culture

The bioreactor was assembled for the batch culture (Section 3.6.1) and operated as a batch for the first 29-40 days. The operation was then switched to a constant volume continuous culture. The feed medium was pumped into the reactor at a specified dilution rate (Masterflex® Tygon® LFL L/S14 tubing; Cole-Palmer, USA). The harvest overflow peristaltic pump was set to operate at a higher flow rate than the feed pump. The harvest was collected in a chilled (4°C) effluent bottle. The bioreactor illuminated with fluorescent lights and arranged for continuous flow operation is shown in Figure 3.12.

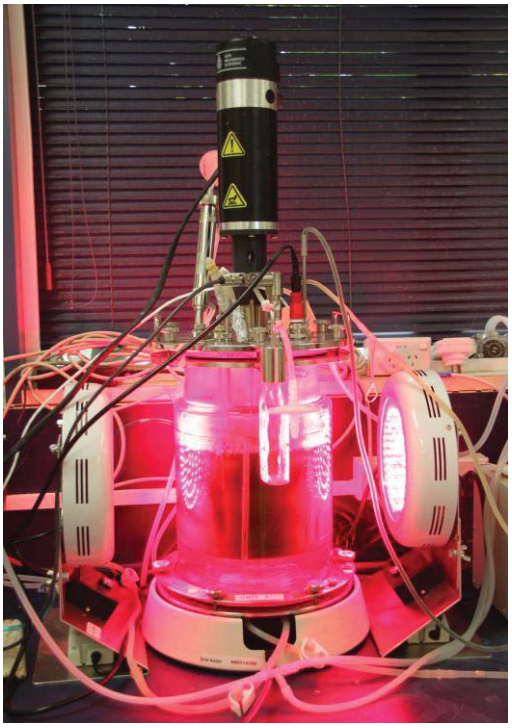

Figure 3.11 A stirred tank photobioreactor illuminated using LED lamps.

Figure 3.12 Continuous culture in a stirred tank photobioreactor.

3.7 A 10 L stirred photobioreactor (Corning photobioreactor)

In some studies, a 10 L stirred photobioreactor (ProCulture spinner flask with 4 vertical sideports; Corning Incorporated, USA) with a working volume of 8 L was used. The reactor vessel had 4 vertical baffles and was made of PYREX® glass. It had an internal diameter of 0.19 m. The depth of broth (unaerated) at working volume was 0.2 m. A 3-bladed impeller, 56 mm in diameter, was used for mixing at an agitation speed of 200 rpm. The agitator was mounted on a central shaft with a vertical distance of 0.26 m from the underside of the cover. The shaft was connected to a motor (model 350 CE: 230 VAC, 50 Hz, Arrow Engineering Co. Inc, USA). The distance between the agitator and the base of the bioreactor flask was 50 mm. The bioreactor was bubbled with 5% (vol/vol) mixture of carbon dioxide in air at a flow rate of 3 L min^{-1} through a single hole sparger (4 mm diameter hole). The pH and the concentration of dissolved oxygen (DO) in the broth were not controlled but the pH was monitored by using a pH meter with silicon chip sensor (model IQ 125; IQ Scientific Instruments, Inc, USA).

The temperature was automatically controlled at 25 °C by re-circulating 25 °C water from a cooler (FE500, Julabo, Germany) through a stainless steel coil located in the vessel.

The bioreactor was continuously illuminated by using 16 vertical fluorescent lamps (NEC FL10EX-N-HG, TRI-PHOSPHOR T5, 26×330 mm, 10 W each) that were placed around the bioreactor (Figure 3.13). The irradiance level at the surface of the bioreactor was 484 μmol $m^{-2}s^{-1}$. The bioreactor was operated aseptically.

Figure 3.13 The 10 L Corning stirred photobioreactor.

3.8 Biomass separation by centrifugation

3.8.1 Batch centrifugation

The culture broth was transferred to a centrifuge bottle. The bottles (including lids) were balanced to have the same weight. The bottles were then centrifuged at 9280-g for 10 min. A 4 °C refrigerated centrifuge (CR22GII, Hitachi, Japan) was used. The cell paste was washed by resuspending in distilled water at the same volume as the volume of the initial broth sample. The centrifugation was repeated. A second wash step followed. After the last centrifugation, the wet cell paste (Figure 3.14) was transferred to a container for freeze-drying.

Figure 3.14 The cell paste after centrifugation.

3.8.2 Continuous centrifugation

Continuous centrifugation was used to process the large volume of the broth from the tubular photobioreactor. A 1 L rotor (R18C) was used. MasterFlex silicone tubing L/S18 (Cole-Palmer, USA) was used to connect the broth tank, the waste bottle and the rotor (Figure 3.15). The rotor was switched on at 520-g and filled by using the peristaltic pump (MasterFlex® L/S®, USA). Then, the pumping was stopped and the centrifuge speed was increased to 13,100-g. The pumping of the broth into the rotor then resumed at a flow rate of 690 mL min^{-1}. After all the broth had been processed, the 3 L of distilled water was pumped though the rotor. The centrifuge was then stopped, the biomass was recovered from the rotor and resuspended in 3 L of distilled water. A batch centrifuge step (Section 3.7.1) followed. The recovered biomass was once again suspended in 3 L of distilled water and centrifuged (Section 3.8.1). The final recovered biomass paste was freeze-dried (Section 3.9).

Figure 3.15 Continuous centrifugation.

3.9 Biomass freeze drying

The biomass paste recovered by centrifugation was stored at −80 °C overnight. The next day it was dried in a vacuum laboratory freeze-dryer (CRYODOS, TeLStaR, Spain) for at least 24 h. A dried biomass sample is shown in Figure 3.16.

Figure 3.16 Freeze-dried biomass

3.10 Measurements

3.10.1 Biomass concentration

Biomass concentration was measured by spectrophotometry (Uttrospec 2000 UV/Visible spectrophotometer, Phamacia Biotech) at 680 nm. The spectrophotometer was zeroed using a sample of the fresh uninoculated culture medium. A 2 mL sample of the culture broth was appropriately diluted with the fresh medium so that the measured absorbance was below 0.6. The dilution factor and the absorbance were recorded.

For a calibration curve, 5 mL of the broth was filtered through a glass microfibre filter (GF-C (1.2μm), diameter 90 mm, Whatman), washed twice with 5 mL of distilled water and then placed in an oven at 105 ºC for 24 h. The biomass was then cooled in a

desiccator for 24 h before weighing. This provided the dry biomass concentration, or dry cell weight (DCW), in the broth. A sample of the same broth was serially diluted and each dilution was measured by a spectrophotometer at 680 nm. The absorbance, the biomass dry weight concentration and the known dilution factors were used to calculate the biomass concentration in the samples to obtain the calibration relationships for the different algae. The various calibration curves are shown in Figures 3.17-3.23. The calibration curve equations corresponding to Figure 3.17-3.23 were as follows:

Chlorella vulgaris (BG-11 made in freshwater)

$$\text{DCW (g L}^{-1}) = \frac{A_{680}}{5.2459} \quad (1)$$

Chlorella vulgaris (BG-11 made in seawater)

$$\text{DCW (g L}^{-1}) = \frac{A_{680}}{2.8500 \pm 0.0058} \quad (2)$$

Choricystis minor (BG-11 made in freshwater)

$$\text{DCW (g L}^{-1}) = \frac{A_{680}}{7.5819} \quad (3)$$

Neochloris sp. (BG-11 made in freshwater)

$$\text{DCW (g L}^{-1}) = \frac{A_{680}}{3.3149} \quad (4)$$

Pseudococcomyxa simplex (BG-11 made in freshwater)

$$\text{DCW (g L}^{-1}) = \frac{A_{680}}{5.3078} \quad (5)$$

Scenedesmus sp. (BG-11 made in freshwater)

$$\text{DCW (g L}^{-1}) = \frac{A_{680}}{1.6032} \quad (6)$$

MGA-1-NZ (BG-11 made in seawater)

$$\text{DCW (g L}^{-1}) = \frac{A_{680}}{6.8372} \tag{7}$$

The replicate spectrophotometric measurements of the biomass concentration of a given sample were reproducible to ±0.79% of the measured value.

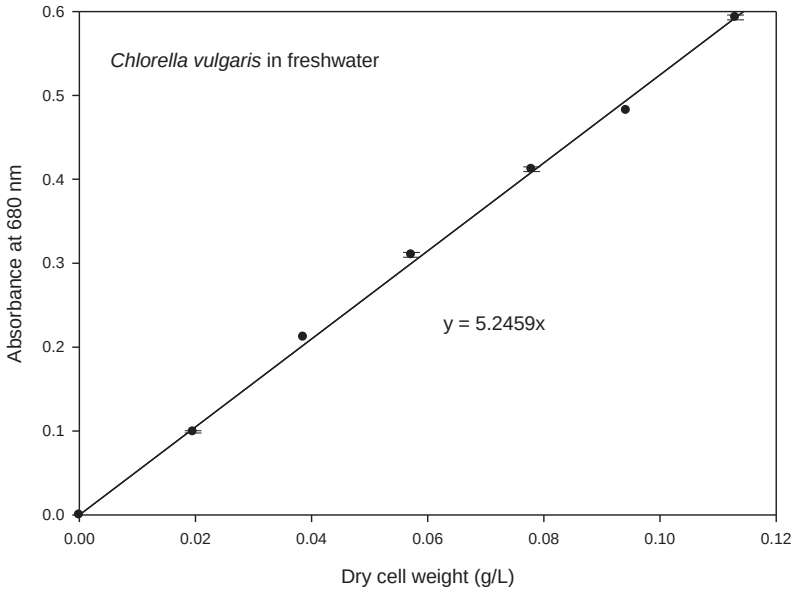

Figure 3.17 The calibration curve for *Chlorella vulgaris* in BG-11 made in freshwater.

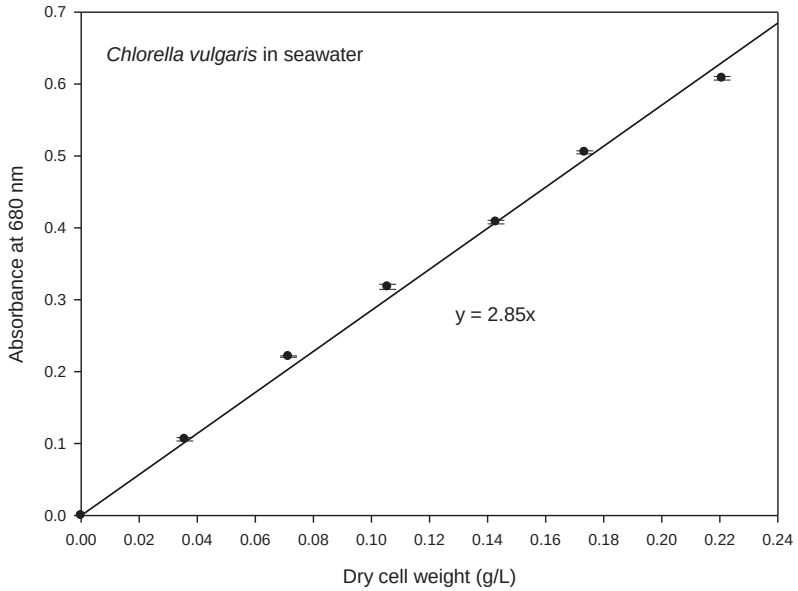

Figure 3.18 The calibration curve for *Chlorella vulgaris* in BG-11 made in seawater.

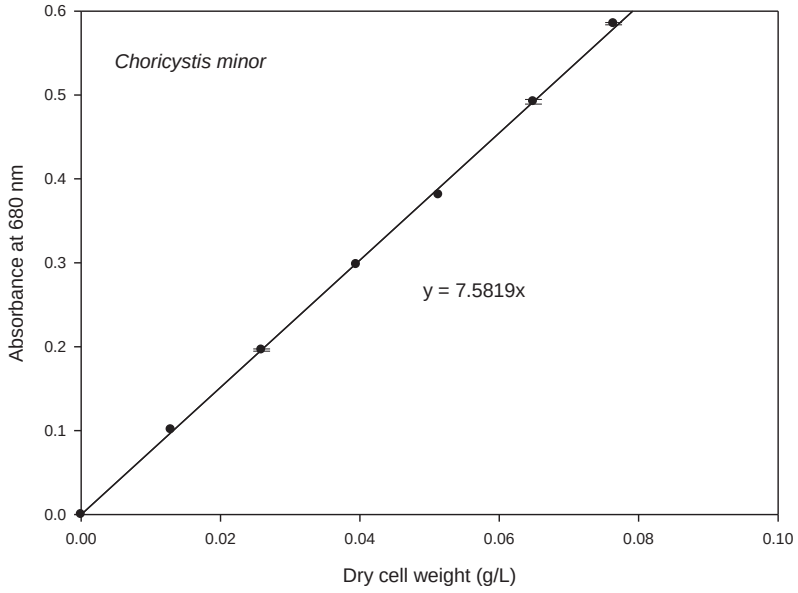

Figure 3.19 The calibration curve for *Choricystis minor* in BG-11 made in freshwater.

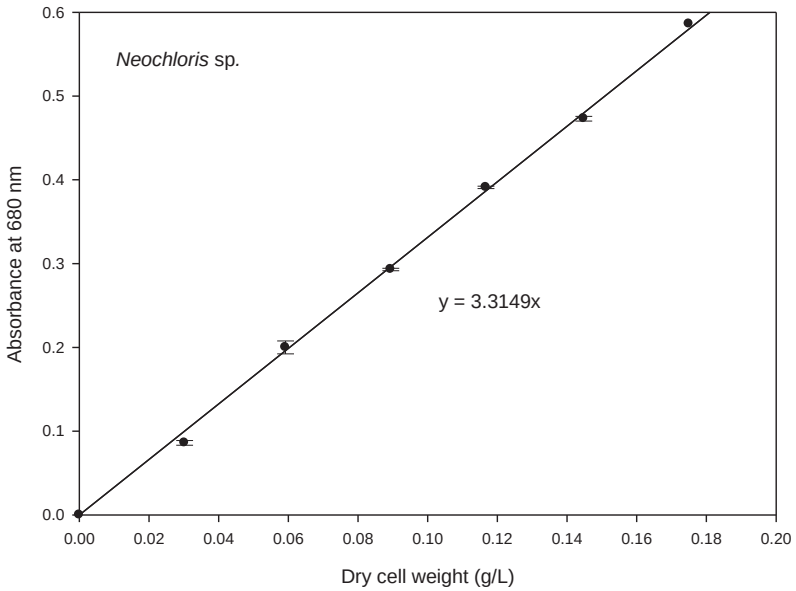

Figure 3.20 The calibration curve for *Neochloris* sp. in BG-11 made in freshwater.

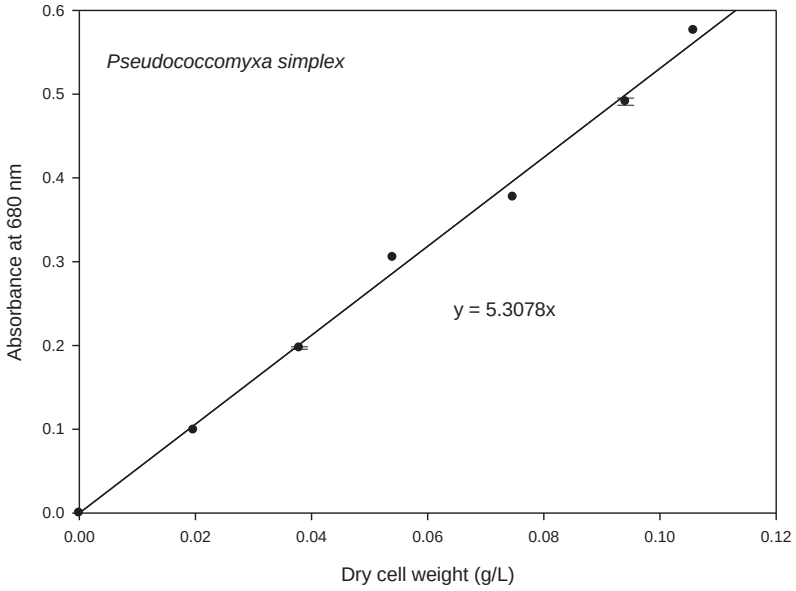

Figure 3.21 The calibration curve for *Pseudococcomyxa simplex* in BG-11 made in freshwater.

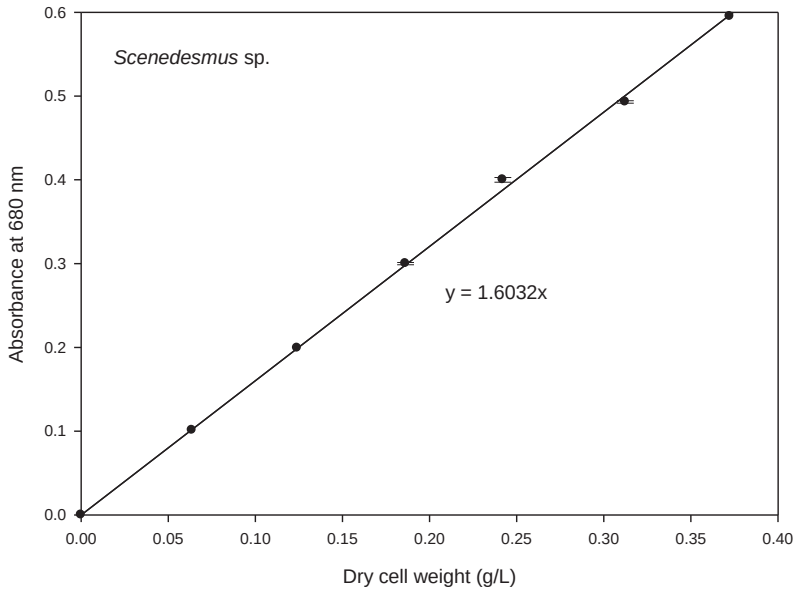

Figure 3.22 The calibration curve for *Scenedesmus* sp. in BG-11 made in freshwater.

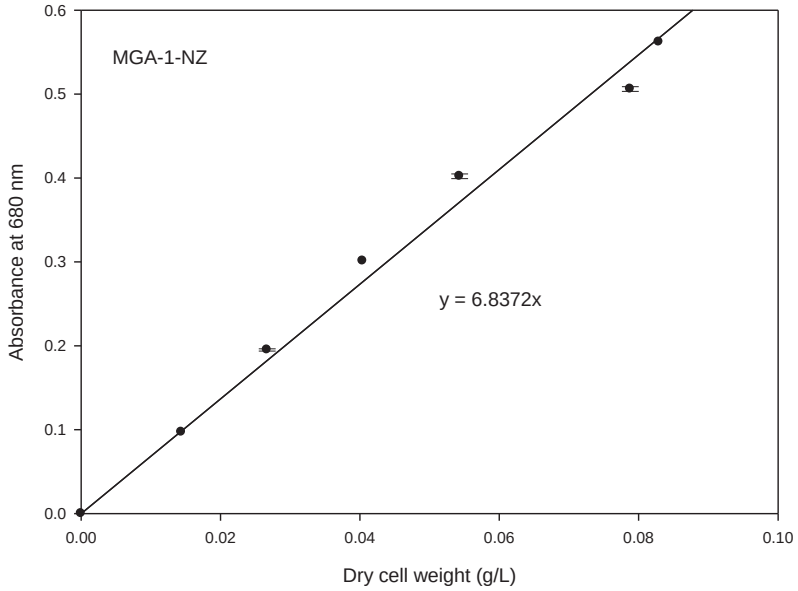

Figure 3.23 The calibration curve for MGA-1-NZ in BG-11 made in seawater.

3.10.2 Irradiance

Photosynthetically active radiation (PAR) level was measured at specified locations on the surface of a culture vessel, or within a fluid, using either a QSL-2101 quantum scalar irradiance sensor (Biospherical Instruments Inc, San Diego, CA, USA) or a Li-Cor LI-189 quantum irradiance meter (Li-Cor Inc., Lincoln, NE, USA). Both instruments gave comparable readings.

The relationship between the percentage of light output and the irradiance for light emission diodes which were used for the tubular photobioreactor and the stirred tank photobioreactors are shown in Figures 3.24 and 3.25-3.26.

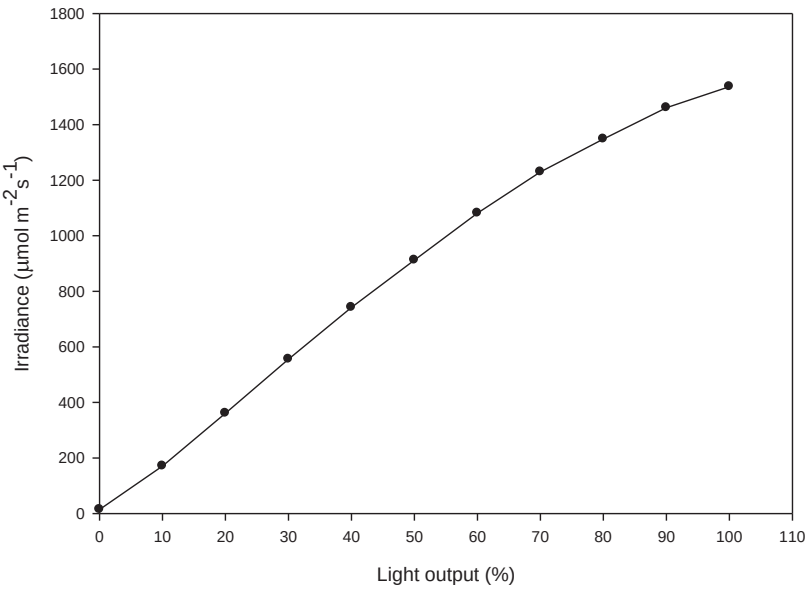

Figure 3.24 Relationship between the percentage light output and irradiance (QSL-2101 sensor) for LEDs of tubular photobioreactor. Irradiance was measured at the outer surface of the tubes.

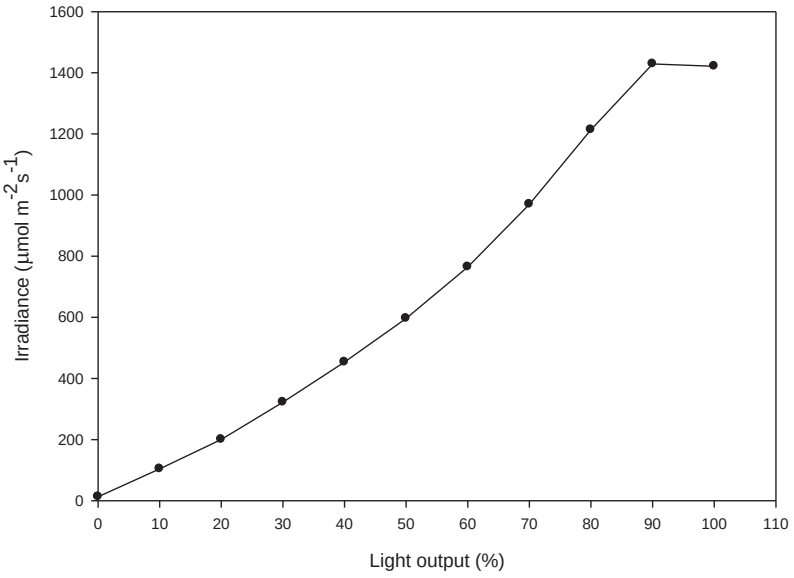

Figure 3.25 Relationship between the percentage light output and irradiance (QSL-2101 sensor) for LEDs units A and B of the stirred tank photobioreactor unit 2. Irradiance was measured at the outer surface of the tank with LED lamps placed 10 cm away.

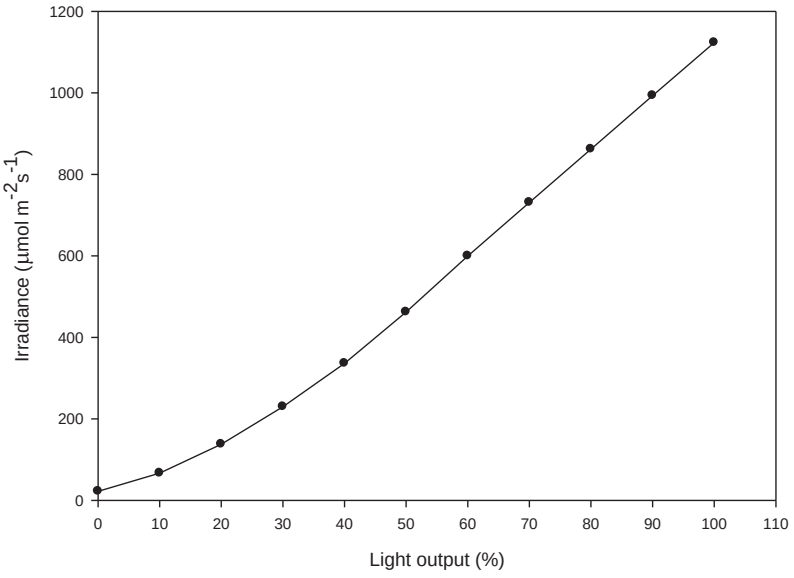

Figure 3.26 Relationship between the percentage light output and irradiance (QSL-2101 sensor) for LEDs units C and D of the stirred tank photobioreactor unit 1. Irradiance was measured at the outer surface of the tank with LED lamps placed 10 cm away.

3.10.3 Nitrate

More than 99.9% of the total nitrogen in the BG11 medium occurs as nitrate and the small amount of ammonium ions present (less than 0.1% of the total nitrogen) can be disregarded. Inorganic nitrogen concentration was therefore measured as nitrate, disregarding any nitrogen present as ammonium.

Residual nitrate was measured in prefiltered (0.45 μm membrane filter; 33 mm diameter Millex®-HA syringe driven filter unit; Millipore Corporation, Billerica, MA, USA) culture fluid using the cadmium reduction method (Hach, 2009) as commercially available from Hach Company, Loveland, CO, USA (catalog no. 216169). The absorbance of samples (525 nm) was compared to a calibration curve prepared using serial dilutions of the BG11 medium to obtain a nitrate concentration range of 0–30 mg L^{-1}. 10 mL of each dilution was mixed with the contents of 1 sachet of the Hach kit for 1 min. This mixture was then left standing for 5 min. The absorbance was then measured with a spectrophotometer at 525 nm.

The calibration curve had been prepared using BG-11 media diluted with deionized water or with seawater, as appropriate. The absorbance versus the known nitrate concentration of each dilution of BG-11 were plotted as shown in Figure 3.27 and Figure 3.28 for freshwater and seawater, respectively.

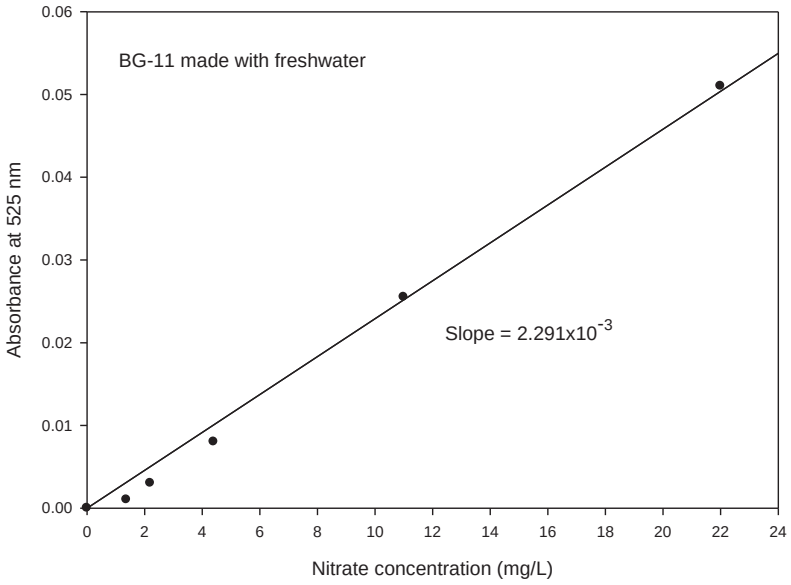

Figure 3.27 A nitrate calibration curve for BG-11 made with freshwater.

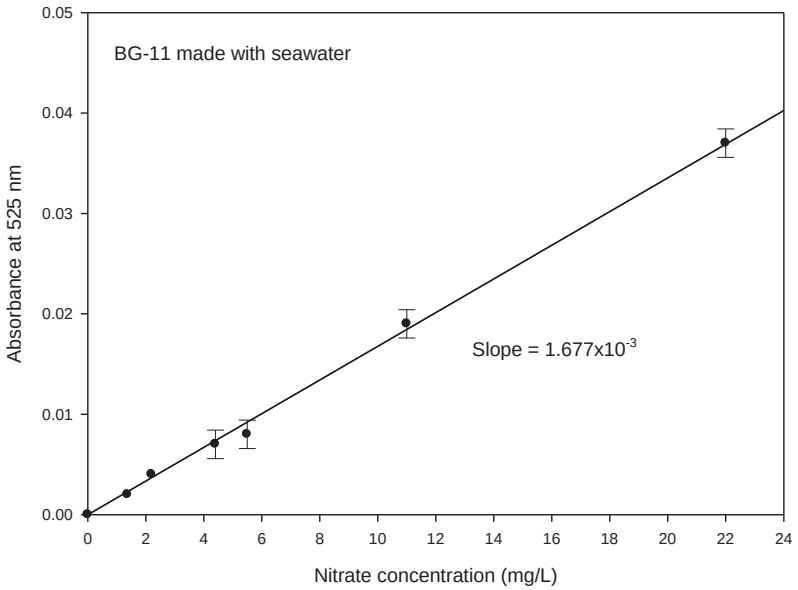

Figure 3.28 A nitrate calibration curve for BG-11 made with seawater.

The calibration relationships were as follows:

BG-11 made with freshwater

$$\text{Nitrate concentration (mg L}^{-1}) = \frac{A_{525}}{2.291\times10^{-3}} \quad (8)$$

BG-11 made with seawater

$$\text{Nitrate concentration (mg L}^{-1}) = \frac{A_{525}}{1.677\times10^{-3}} \quad (9)$$

Replicate measurements of the nitrate concentration of a given sample were reproducible to ±10.3% of the measured value.

3.10.4 Phosphate

Residual phosphate was determined in prefiltered (0.45 μm membrane filter; 33 mm diameter Millex®-HA syringe driven filter unit; Millipore Corporation, Billerica, MA, USA) culture fluid appropriately diluted with distilled water to give a concentration that was within the range of 0–1 mg PO_4^{2-} per liter. Ascorbic acid-molybdate method was used (Strickland & Parsons, 1972). A 0.5 mL of a mixed reagent (50 mL of ammonium heptamolybdate tetrahydrate (AnalaR NORMAPUR BDH(PROLABO, Belgium; 30 g L^{-1}) solution + 25 mL of sulfuric acid (J. T. Baker, USA; 140 mL of concentrated (~2.4 M) acid dissolved in 900 mL of distilled water) + 50 mL of L(+) ascorbic acid (reagent grade; Scharlau S. L., Spain; 5.4 g/100 mL distilled water) + 25 mL of antimonyl potassium (+)-tartrate (AnalaR, BDH Chemicals Ltd., England; 0.272 g dissolved in 200 mL of distilled water) was mixed with 5 mL of the prefiltered diluted sample. The mixed solution was allowed to stand for at least 20 min but not longer than 1 h. Then, the absorbance was measured at 885 nm using a

spectrophotometer. The absorbance was compared to a calibration curve to obtain the phosphate concentration. The ascorbic acid solution used in the mixed reagent was prepared fresh daily. The equation of the calibration curve (Figure 3.29) was:

$$\text{Phosphate concentration (mg L}^{-1}) = \frac{A_{885}}{0.226} \qquad (10)$$

The calibration curve (Figure 3.29) had been prepared by using serial dilutions of a standard solution of pre-dried KH_2PO_4 (Fisher Scientific, UK) in distilled water instead of the culture fluid in the above procedure. All dilution was made using distilled water.

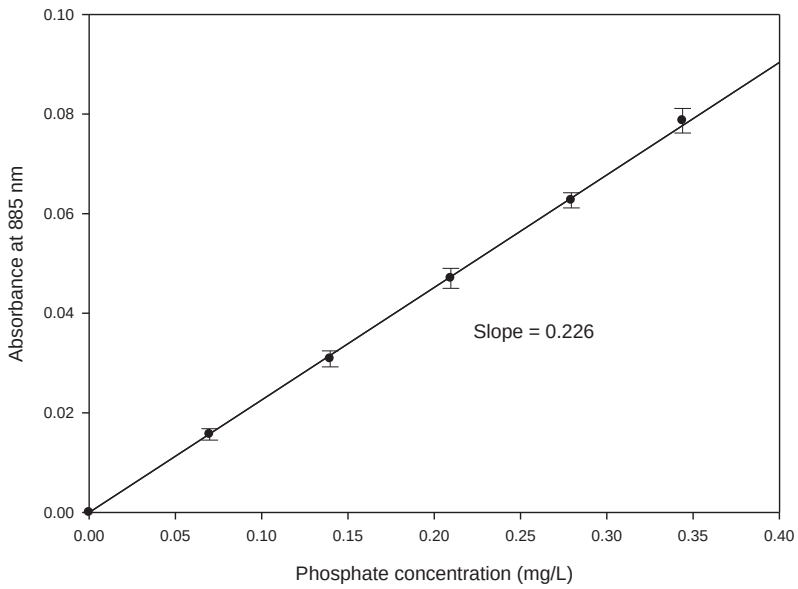

Figure 3.29 A phosphate calibration curve.

All glassware used in the assay had been rigorously cleaned with distilled water to prevent interference from phosphate that is present in commercial detergents. Replicate

measurements of the phosphate concentration of a given sample were reproducible to ±4.5% of the measured value.

3.10.5 Total lipids

An adaptation of the Bligh & Dyer (1959) method was used to extract the total lipids from freeze-dried biomass. Dry biomass (20 g) was homogenized with a solvent mixture of 100 mL of chloroform, 200 mL of methanol and 80 mL of distilled water, for 2 minutes, and stirred for a further 4 h (magnetic stirrer) at room temperature. Chloroform (100 mL) was then added and the slurry was mixed for 30 s. Distilled water (100 mL) was added and mixing was continued for a further 30 s. The suspension was centrifuged (4,150-g, 10-min) and allowed to separate into three layers. The top layer of methanol/water was discarded. The chloroform layer (the third layer from top) was collected. The residual biomass was extracted twice more. The chloroform extracts were combined and left overnight at 4 °C. The volume of the combined chloroform extracts was measured in a graduated cylinder. Total lipids in the chloroform extract were determined gravimetrically by evaporating (50 °C) an aliquot of the extract in a preweighed aluminum dish.

Using the measured volume of the pooled chloroform, the total lipid concentration in the extract and the amount of dry biomass used in extraction, the total lipids content were calculated as weight percent of dry biomass, as follows:

Total lipids (%)

$$= \frac{\text{volume of chloroform extract (mL)} \times \text{total lipid concentration in extract (mg/mL)}}{\text{mass of biomass extracted (mg)}} \times 100 \qquad (11)$$

Where necessary, the above method was scaled down (e.g. for 1 g biomass samples) such that the volume ratio of chloroform, methanol and water was always 1:2:0.8 in the extraction step and 2:2:1.8 in the biphasic separation step.

3.10.6 Neutral lipids

Neutral lipids were separated from the total lipids fraction using a method described by Kates (1986). A pre-packed silicic acid column (Extract Clean™ Silica; SPE SI 20000 mg/75 mL, Grace, Australia) was used. The column was first washed with 60 mL of chloroform. Total lipids (200-250 mg) dissolved in 5 mL of chloroform were applied to the column. The residual lipids from the glassware were washed into the column using 3 mL of chloroform. The column was eluted sequentially with 300 mL of chloroform, 1200 mL of acetone, and 300 mL of methanol. These fractions were collected separately. The acetone and methanol fractions contained polar lipids such as mono-and di-galactosyl diglycerides (Kates, 1986). The chloroform fraction contained the neutral lipids (Kates, 1986). A known volume of each fraction was evaporated (50 °C) separately in pre-weighed aluminum dishes. The dishes were cooled in a desiccator and weighed.

The fraction of the neutral lipids in total lipids was calculated as follow:

$$\text{Neutral lipid (as \% of total lipids)} = \frac{\text{mass of neutral lipids recovered (mg)}}{\text{mass of total lipids applied (mg)}} \times 100 \qquad (12)$$

3.10.7 Triglyceride in neutral lipids

Triglycerides were separated from the neutral lipids fraction following the method described by Kates (1986). Pre-packed silicic acid columns (Extract Clean™ Silica; SPE SI 10000

mg/25 mL, Grace, Australia) were used. The column was first washed with 30 mL of hexane. A known amount 120-180 mg of neutral lipid dissolved in 5 mL of hexane was applied to the column. The residual material from the glassware was washed into the column using 3 mL of hexane. The column was eluted sequentially with 45 mL of hexane, 95 mL of hexane: ethyl ether (99:1 vol/vol), and 60 mL of hexane: ethyl ether (95:5 vol/vol). The last fraction was collected separately and contained the triglycerides. A known volume of the triglyceride fraction was evaporated to dryness (50 °C) in a pre-weighed aluminum dish. The dish was then cooled in a desiccator and weighed.

Triglycerides (as % of neutral lipids (NL))

$$= \frac{\text{mass of triglycerides recoverd (mg)}}{\text{mass of neutral lipids applied (mg)}} \times \%\ \text{of neutral lipids in total lipids} \qquad (13)$$

3.10.8 Calorific values

Calorific value (i.e. the heat of combustion) of the freeze-dried algal biomass was measured by bomb calorimetery. A Leco AC-350 calorimeter (Leco Corporation, St Joseph, MI, USA) was used. Measurements were done by the Nutritional Laboratory, Institute of Food, Nutrition and Human Health (Massey University, Palmerston North, New Zealand). About 1 g of dried biomass was used for each measurement. The calorific value of a given sample was reproducible to ±2.8% of the measured value.

3.10.9 Nile red staining of cells (modified from Elsey *et al.*, 2007)

This procedure was used to visualize the intracellular lipids. A 3 mL sample of the diluted broth with an absorbance at 720 nm of between 0.3-0.5 was mixed with 10 μL of nile red (9-

diethylamino-5H-benzo[α]phenoxazine-5-one, $C_{20}H_{18}N_2O_2$; 7.8×10^{-4} M in acetone) for 1 min. The mixture was then held at room temperature for at least 30 min but not longer than 40 min. The sample was then placed on a microscopic slide, covered with a cover slip, and photographed under a fluorescent microscope.

3.10.10 Gram staining (Mudili, 2007; Cappuccino & Natalie, 2011)

This procedure was used to check for bacterial contamination of the algae cultured in bioreactors. A drop of algae cell broth was placed on a microscope slide and heat-fixed. The slide was then stained with crystal violet as a primary stain for 1 min and rinsed with water. The slide was then treated by iodine solution as a mordant for 1 min and rinsed with water. The slide was then decolorized rapidly with alcohol and rinsed with water. Finally, the slide was counterstained with safraninO for 1 min and rinsed with water and examined under the microscope.

3.10.11 Algae morphology

Algal morphology was documented by optical microscopy and imaging. Most of the microscopic examinations were done by the author at the facilities of Manawatu Microscopy and Imaging Centre, Massey University, Palmerston North. A sample of the algal broth (diluted with the appropriate medium, if necessary) was placed on a microscopic slide with a cover slip, and photographed at specified magnification.

3.10.12 Calculations of kinetic parameters (Doran, 1995; Shuler & Kargi, 2002)

In batch culture, the specific nitrate and phosphate consumption rates (q_N and q_P; mg $g^{-1}d^{-1}$), the biomass yield coefficients on nitrate, phosphate and light ($Y_{X/N}$, $Y_{X/P}$; g mg^{-1} and $Y_{X/Light}$;

g μmol^{-1}), the lipid yield on light ($Y_{L/Light}$; g μmol^{-1}), the final biomass productivity (Q_X; g $L^{-1}d^{-1}$), and the final lipid productivity (Q_L; g $L^{-1}d^{-1}$) were calculated as follows:

$$q_N = \frac{N_i - N_f}{t_f - t_i} \times \frac{1}{X_f - X_i} \tag{14}$$

$$q_P = \frac{P_i - P_f}{t_f - t_i} \times \frac{1}{X_f - X_i} \tag{15}$$

$$Y_{X/N} = \frac{X_f - X_i}{N_i - N_f} \tag{16}$$

$$Y_{X/P} = \frac{X_f - X_i}{P_i - P_f} \tag{17}$$

$$Y_{X/Light}^{*} = \frac{(X_f - X_i)V}{IA(t_f - t_i)} \tag{18}$$

$$Y_{L/Light}^{*} = Y_{X/Light}y \tag{19}$$

$$Q_X = \frac{X_f - X_i}{t} \tag{20}$$

$$Q_L = \frac{X_f - X_i}{t}y \tag{21}$$

The specific growth rate was estimated as the maximum slope of a plot of the natural logarithm of the biomass concentration versus time.

In the above equations, N_f, P_f, and X_f are the final concentrations of nitrate, phosphate, and biomass; N_i, P_i, and X_i are the initial concentrations of nitrate, phosphate, and biomass; t is the duration of the batch; t_i is the initial time and t_f is the final time; V is the working volume of the reactor; I is the light irradiance; A is the area that was illuminated by the light; y is the weight fraction of lipids in the biomass. (* These equations are modified

forms of equation (16) assuming the light to be the substrate.) In all cases, the parameters were calculated at a value of t (or t_f) corresponding to the instance of the maximum biomass concentration.

In continuous culture, the dilution rate (D; d^{-1}), the specific nitrate and phosphate consumption rates (q_N and q_P; mg $g^{-1}d^{-1}$), the specific lipid production rate (q_L; d^{-1}), the biomass yield coefficients on nitrate, phosphate and light ($Y_{X/N}$, $Y_{X/P}$; g mg^{-1} and $Y_{X/Light}$; g μmol^{-1}), the lipid yield coefficients on nitrate, phosphate and light ($Y_{L/N}$, $Y_{L/P}$; g mg^{-1} and $Y_{L/Light}$; g μmol^{-1}), the final biomass productivity (Q_X; g $L^{-1}d^{-1}$), and the final lipid productivity (Q_L; g $L^{-1}d^{-1}$) were calculated as follows:

$$D = \frac{F}{V} \tag{22}$$

$$q_N = \frac{D(N_i - N_f)}{X} \tag{23}$$

$$q_P = \frac{D(P_i - P_f)}{X} \tag{24}$$

$$q_L = Dy \tag{25}$$

$$Y_{X/N} = \frac{X}{(N_i - N_f)} \tag{26}$$

$$Y_{X/P} = \frac{X}{(P_i - P_f)} \tag{27}$$

$$Y_{X/Light}^{*} = \frac{FX}{IA} \tag{28}$$

$$Y_{L/N} = \frac{Xy}{(N_i - N_f)} \tag{29}$$

$$Y_{L/P} = \frac{Xy}{(P_i - P_f)} \tag{30}$$

$$Y_{L/Light}^{*} = Y_{X/Light}y \tag{31}$$

$$Q_X = DX \quad (32)$$

$$Q_L = DXy \quad (33)$$

In the above equations, F is the flow rate of the feed; V is the working volume of the reactor; N_f and P_f are the concentrations of nitrate and phosphate in the reactor at steady state; N_i and P_i are the initial concentrations of nitrate and phosphate in the feed; X is the biomass concentration at steady state in the reactor; y is the weight fraction of lipids in the biomass; I is the light irradiance; A is the area that was illuminated by the light. (* These equations are modified forms of equation (26) assuming the light to be the substrate.)

In continuous culture operations at steady state, the dilution rate was taken to equal the specific growth rate.

Chapter 4

Results and Discussion

4.1 Studies in Duran bottles

4.1.1 Salinity effects on growth

Because the interest was in eventually using the abundant seawater for culturing the algae for oils, all algae were assessed for growth capability in BG11 formulated in seawater. For comparison, growth was also measured in the same medium formulated with brackish water (i.e. a 1:1 by volume mixture of artificial seawater and freshwater) and freshwater. Cultures were grown in 1 L Duran bottles (900 mL initial working volume) bubbled with a prehumidified mixture of 5% (v/v) carbon dioxide in air. The culture temperature was 22–25 °C. Cultures were illuminated continuously at an irradiance value of 126-173 $\mu mol \cdot m^{-2}s^{-1}$ (daylight fluorescent light) at the surface of the bottles. The growth profiles are shown in Figures 4.1-4.4 for *Chlorella vulgaris*, *Choricystis minor*, *Neochloris* sp. and *Pseudococcomyxa simplex*, respectively. The total lipids contents of the biomass harvested at the end of the culture period were determined. The relevant data and the kinetic parameters for the algae based on the data of Figure 4.1-4.4 are shown in Table 4.1.

From Figures 4.1-4.4, only *C. vulgaris* could grow in a seawater based medium to achieve a biomass concentration (3.7-4.0 g L^{-1} on day 33) comparable to that found in the freshwater medium. *Choricystis minor* had a good biomass productivity (Table 4.1) (a biomass concentration 5 g L^{-1} on day 37), but only in freshwater medium. In contrast, this alga completely failed to grow in even half-strength seawater. *Neochloris* sp. and *P. simplex* grew in seawater, but extremely slowly when compared to growth in the freshwater medium.

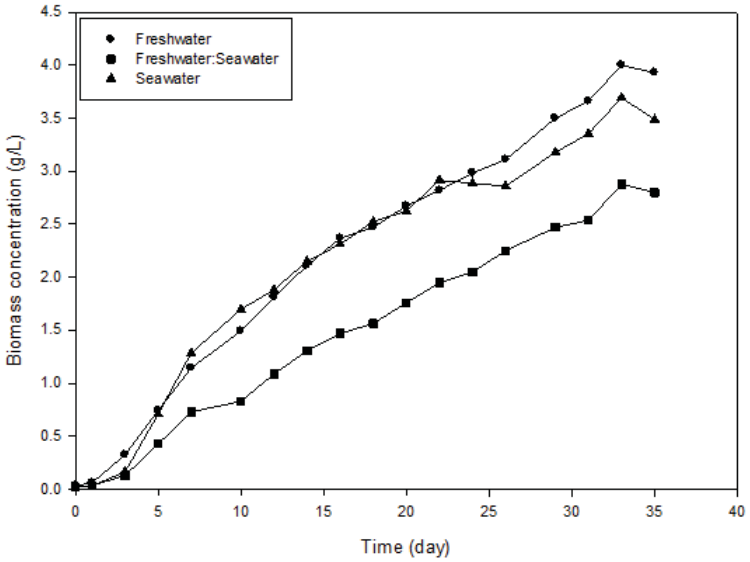

Figure 4.1 Growth curves of *Chlorella vulgaris* in different BG11 formulations in 1 L culture bottles.

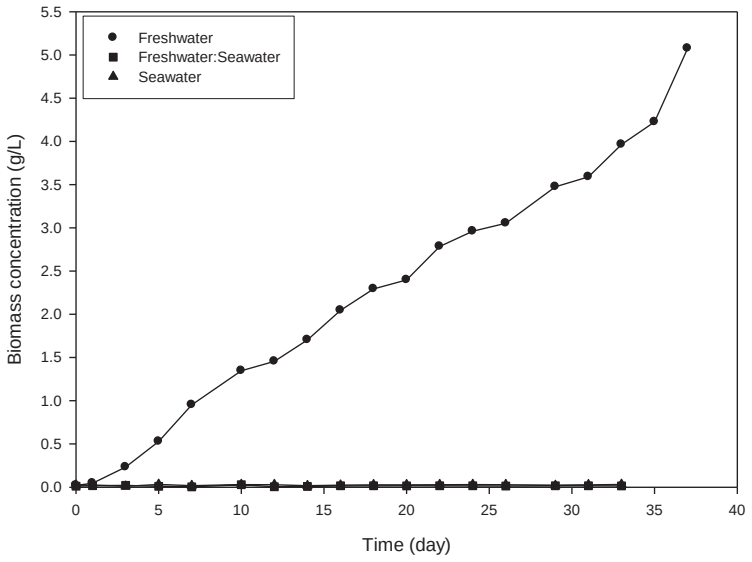

Figure 4.2 Growth curves of *Choricystis minor* in different BG11 formulations in 1 L culture bottles.

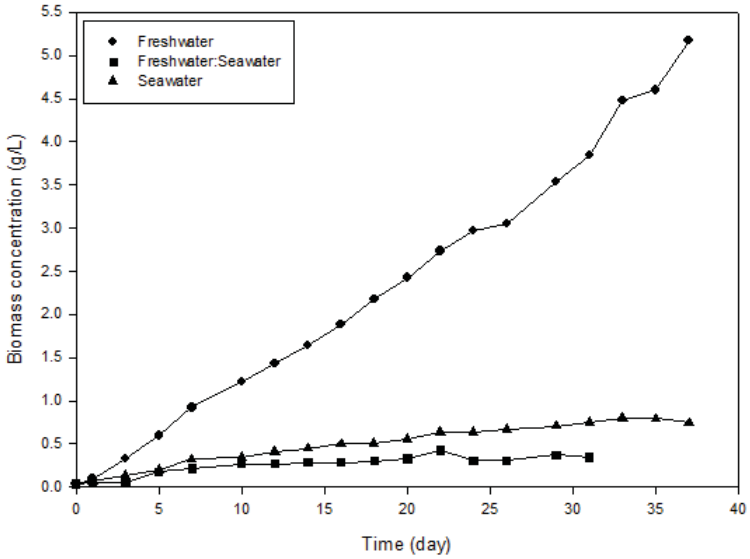

Figure 4.3 Growth curves of *Neochloris* sp. in different BG11 formulations in 1 L culture bottles.

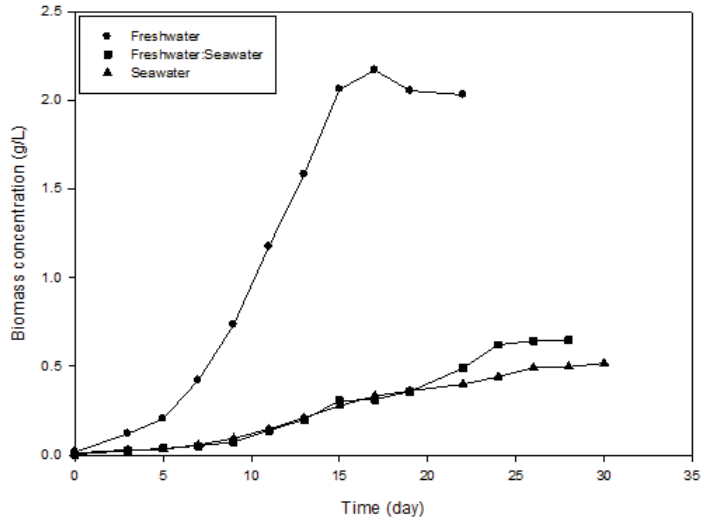

Figure 4.4 Growth curves of *Pseudococcomyxa simplex* in different formulations of BG11 in 1 L culture bottles.

Table 4.1 Kinetic parameters for the algae cultured in 1 L bottles (Figures 4.1-4.4)

Algae in BG-11 made with	Specific growth rate (μ; d^{-1})	Biomass productivity (Q_X; g $L^{-1}d^{-1}$)	Lipid productivity (Q_L; mg $L^{-1}d^{-1}$)
Freshwater			
Chlorella vulgaris	0.649	0.120	18.3
Choricystis minor	0.698	0.137	45.4
Neochloris sp.	0.517	0.139	32.0
Pseudococcomyxa simplex	0.423	0.127	22.9
Freshwater:seawater (1:1 by vol.)			
Chlorella vulgaris	0.537	0.087	23.0
Choricystis minor	ND	ND	ND
Neochloris sp.	0.224	0.018	7.1
Pseudococcomyxa simplex	0.323	0.023	9.2
Seawater			
Chlorella vulgaris	0.590	0.111	37.1
Choricystis minor	ND	ND	ND
Neochloris sp.	0.300	0.023	7.8
Pseudococcomyxa simplex	0.237	0.017	7.0

ND – not determined because of insufficient growth.

In view of Table 4.1, the specific growth rates and biomass productivities of the four algae that grew in BG-11 made with freshwater are broadly similar. *C. minor* and *Neochloris* sp. had the lipid productivity 2.5- and 1.7-fold higher than *C. vulgaris*, respectively. However, only *C. vulgaris* tolerated full-strength seawater without much reduction in growth

rate or in the final biomass productivity relative to freshwater (Table 4.1). Also, the lipid productivity for *C. vulgaris* in seawater medium was much higher than for the other algae in seawater (Table 4.1).

The above identified effects of salinity on growth and lipids contents were confirmed by growing the algae in scaled up 2 L Duran bottles (1800 mL initial working volume) under the same conditions as mentioned earlier in this section. The growth profiles are shown in Figures 4.5-4.9 for the various algae. Measurements are reported also for a new freshwater alga, *Scenedesmus* sp., that had become available for evaluations. The total lipid content of the final biomass samples and the calorific value of the biomass are shown in Table 4.2. The culture kinetic parameters for the algae are shown in Table 4.3.

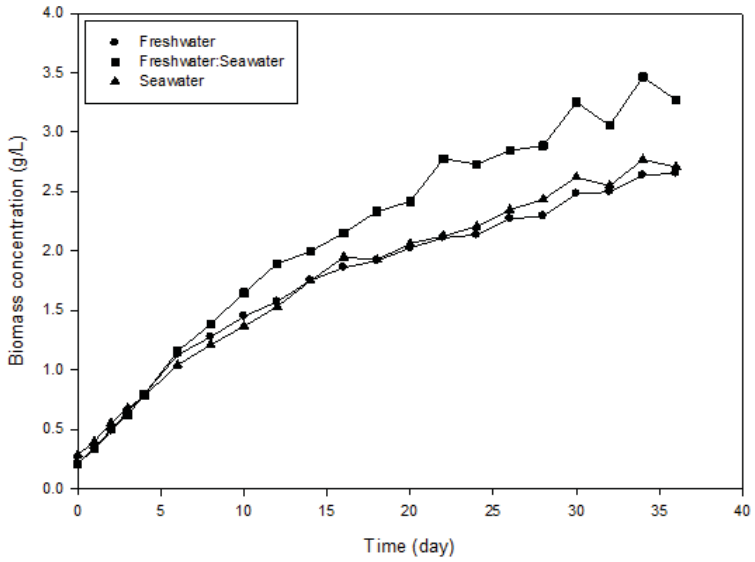

Figure 4.5 Growth curves of *Chlorella vulgaris* in different BG11 formulations in 2 L culture bottles.

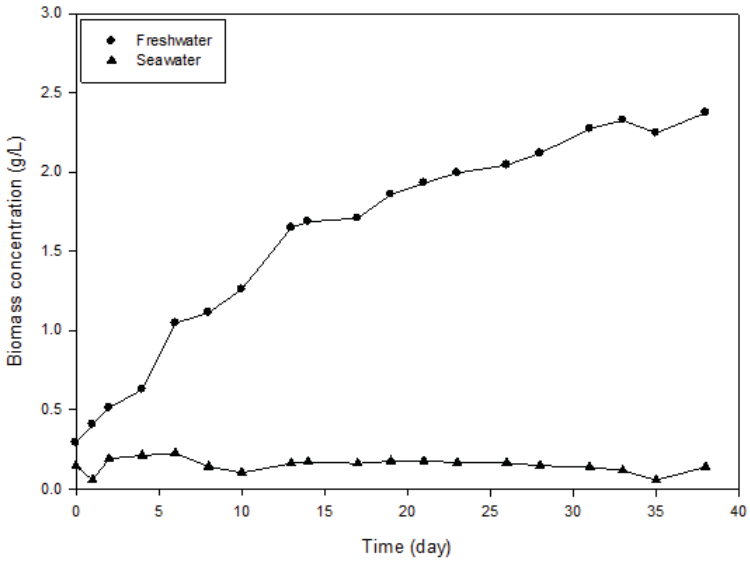

Figure 4.6 Growth curves of *Choricystis minor* in different BG11 formulations in 2 L culture bottles.

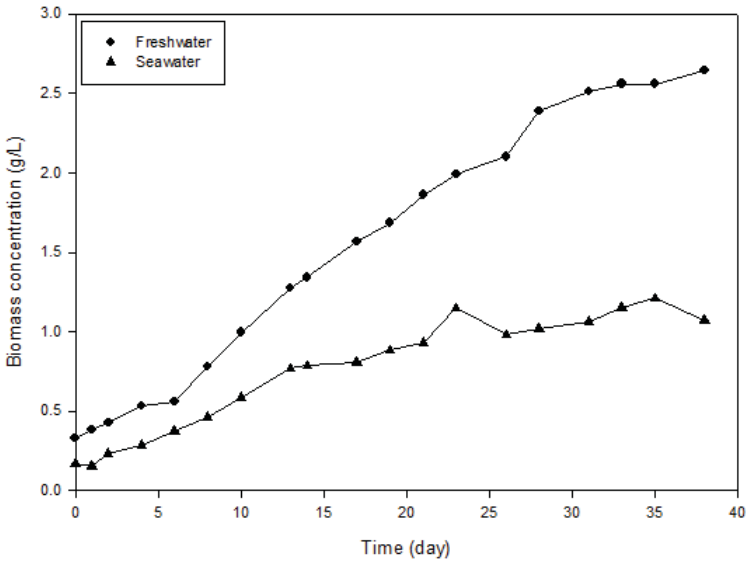

Figure 4.7 Growth curves of *Neochloris* sp. in different BG11 formulations in 2 L culture bottles.

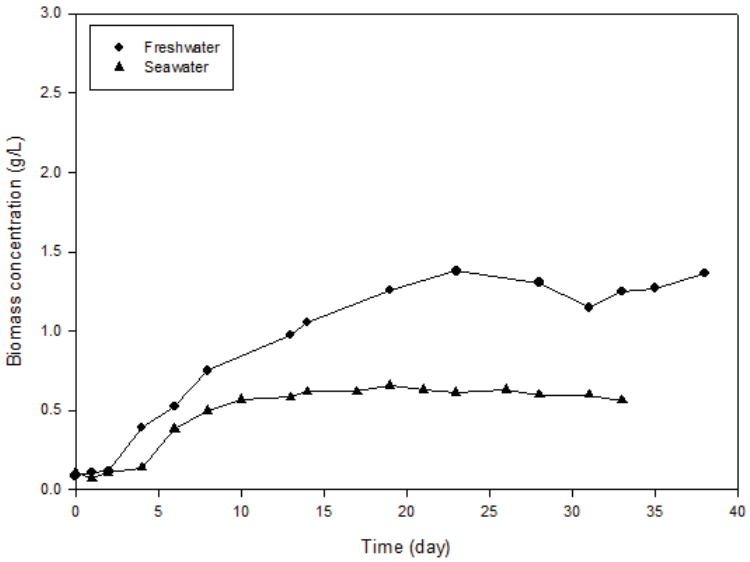

Figure 4.8 Growth curves of *Psuedococcomyxa simplex* in different formulations of BG11 in 2 L culture bottles.

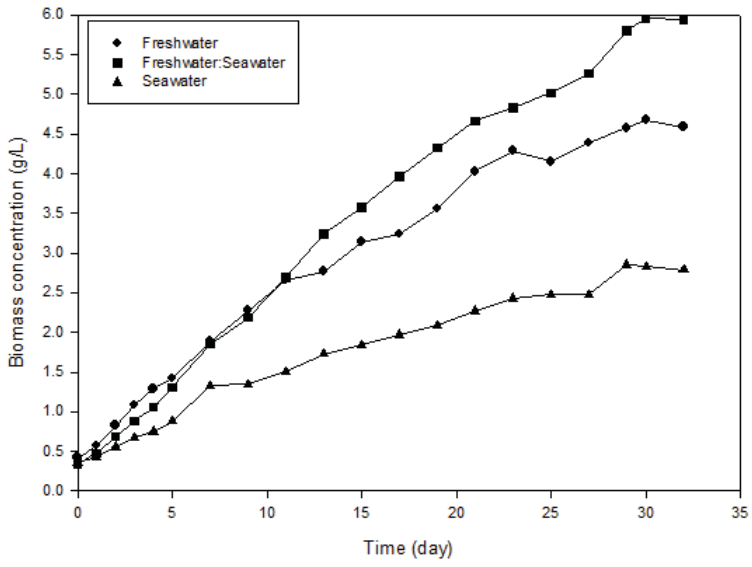

Figure 4.9 Growth curves of *Scenedesmus* sp. in different formulations of BG11 in 2 L culture bottles.

Table 4.2 Total lipid contents and calorific values for the algae cultured in 2 L bottles

Algae in BG-11 made with	Total lipid content (%, w/w)[a]	Calorific value (kJ g^{-1})[b]
Freshwater		
Chlorella vulgaris	7.1±0.0	26.0
Choricystis minor	29.1±0.0	27.7
Neochloris sp.	14.9±0.1	23.7
Pseudococcomyxa simplex	13.6±2.4	23.6
Scenedesmus sp.	6.2±0.2	21.3
Freshwater:seawater (1:1 by vol.)		
Chlorella vulgaris	16.2±0.4	24.5
Scenedesmus sp.	10.9±1.2	22.1
Seawater		
Chlorella vulgaris	15.6±0.2	25.2
Choricystis minor	ND	ND
Neochloris sp.	19.0±0.2	24.5
Pseudococcomyxa simplex	15.2±0.0	23.9
Scenedesmus sp.	15.9±0.9	23.1

ND – not determined because of insufficient growth.

[a] – mean value ± standard deviation.

[b] – previously shown to be reproducible to ± 2.8% of the mean value (Section 3.10.8).

Table 4.3 Kinetic parameters for the algae cultured in 2 L bottles

Algae in BG-11 made with	Biomass yield on phosphate ($Y_{X/P}$; g mg^{-1})	Specific phosphate consumption rate (q_P; mg $g^{-1}d^{-1}$)	Specific growth rate (μ; d^{-1})	Biomass productivity (Q_X; g $L^{-1}d^{-1}$)	Lipid productivity (Q_L; mg $L^{-1}d^{-1}$)
Freshwater					
Chlorella vulgaris	0.147	0.189	0.359	0.068	4.80±0.00
Choricystis minor	0.120	0.253	0.212	0.062	17.90±0.00
Neochloris sp.	0.136	0.193	0.105	0.061	9.05±0.07
Pseudococcomyxa simplex	0.076	0.573	0.291	0.056	7.60±1.32
Scenedesmus sp.	0.262±0.000	0.127±0.000	0.300	0.142	8.84±0.22
Freshwater:seawater (1:1 by vol.)					
Chlorella vulgaris	0.190	0.155	0.362	0.096	15.50±0.37
Scenedesmus sp.	0.336±0.000	0.099±0.000	0.284	0.187	20.34±2.30

Table 4.3 Kinetic parameters of the algae cultured in 2 L bottles (Cont.)

Algae in BG-11 made with	Biomass yield on phosphate ($Y_{X/P}$; g mg^{-1})	Specific phosphate consumption rate (q_P; mg $g^{-1}d^{-1}$)	Specific growth rate (μ; d^{-1})	Biomass productivity (Q_X; g $L^{-1}d^{-1}$)	Lipid productivity (Q_L; mg $L^{-1}d^{-1}$)
Seawater					
Chlorella vulgaris	0.144	0.204	0.303	0.073	11.43±0.13
Choricystis minor	ND	ND	ND	ND	ND
Neochloris sp.	0.056	0.773	0.119	0.042	8.06±0.06
Pseudococcomyxa simplex	0.032	1.657	0.182	0.029	4.39±0.00
Scenedesmus sp.	0.149±0.000	0.232±0.000	0.188	0.086	13.67±0.81

ND – not determined because of insufficient growth.

Standard deviations are shown for selected measurements.

The data in 2 L Duran bottles (Figures 4.5-4.8) were generally consistent with the data in 1 L bottles (Figures 4.1-4.4). The data confirmed that of the freshwater algae tested, only *C. vulgaris* could grow almost as well in the seawater medium as in freshwater medium. For the other algae, the biomass productivity in seawater was greatly reduced compared to in freshwater. *Scenedesmus* sp. grew exceptionally well (Figure 4.9) in both freshwater and brackish water (i.e. 1:1 v/v mixture of seawater and freshwater), but had a much reduced biomass productivity in seawater. In BG-11 made with brackish water, *Scenedesmus* sp. attained an exceptionally high biomass concentration of 6 g L^{-1} within 30 days (Figure 4.9).

For all algae, in a given medium, the specific growth rate and the final biomass productivity were reduced by scale up from 1 L to 2 L culture bottles (Table 4.1, Table 4.3). This was a consequence of a reduced availability of light per unit culture volume in the larger bottles (diameter = 136 mm) compared to smaller bottles (diameter = 101 mm). This effect is well known (Richmond, 2004; Sirisansaneeyakul *et al.*, 2011). For a fixed depth of culture in a bottle of diameter d, the surface area A for light capture is proportional to πd whereas the culture volume is proportional to $\frac{\pi d^2}{4}$. Therefore, the area-to-volume ratio (A/V) is 4/d. Thus, as the bottle diameter increases the area-to-volume ratio decreases and less light is received per unit volume of the culture.

Of the algae that could be grown in seawater, *Neochloris* sp. had the highest lipid content in the biomass (Table 4.2), but a lower lipid productivity compared to *C. vulgaris* and *Scenedesmus* sp. (Table 4.3). The total lipid content in *C. vulgaris* and *Scenedesmus* sp. were similar (Table 4.2), but *C. vulgaris* tended to have a higher total energy content than *Scenedesmus* sp. as revealed by the calorific values in Table 4.2. In seawater, the total lipid productivity of *C. vulgaris* and *Scenedesmus* sp. were similar (Table 4.2). Overall, therefore, *C. vulgaris* and *Scenedesmus* sp. were almost equal as candidate algae for lipid production in

a seawater medium. As the calorific value of *C. vulgaris* tended to be consistently higher than the calorific value of *Scenedesmus* sp. (Table 4.2), *C. vulgaris* was selected as the focus of this study as having a higher total energy content per unit of biomass. The rationale was that once the oil has been extracted, the residual biomass could be used as a further source of energy, by anaerobic digestion to methane (Samson & Le Duy, 1982; Sánchez Hernández & Travieso Córdoba, 1993; Vergara-Fernández *et al.*, 2008; Ras *et al.*, 2011; Chisti, 2012), for example. Further examination of the residual biomass and its uses were of course not within the scope of this thesis.

Preliminary results obtained in 1 L culture bottles suggest that the oil productivity of *C. vulgaris* was improved by growing the alga in seawater instead of in freshwater (Table 4.1). This was confirmed by the data obtained in 2 L culture bottles (Table 4.3). The reasons why most of the freshwater algae failed to thrive under high salinity media are not relevant here, but likely have to do with the increased osmolality that accompanies an increase in salinity of the medium (Avron, 1986; Bisson & Kirst, 1995; Ladas & Papageorgiou, 2000; Rathinasabapathi, 2000; Ferroni *et al.*, 2007; Affenzeller *et al.*, 2009). *C. vulgaris* is normally a freshwater alga. Many *C. vulgaris* strains do not tolerate a high salinity (Gustavs *et al.*, 2010), but some strains are able to grow in full strength seawater (Kessler, 1974).

4.1.2 Light/dark cycle effects on *Chlorella vulgaris*

Chlorella vulgaris was cultured in 2 L Duran bottles (1.8 L working volume) in BG-11 made with seawater. The bottles were bubbled with 5% (v/v) carbon dioxide in air. The culture temperature was 22–25 °C. Cultures were illuminated either continuously or under a light-dark cycle (12 h/12 h) at an irradiance value of 126-173 $\mu E \cdot m^{-2}s^{-1}$ (daylight fluorescent light) at the surface of the bottles. The growth profiles are shown in Figure 4.10. Total lipid

content of the biomass, the calorific value of the biomass, and the kinetic parameters relating to these cultures are given in Table 4.4.

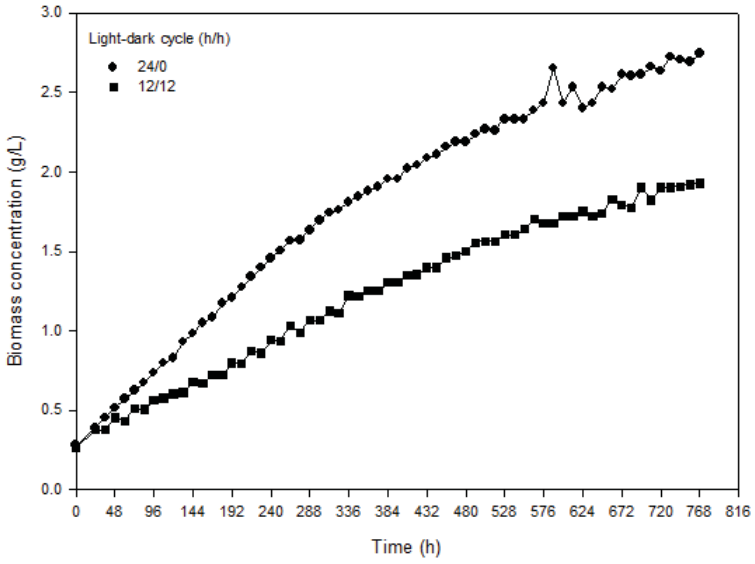

Figure 4.10 Growth curves of *Chlorella vulgaris* in BG11 made with seawater, illuminated continuously (24/0) and every 12 h (12/12) by fluorescent lamps.

In view of Figure 4.10 and Table 4.4, the cultures that were continuously illuminated grew more rapidly and produced a higher final biomass concentration of 2.75 g L^{-1}, compared with the day-night cycled cultures. This was because the alga stopped growing in the dark and the growth resumed in the next light period. In fact, during the dark there was some loss of biomass as revealed by a close look at the data in Figure 4.10. Stored starch is consumed by algae in the dark to obtain energy for metabolism (Markager *et al.*, 1992; Post, 1993; Stal & Moezelaar, 1997). In the light/dark cycled culture, the final biomass concentration was 1.93 g L^{-1}, or 70% of the value obtained in the continuously illuminated culture (Figure 4.10).

The lipid content of the biomass and its calorific value were not affected much by the illumination regime (Table 4.4) even though the lipid productivity of the culture illuminated continuously was nearly double that of the light-dark cycled culture. The light-dark cycling also affected on the average specific growth rate (Table 4.4). These experiments provided data for possible use in correcting the productivity values of the continuously illuminated cultures for estimating the expected productivity in a natural outdoor light-dark cycle.

Table 4.4 Comparison of continuous illumination and light-dark cycling (12 h/12 h) on culture kinetics and biomass properties of *Chlorella vulgaris*

Illumination	Total lipid content (% w/w) (final harvest)	Calorific value (kJ g^{-1}) (final harvest)	Specific growth rate (μ; d^{-1})	Biomass productivity (Q_X; g $L^{-1}d^{-1}$)	Lipid productivity (Q_L; mg $L^{-1}d^{-1}$)
Continuous	14.7±0.1	25.2	0.288	0.077	11.34±0.11
12 h/12 h light-dark cycle	15.0±0.5	23.3	0.216	0.052	7.80±0.26

Standard deviations are shown for selected measurements.

4.1.3 *Chlorella vulgaris* biomass loss in the dark

The objective was to characterize the kinetics of biomass loss in the dark (no photosynthesis) by self consumption at various temperatures. A characterization of self-consumptive loss by respiration is important as in a sunlight illuminated outdoor culture, periodic loss would occur each night (Sánchez Mirón *et al.*, 2000; Miron *et al.*, 2002).

C. vulgaris broth (200 mL per sample) from PBR 1 (Section 4.2) was placed in 500 mL Erlenmeyer flasks. All flasks were wrapped with aluminium foil to prevent light penetration. The flasks, plugged with sterile cotton wool, were incubated separately at temperatures of 20 °C, 25 °C and 30 °C on an orbital shaker at 100 rpm. Two parallel flasks were incubated at 25 °C for reproducibility checks. The biomass concentration was measured periodically. The resulting biomass loss profiles are shown in Figure 4.11.

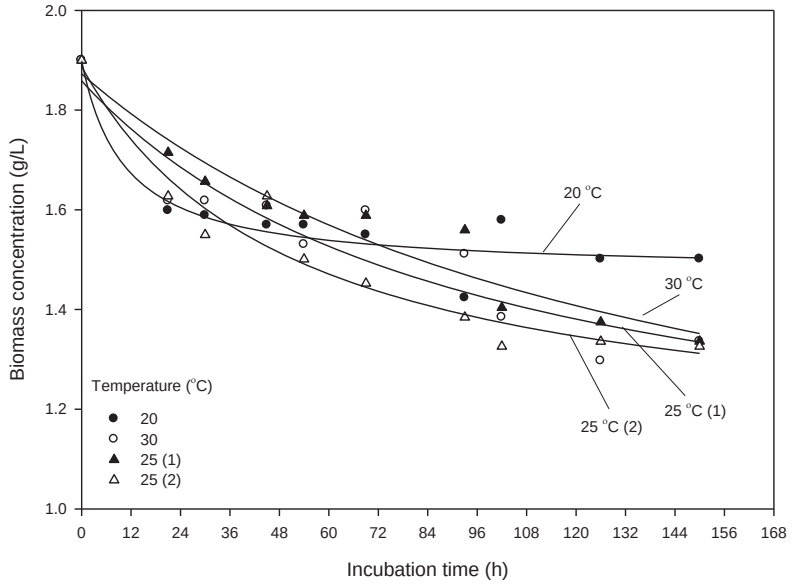

Figure 4.11 *Chlorella vulgaris* biomass loss in the dark during incubation at various temperatures. At 25 °C, the data sets marked (1) and (2) are from two parallel flasks.

From Figure 4.11, in the temperature range of 20-30 °C the rate of biomass loss was not strongly dependent on temperature. The biomass was lost because of respiration. Night-time loss of biomass is well documented for other microalgae (Sánchez Mirón *et al.*, 2000; Miron *et al.*, 2002), but not been previously characterized for *C. vulgaris* in a seawater medium.

The data in Figure 4.11 (excluding the first data point because the culture temperature for this measurement had not reached equilibrium with the incubator temperature) were used to model the biomass loss kinetics as follows:

$$-\frac{dC}{dt} = kC \tag{34}$$

In Equation (34), C and C_0 are the biomass concentrations at time t and time 0 h, respectively. (The time was taken to be 0 h after 21 h of incubation at which time the culture had attained the incubation temperature.) The k (h^{-1}) in Equation (34) is the first-order rate constant for biomass loss. At a constant temperature, Equation (34) could be integrated between the limits $t = 0$, $C = C_0$ and $t = t$, $C = C$, to the following form:

$$-\ln\left(\frac{C}{C_0}\right) = kt \tag{35}$$

From Equation (35), $\ln(C/C_0)$ and t for four fixed incubation temperatures were plotted to obtain the slope $-k$ by linear regression as shown in Figure 4.12.

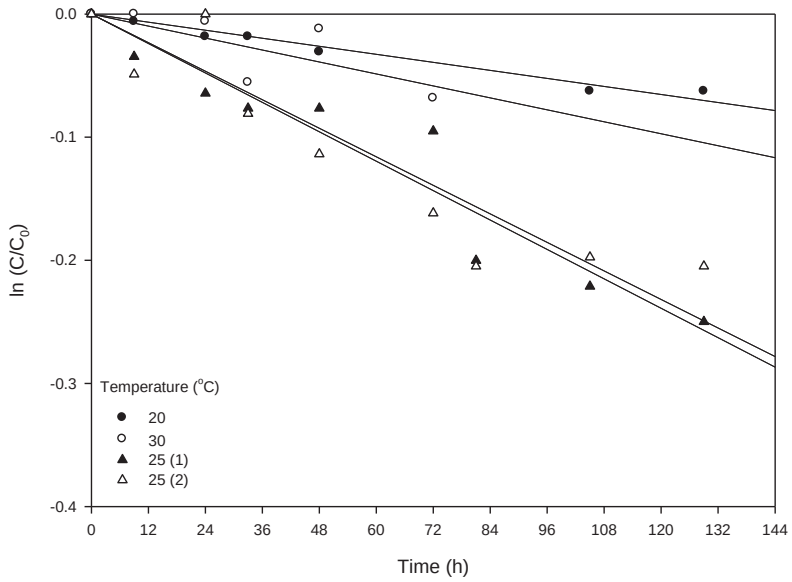

Figure 4.12 Plots of ln(C/C_0) versus time for *C. vulgaris* at various temperatures in the dark. At 25 °C, the data sets marked (1) and (2) are from two parallel flasks.

The *k*-values obtained from Figure 4.12 are shown in Table 4.5. The *k*-values (Table 4.5) for the two duplicate samples incubated at 25 °C were in good agreement (±2% of the averaged value) demonstrating good reproducibility. The *k*-value at 20 °C was substantially lower than the *k*-values at 25 °C while the *k*-value at 25 °C was unexpectedly higher than at 30 °C. This did not agree with the expectation that an increase in temperature should generally increase the self-consumption rate. However, a reason might be that incubation at 30 °C may have been damaging to the normal respiratory metabolism of the alga.

Table 4.5 *C. vulgaris* biomass consumption rate constant *k* in the dark at various temperatures

Incubation temperature (°C)	k (h^{-1}) × 10^{-3}
20	0.545
25 (1)	1.992
25 (2)	1.932
30	0.811

4.2 Culture profiles in tubular photobioreactor

Chlorella vulgaris was cultured in the tubular photobioreactor under various conditions as summarized in Table 4.6 for the 15 separate runs (PBR 1-15). The objective of the initial two runs (PBR 1-2) was to attempt to reproduce in the tubular photobioreactor the growth performance that had been earlier observed in 1 L Duran bottles. This proved impossible because of continual biomass loss through foaming (Section 4.2.1.1) and because the presence of the many tiny gas bubbles in seawater impeded the penetration of light in the culture broth. The other runs (PBR 3-15) attempted to delineate: the effects of nitrate concentration on productivity in batch and continuous operations; the effects of possible contamination with copper on productivity; the effects of incident irradiance on productivity in batch and continuous operations; and possible differences between batch and continuous modes of operation in terms of biomass/lipid productivity. As nearly all the runs were different, a statistical comparison among runs is not feasible.

Table 4.6 Summary of *C. vulgaris* production in the photobioreactor runs

Batch	Conditions
PBR 1	Started with a 9.7% inoculum in a working volume of 77.5 L, using BG-11 seawater medium with full nitrate concentration; 25 °C; pH of 6.8; dissolved oxygen concentration of 6.8-7.0 ppm; recirculation rate of 105.8 L min^{-1}; and illumination by LED lights at 115-171 μmol $m^{-2}s^{-1}$.
PBR 2	Same culture conditions as PBR1. On day 2, culture started foaming.
PBR 3	Started with a 8% inoculum in a working volume of 75 L, using BG-11 seawater medium with full nitrate concentration; 25 °C; pH of 6.8; dissolved oxygen concentration of 6.8-7.0 ppm; recirculation rate of 97 L min^{-1}; and illumination by LED lights at 251-361 μmol $m^{-2}s^{-1}$. On day 6, decreased the illumination level to 115-171 μmol $m^{-2}s^{-1}$. On day 8, humidity unit was installed to prevent evaporation. On day 26, reduced the recirculation rate to 45.2 L min^{-1}. On day 29, increased the illumination level to 251-361 μmol $m^{-2}s^{-1}$. The broth after harvesting on day 49 was kept at 4 °C for 6 days because of a breakdown of the centrifuge.
PBR 4	Same as PBR 3 except: started with a 10% inoculum and recirculation rate of 102.3 L min^{-1}. The broth was harvested on day 38 and held at 4 °C for 7 days because of a breakdown of the centrifuge.
PBR 5	Same culture conditions as PBR 4 except: recirculation rate of 103.3 L min^{-1} and illumination by LED lights at 115-171 μmol $m^{-2}s^{-1}$.

Table 4.6 Summary of *C. vulgaris* production in the photobioreactor runs (Cont.)

Batch	Conditions
PBR 5 (Cont.)	On day 12, started foaming and the foam overflowed from the degassing column. On day 19, washed the deposited biomass from the walls by spraying with tap water (~500 mL) manually. On day 20, a spray head was inserted on the top of the column and continuous spraying with recycled broth was implemented to wash the biomass deposits from the walls into the broth. On day 29, increased the illumination level to 251-361 μmol $m^{-2}s^{-1}$.
PBR 6	Same as PBR 5 except: started with a 9.7% inoculum in a working volume of 77.5 L and a recirculation rate of 104.7 L min^{-1}. On day 0, 3.5 L of broth overflowed because of problems with the dissolved oxygen controller. On day 9, added water (~3.5 L) to bring the volume to 77.5 L. On day 20, culture started foaming. 3 L of broth was harvested and 3 L of the fresh medium without nitrate and copper was added to the reactor on each of days 22, 36, 50, and 64. On day 61, the culture was contaminated with Gram negative bacteria.
PBR 7	Same as PBR 5 except: started with a 9.6% inoculum; dissolved oxygen concentration of 7.9-8.5 ppm; and a recirculation rate of 117.8 L min^{-1} On day 15, the dissolved oxygen probe broke. On day 19, the reactor was shut down for about 1.5 h to replace the

Table 4.6 Summary of *C. vulgaris* production in the photobioreactor runs (Cont.)

Batch	Conditions
PBR 7 (Cont.)	dissolved oxygen probe. On day 24, 4.5 L of BG-11 without nitrate and phosphate was added to bring the broth level up to cover the tip of the pH probe.
PBR 8	Started with a 10% inoculum in a working volume of 75 L, using BG-11 seawater medium with 200 mg L^{-1} of nitrate concentration; 25 °C; pH of 6.8; dissolved oxygen concentration of 8-9 ppm; recirculation rate of 100.8 L min^{-1}; and illumination by LED lights at 115-171 μmol $m^{-2}s^{-1}$. On day 2, 5 L of broth overflowed so 5 L of fresh medium without nitrate and phosphate was added. Also, the dissolved oxygen set point was changed to 9.6-10.0 ppm. On day 24, the culture was contaminated with Gram negative bacteria. On day 35, switched the culture to a continuous mode of operation. The feed medium was BG-11 seawater with 200 mg L^{-1} of nitrate concentration at a dilution rate of 0.3 d^{-1}. After running for 6 days, the culture was washed out.
PBR 9	Same as PBR 8 except: using BG-11 seawater medium with half nitrate concentration; dissolved oxygen concentration of 12.5-14.0 ppm; and recirculation rate of 97.6 L min^{-1}. On day 3 and day 12, 5 L and 1.2 L of broth overflowed, respectively, so 5 L (day 3) and 1.2 L (day 12) of fresh medium without nitrate and phosphate was added to bring up the volume to cover the tip of the pH probe.

Table 4.6 Summary of *C. vulgaris* production in the photobioreactor runs (Cont.)

Batch	Conditions
PBR 9 (Cont.)	On day 12, the culture was switched to continuous mode of operation. The feed was BG-11 seawater medium with 200 mg L^{-1} of nitrate concentration at a dilution rate of 0.12 d^{-1}. On day 26, increased the illumination level to 314-458 μmol $m^{-2}s^{-1}$. On day 32, increased the illumination level to 644-912 μmol $m^{-2}s^{-1}$. On day 33, increased the illumination level to 909-1289 μmol $m^{-2}s^{-1}$. On day 39, the illumination level was decreased to 644-912 μmol $m^{-2}s^{-1}$. On day 46, stopped continuous operation and switched to batch operation.
PBR 10	Same as PBR 9 except: using BG-11 seawater medium with full nitrate concentration; recirculation rate of 118 L min^{-1}, and illumination by LED lights at 314-458 μmol $m^{-2}s^{-1}$. On day 1, 4.5 L of broth overflowed so 4.5 L of fresh medium without nitrate and phosphate was added. On day 13 some biomass was deposited on the walls of the tubes; therefore, increased the recirculation rate to 150-160 L min^{-1} to remove the deposits.
PBR 11	Same culture conditions as PBR 4; recirculation rate of 98.2 L min^{-1} and illumination by LED lights at 314-458 μmol $m^{-2}s^{-1}$. On day 9, 3.5 L of broth was lost because the spray pump leaked; therefore, 3.5 L of BG-11 seawater without nitrate and phosphate was added to the reactor.

Table 4.6 Summary of *C. vulgaris* production in the photobioreactor runs (Cont.)

Batch	Conditions
PBR 12	Same as PBR 9 except: run with a working volume of 77.5 L, using BG-11 seawater medium with 240 mg L^{-1} of nitrate concentration; and recirculation rate of 102.8 L min^{-1}.
PBR 13	Same as PBR 12 except: recirculation rate of 103.8 L min^{-1}. On days 41, 55 and 65, 5 L of nitrate-free fresh medium (with phosphate) was added.
PBR 14	Same as PBR 13 except: recirculation rate of 80 L min^{-1} and illumination by LED lights at 314-458 μmol $m^{-2}s^{-1}$.
PBR 15	Same as PBR 14 except: recirculation rate of 78.9 L min^{-1}.

The total lipid contents and the calorific values of the biomass recovered from the various runs are shown in Table 4.7. The kinetic parameters of the various runs are shown in Table 4.8.

Table 4.7 Total lipid content and calorific value of *C. vulgaris* biomass produced in the photobioreactor

Batch	Total lipid content (%)[a]	Calorific value (kJ g^{-1})[b]
PBR 1	8.5±0.0	25.4
PBR 2	7.8±0.1	24.1
PBR 3	10.3±0.3	25.6
PBR 4	10.9±0.1	21.3
PBR 5	6.3±0.3	23.9
PBR 6	9.6±0.1	23.8
PBR 7	12.3±0.2	24.1
PBR 8	10.7±0.0	22.8
PBR 9	ND	ND
PBR 10	14.4±0.0	24.2
PBR 11	9.9±0.2	22.5
PBR 12	4.2±0.0	14.8
PBR 13	6.2±0.2	21.1
PBR 14	ND	ND
PBR 15	1.9±0.4	16.6

ND – not determined because of insufficient growth.

[a] – mean value ± standard deviation.

[b] – previously shown to be reproducible to ± 2.8% of the mean value (Section 3.10.8).

Table 4.8 Kinetic parameters of *C. vulgaris* production in tubular photobioreactor

Batch	Biomass yield on nitrate ($Y_{X/N}$; g mg^{-1})	Biomass yield on phosphate ($Y_{X/P}$; g mg^{-1})	Specific nitrate consumption rate (q_N; mg $g^{-1}d^{-1}$)	Specific phosphate consumption rate (q_P; mg $g^{-1}d^{-1}$)	Specific growth rate (μ; d^{-1})	Biomass productivity (Q_X; g $L^{-1}d^{-1}$)	Lipid productivity (Q_L; mg $L^{-1}d^{-1}$)
PBR 1	0.005±(4.6×10^{-4})	0.176±0.000	13.14±1.19	0.38±0.00	0.335	0.176	15.08±0.00
PBR 2	0.003±(11.6×10^{-4})	0.055±0.000	11.17±3.74	0.70±0.00	0.169	0.034	2.63±0.00
PBR 3	0.003±(7.46×10^{-4})	0.091±0.002	11.97±3.09	0.38±0.01	0.114	0.047	4.87±0.01
PBR 4	0.000±(3.5×10^{-4})	0.008±0.000	79.37±59.37	4.59±0.28	0.200	0.003	0.32±0.00
PBR 5	0.003±0.000	0.039±0.000	18.51±0.00	1.62±0.00	0.258	0.038	2.37±0.01
PBR 6	0.004±(2.6×10^{-4})	0.091±0.002	14.16±0.87	0.65±0.01	0.266	0.084	8.04±0.00
PBR 7	0.008±(8.8×10^{-4})	0.106±0.000	8.02±0.84	0.63±0.00	0.275	0.111	13.62±0.02
PBR 8	0.004±(9.3×10^{-4})	0.081±0.002	12.43±2.82	0.62±0.01	0.225	0.066	7.03±0.00
PBR 9	0.002±(2.9×10^{-4})	0.035±0.001	42.82±6.46	2.39±0.05	0.140	0.045	ND
PBR 10	0.002±0.000	0.022±0.000	57.34±0.00	5.76±0.11	0.180	0.049	7.02±0.00
PBR 11	0.002±(8.0×10^{-4})	0.020±0.001	54.91±29.12	4.11±0.10	0.124	0.030	3.00±0.00

ND – not determined because of insufficient growth.

Standard deviations are shown for selected measurements.

Table 4.8 Kinetic parameters of *C. vulgaris* production in tubular photobioreactor (Cont.)

Batch	Biomass yield on nitrate ($Y_{X/N}$; g mg^{-1})	Biomass yield on phosphate ($Y_{X/P}$; g mg^{-1})	Specific nitrate consumption rate (q_N; mg $g^{-1}d^{-1}$)	Specific phosphate consumption rate (q_P; mg $g^{-1}d^{-1}$)	Specific growth rate (μ; d^{-1})	Biomass productivity (Q_X; g $L^{-1}d^{-1}$)	Lipid productivity (Q_L; mg $L^{-1}d^{-1}$)
PBR 12	$0.002\pm(9.9\times10^{-4})$	0.010±0.000	57.26±32.55	9.60±0.10	0.194	0.016	0.68±0.00
PBR 13	$0.001\pm(0.6\times10^{-4})$	0.019±0.000	21.28±0.92	1.43±0.02	0.242	0.009	0.56±0.00
PBR 14	0.001±0.000	0.010±0.000	88.10±0.00	12.11±0.12	0.176	0.021	ND
PBR 15	$0.002\pm(1.3\times10^{-4})$	0.020±0.000	30.86±1.68	3.51±0.07	0.170	0.023	0.44±0.01

ND – not determined because of insufficient growth.

Standard deviations are shown for selected measurements.

4.2.1 Batch cultures

4.2.1.1 Effect of nitrate concentration

The runs PBR 1, PBR 9 and PBR 13 were cultured at different initial nitrate concentrations of 1133, 537, and 291 mg L^{-1}, respectively, under a light intensity of 115-171 μmol $m^{-2}s^{-1}$. The culture profiles for PBR 1, PBR 9 and PBR 13 are shown in Figures 4.13-4.15.

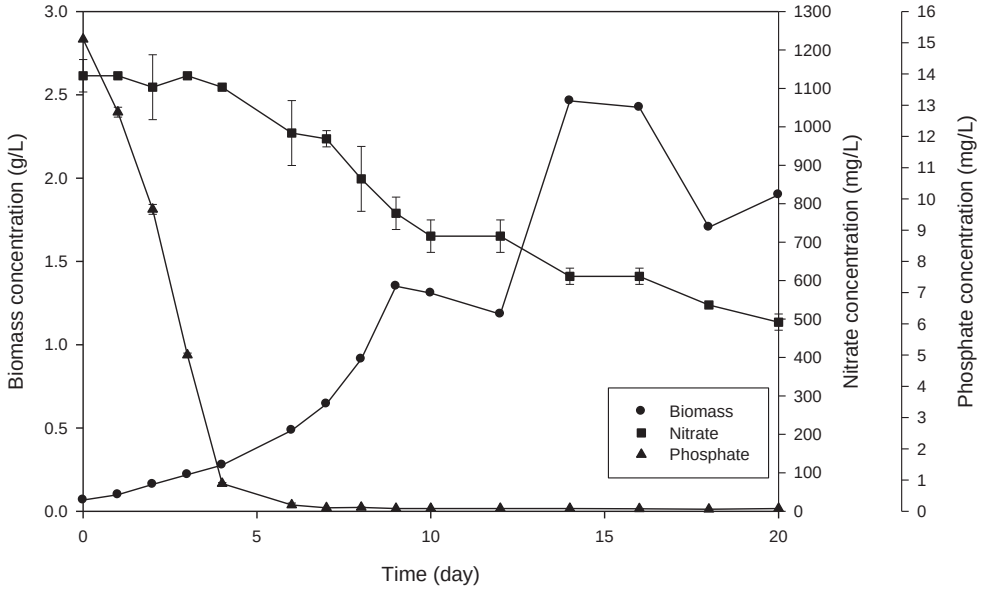

Figure 4.13 Culture profile of *C. vulgaris* in the run PBR 1 with 1133 mg L^{-1} of initial nitrate concentration.

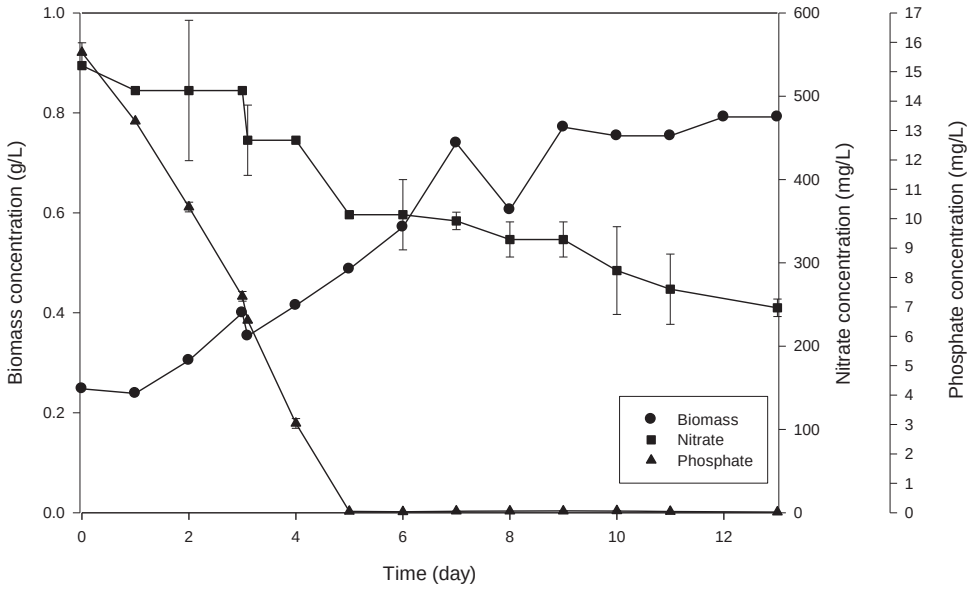

Figure 4.14 Culture profile of *C. vulgaris* in the run PBR 9 with 537 mg L^{-1} of initial nitrate concentration and 0.02 mg L^{-1} of copper concentration.

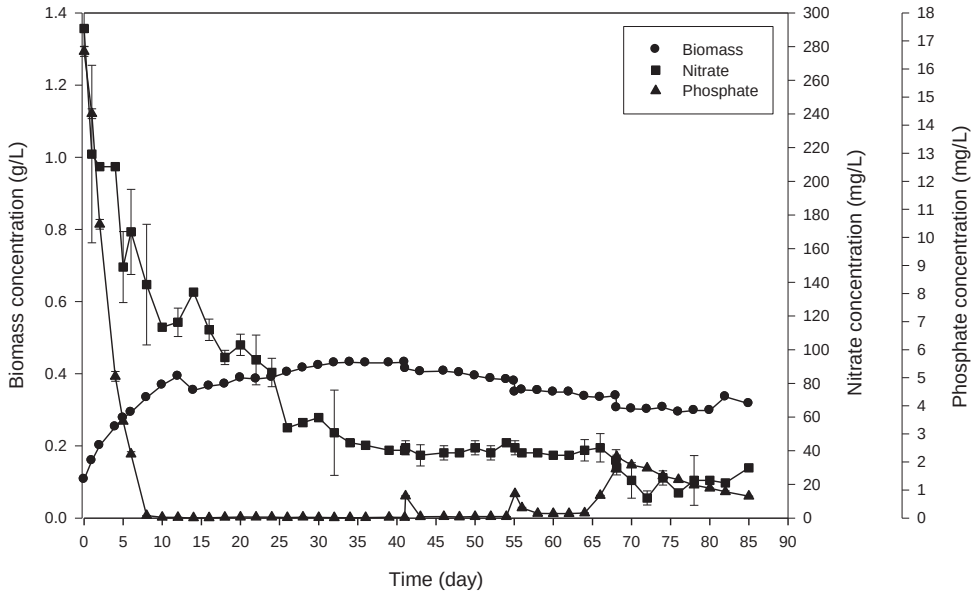

Figure 4.15 Culture profile of *C. vulgaris* in the run PBR 13 with 291 mg L^{-1} of initial nitrate concentration. See Table 4.6 for further details.

As shown in Figures 4.13-4.15, the phosphate was completely consumed in all the runs by day 6-8. As discussed in Section 4.3.1, this does not limit biomass production. The normal initial phosphate concentration of 16.7 mg L^{-1} in the BG-11 medium can support a final biomass concentration of at least 3.7-4.0 g L^{-1} (Section 4.1.1). None of the runs (Figures 4.13-4.15) attained a biomass concentration of >2.7 g L^{-1}. Except possibly in the run PBR 13 (Figure 4.15), the biomass growth was not limited by nitrate as more than 250 mg L^{-1} of nitrate remained in the media by the end of the runs PBR 1 and PBR 9.

Normally, the *C. vulgaris* growth curves tend to be quite smooth (e.g. Figure 4.1). The fluctuation seen in biomass concentration in the tubular photobioreactor (e.g. Figure 4.13 and Figure 4.14) are a consequence of the biomass being removed from the broth by foaming and being washed in again as shown in Figure 4.16.

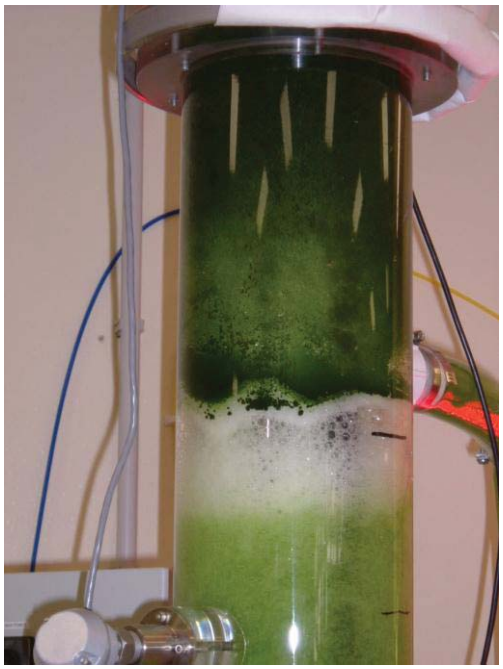

Figure 4.16 Broth foaming in the degassing column.

The total lipid content of the biomass harvested from the runs PBR 1 and PBR 13 (Table 4.7) were relatively low at <10% as none of these cultures were nitrogen starved (Figure 4.14, Figure 4.15). The lipid contents and calorific values could not be measured for the run PBR 9 as insufficient biomass was recovered for these measurements. The biomass from the run PBR 13 harvested on day 41 had a relatively low calorific value (21.1 kJ kg^{-1}) compared with the biomass harvested on day 20 in the run PBR 1 (25.4 kJ kg^{-1}). This difference is substantial considering the ±2.8% reproducibility of measurements of the calorific value (see Section 3.9.8). This suggests that a long duration of a stationary phase (Figure 4.15) has the potential to affect the lipid profiles and therefore the calorific value of the biomass.

In Figure 4.15, the spikes in phosphate concentration (i.e. on day 41, 55, and 65) coincided with the addition of the phosphate-containing nitrate-free fresh medium (Table 4.6). After the last addition (day 65) phosphate was not consumed possibly because the cells had attained the maximum possible level of intracellular phosphate.

The runs PBR 10 and PBR 14 were conducted identically except for the initial nitrate concentrations which were 1372 and 236 mg L^{-1}, respectively. Both these runs took place at a relatively high illumination level of 314-458 μmol $m^{-2}s^{-1}$. (This was nearly 270% of the light level used in the previously mentioned runs PBR 1, PBR 9 and PBR 13.) The culture profiles of the runs PBR 10 and PBR 14 are shown in Figure 4.17 and Figure 4.18, respectively.

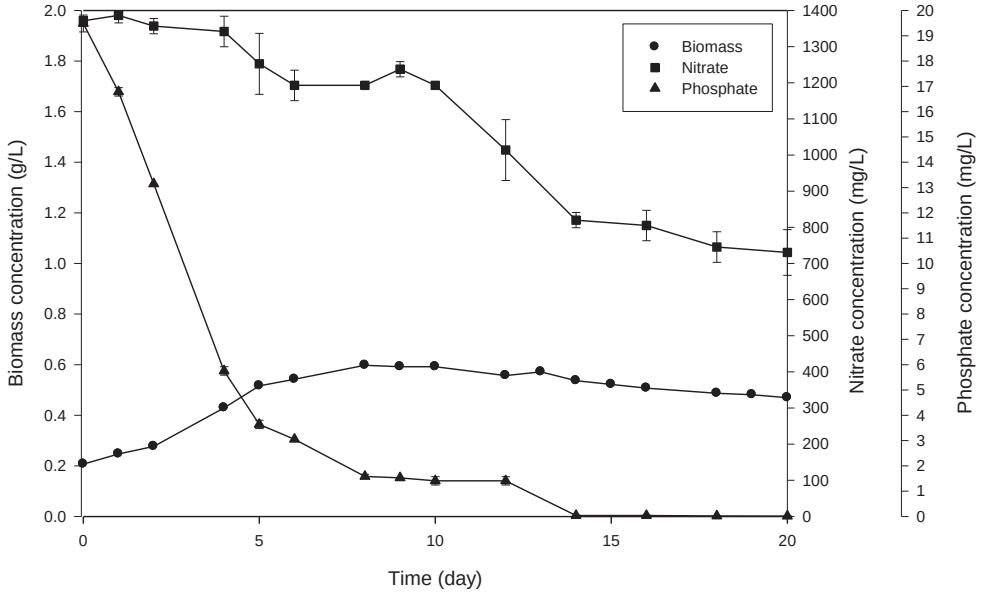

Figure 4.17 Culture profile of *C. vulgaris* in the run PBR 10 with 1372 mg L^{-1} of initial nitrate concentration under a light level of 314-458 μmol $m^{-2}s^{-1}$.

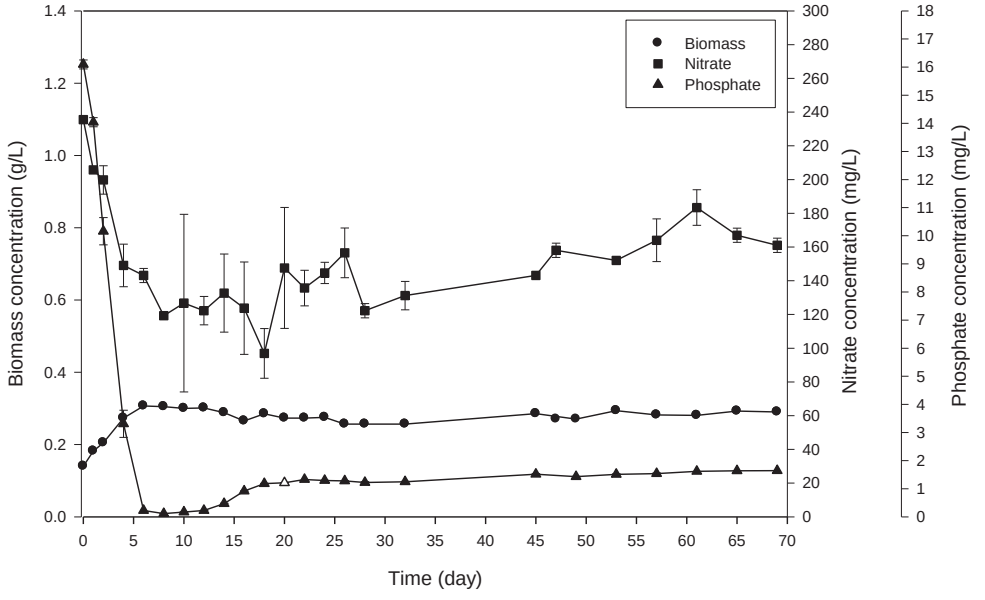

Figure 4.18 Culture profile of *C. vulgaris* in the run PBR 14 with 236 mg L^{-1} of initial nitrate concentration under a light level of 314-458 μmol $m^{-2}s^{-1}$.

The runs PBR 10 and PBR 14, failed to grow well: in PBR 10 the biomass concentration increased to a maximum of about 0.6 g L^{-1} from an inoculation level of about 0.2 g L^{-1} (Figure 4.17) and in PBR 14 the maximum biomass concentration was about 0.3 g L^{-1} (Figure 4.18). The phosphate uptake behaviour of these runs was also unusual: in run PBR 10, phosphate could be detected in the culture supernatant past day 10 (Figure 4.17). In the run PBR 14, phosphate was released from the cells soon after day 10 (Figure 4.18). None of these runs was limited by either nitrate or phosphate, or any other nutrient. The poor growth and the abnormal phosphate consumption behaviour were a likely consequence of a continuous high light level, a level that was photoinhibitory. An irradiance level ≥185 μmol $m^{-2}s^{-1}$ is photoinhibitory for many microalgae (Chisti, 2007). For *C. vulgaris* specifically in freshwater, onset of photoinhibition has been observed at irradiance of >300 μmol $m^{-2}s^{-1}$ (Ratchford & Fallowfield, 2003). Photoinhibition is further discussed by Powles (1984) and Henley (1993).

4.2.1.2 Effect of light

The effects of incident irradiance were further evaluated using the runs PBR 1, PBR 3 and PBR 10 which contained similar initial amounts of nitrate (~1088-1372 g L^{-1}). The incident irradiance levels for the runs PBR 1, PBR 3 and PBR 10 were 115-171, 251-361, and 314-458 μmol $m^{-2}s^{-1}$, respectively. The culture profiles for these runs are shown in Figure 4.13, Figure 4.19 and Figure 4.17.

The specific growth rate (Table 4.8, $\mu = 0.335$ d^{-1}) was the highest for the nonphotoinhibited run PBR 1. In comparison with this, both the runs PBR 3 and PBR 10 were continuously exposed to a photoinhibitory level of irradiance and consequently had specific growth rates that were 34% (PBR 3) and 56% (PBR 10) compared with the specific

growth rate of the run PBR 1 (Table 4.8). Although the incident irradiance level in the run PBR 10 was ~26% greater than the incident irradiance in the run PBR 3 (Table 4.6), the specific growth rate in run PBR 10 was ~58% greater than in the run PBR 3 (Table 4.8). This is because the initial biomass concentration (X_0 = 0.21 g L^{-1}, Figure 4.17) in the run PBR 10 was about 4-fold greater than in the run PBR 3 (X_0 = 0.05 g L^{-1}, Figure 4.19). Both the incident irradiance and the biomass concentration determine the average irradiance level seen by the cells. Thus, if the initial cell density is high, only the cells at the walls experience photoinhibitory irradiance. The cells deeper in the culture broth do not experience photoinhibitory level of irradiance because of self shading. The biomass productivities of the runs PBR 10 and PBR 3 were similar at 0.048±0.001 g $L^{-1}d^{-1}$ (Table 4.8) because in batch cultures of algae the specific growth rate always declines rapidly (exponentially) with an increasing cell concentration that reduces light availability per cell (at a constant incident irradiance). Therefore, the initial difference in the values of the specific growth rates of the cultures does not persist as growth progresses.

4.2.1.3 Effect of copper

Too much copper (Cu^{2+}) is toxic to microalgae (Polynov *et al.*, 1993; Mi-Kyung & Smith, 2001), as Cu^{2+} is a known inhibitor of photosynthesis (Oukarroum *et al.*, 2012). The normal BG-11 medium contains Cu^{2+} at a concentration of 20.1 μg L^{-1}. This level does not inhibit *C. vulgaris* as evidenced by the high specific growth rates and final biomass concentration achieved in Duran bottle cultures (Section 4.1). There was some concern that the generally lower biomass productivities in the tubular photobioreactor (Table 4.8) relative to the Duran bottles (Table 4.1), were due to a possible leaching of Cu^{2+} from the bronze housing of the

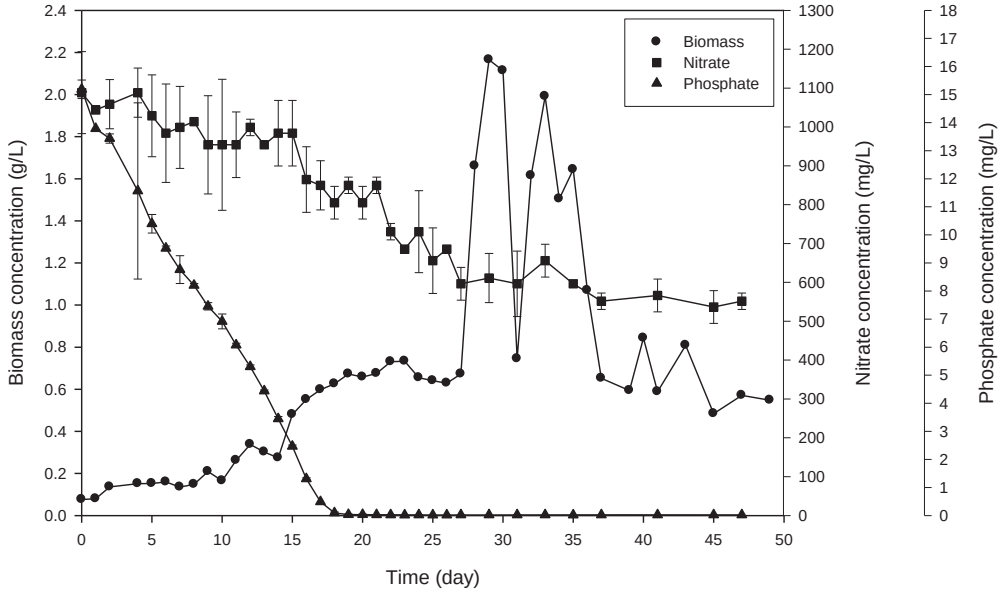

Figure 4.19 Culture profile of *C. vulgaris* in the run PBR 3 with 1088 mg L^{-1} of initial nitrate concentration under a light level of 251-361 μmol $m^{-2}s^{-1}$.

circulation pump (Section 3.5) installed on the photobioreactor. A bronze pump was used because bronze is highly resistant to corrosion by seawater. Modern bronze alloy contains ~88% copper and 12% tin. The directly measured Cu^{2+} concentration in the BG-11 seawater medium was 38 μg L^{-1} (this was higher than in the BG-11 freshwater formulation because sea salt (typically contains <0.5 mg kg^{-1} of copper) contributed about 20 μg L^{-1} of copper) and the measured Cu^{2+} concentration in the BG-11 culture broth harvested from the bioreactor was 43 μg L^{-1}. The measurements failed to reveal any increase in the Cu^{2+} concentration relative to the standard BG-11 seawater medium. Also, an examination of the interior of the pump housing failed to reveal the slightest evidence of corrosion. Therefore, a possible elevated concentration of Cu^{2+} was dismissed as a probable cause of the relatively low productivity of the tubular photobioreactor.

Prior to direct measurements of Cu^{2+} in the culture medium, two identical runs, PBR 6 (Figure 4.20) and PBR 9 (Figure 4.14) (Table 4.6), were carried out to see if Cu^{2+} concentration was being toxic to *C. vulgaris* growth. The runs PBR 6 and PBR 9 were identical in every respect except that no copper was added to the BG-11 seawater formulation used in PBR 6. (A small amount of copper at ~2 μg L^{-1} final concentration, was present because the inoculum (9.7% v/v) contained the normal level of copper at 38 μg L^{-1}.)

The reduced copper run PBR 6 actually had a lower specific growth rate at ~53% of the specific growth rate of the normal copper run PBR 1 (Table 4.8). Also, the biomass productivity of the low copper run PBR 6 was only 87% of the productivity of the normal copper run PBR 9 (Table 4.8). Therefore, reducing the copper level in the culture medium relative to the normal BG-11 level was actually detrimental to biomass production. Previously, a Cu^{2+} concentration of 26 μg L^{-1} has been found to stimulate the growth of the green alga *Selenastrum capricornutum* but a Cu^{2+} concentration of 130 μg L^{-1} has been found to be toxic (Mi-Kyung & Smith, 2001). In *C. vulgaris* grown in a freshwater medium, a Cu^{2+} concentration in the range of 5-100 μg L^{-1} has been found to inhibit growth (Polynov *et al.*, 1993). The Cu^{2+} concentration in the BG-11 medium is about 38 μg L^{-1}, or well below the level that has been found to inhibitory the alga.

The copper-free run PBR 6 attained a peak biomass concentration of ~1.6 g L^{-1} likely because of the carry over of some copper in the inoculum.

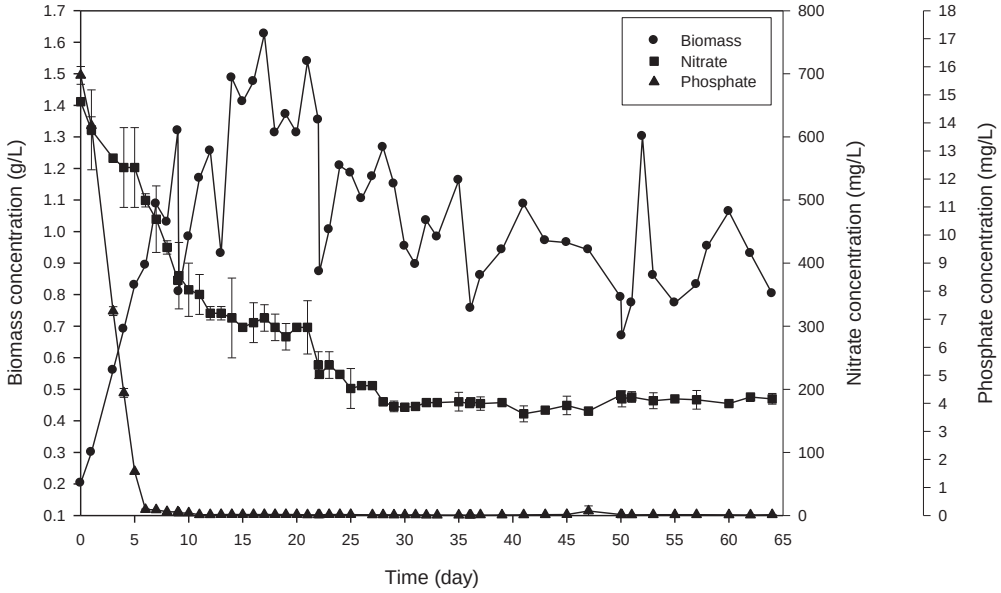

Figure 4.20 Culture profile of *C. vulgaris* in the run PBR 6 without copper under a light level of 115-171 μmol $m^{-2}s^{-1}$.

4.2.2 Continuous cultures

Two of the tubular photobioreactor cultures, the runs PBR 8 and PBR 9, were switched to a continuous mode of operation after a batch operation period. During the continuous cultures the feed was BG-11 seawater medium that contained 200 mg L^{-1} of nitrate concentration. The dilution rates were 0.3 d^{-1} and 0.12 d^{-1} for the runs PBR 8 and PBR 9, respectively. The culture profiles of these runs are shown in Figures 4.21 and 4.22.

For PBR 8 from Figure 4.21, the cell concentration in batch operation increased to >1 g L^{-1}. The subsequent decline and fluctuations were a result of biomass removal in the foam and redeposition as explained in Section 4.2.1.1. The sharp drop in nitrate concentration and biomass concentration on day 29 was because 15 L of the broth was harvested from the reactor and the same volume of the fresh BG-11 seawater medium without nitrate and phosphate was added. All phosphate had been consumed by day 6 of the batch operation. On

day 35, the culture was switched to continuous mode of operation at a dilution rate of 0.3 d^{-1}. In this mode of operation, the phosphate concentration began to rise as the dilution rate was too high. Also, the biomass concentration progressively declined to washout.

For PBR 9, from Figure 4.22, the phosphate was fully consumed by day 6 in the batch operation in keeping with expectations. The biomass concentration increased to a peak of about 0.8 g L^{-1} on day 12. The culture was then switched from batch mode of operation to continuous culture at a dilution rate of 0.12 d^{-1}. In the continuous mode of operation, the phosphate concentration remained essentially nil until day 35. Afterwards, the decrease in biomass concentration because of changed illumination led to a slow increase in phosphate concentration. At day 26, the illumination was increased from 143 to 386 μmol $m^{-2}s^{-1}$ (point A, Figure 4.22). The biomass concentration that was previously dropping stabilized to a steady value possibly because more light could support an increased rate of growth. The light intensity was then further raised up to 778 μmol $m^{-2}s^{-1}$ (point B, Figure 4.22) and the biomass concentration increased to ~0.33 g L^{-1}. The day after, the light illumination was increased still more to 1099 μmol $m^{-2}s^{-1}$ (point C, Figure 4.22) for 6 days. The biomass concentration increased until day 42 and then began to decline. In view of the low biomass concentration in the bioreactor, apparently all biomass was experiencing photoinhibition and possibly photooxidation damage. Therefore on day 39-46, the illumination was reduced to 778 μmol $m^{-2}s^{-1}$ (point D, Figure 4.22) but the algal biomass concentration kept decreasing to eventually stabilize at 0.139 g L^{-1}. At this stage the biomass had recovered from any damage from the previous illumination period. The continuous mode of operation was then switched to a batch mode of operation.

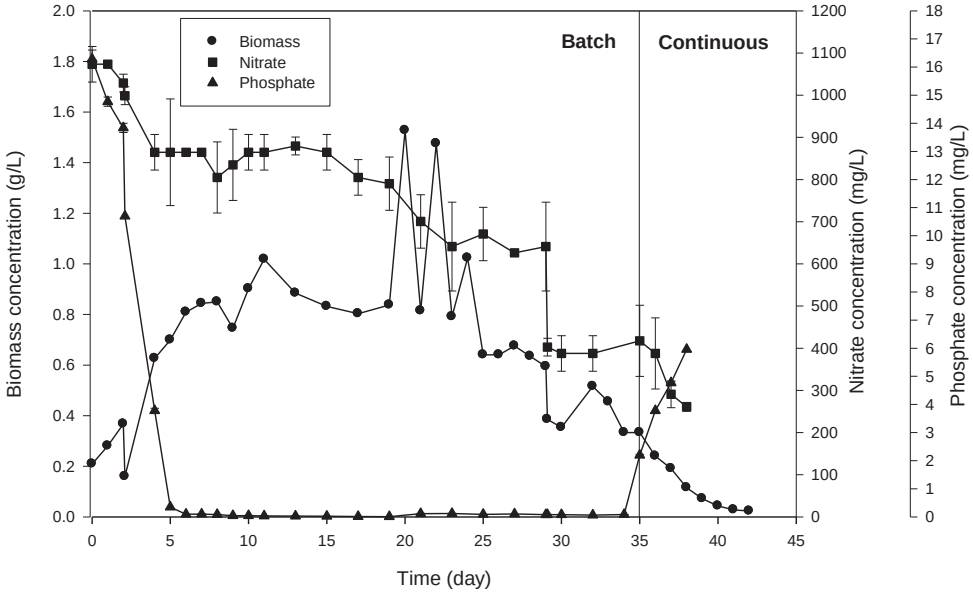

Figure 4.21 Continuous growth profile of *C. vulgaris* in PBR 8 at a dilution rate of 0.3 d^{-1}.

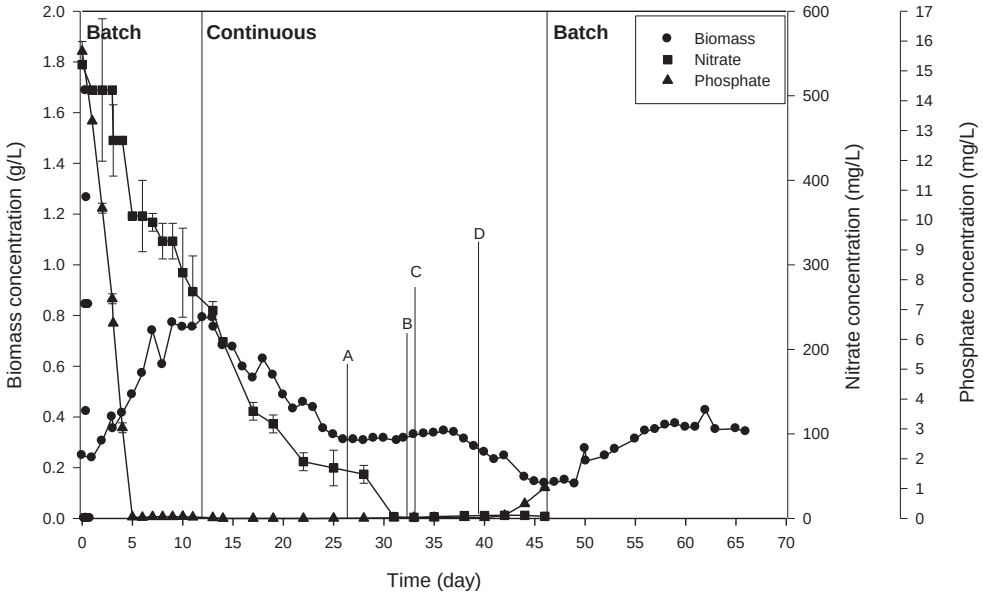

Note A - Light level changed from ~143 μmol $m^{-2}s^{-1}$ to ~386 μmol $m^{-2}s^{-1}$
B - Light level changed from ~386 μmol $m^{-2}s^{-1}$ to ~778 μmol $m^{-2}s^{-1}$
C - Light level changed from ~778 μmol $m^{-2}s^{-1}$ to ~1099 μmol $m^{-2}s^{-1}$
D - Light level changed from ~1099 μmol $m^{-2}s^{-1}$ to ~778 μmol $m^{-2}s^{-1}$

Figure 4.22 Continuous growth profile of *C. vulgaris* in PBR 9 at a dilution rate of 0.12 d^{-1}.

The above changes in light levels during continuous mode of operation were to gain some insight on how growth might be affected by irradiance. As explained above, the responses of the biomass concentration to changes in irradiance were consistent with the expected behaviour: an increase in biomass concentration with increasing light level until the light level was photoinhibitory then a decrease in biomass concentration.

4.3 Culture profiles in stirred-tank bioreactor

Chlorella vulgaris was cultured aseptically in stirred-tank bioreactors (Section 3.6) under various conditions in several batch and continuous cultures, as summarized in Table 4.9.

Table 4.9 Summary of *C. vulgaris* cultures in stirred-tank bioreactors

Batch	Conditions
STR 1	A 10% inoculum in a working volume of 4 L; BG-11 made in seawater as the culture medium (full nitrate concentration); 25 °C; bubbled with 5% (vol/vol) carbon dioxide in air at a flow rate of 1 L min^{-1}; 200 rpm impeller rotational speed; pH of 7.1±0.3 (not controlled); dissolved oxygen concentration of 132±11% (not controlled); illumination by fluorescent lights at 292 μmol $m^{-2}s^{-1}$.
STR 2	Same culture conditions as STR 1 except: using the culture from STR 1 as the inoculum and using 50% of normal nitrate concentration in BG-11 seawater medium; pH of 7.0±0.1 (not controlled); dissolved oxygen concentration of 136±7% (not controlled). On day 39, the temperature controller failed so the culture temperature decreased to 10 °C. The

Table 4.9 Summary of *C. vulgaris* cultures in stirred-tank bioreactors (cont.)

Batch	Conditions
STR 2 (Cont.)	temperature was raised to 20 °C by using a water bath until harvest on day 50.
STR 3	Same culture conditions as STR 1; pH of 6.6±0.3 (not controlled); dissolved oxygen concentration of 96±5% (not controlled).
STR 4	Same culture conditions as STR 2; pH of 6.7±0.1 (not controlled); dissolved oxygen concentration of 124±6% (not controlled). On day 48, the temperature was reduced to 10 °C for overnight. On day 49, the temperature was increased to 20 °C until harvest on day 59.
STR 5	Same culture conditions as STR 4; pH of 6.7±0.3 (not controlled); dissolved oxygen concentration of 124±1% (not controlled). Broth was harvested on day 23, 38, and 60 (final harvest). After each harvest, fresh BG-11 seawater medium without nitrate and phosphate was added. On day 38, after harvesting and adding fresh medium, the temperature was set at 20 °C.
STR 6	Same culture conditions as STR 5; pH of 6.7±0.2 (not controlled); dissolved oxygen concentration of 113±10% (not controlled). The broth was harvested on day 29, 31, 33, 35, 37, 39, and 42 (final harvest), as in STR 5, but the temperature remained constant at the normal set point of 25 °C.
STR 7	Same culture conditions as STR 6; pH of 6.6±0.1 (not controlled); dissolved oxygen concentration of 210±10% (not controlled).

Table 4.9 Summary of *C. vulgaris* cultures in stirred-tank bioreactors (cont.)

Batch	Conditions
STR 7 (cont.)	On day 20, BG-11 seawater medium without nitrate and phosphate was added to bring the volume to 3.5 L. (The volume had declined because of sampling.) On day 28, BG-11 seawater medium without nitrate and phosphate was added to bring volume to 4 L. On day 31, the culture was switched to continuous mode of operation at a feed rate of 26.1 mL h^{-1} and fed with BG-11 seawater medium with 25% of the normal nitrate concentration in the medium. Also, the air flow rate was changed from 2 L min^{-1} to 1 L min^{-1}. On day 37 and 45 (at steady state), the effluent from the reactor was collected. On day 48, the agitation speed was increased up to 400, 600 and then 800 rpm to dislodge some biomass that was stuck to the walls and then reset to 200 rpm. On day 52, at steady state, the effluent from the reactor was harvested. The entire culture broth was harvested on day 59.
STR 8	Same culture conditions as STR 1 except using light-emitting diodes as the light source with an irradiance of 1123 μmol $m^{-2}s^{-1}$; pH of 6.7±0.1 (not controlled); dissolved oxygen concentration of 149±28% (not controlled). On day 27, BG-11 seawater medium without nitrate and phosphate was added to bring volume to 4 L. On day 30, the batch culture was switched to continuous mode of operation

Table 4.9 Summary of *C. vulgaris* cultures in stirred-tank bioreactors (cont.)

Batch	Conditions
STR 8 (Cont.)	at a feed rate of 36.6 mL h^{-1}. The feed medium was the normal BG-11 seawater medium. On day 36 and 41, harvested the effluent from the reactor. On day 48 and 54, harvested the effluent from the reactor at steady state as SS1. On day 55, decreased the feed rate to 13.2 mL h^{-1}. On day 63, the culture was found to be contaminated. On day 68, the feeding was stopped because the volume in the vessel had risen to 5 L because of a blockage of the effluent tube. On day 70 and 86, harvested the effluent from the reactor at steady state as SS2.
STR 9	Same culture conditions as STR 1 except an impeller rotational speed of 400 rpm; pH of 6.6±0.2 (not controlled); dissolved oxygen concentration was not measured because the dissolve oxygen probe had broken down during the run. On day 41, switched the culture to continuous mode of operation at a feed rate of 13.2 mL h^{-1}. The feed was normal BG-11 seawater medium. On day 42, reduced the impeller rotational speed to 200 rpm. On day 54 and 69, harvested the effluent from the reactor. On day 83, harvested the effluent from the reactor at steady state. On day 98, harvested the entire culture in the vessel.
STR 10	Same culture conditions as STR 9 except using light-emitting diodes as the

Table 4.9 Summary of *C. vulgaris* cultures in stirred-tank bioreactors (cont.)

Batch	Conditions
STR 10 (Cont.)	light source with an irradiance of 200 μmol $m^{-2}s^{-1}$; pH of 6.9±0.3 (not controlled); dissolved oxygen concentration of 162±22% (not controlled).
STR 11	Same culture conditions as STR 10 except using light-emitting diodes as the light source with an irradiance of 600 μmol $m^{-2}s^{-1}$; pH of 7.2±5 (not controlled); dissolved oxygen concentration of 129±12% (not controlled). On day 1, reduced the impeller rotational speed to 300 rpm because of foaming. On day 27, reduced the impeller rotational speed to 200 rpm because of foaming. On day 35, switched the batch culture to a continuous mode of operation at a feed rate of 13.2 mL h^{-1}. The feed was the normal BG-11 seawater medium. On day 93, harvested the effluent from the reactor at steady state as SS11. Then, increased the feed rate to 26.1 mL h^{-1}. On day 116, the temperature rose up to 30 °C because of a power failure. On day 121, harvested the effluent from the reactor at steady state as SS12. Then, increased the feed rate to 36.6 mL h^{-1}. On day 160, harvested the effluent from the reactor at steady state as SS13. Then, increased the feed rate to 57 mL h^{-1}. On day 177, harvested the effluent from the reactor at steady state as SS14. Then, decreased the feed rate to 13.2 mL h^{-1} and increased the light level to 862 μmol $m^{-2}s^{-1}$.

Table 4.9 Summary of *C. vulgaris* cultures in stirred-tank bioreactors (cont.)

Batch	Conditions
STR 11 (Cont.)	On day 234, harvested the effluent from the reactor at steady state as SS21. Then, increased the feed rate to 26.1 mL h^{-1}. On day 282, harvested the effluent from the reactor at steady state as SS22. Then, increased the feed rate to 36.6 mL h^{-1}. On day 299, harvested the effluent from the reactor at steady state as SS23. Then, increased the feed rate to 57 mL h^{-1}. On day 310, harvested the effluent from the reactor at steady state as SS24.
STR 12	Same culture conditions as STR 11 except using light-emitting diodes as the light source with an irradiance of 177 μmol $m^{-2}s^{-1}$ and the impeller rotational speed of 300 rpm; pH of 6.9±0.3 (not controlled); dissolved oxygen concentration of 161±123% (not controlled). (This high level of fluctuation in the dissolved oxygen concentration was apparently due to a faulty electrode.) On day 26, reduced the impeller rotational speed to 200 rpm because of foaming. On day 34, switched the batch culture to a continuous mode of operation at a feed rate of 13.2 mL h^{-1}. The feed was the normal BG-11 seawater medium. On day 86, harvested the effluent from the reactor at steady state as SS11. Then, increased the feed rate to 26.1 mL h^{-1}. On day 115, the temperature rose up to 29 °C because of a power failure. On day 119, harvested the effluent from the reactor at steady state as SS12.

Table 4.9 Summary of *C. vulgaris* cultures in stirred-tank bioreactors (cont.)

Batch	Conditions
STR 12 (cont.)	Then, increased the feed rate to 36.6 mL h^{-1}. On day 138, stopped feeding because the volume in the vessel had risen to nearly 6 L because of the blocked effluent tube. On day 162, harvested the effluent from the reactor at steady state as SS13. Then, increased the feed rate to 57 mL h^{-1}. On day 180 and 196, harvested the effluent from the reactor at steady state as SS14. Then, decreased the feed rate to 13.2 mL h^{-1} and also reduced the light level to 76 μmol $m^{-2}s^{-1}$. On day 261, harvested the effluent from the reactor at steady state as SS21. Then, increased the feed rate to 26.1 mL h^{-1}. On day 277, harvested the effluent from the reactor at steady state as SS22. Then, increased the feed rate to 36.6 mL h^{-1}. On day 297, harvested the effluent from the reactor at steady state as SS23. Then, increased the feed rate to 57 mL h^{-1}. On day 303, stopped feeding because the volume in the vessel had risen to over 6 L as a result of the effluent tube blocking. On day 311, harvested the effluent from the reactor at steady state as SS24.

The total lipid contents and the calorific values of the harvested biomass are shown in Table 4.10. Also, the culture kinetic parameters for all the runs are shown in Table 4.11 and Table 4.12.

Table 4.10 Total lipid contents and calorific values of *C. vulgaris* biomass from stirred-tank bioreactors

Run	Total lipid content (%)[a]	Calorific value (kJ g^{-1})[b]
STR 1	17.5±0.22	27.6
STR 2	59.1±0.34	27.0
STR 3	26.9±0.91	ND
STR 4	53.4±0.64	30.8
STR 5 (Day 23)	21.8±1.11	28.6
(Day 38)	48.3±0.06	30.4
(Day 60)	49.0±1.78	32.1
STR 6 (Day 29)	15.0±0.31	29.0
(Day 31)	16.9±0.16	29.2
(Day 33)	18.7±0.90	29.6
(Day 35)	27.8±5.32	29.7
(Day 37)	27.8±0.64	30.0
(Day 39)	35.1±0.69	29.6
(Day 42)	37.5±0.35	30.1
STR 7 at steady state 1 (SS1)	12.1±0.45	24.7
STR 8 at steady state 1 (SS1)	7.1±0.13	23.6
steady state 2 (SS2)	5.1±0.11	24.4

ND – not determined because of insufficient growth.

[a] – mean value ± standard deviation.

[b] – previously shown to be reproducible to ± 2.8% of the mean value (Section 3.10.8).

Table 4.10 Total lipid contents and calorific values of *C. vulgaris* biomass from stirred-tank bioreactors (cont.)

Run	Total lipid content (%)[a]	Calorific value (kJ g^{-1})[b]
STR 9 at steady state (SS1)	15.6±0.20	22.9
STR 10	20.11±0.03	26.6
STR 11 at SS11	9.5±0.03	25.0
SS12	10.4±0.19	23.3
SS13	11.3±0.39	23.2
SS14	13.7±0.29	22.9
SS21	12.1±0.78	23.0
SS22	9.4±0.32	22.7
SS23	11.6±0.05	22.6
SS24	14.1±0.23	22.2
STR 12 at SS11	7.6±0.31	24.9
SS12	14.4±0.30	23.4
SS13	11.7±0.03	22.6
SS14	14.9±1.19	23.0
SS21	9.5±0.66	23.1
SS22	12.2±0.46	22.9
SS23	15.5±0.58	23.1
SS24	17.7±0.46	22.4

[a] – mean value ± standard deviation.

[b] – previously shown to be reproducible to ± 2.8% of the mean value (Section 3.10.8).

Table 4.11 Culture kinetic parameters for *C. vulgaris* from stirred-tank bioreactors

Run	Biomass yield on nitrate ($Y_{X/N}$; g mg^{-1})	Biomass yield on phosphate ($Y_{X/P}$; g mg^{-1})	Specific nitrate consumption rate (q_N; mg $g^{-1}d^{-1}$)	Specific phosphate consumption rate (q_P; mg $g^{-1}d^{-1}$)	Biomass yield on light ($\times10^{-7}$) ($Y_{X/light}$; g μmol^{-1})	Specific growth rate (μ; d^{-1})	Biomass productivity (Q_X; g $L^{-1}d^{-1}$)
STR 1	0.004±(0.5×10^{-4})	0.355±0.005	8.85±0.10	0.10±0.00	2.35	0.438	0.134
STR 2	0.008±(5.2×10^{-4})	2.573±0.000	3.51±0.23	0.01±0.00	1.25	0.048	0.071
STR 3	0.002±(0.9×10^{-4})	0.134±0.003	11.15±0.51	0.17±0.00	7.97	0.432	0.046
STR 4	0.005±(1.5×10^{-4})	0.212±0.007	3.72±0.11	0.09±0.00	1.07	0.491	0.061
STR 5 (day 23)	0.003±(0.1×10^{-4})	0.178±0.007	9.08±0.02	0.25±0.01	2.08	0.327	0.119
STR 6 (day 29)	0.006±(1.3×10^{-4})	0.225±0.004	5.47±0.11	0.15±0.00	1.94	0.265	0.111
STR 7 at SS1	0.002±(0.9×10^{-4})	0.044±0.000	95.63±5.08	3.53±0.00	19.00	0.157	0.110
STR 8 at SS1	0.001±(1.0×10^{-4})	0.046±0.001	184.02±14.97	4.83±0.06	6.00	0.220	0.142
SS2	0.001±(1.0×10^{-4})	0.065±0.001	59.29±4.26	1.21±0.01	3.00	0.079	0.073
STR 9 at SS1	0.002±(3.7×10^{-4})	0.064±0.001	34.44±5.54	1.24±0.03	13.00	0.079	0.075
STR 10	0.003±(1.4×10^{-4})	0.156±0.010	9.05±0.39	0.20±0.01	4.54	0.374	0.071
STR 11 at SS11	0.002±(3.0×10^{-4})	0.052±0.000	36.59±5.11	1.52±0.01	5.00	0.079	0.057
SS12	0.002±(2.6×10^{-4})	0.065±0.001	69.80±8.22	2.41±0.02	11.00	0.157	0.141

Table 4.11 Culture kinetic parameters for *C. vulgaris* from stirred-tank bioreactors (cont.)

Run		Biomass yield on nitrate ($Y_{X/N}$; g mg^{-1})	Biomass yield on phosphate ($Y_{X/P}$; g mg^{-1})	Specific nitrate consumption rate (q_N; mg $g^{-1}d^{-1}$)	Specific phosphate consumption rate (q_P; mg $g^{-1}d^{-1}$)	Biomass yield on light ($\times10^{-7}$) ($Y_{X/light}$; g μmol^{-1})	Specific growth rate (μ; d^{-1})	Biomass productivity (Q_X; g $L^{-1}d^{-1}$)
	SS13	0.006±(19.5×10^{-4})	0.053±0.000	38.70±13.32	4.16±0.03	13.00	0.220	0.161
	SS14	0.001±(3.1×10^{-4})	0.029±0.000	246.36±54.44	11.68±0.10	11.00	0.342	0.139
	SS 21	0.002±(2.2×10^{-4})	0.063±0.001	39.36±4.36	1.25±0.01	4.00	0.079	0.070
	SS22	0.004±(7.77×10^{-4})	0.077±0.001	39.05±7.47	2.04±0.02	9.00	0.157	0.167
	SS23	0.006±(19.8×10^{-4})	0.060±0.000	35.33±11.26	3.66±0.03	10.00	0.220	0.183
	SS24	0.005±(19.9×10^{-4})	0.041±0.000	67.74±26.67	8.24±0.07	11.00	0.342	0.197
STR 12 at	SS11	0.004±(8.2×10^{-4})	0.069±0.002	22.73±5.37	1.15±0.04	21.00	0.079	0.076
	SS12	0.007±(34.8×10^{-4})	0.064±0.002	23.56±12.32	2.46±0.09	38.00	0.157	0.140
	SS13	0.002±(9.8×10^{-4})	0.022±0.001	110.58±54.44	10.18±0.36	18.00	0.220	0.066
	SS14	–0.008±(116×10^{-4})	0.030±0.001	–41.73±59.26	11.32±0.44	36.00	0.342	0.131
	SS 21	0.004±(14.2×10^{-4})	0.052±0.002	21.76±8.45	1.54±0.05	36.00	0.079	0.057
	SS22	0.005±(29.7×10^{-4})	0.039±0.001	31.13±18.38	4.05±0.14	54.00	0.157	0.085
	SS23	–0.018±(543×10^{-4})	0.038±0.001	–11.90±35.05	5.77±0.22	69.00	0.220	0.109
	SS24	0.018±(867×10^{-4})	0.027±0.001	18.68±88.48	12.57±0.62	59.00	0.342	0.093

Table 4.12 Lipid production by *C. vulgaris* in stirred-tank bioreactors

Run	Lipid yield on nitrate ($Y_{Lipid/N}$; g mg^{-1})	Lipid yield on phosphate ($Y_{Lipid/P}$; g mg^{-1})	Specific lipid production rate (q_{Lipid}; mg $g^{-1}d^{-1}$)	Lipid yield on light ($\times 10^{-7}$) ($Y_{Lipid/light}$; g μmol^{-1})	Lipid productivity (Q_L; mg $L^{-1}d^{-1}$)
STR 1	-	-	-	0.41±0.01	23.46±0.29
STR 2	-	-	-	0.74±0.00	42.24±0.25
STR 3	-	-	-	0.22±0.01	12.27±0.41
STR 4	-	-	-	0.57±0.01	32.71±0.39
STR 5 (Day 38)	-	-	-	0.45±0.02	27.16±0.03
STR 6 (Day 29)	-	-	-	0.29±0.01	16.63±0.34
STR 7 at SS1	0.000±(1.9×10^{-5})	0.0053±0.0003	0.019±0.001	2.33±0.08	13.31±0.50
STR 8 at SS1	0.000±(1.1×10^{-5})	0.0032±0.0001	0.016±0.000	0.44±0.01	10.13±0.19
SS2	0.000±(0.5×10^{-5})	0.0033±0.0001	0.004±0.000	0.16±0.00	3.71±0.08
STR 9 at SS1	0.000±(6.1×10^{-5})	0.0100±0.0003	0.012±0.000	2.05±0.03	11.69±0.15
STR 10	-	-	-	0.91±0.00	19.07±0.02
STR 11 at SS11	0.000±(3.9×10^{-5})	0.0049±0.0001	0.008±0.000	0.44±0.00	5.43±0.02
SS12	0.000±(3.1×10^{-5})	0.0068±0.0001	0.016±0.000	1.19±0.02	14.75±0.23

Table 4.12 Lipid production by *C. vulgaris* in stirred-tank bioreactors (cont.)

Run	Lipid yield on nitrate ($Y_{Lipid/N}$; g mg^{-1})	Lipid yield on phosphate ($Y_{Lipid/P}$; g mg^{-1})	Specific lipid production rate (q_{Lipid}; mg $g^{-1}d^{-1}$)	Lipid yield on light ($\times10^{-7}$) ($Y_{Lipid/light}$; g μmol^{-1})	Lipid productivity (Q_L; mg $L^{-1}d^{-1}$)
SS13	$0.001\pm(30.4\times10^{-5})$	0.0060±0.0003	0.025±0.001	1.47±0.05	18.29±0.62
SS14	$0.000\pm(10.3\times10^{-5})$	0.0040±0.0002	0.047±0.001	1.53±0.03	19.01±0.40
SS 21	$0.000\pm(3.5\times10^{-5})$	0.0076±0.0006	0.010±0.001	0.47±0.03	8.40±0.54
SS22	$0.000\pm(6.9\times10^{-5})$	0.0072±0.0003	0.015±0.001	0.88±0.03	15.71±0.54
SS23	$0.001\pm(27.6\times10^{-5})$	0.0070±0.0001	0.026±0.000	1.19±0.06	21.28±0.10
SS24	$0.001\pm(48.5\times10^{-5})$	0.0058±0.0002	0.048±0.001	1.56±0.02	27.78±0.45
STR 12 at SS11	$0.000\pm(6.6\times10^{-5})$	0.0050±0.0003	0.006±0.000	1.57±0.06	5.75±0.24
SS12	$0.001\pm(56.0\times10^{-5})$	0.0090±0.0002	0.022±0.000	5.48±0.10	20.06±0.42
SS13	$0.000\pm(38.1\times10^{-5})$	0.0025±0.0003	0.026±0.000	2.12±0.01	7.75±0.02
SS14	$-0.001\pm(453\times10^{-5})$	0.0045±0.0010	0.051±0.004	5.36±0.43	19.62±1.56
SS 21	$0.000\pm(19.0\times10^{-5})$	0.0049±0.0005	0.008±0.001	3.45±0.23	5.43±0.38
SS22	$0.001\pm(67.0\times10^{-5})$	0.0047±0.0004	0.019±0.001	6.53±0.25	10.27±0.39
SS23	$-0.003\pm(1704\times10^{-5})$	0.0059±0.0006	0.034±0.001	10.73±0.40	16.88±0.63
SS24	$0.003\pm(4.6\times10^{-5})$	0.0048±0.0010	0.060±0.002	10.49±0.27	16.51±0.43

4.3.1 Batch cultures

The batch cultures focused on characterizing algal biomass growth and oil production particularly under conditions of nitrogen limitation that are known to enhance the total lipid level in *C. vulgaris* biomass grown in freshwater (Converti *et al.*, 2009). For example, in freshwater media, (Illman *et al.*, 2000; Scragg *et al.*, 2002) reported an increased calorific value of *Chlorella* strains grown under nitrogen limitation. Nitrogen is of course essential for growth of biomass as it is needed for making proteins, DNA, RNA, chlorophyll and other metabolites. A nitrogen limitation imposed after the biomass has been grown to a certain level prevents or slows further biomass growth. Under these conditions in many algae, the starch formed as a result of photosynthesis is used to produce storage lipids while the concentration of the biomass declines to some extent. An increased concentration of energy-rich oils in the cell results in an increased calorific value.

Prior to studies of nitrogen limited growth, a baseline culture profile was generated (Figure 4.23) for *C. vulgaris* growing in BG-11 seawater medium with the normal full nitrate level. Subsequently, the alga was grown in BG-11 seawater medium containing 50% of the normal initial nitrate concentration (Figure 4.24).

Both cultures (Figure 4.23, Figure 4.24) attained a biomass concentration of ~4 g L^{-1} on day 28 and 36, but the actual growth, i.e. the change in biomass concentration from inoculation to day 36, was smaller (2.57 g L^{-1}) in the nitrogen limited (half nitrate) culture (Figure 4.24) compared with 3.76 g L^{-1} in the nonlimited culture (Figure 4.23). In the nonlimited culture, 142 mg L^{-1} (or 13% of the initial nitrate) of nitrate remained on day 28 (Figure 4.23). In contrast, in the nitrate limited culture (Figure 4.24), 95% of the initial nitrate had been consumed by day 36. In both cultures (Figure 4.23, Figure 4.24), the phosphate concentration declined sharply to nearly zero within 4 days. This might suggest an

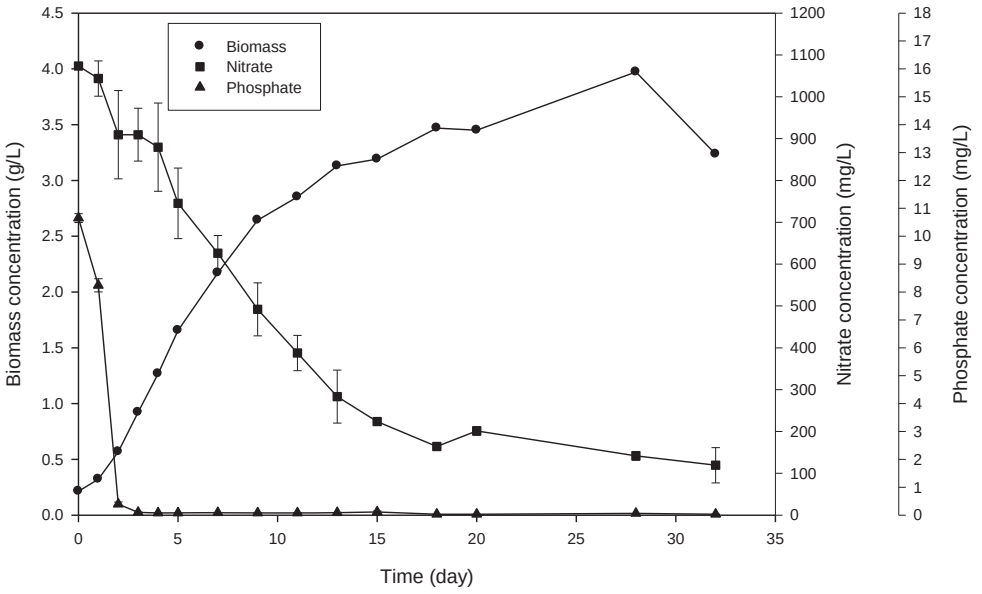

Figure 4.23 Growth profile of *C. vulgaris* in STR 1 with normal nitrate (BG-11 seawater) under illumination of 292 μmol $m^{-2}s^{-1}$ by fluorescent lights.

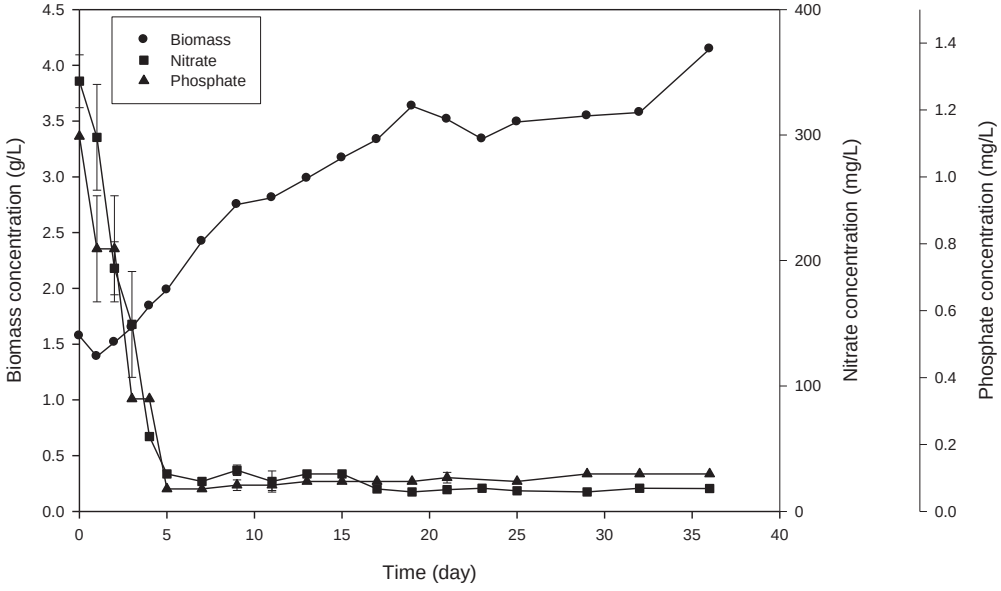

Figure 4.24 Growth profile of *C. vulgaris* in STR 2 with half nitrate under illumination of 292 μmol $m^{-2}s^{-1}$ by fluorescent lights.

insufficiency of phosphate in the medium, but this was not so. The rapid decline in phosphate concentration as in Figures 4.23 and 4.24 is common for microalgae, especially for *C. vulgaris* which is known to accumulate excess phosphorus as intracellular polyphosphate when growing in a phosphorus rich medium (Miyachi & Miyachi, 1961; Miyachi & Tamiya, 1961; Miyachi *et al.*, 1964; Cembella *et al.*, 1984; John & Flynn, 2000; Eixler *et al.*, 2005). The rate of phosphate absorption is enhanced if the algae are transferred from a phosphorus short culture to a phosphorus rich medium (Hernández *et al.*, 2006). The intracellular accumulation of phosphate assures that the alga can continue to grow without limitation for many generations as in Figure 4.23.

Based on the atomic ratio of carbon, nitrogen and phosphorus in phytoplankton (i.e. the Redfield ratio, C:N:P = 106:16:1), the normal maximum phosphorus content of algal biomass should be around 2% by weight. The normal BG-11 medium contains 5.45 mg L^{-1} of elemental phosphorus (based on 16.7 mg L^{-1} of PO_4^{3-}); therefore, based on Redfield ratio, the medium can support a maximum biomass concentration of 0.45 g L^{-1}. In practice, the standard BG-11 seawater medium could provide a maximum measured biomass concentration of 3.7 g L^{-1} in Duran bottles (Section 4.1.1). This is inconsistent with the estimate based on the Redfield ratio, but in practice, the Redfield ratio is quite plastic (Geider & Roche, 2002; Hakanson & Stenstrom-Khalili, 2009). For example, in phytoplankton, under nutrient replete conditions, the value of N:P atomic ratio can range from 5:1 to 19:1 (Geider & Roche, 2002). Similarly, the C:P ratio can range from 27:1 to 135:1 (Geider & Roche, 2002). A revised Redfield ratio consistent with the above mentioned ranges would be C:N:P of 135:19:1, corresponding to a P content in the biomass of 1.6% by weight. The mean molecular formula of the algal biomass of $CO_{0.48}H_{1.83}N_{0.11}P_{0.01}$ available in the literature (Grobbelaar, 2004; Chisti, 2007) suggests a P mass fraction in the biomass of

1.3% w/w, or ~65% of the Redfield ratio. In practice, the measured biomass concentration of 3.7 g L^{-1} suggests that the P content in the biomass could be as low as 0.15%.

Studies conducted by others at Massey University with *C. vulgaris* have confirmed that further supplementation of P to above the normal level in BG-11 does not increase the final attainable biomass concentration in a 2 L Duran batch culture (Y. Chisti, Personal Communication) as near a concentration of 4 g L^{-1} the culture is strongly light limited.

For STR 2 (Figure 4.24), the biomass from STR 1 was used as the inoculum. In nitrogen limited culture (Figure 4.24), the nitrate was consumed much earlier than in the nitrogen sufficient culture (Figure 4.23). The kinetic parameters for the culture STR 1 (Figure 4.20) and STR 2 (Figure 4.24) are shown in Table 4.11. Clearly, the specific growth rate of the biomass was nearly 9-fold greater (Table 4.11) under nitrogen sufficiency (STR 1) when compared with STR 2. However, in the low nitrogen environment of STR 2, the biomass yield on nitrate was twice the yield in the nitrogen sufficient STR 1 (Table 4.11). Therefore, nitrate was more efficiently used by the alga in a low nitrogen environment. A low nitrogen environment also improved the efficiency of utilization of phosphorus (Table 4.11). The biomass productivity of the nonlimited culture (STR 1) was nearly 1.9 fold the biomass productivity of the nitrogen limited culture (STR 2) (Table 4.11). However, the nitrogen limited culture had a total lipid productivity that was 1.8 fold greater compared with the lipid productivity of the nitrate sufficient STR 1 (Table 4.12). This confirmed that in seawater-based media, the effect of nitrogen limitation on lipid contents previously reported in freshwater *C. vulgaris* (Converti *et al.*, 2009), does occur. As shown in Table 4.10, the lipid content in the biomass of the low nitrate run (STR 2) was nearly 3.4 fold greater than the lipid content of the biomass from the nitrate sufficient run (STR 1). The difference in the lipid contents of the biomass from the runs STR 1 and STR 2 did not translate into a difference in the calorific value of the biomass (Table 4.10). The calorific value of the

biomass samples of STR 1 and STR 2 were within 1% of each other and were not significantly different. (For replicate samples, the reproducibility of measurements of the calorific value is ±2.8%, based on experience with other biomass samples.) This suggests that the composition of the lipids in the biomass samples of the runs STR1 and STR 2 was different as different oils have different calorific values.

The low nitrate run STR 2 was repeated as the run STR 4. The culture profile for this replicated run is shown in Figure 4.25.

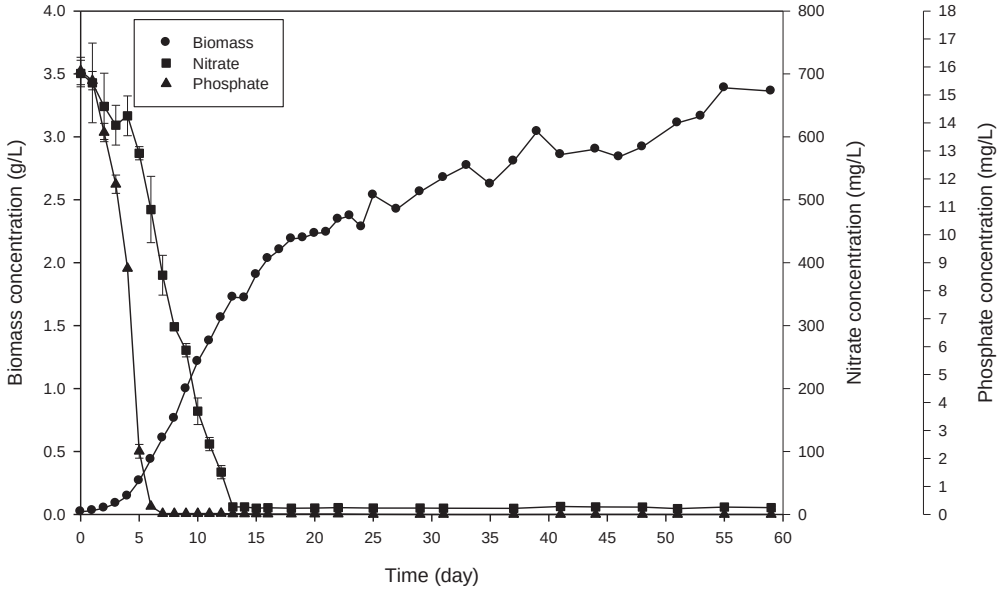

Figure 4.25 Growth profile of *C. vulgaris* in STR 4 with half nitrate under illumination of 292 μmol $m^{-2}s^{-1}$ by fluorescent lights.

The culture profiles in Figure 4.25 are generally similar to those shown in Figure 4.24. The nitrate and phosphate consumption rates in Figure 4.25 are lower than in Figure 4.24 because the initial concentration of the biomass (i.e. concentration at inoculation) is lower in Figure 4.25.

Once again, the lipid productivity of the nitrogen limited run STR 4 (Figure 4.25) is substantially higher (~1.4 fold higher) compared with the lipid productivity of the nitrate sufficient run STR 1 (Table 4.12). The lipid contents of the biomass from the replicate runs STR 2 and STR 4 were in good agreement at 59.1% and 53.4% (Table 4.10), respectively. The calorific value of the biomass of STR 4 was ~14% greater than the calorific value of the biomass from the run STR 2 (Table 4.10), suggesting possible differences in the composition of the oils. In Table 4.11, the biomass productivities of the replicate runs STR 2 and STR 4 are in close agreement, within ±8% of the average value. The specific growth rate for the run STR 4 was nearly 10-fold greater than for the run STR 2 (Table 4.11). This was because at inoculation, the biomass concentration in STR 4 (Figure 4.25) was much lower (~75-fold) than the concentration at inoculation in the run STR 2 (Figure 4.24). The specific growth rate is calculated during the exponential growth phase when the culture is dilute and growing most rapidly. In exponential growth, the culture STR 4 was more dilute (concentration range of 0.4-1.0 g L^{-1}, Figure 4.25) compared with the culture STR 2 (concentration range of 1.5-2.0 g L^{-1}, Figure 4.24). The dilute culture had more light available (better light penetration) than the self-shaded darker culture and grew more rapidly in the exponential phase.

The runs STR 5 (Table 4.9) and STR 6 (Table 4.9) were intended to determine if there was a progressive increase in the lipid content of the biomass harvested after different periods of nitrogen starvation in a batch culture. The growth profiles of STR 5 and STR 6 are shown in Figure 4.26 and Figure 4.27, respectively. The biomass samples were harvested as explained in Table 4.8, after various periods of nitrate having run out. The culture history of STR 5 and STR 6 was the same as that of STR 4 (Table 4.9), but STR 4 was harvested on day 59.

The total lipid contents and the calorific values for the biomass harvested at various times are shown in Table 4.10. As shown in Table 4.10, the lipid contents of the biomass

progressively increased with the duration of exposure to nitrate starved condition in both the runs STR 5 and STR 6. For example, in the biomass of the run STR 6 (Figure 4.27), the lipid contents rose from 15% (day 29; Table 4.10) to nearly 38% (day 42; Table 4.10). The calorific values of the biomass samples were high (i.e. 29.0-30.1 kJ g^{-1}; Table 4.10, run STR 6) in comparison with the biomass that had been grown without nitrogen starvation (STR 1, Table 4.10). The lipid content of the biomass harvested on day 60 for the run STR 5 (Table 4.10) was 49%, or quite close to the lipid content of the biomass harvested in the similarly conducted run STR 4, on day 59 (i.e. 53.4%, Table 4.10). All this data is substantial repeatable evidence that the lipid contents of the biomass progressively increase to some extent on nitrate starvation of the biomass.

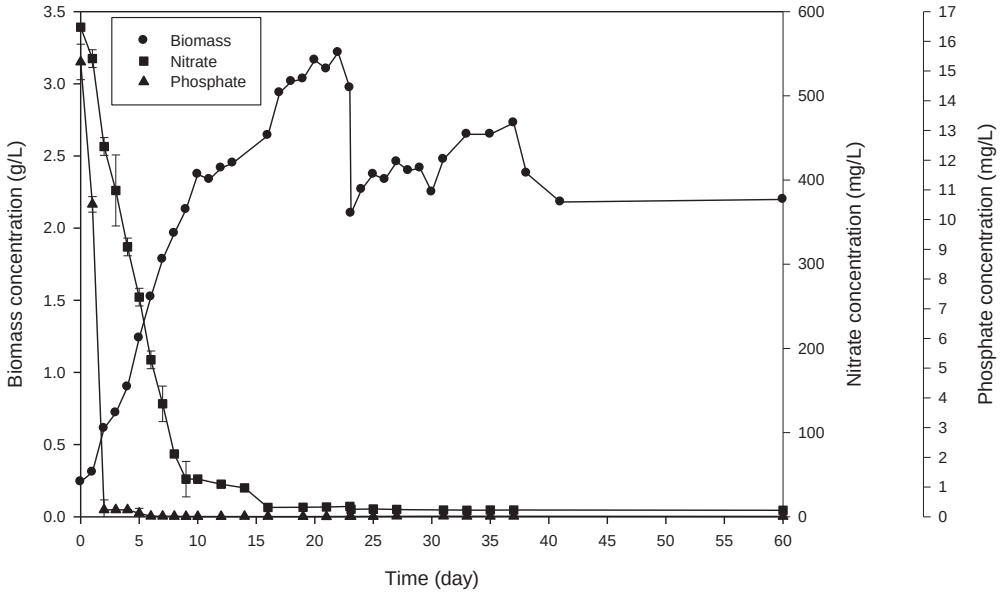

Figure 4.26 Growth profile of *C. vulgaris* in STR 5 with half nitrate under illumination of 292 μmol $m^{-2}s^{-1}$ by fluorescent lights.

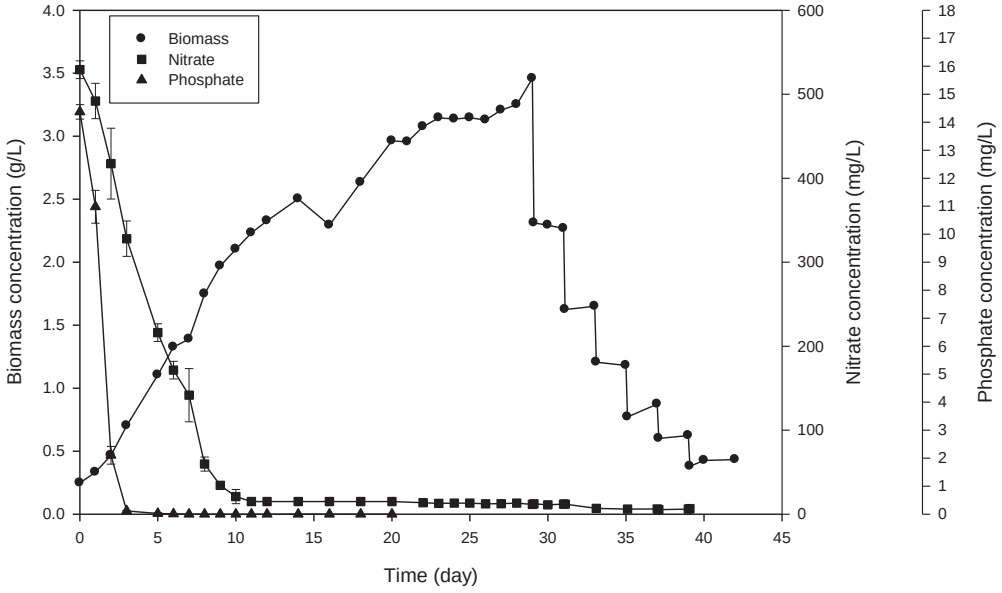

Figure 4.27 Growth profile of *C. vulgaris* in STR 6 with half nitrate under illumination of 292 μmol $m^{-2}s^{-1}$ by fluorescent lights.

All previous batch cultures (STR 1-6) used fluorescent light at an irradiance of 276 μmol $m^{-2}s^{-1}$. One batch culture (STR 10) was carried out using the light-emitting diodes as the light source. The irradiance level was 200 μmol $m^{-2}s^{-1}$. The culture medium was the normal BG-11 seawater medium. The growth profile of STR 10 is shown in Figure 4.28.

In principle, the value of irradiance determines the rate of photosynthesis, not the nature of the light source providing the PAR (photosynthetically active radiation). Irradiance is the micromoles of photosynthetically active photons received per unit surface area per unit time and has the units of μmol $m^{-2}s^{-1}$, or μE $m^{-2}s^{-1}$ (microEienstein per square meter per second; 1 μmol of photosynthetically active radiation = 1 μE). The PAR provided by the red light-emitting diodes (LEDs) was used in some experiments as the irradiance output of LED lamps could be varied using a potentiometer, something that is not possible to do with fluorescent lights. Also, compared with fluorescent lights, LEDs produce more PAR per unit

of electrical energy consumed and generate less heat. Red LEDs have been previously successfully used as the sole light source in growing certain fresh water *Chlorella* species, e.g. *Chlorella pyrenoidosa* (Matthijs *et al.*, 1996) and *C. vulgaris* (Lee & Palsson, 1996).

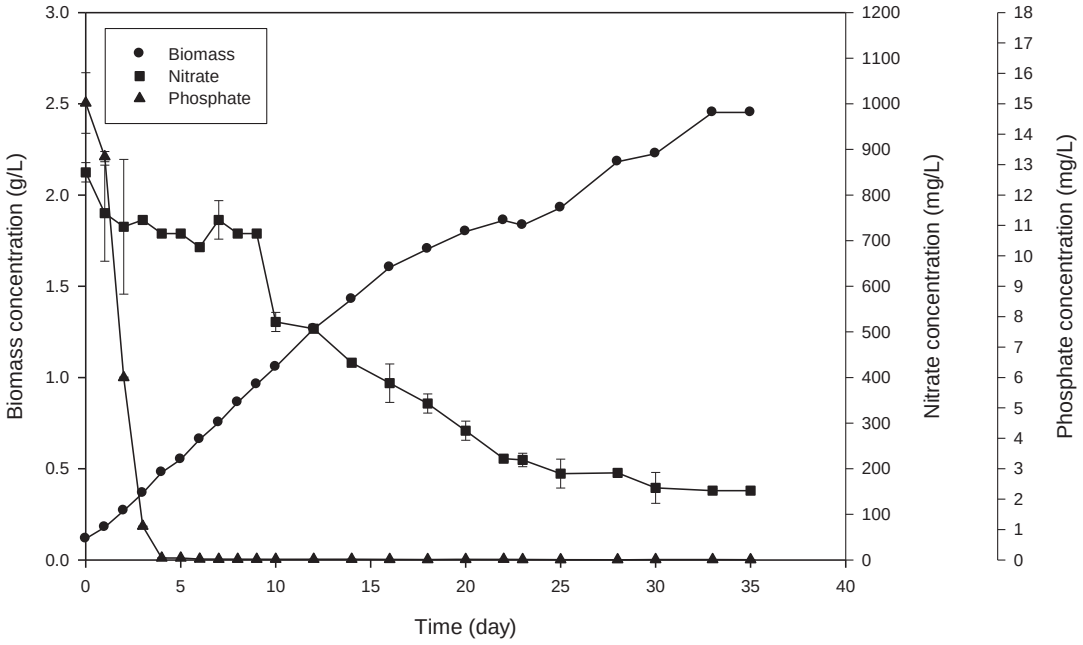

Figure 4.28 Growth profile of *C. vulgaris* in STR 10 with normal nitrate under illumination of 200 μmol $m^{-2}s^{-1}$ by light-emitting diodes.

For otherwise identical conditions, the growth profiles for LED illuminated culture (STR 10, Figure 4.28) were quite comparable to the profiles obtained for the culture illuminated with fluorescent lights (STR 1, Figure 4.23). The growth kinetic parameters for these cultures are shown in Table 4.11 and the lipid production data are shown in Table 4.12.

The specific growth rate in STR 1 (fluorescent light) was ~17% greater than in STR 10 (LEDs) (Table 4.11) because the incident irradiance for the latter was lower (~30% of the incident irradiance of STR 1). Because of differences in incident irradiance, the biomass

productivity of STR 1 was ~89% greater than the biomass productivity of STR 10 (Table 4.11). The lipid contents of the biomass for the runs STR 1 and STR 10 were 17.5% and 26.9% (Table 4.10), respectively, but the calorific values were similar at 27.1±0.5 kJ g^{-1} (Table 4.10).

4.3.2 Continuous cultures

Well mixed continuous culture studies focused on the effects of irradiance level and the dilution rate on the productivity of the biomass and the lipids. The culture runs STR 7-STR 9 and STR 11-STR 12 (Table 4.9) were initiated as batch cultures and later switched to a constant volume continuous flow operation. The biomass growth and nutrient concentration profiles for these runs are shown in Figures 4.29-4.33. The cell concentrations at steady state in various conditions are summarized in Table 4.13.

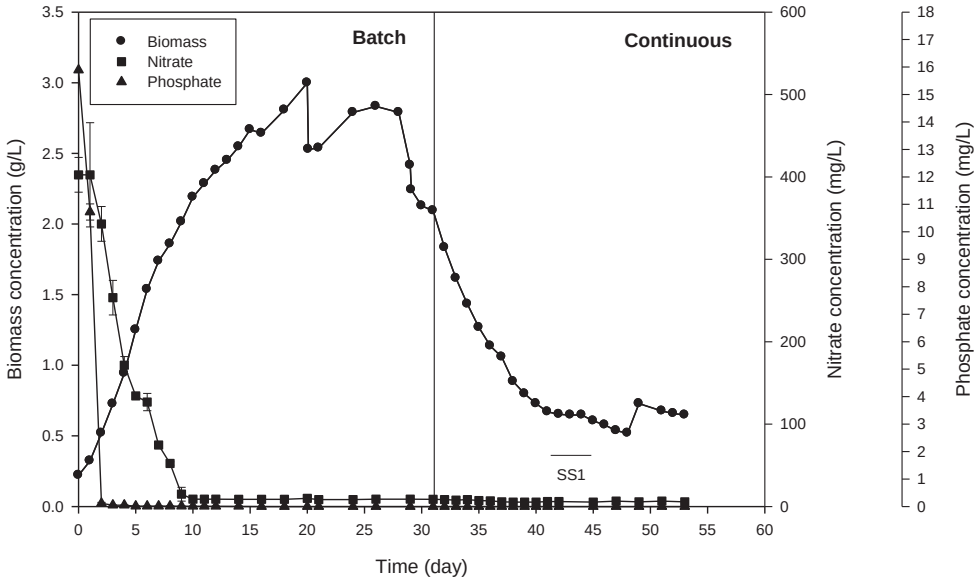

Figure 4.29 Culture profile of *C. vulgaris* in STR 7. On day 31, the dilution rate was set at 0.157 d^{-1}. Irradiance level was 292 μmol $m^{-2}s^{-1}$ (fluorescent light).

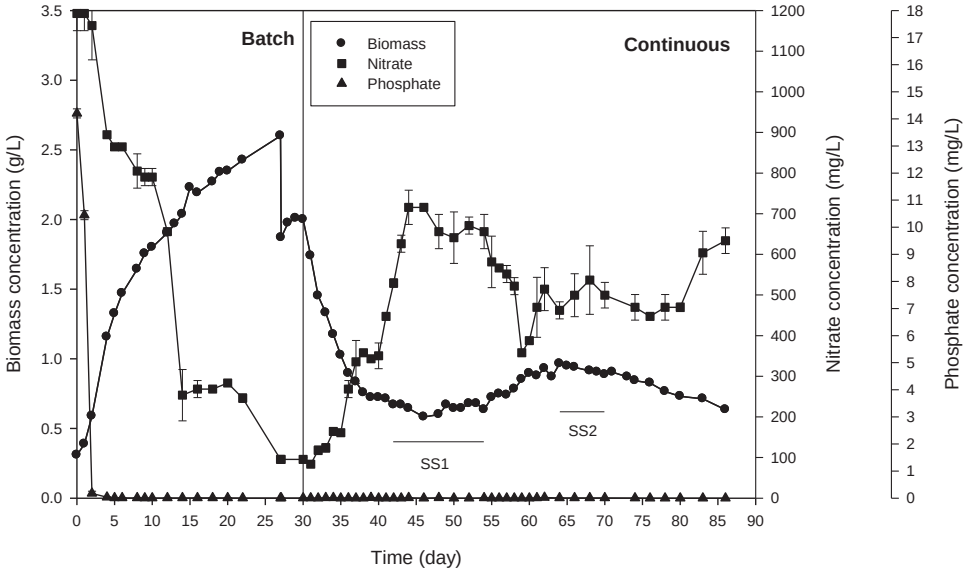

Figure 4.30 Culture profile of *C. vulgaris* in STR 8. The dilution rate was 0.22 d^{-1} (day 30) and 0.079 d^{-1} (day 55). Irradiance level was 1123 μmol $m^{-2}s^{-1}$ (light emitting diodes).

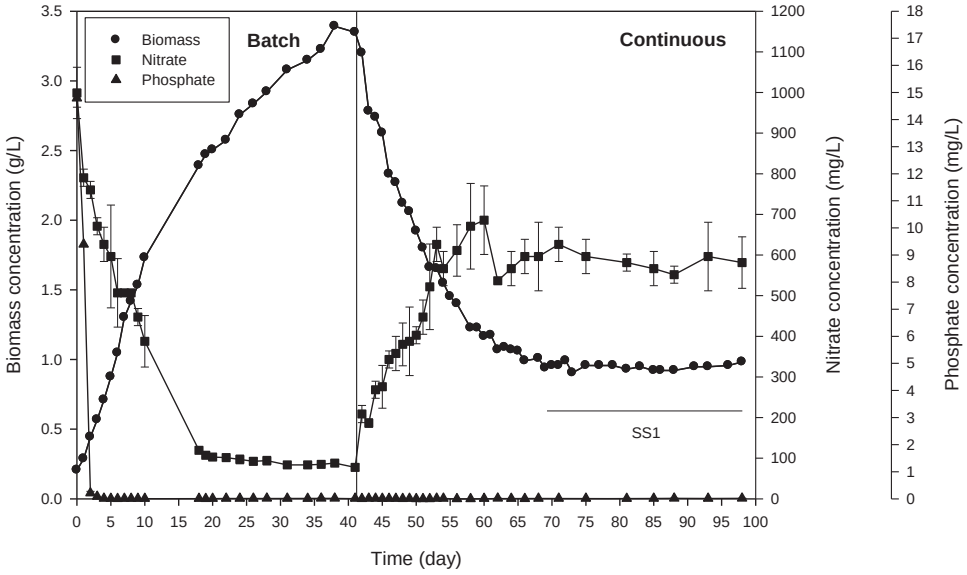

Figure 4.31 Culture profile of *C. vulgaris* in STR 9. On day 41, the dilution rate was set at 0.079 d^{-1}. Irradiance level was 292 μmol $m^{-2}s^{-1}$ (fluorescent light).

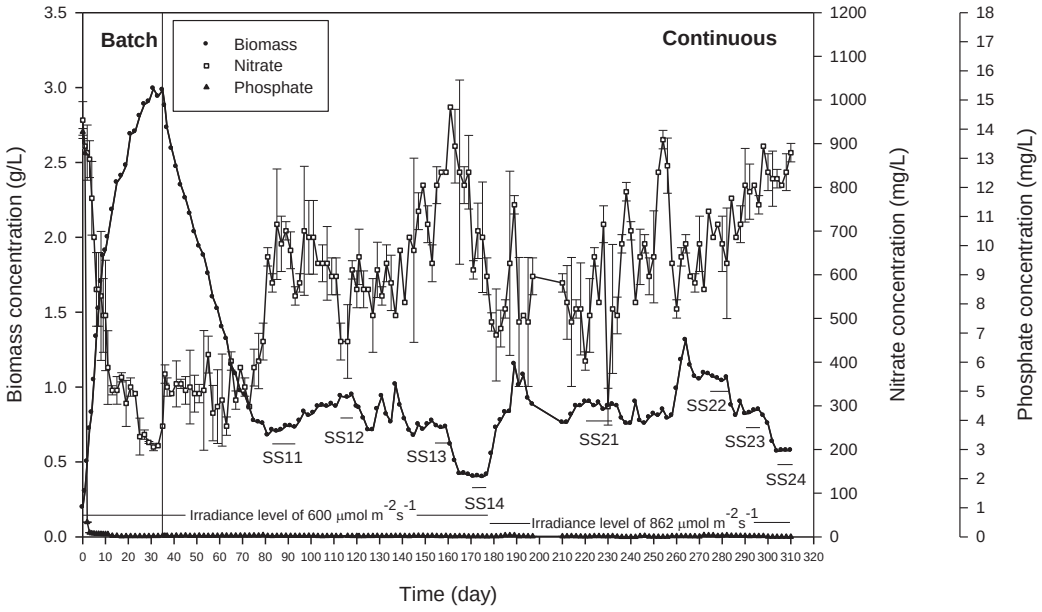

Figure 4.32 Culture profile of *C. vulgaris* in STR 11 at various dilution rates (Table 4.8). The incident irradiance levels were 600 and 862 μmol $m^{-2}s^{-1}$ (light-emitting diodes) as noted in Table 4.8.

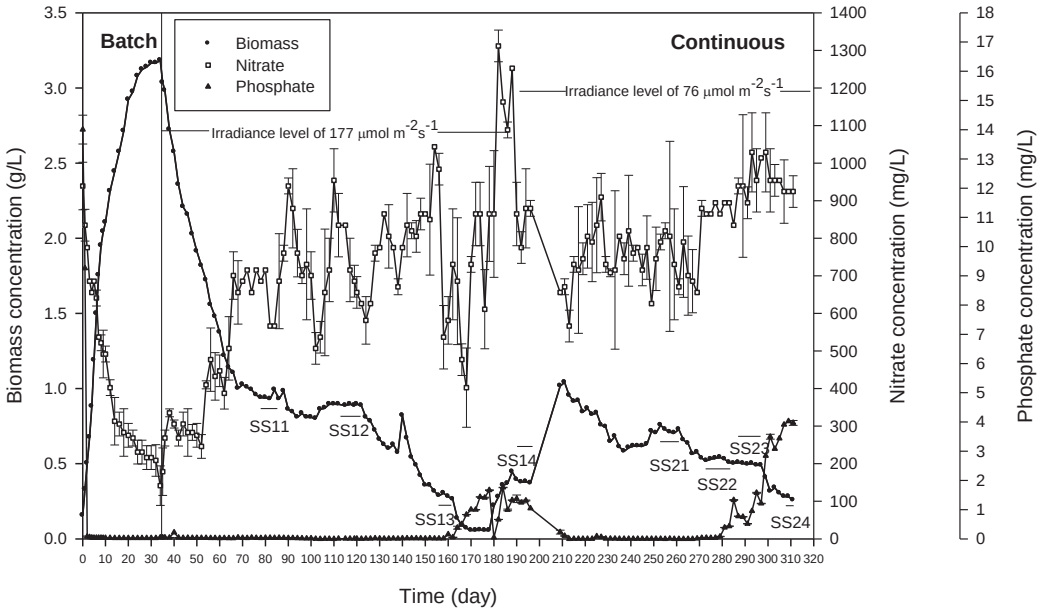

Figure 4.33 Culture profile of *C. vulgaris* in STR 12 at various dilution rates (Table 4.8). The incident irradiance level were 177 and 76 μmol $m^{-2}s^{-1}$ (light-emitting diodes) as noted in Table 4.8.

Table 4.13 Summary of biomass concentrations at various steady states

Run	Light level ($\mu mol\ m^{-2}s^{-1}$)	Dilution rate (d^{-1})	Cell concentration at steady state ($g\ L^{-1}$)
STR 7 at SS1	292 (Fluorescent light)	0.157	0.70
STR 8 at SS1	1123 (LEDs)	0.220	0.65
SS2	1123 (LEDs)	0.079	0.93
STR 9 at SS1	292 (Fluorescent light)	0.079	0.95
STR 11 at SS11	600 (LEDs)	0.079	0.72
SS12	600 (LEDs)	0.157	0.90
SS13	600 (LEDs)	0.220	0.73
SS14	600 (LEDs)	0.342	0.41
SS21	862 (LEDs)	0.079	0.88
SS22	862 (LEDs)	0.157	1.06
SS23	862 (LEDs)	0.220	0.83
SS24	862 (LEDs)	0.342	0.58
STR 12 at SS11	177 (LEDs)	0.079	0.96
SS12	177 (LEDs)	0.157	0.89
SS13	177 (LEDs)	0.220	0.30
SS14	177 (LEDs)	0.342	0.38
SS21	76 (LEDs)	0.079	0.72
SS22	76 (LEDs)	0.157	0.54
SS23	76 (LEDs)	0.220	0.50
SS24	76 (LEDs)	0.342	0.27

The runs STR 7-9 and STR 11-12 all started as batch cultures in the normal BG-11 seawater medium (Figures 4.29-4.33). All cultures grew to a high biomass concentration (2.5-3.2 g L^{-1}) towards the end of the batch phase, until the culture was switched to a constant volume continuous culture operation.

In STR 7 (Figure 4.29), some broth was harvested on day 20 and fresh BG-11 (without nitrate and phosphate) was added to bring the volume to 3.5 L. On day 26, this procedure was repeated and the volume was brought to 4 L (Table 4.9). The culture was then switched to continuous flow operation at a dilution rate of 0.157 d^{-1}. The biomass concentration progressively declined due to washout until around day 38-45 when a steady state was reached at a biomass concentration of about 0.70 g L^{-1}. The biomass concentration increased a little after the steady state (Figure 4.29). This was because the alga attached on the walls was dislodged by increasing the impeller speed (Table 4.9). The nitrate and phosphate were consumed by the time of the steady state. The biomass harvested at steady state contained 11.9% of total lipid and had a calorific value of 24.7 kJ g^{-1} (Table 4.10).

Run STR 8 (Figure 4.30) intended to examine the effects of the dilution rate on steady state biomass concentrations and nutrient levels. Dilution rate values of 0.220 and 0.079 d^{-1} were used. In STR 8 (Figure 4.30), the drop in biomass concentration on day 27 was due to the working volume being raised to 4 L by adding 1 L of BG-11 seawater medium without nitrate and phosphate. The alga began to grow again (Figure 4.30) on day 30 and the culture was switched to continuous culture. More than 99.9% of phosphate and >91% of nitrate had been consumed during batch culture. In continuous culture (fed with the normal BG-11 seawater medium), the first steady state was reached on day 42 using a feed rate of 0.61 mL min^{-1}. At the steady state, the biomass concentration remained stable at ~0.65 g L^{-1} for 12 days and then the feed rate was reduced to 0.22 mL min^{-1}. The biomass concentration rose for around 8 days and became stable at the second steady state at a

concentration of ~0.93 g L^{-1}. The nitrate concentration increased during feeding because the BG-11 seawater medium with the original nitrate concentration was fed. The nitrate concentration stabilized at approximately 651 mg L^{-1} in the first steady state. The nitrate concentration then dropped because the dilution rate was reduced and the concentration of the consuming cells increased (Figure 4.30). At the second steady state, the nitrate concentration stabilized at ~485 mg L^{-1}. Although the feed contained phosphate at the same level as in the normal BG-11, the phosphate concentration remained around 0 mg L^{-1} during all of continuous culture. This meant virtually instant absorption of phosphate by the algal cells.

At both steady states, the lipid contents of the biomass and the calorific values were relatively low (Table 4.10) as the culture medium at these steady states contained a substantial amount of nitrate (≥ 485 mg L^{-1}, Figure 4.30).

Another continuous culture was run using fluorescent lights and a lower dilution rate (0.079 d^{-1}) to examine the effect of dilution rate on growth. This was the run STR 9 profiled in Figure 4.31. The biomass profile in Figure 4.31 had the same general behavior as previously discussed for the run STR 8. Continuous culture operation began on day 38. In continuous operation, the biomass continuously declined until stabilizing at a steady state concentration of 0.947 g L^{-1} on day 69. The nitrate and phosphate concentrations were also stable. By the end of the batch phase >92% of the initial nitrate had been consumed (Figure 4.31). The nitrogen concentration rose during feeding until reaching a steady state value of ~586 mg L^{-1}. As was seen before, the phosphate concentration remained well below 0.5 mg L^{-1} during the feeding even though the feed contained phosphate.

Comparing the steady state biomass samples of the runs STR 7 (half nitrate) and STR 9 (~ 989 mg L^{-1} nitrate), the biomass of STR 9 had a higher lipid contents of 15.6% (Table 4.10) compared with a lipid contents of 11.9% for the biomass of the run STR 7 (Table

4.10). In contrast, the specific lipid production rate and the lipid productivity (Table 4.12) of the run STR 7 were slightly greater than for the run STR 9. Therefore, a low nitrate environment enhanced lipid production and the higher lipid level in the biomass of the run STR 9 was likely because the biomass was harvested much later (day 83) than the biomass of the run STR 7 (day 37 and day 45).

The runs STR 11 and STR 12 were conducted to investigate the effects of the irradiance levels of light-emitting diodes and the dilution rate on the biomass and lipid productivity. The incident irradiance in the runs STR 11 and STR 12 was 600 μmol $m^{-2}s^{-1}$ and 177 μmol $m^{-2}s^{-1}$, respectively. The culture profiles of STR 11 and STR 12 are shown in Figure 4.32 and Figure 4.33, respectively.

At the end of the batch phase, the lower irradiance run (i.e. STR 12) actually attained a slightly higher biomass concentration (Figure 4.33, day 32) than the higher irradiance run STR 11 (Figure 4.32, day 33). This was likely because the high irradiance value of 600 μmol $m^{-2}s^{-1}$ caused photoinhibition as has been reported for many other microalgae (Powles, 1984; Maxwell *et al.*, 1995; Camacho Rubio *et al.*, 2003). On day 33 (STR 11) and day 32 (STR 12), both cultures were switched to a continuous culture mode of operation. In continuous culture at the dilution rate of 0.079 d^{-1} and irradiance of 600 μmol $m^{-2}s^{-1}$, the biomass became steady during days 79-93 at about 0.72 g L^{-1} (Figure 4.32). Increasing the dilution rate to 0.157 d^{-1} increased the steady state biomass concentration to about 0.90 g L^{-1} (Figure 4.32). A further increase in dilution rate to 0.22 d^{-1}, led to oscillations and eventually a steady state on day 155 with a biomass concentration of 0.73 g L^{-1}. At the highest dilution rate of 0.342 d^{-1}, the biomass concentration declined and stabilized on days 173-177 at 0.41 g L^{-1} (Figure 4.32).

Increasing the light intensity to 862 μmol $m^{-2}s^{-1}$ (80% of full irradiance), at the lowest dilution rate of 0.079 d^{-1}, the biomass concentration reached a steady state during

days 218-234 at a concentration of 0.88 g L^{-1} (Figure 4.32). After the dilution rate was increased to 0.157 d^{-1}, the biomass concentration fluctuated and took around 38 days to become steady at 1.06 g L^{-1}. At a higher dilution rate of 0.22 d^{-1}, the biomass concentration slightly reduced to attain a steady state at 0.83 g L^{-1} after about 10 days of operation. At the highest dilution rate of 0.342 d^{-1}, the biomass concentration dropped to stabilize at 0.58 g L^{-1} on days 306-310.

In the runs STR 11 and STR 12, the feed medium was the normal BG-11 seawater medium. In general, the nitrate concentration increased with the increasing dilution rate (Figure 4.32 and 4.33). In STR 11 where the biomass concentration never dropped to below 0.4 g L^{-1}, the phosphate concentration was nearly nil throughout continuous operation (Figure 4.32).

In the run STR 12 (Figure 4.33) during periods when the biomass concentration reduced to quite low levels, the phosphate concentration tended to rise. This was because the biomass in the reactor was insufficient to absorb all the phosphate.

The relationship between the dilution rate and the steady state biomass productivity at different light levels is shown in Figure 4.34. A similar relationship for steady state lipid productivity is shown in Figure 4.35.

From Figure 4.34, the increasing dilution rate tended to increase the biomass productivity at a given light level to a maximum value (not reached in all cases), suggesting that there is an optimal dilution rate for attaining the peak biomass productivity at a given irradiance. Exactly the same observation has been reported for other algae being grown in pseudo steady state continuous culture in large outdoor tubular photobioreactors (Molina Grima *et al.*, 1996). At a given dilution, productivity tended to increase with increasing irradiance as irradiance controls the biomass growth in nutrient sufficient continuous culture.

As shown in Figure 4.35, the pattern of variation of the steady state lipid productivity with changes in dilution rate and irradiance was completely consistent with the pattern seen in Figure 4.34 for biomass productivity. Anything that affects biomass productivity would identically affect the lipid productivity so long as the lipids constitute a fixed fraction of the biomass.

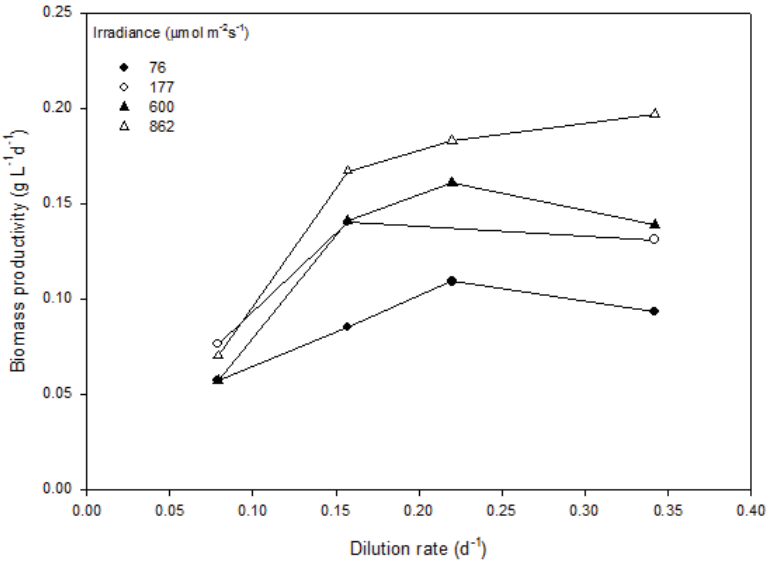

Figure 4.34 Relationship between dilution rate and the steady state biomass productivity.

Note – A data point obtained at a dilution rate of 0.22 d^{-1} and irradiance level of 177 µmol $m^{-2}s^{-1}$ has been ignored because a blockage (Table 4.9) of the bioreactor outlet tube led to an increase in volume and an erroneously low measurement of the biomass concentration.

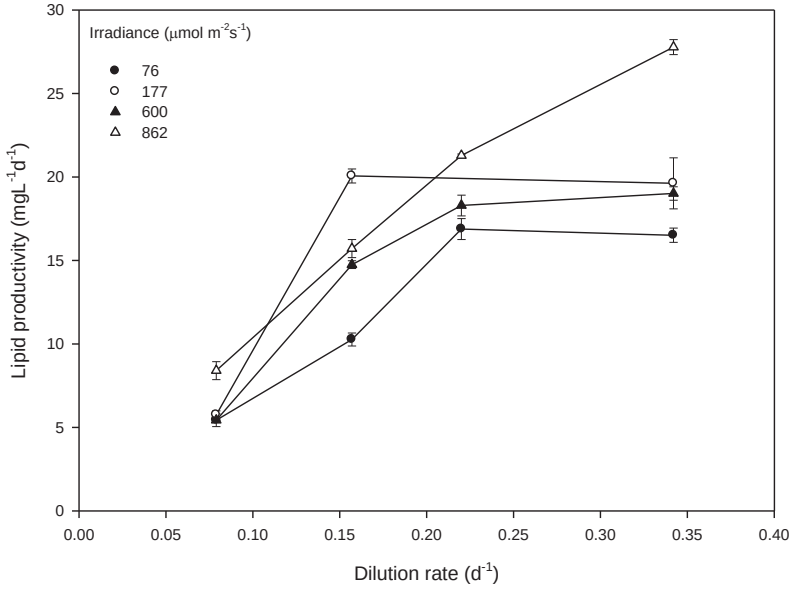

Figure 4.35 Relationship between dilution rate and the steady state lipid productivity.

Note – A data point obtained at a dilution rate of 0.22 d^{-1} and irradiance level of 177 μmol $m^{-2}s^{-1}$ has been ignored because a blockage (Table 4.9) of the bioreactor outlet tube led to an increase in volume and an erroneously low measurement of the biomass concentration.

4.4 Investigation of MGA-1-NZ cultures

4.4.1 MGA-1-NZ culture in Duran bottles

MGA-1-NZ was grown in 2 L Duran bottles (1.8 L initial working volume) bubbled with a prehumidified mixture of 5% (v/v) carbon dioxide in air. The culture temperature was 22–25 °C. The culture was illuminated continuously at an irradiance value of 126-173 $\mu E \cdot m^{-2}s^{-1}$ (daylight fluorescent light) at the surface of the bottle. The growth profiles are shown in Figure 4.36.

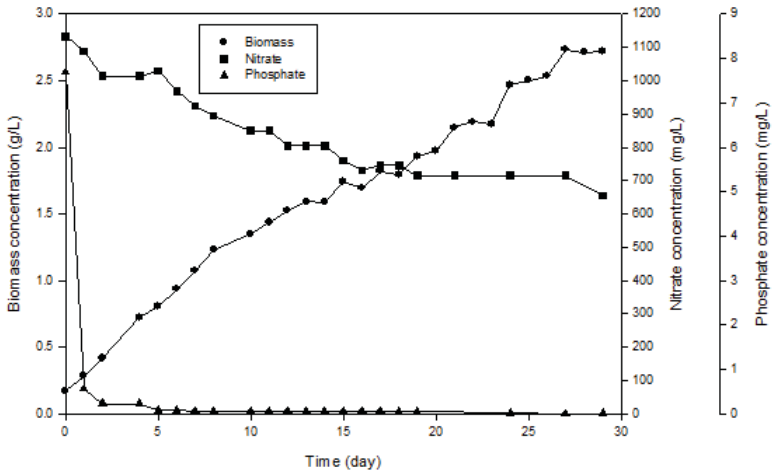

Figure 4.36 Culture profiles of MGA-1-NZ in BG11 seawater medium in 2 L Duran bottle.

From Figure 4.36, the alga attained a peak biomass concentration of 2.74 g L^{-1} on day 27. As seen with the other algae discussed in Section 4.1.1, the phosphate was consumed rapidly until nearly nil in just 5 days (>99.9% consumption). By the end of the culture period, nearly 37% of the initial nitrate had been consumed and nearly 716 mg L^{-1} of nitrate remained.

In view of the fairly high biomass concentration attained in 27 days, the alga MGA-1-NZ was further investigated as discussed next. The kinetic parameters of the culture in Figure 4.36 are discussed later during comparison with the photobioreactor culture profiles.

4.4.2 MGA-1-NZ culture in 10 L Corning stirred photobioreactor

Three batch cultures of MGA-1-NZ were grown in Corning stirred photobioreactors (Section 3.7) as summarized in Table 4.14. The incident irradiance of the runs BR 1-3 was 484 μmol

$m^{-2}s^{-1}$ (fluorescent light). The relevant culture profiles are shown in Figures 4.37-4.39 for BR 1-3, respectively.

The maximum biomass concentration in the normal BG-11 seawater medium was ~1.25 g L^{-1} (Figure 4.37) or only ~46% of the concentration attained around the same time in the 2 L culture bottle (Figure 4.36). This difference was a consequence of a lower average light level in the photobioreactor. Although the incident irradiance for the bioreactor runs was nearly 3.2-fold than in the 2 L bottle, the internal diameter of the photobioreactor tank was 0.19 m compared to an internal diameter of 0.136 m for the Duran bottle. Average irradiance was therefore low in the photobioreactor compared with the Duran bottle, as discussed in Section 4.1.1.

In all the runs BR 1-3, the phosphate consumption was consistent with the profiles previously discussed for *C. vulgaris* (Section 4.3.1). In BR 1, the step change in the biomass concentration is a consequence of harvesting on day 34 and replenishment with nitrate and phosphate free medium (Figure 4.37). Although the culture medium had plenty of residual nitrate (Figure 4.37), there was no growth after day 34 as phosphate had run out (the added medium was phosphate free).

In BR 2 (Figure 4.38), the initial nitrate level was ~27% of the normal level and, therefore, the nitrate concentration declined to a low value by day 6. The same happened in BR 3 which was a replicate of BR 2. In BR 2, the stepped changes in biomass concentration (Figure 4.38) are a consequence of harvesting and replenishment with media devoid of nitrate and phosphate.

Table 4.14 Summary of MGA-1-NZ cultures in 10 L Corning stirred photobioreactor

Batch	Conditions
BR 1	Starting with 10% inoculum in a working volume of 8 L, using BG-11 made in seawater (full nitrate) as the culture medium; 25 °C; bubbling with 5% (vol/vol) carbon dioxide in air; 200 rpm impeller rotational speed; pH of 6.6±0.4 (not controlled); and illuminated by fluorescent light at 484 μmol $m^{-2}s^{-1}$. On day 34, 1.8 L of broth was harvested and the bioreactor was refilled with BG-11 (seawater) without nitrate and phosphate. On day 50, harvested 1.8 L and refilled with the same volume of BG-11 without nitrate and phosphate and reduced the temperature to 20 °C. On day 46, the broth colour was a little faded. On day 65, harvested 1.8 L.
BR 2	Same culture conditions as BR 1 except used 300 mg L^{-1} of initial nitrate concentration in the BG-11 seawater medium; pH of 6.8±0.4 (not controlled). The broth (1.8 L) was harvested and the bioreactor was refilled with the same volume of BG-11 (seawater) without nitrate and phosphate every two days from day 34 to day 48.
BR 3	Same culture conditions as BR 2; pH of 6.8±0.3 (not controlled).

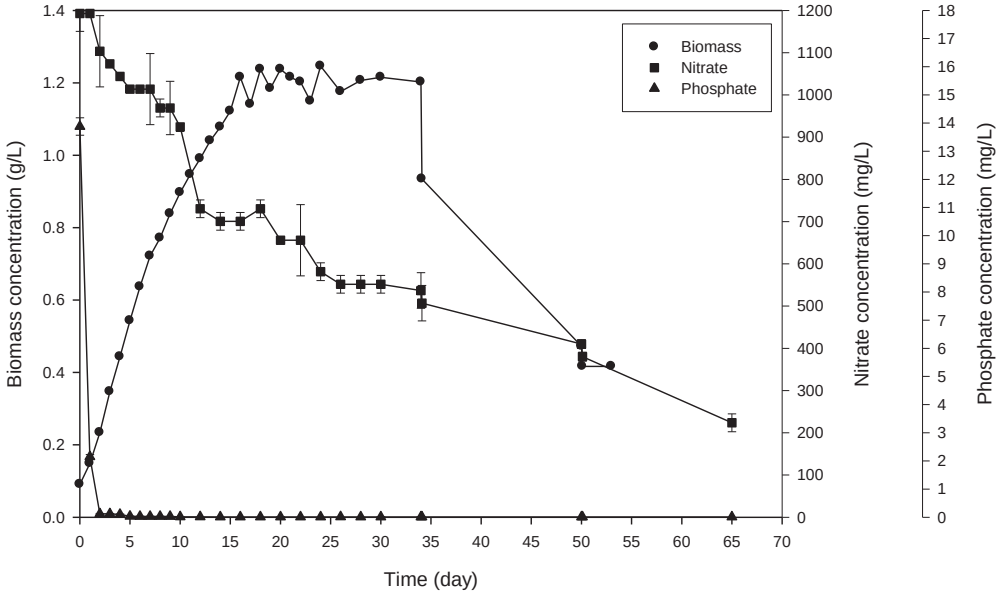

Figure 4.37 Culture profile of MGA-1-NZ in BR 1.

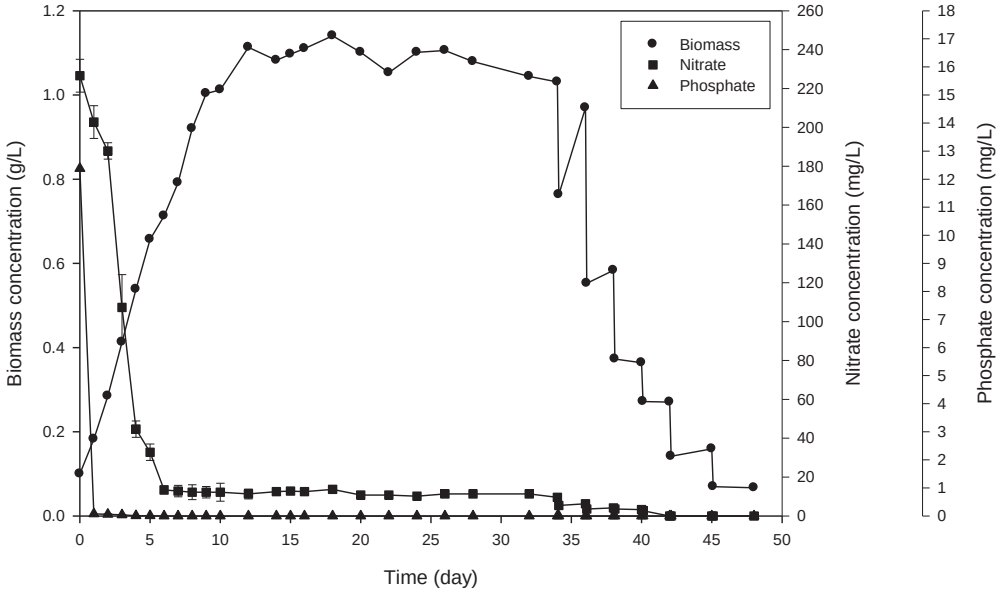

Figure 4.38 Culture profile of MGA-1-NZ in BR 2.

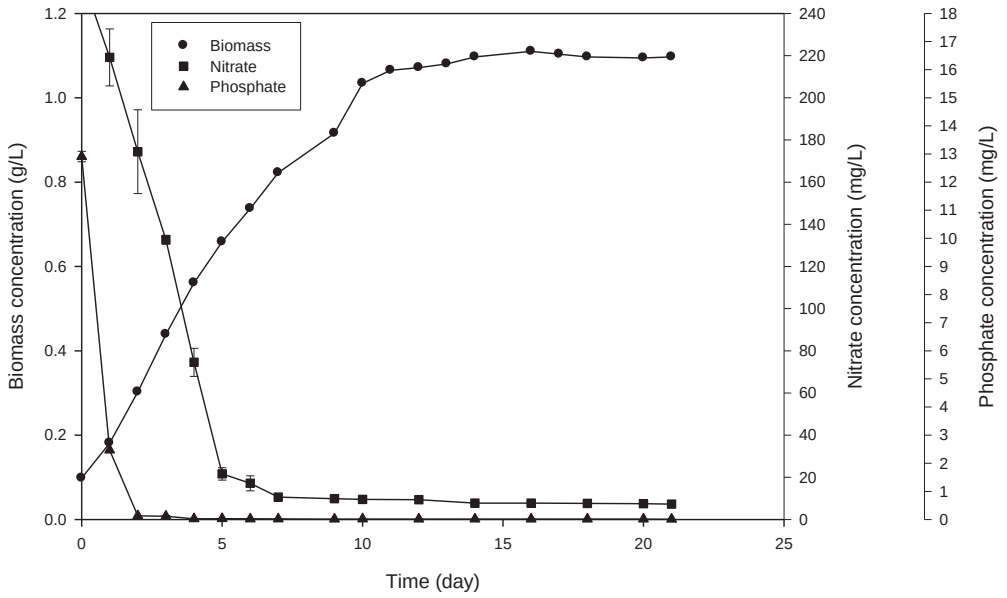

Figure 4.39 Culture profile of MGA-1-NZ in BR 3.

The total lipid contents and the calorific values for the biomass harvested at various stages of BR 1-3 are shown in Table 4.15. The culture kinetic parameters of the various runs are shown in Table 4.16 and Table 4.17.

Table 4.15 Total lipid contents and calorific values of MGA-1-NZ biomass

Batch	Total lipid content (%)	Calorific value (kJ g^{-1})
2 L bottle	24.0±0.7	23.4
BR 1 (Day 34)	24.0±0.7	26.0
(Day 50)	6.2±0.0	17.4
(Day 65)	13.5±0.3	22.1
BR 2 (Day 34)	24.4±5.2	26.3
(Day 36)	12.5±0.4	25.9
(Day 38)	11.4±0.3	25.4
(Day 40)	17.0±0.2	25.0
(Day 42)	14.8±0.5	25.4
(Day 45)	19.8±3.8	24.4
(Day 48)	13.7±0.7	ND
BR 3	33.7±0.7	25.3

ND – not determined because of insufficient growth.

[a] – mean value ± standard deviation.

[b] – previously shown to be reproducible to ± 2.8% of the mean value (Section 3.10.8).

Table 4.16 Growth kinetic parameters of MGA-1-NZ

Batch	Biomass yield on nitrate ($Y_{X/N}$; g mg^{-1})	Biomass yield on phosphate ($Y_{X/P}$; g mg^{-1})	Biomass yield on light ($\times 10^{-7}$) ($Y_{X/light}$; g μmol^{-1})	Specific nitrate consumption rate (q_N; mg $g^{-1}d^{-1}$)	Specific phosphate consumption rate (q_P; mg $g^{-1}d^{-1}$)	Specific growth rate (μ; d^{-1})	Biomass productivity (Q_X; g $L^{-1}d^{-1}$)
2 L bottle	0.006±0.001	0.333±0.014	-	6.037±1.220	0.111±0.005	0.339	0.095
BR 1*	0.002±0.3×10^{-4}	0.083±0.002	1.430	22.049±0.380	0.500±0.011	0.336	0.048
BR 2*	0.005±4.8×10^{-4}	0.084±0.000	1.719	11.361±1.125	0.661±0.000	0.458	0.058
BR 3	0.004±4.2×10^{-4}	0.078±0.001	1.880	15.449±1.595	0.797±0.009	0.478	0.063

* Using data for Day 34.

Standard deviations are shown for selected measurements.

Table 4.17 Lipid production parameters of MGA-1-NZ

Batch	Lipid yield on nitrate ($Y_{Lipid/N}$; g mg^{-1})	Lipid yield on phosphate ($Y_{Lipid/P}$; g mg^{-1})	Lipid yield on light ($\times 10^{-7}$) ($Y_{Lipid/light}$; g μmol^{-1})	Lipid productivity (Q_L; mg $L^{-1}d^{-1}$)
2L bottle	-	-	-	22.73±0.71
BR 1*	0.0002±0.000	0.007±0.000	0.34±0.01	11.55±0.03
BR 2*	0.0004±0.000	0.007±0.000	0.42±0.02	14.12±0.30
BR 3	0.0014±0.000	0.026±0.000	0.63±0.01	21.28±0.05

* Using data for Day 34.

Standard deviations are shown for selected measurements.

As shown in Table 4.15, the lipid contents in the biomass tended to be high for the nutrient sufficient conditions (i.e., 2 L bottle; BR 1, day 34; BR 2, day 34; BR3) and was not increased by nitrate starvation (e.g. BR 2, day 36-45; Table 4.15). Nutrient starvation actually reduced the total lipids in the biomass (Table 4.15). Not all microalgae increase their lipid content in response to nitrate starvation. For example, nitrogen starvation does not affect the lipid content of the biomass of the marine microalga *Nannochloropsis salina* (Boussiba *et al.*, 1987).

The highest lipid productivity for this alga occurred in the nutrient sufficient medium (2 L bottle, Table 4.17). This was 22.7 mg $L^{-1}d^{-1}$. The alga MGA-1-NZ was not further investigated in this thesis because it tended to have lower biomass productivity and lipid productivity (Tables 4.16, 4.17) compared with the alga *C. vulgaris* (Tables 4.11, 4.12; Section 4.3.1). The total lipid contents and the calorific values of MGA-1-NZ biomass were generally lower than for *C. vulgaris*. Also, the total lipid contents and the calorific values of MGA-1-NZ were not susceptible to enhancement by nitrate limitation (Table 4.15) unlike the situation in *C. vulgaris* (Table 4.10; Section 4.3.1).

4.5 Characteristics of the algal lipids

The lipid extracts of a few algal biomass samples were preliminarily characterized in terms of their compositions, although a characterization of lipids per se was not an objective of this research. Concentrations of certain elements (Ca, Cu, Fe, Mg, N, P, Na, S) in some crude oil samples were measured as these elements have the potential to interfere with certain catalytic processes (Chisti, 2012) that may be potentially used to convert algal crude oil to conventional gasoline, kerosene (jet fuel) and diesel.

4.5.1 *Chlorella vulgaris*

4.5.1.1 Concentrations of elements in *Chlorella vulgaris* total lipid extract

The concentrations of various elements were measured in the total lipids extracted from *C. vulgaris* by using inductively coupled plasma optical emission spectrometry (ICP-OES), inductively coupled plasma mass spectrometry (ICP-MS) and Dumas combustion (*Official Methods of Analysis of AOAC (OMA)*, 18th edition, AOAC International, Gaithersburg, MD, USA, 2006). The analyses were performed by R J Hill Laboratories Limited, Hamilton, New Zealand. The concentrations of various elements in *C. vulgaris* oil from stirred-tank photobioreactor runs STR 1 and STR 2 are shown in Table 4.18

Table 4.18 Concentrations of various elements in *C. vulgaris* total lipid extract from stirred-tank photobioreactor runs STR 1 and STR 2

Element	Concentration (mg g^{-1} oil)		Method used	Detection limit (mg g^{-1})
	STR 1	STR 2		
Calcium, Ca	0.34	3.50	ICP-OES	0.0002
Copper, Cu	80	52	ICP-MS	0.005×10^{-4}
Iron, Fe	110	910	ICP-OES	0.1×10^{-4}
Magnesium, Mg	2.60	3.10	ICP-OES	0.0002
Nitrogen, N	6.30	0.77	Dumas combustion	0.02
Phosphorus, P	0.88	0.35	ICP-OES	0.001
Sodium, Na	0.14	< 0.05	ICP-OES	0.005
Sulfur, S	2.60	0.24	ICP-OES	0.001

The measured elemental concentrations were higher than would be acceptable in processes for catalytic processing of algal oils (Y. Chisti, Personal Communication). Therefore, in the future, methods will need to be developed to remove the unwanted trace elements from the algal crude oil. This may be done, for example, by washing the oil with a dilute aqueous acid, or with a mixture of a metal chelating agent (e. g. Ethylenediaminetetraacetic acid) and dilute aqueous acid.

4.5.1.2 Fractionation of *Chlorella vulgaris* total lipid extract

The total lipids extracted from *C. vulgaris* biomass from several different photobioreactor and stirred-tank photobioreactor runs were separated into neutral lipids (including triglycerides) and other oils (e.g. chlorophyll, carotenoids). In addition, in some cases the neutral lipids were further analyzed to determine the type of fatty acids present. The neutral lipid contents and the triglyceride contents of the oils are shown in Table 4.19.

From Table 4.19, the *C. vulgaris* crude oil commonly contained >45% neutral lipids although the percentage of neutral lipids could vary from as low as 1.5% to a high of nearly 91%. Of the runs PBR 1-8 and STR 2-5, only PBR 1 and PBR 2 were performed under identical conditions and for these the neutral lipid contents in the oils were similar, or within ±11.4% of the average value of 51.1% (Table 4.19). Although, the neutral lipids as a fraction of total lipids could be quite high, they never contained more than 1.4% of triglycerides. Note that only triglycerides can be used to make the conventional biodiesel (Chisti, 2007), but the entire lipid fraction (i.e. all carbon rich oils) can be used to make diesel that is identical to petrodiesel, jet fuel and gasoline (Chisti, 2012).

Table 4.19 Neutral lipid content and triglyceride content of *C. vulgaris* oils

Lipid sample from	Neutral lipid as percent (w/w) of total lipid	Triglyceride as percent (w/w) of neutral lipid
PBR 1	45.3	ND
PBR 2	56.9	ND
PBR 3	74.3	ND
PBR 4	59.1	ND
PBR 5	58.8	ND
PBR 6	29.8	1.4
PBR 7	1.6	ND
PBR 8	14.4	1.1
STR 2	24.9	ND
STR 3	73.7	ND
STR 4	90.7	1.3
STR 5	1.5	ND

ND – not determined because of insufficient neutral lipid.

4.5.1.3 Fatty acid profiles of *Chlorella vulgaris* total lipid extract

The fatty acids in the total lipids extracted from *C. vulgaris* biomass from several different photobioreactor and stirred-tank photobioreactor runs were quantified by gas chromatography after converting to free fatty acid methyl esters. The analysis was done by Nutrition Laboratory, Institute of Food, Nutrition & Human Health, Massey University, Palmerston North, New Zealand. The fatty acid profiles of the oil produced in tubular photobioreactor and stirred-tank photobioreactors are summarized in Table 4.20 and Table 4.21, respectively. Using the data of Table 4.20 and Table 4.21, the proportion of saturated, unsaturated and polyunsaturated fatty acids in algal oil could be determined as shown in Table 4.22.

Table 4.20 Fatty acid profiles of *C. vulgaris* total lipid extract from photobioreactor runs

Fatty acid	Concentration (g/100 g oil)				
	PBR 1	PBR 2	PBR 3	PBR 6	PBR 7
C6:0 Caproic	ND	ND	ND	ND	ND
C8:0 Caprylic	0.004	ND	ND	ND	ND
C10:0 Capric	ND	ND	ND	ND	ND
C11:0 Undecanoic	ND	ND	ND	ND	ND
C12:0 Lauric	ND	ND	ND	0.01	ND
C13:0 Tridecanoic	ND	ND	ND	ND	ND
C14:0 Myristic	ND	0.023	0.03	0.01	0.02
C14:1-cis9 Myristoleic	ND	ND	ND	ND	ND
C15:1-cis10 Pentadecenoic	ND	ND	ND	ND	ND
C16:0 Palmitic	0.341	0.613	0.55	0.40	0.54
C16:1-cis9 Palmetoleic	ND	0.026	0.09	0.04	0.01
C17:0 Margaric	ND	ND	ND	0.01	0.01
C17:1-cis10 Heptadecenoic	ND	ND	ND	ND	ND
C18:0 Stearic	0.042	0.044	0.04	0.04	0.04
C18:1-tran9 Elaidic	ND	ND	ND	ND	ND
C18:1-tran11 Vaccenic	ND	ND	ND	ND	ND
C18:1-cis9 Oleic	0.826	1.336	1.56	1.33	0.89
C18:1-cis11 Vaccenic	0.093	0.307	0.47	0.09	0.04
C18:2-tran9,12 Linolelaidic	ND	ND	ND	ND	ND
C18:2-cis9,12 Linoleic	0.927	1.102	0.71	0.29	0.25

Table 4.20 Fatty acid profiles of *C. vulgaris* total lipid extract from photobioreactor runs (Cont.)

Fatty acid	Concentration (g/100 g oil)				
	PBR 1	PBR 2	PBR 3	PBR 6	PBR 7
C20:0 Arachidic	ND	ND	ND	ND	ND
C18:3n6-cis6,9,12 γ-Linolenic	ND	ND	ND	ND	ND
C20:1-cis11 Eicosenoic	ND	ND	ND	0.01	0.01
C18:3-cis9,12,15 Linolenic	0.513	ND	0.88	0.41	0.10
C21:0 Heneicosanoic	ND	ND	ND	ND	ND
C20:2-cis11,14 Eicosadienoic	ND	ND	ND	ND	ND
C22:0 Behenic	ND	ND	ND	ND	ND
C20:3n6-cis8,11,14 Eicosatrienoic	ND	ND	ND	ND	ND
C22:1-cis13 Erucic	ND	ND	ND	ND	ND
C20:3n6-cis11,14,17 Eicosatrienoic	ND	ND	ND	ND	ND
C20:4n6-cis5,8,11,14 Arachidonic	ND	ND	ND	ND	ND
C23:0 Tricosanoic	ND	ND	ND	ND	ND
C22:2-cis13,16 Docosadienoic	ND	ND	ND	ND	ND
C24:0 Lignoceric	ND	ND	ND	0.01	ND
C20:5n3-cis5,8,11,14,17 Epa	ND	ND	ND	ND	ND
C24:1-cis15 Nervonic	ND	ND	ND	ND	ND
C22:5-cis7,10,13,16,19 DPA	ND	ND	ND	ND	ND
C22:6n3-cis4,7,10,13,16,19 DHA	ND	ND	ND	ND	ND
Percent total fatty acids	2.75	3.45	4.33	2.64	1.91

ND – not detected.

Table 4.21 Fatty acid profiles of *C. vulgaris* total lipid extract from stirred-tank photobioreactor runs

Fatty acid	Concentration (g/100 g oil)				
	STR 1	STR 2	STR 3	STR 4	STR 5
C6:0 Caproic	ND	ND	ND	ND	ND
C8:0 Caprylic	ND	0.019	ND	ND	ND
C10:0 Capric	ND	ND	ND	ND	ND
C11:0 Undecanoic	ND	ND	ND	ND	ND
C12:0 Lauric	ND	ND	ND	ND	ND
C13:0 Tridecanoic	ND	ND	ND	ND	ND
C14:0 Myristic	ND	ND	0.01	ND	0.02
C14:1-cis9 Myristoleic	ND	ND	ND	ND	ND
C15:1-cis10 Pentadecenoic	ND	ND	ND	ND	ND
C16:0 Palmitic	0.342	0.355	0.39	0.45	0.47
C16:1-cis9 Palmetoleic	ND	ND	0.02	0.02	0.01
C17:0 Margaric	ND	ND	ND	0.01	0.01
C17:1-cis10 Heptadecenoic	ND	ND	ND	ND	ND
C18:0 Stearic	0.031	0.059	ND	0.08	0.05
C18:1-tran9 Elaidic	ND	ND	ND	ND	ND
C18:1-tran11 Vaccenic	ND	0.070	ND	ND	ND
C18:1-cis9 Oleic	0.796	ND	1.09	1.57	2.32
C18:1-cis11 Vaccenic	0.165	ND	0.27	0.05	0.06
C18:2-tran9,12 Linolelaidic	ND	ND	ND	ND	ND
C18:2-cis9,12 Linoleic	0.720	ND	0.78	0.49	0.81

Table 4.21 Fatty acid profiles of *C. vulgaris* total lipid extract from stirred-tank photobioreactor runs (Cont.)

Fatty acid	Concentration (g/100 g oil)				
	STR 1	STR 2	STR 3	STR 4	STR 5
C20:0 Arachidic	ND	ND	ND	ND	ND
C18:3n6-cis6,9,12 γ-Linolenic	ND	ND	ND	ND	ND
C20:1-cis11 Eicosenoic	ND	ND	ND	0.03	0.01
C18:3-cis9,12,15 Linolenic	0.703	ND	0.92	0.25	0.96
C21:0 Heneicosanoic	ND	0.033	ND	ND	ND
C20:2-cis11,14 Eicosadienoic	ND	0.009	ND	ND	ND
C22:0 Behenic	ND	ND	ND	ND	ND
C20:3n6-cis8,11,14 Eicosatrienoic	ND	ND	ND	ND	ND
C22:1-cis13 Erucic	ND	ND	ND	ND	ND
C20:3n6-cis11,14,17 Eicosatrienoic	ND	ND	ND	ND	ND
C20:4n6-cis5,8,11,14 Arachidonic	ND	ND	ND	ND	ND
C23:0 Tricosanoic	ND	ND	ND	ND	ND
C22:2-cis13,16 Docosadienoic	ND	ND	ND	ND	ND
C24:0 Lignoceric	ND	ND	ND	0.01	ND
C20:5n3-cis5,8,11,14,17 Epa	ND	ND	ND	ND	ND
C24:1-cis15 Nervonic	ND	ND	ND	ND	ND
C22:5-cis7,10,13,16,19 DPA	ND	ND	ND	ND	ND
C22:6n3-cis4,7,10,13,16,19 DHA	ND	ND	ND	ND	ND
Percent total fatty acids	2.76	0.55	3.48	2.96	4.72

ND – not detected.

Table 4.22 Proportions of the various classes of fatty acids in lipids from some tubular photobioreactor and stirred-tank photobioreactor runs

Run	Fatty acid class as percent of total fatty acid present (% w/w)		
	Saturated	Monounsaturated	Polyunsaturated
PBR 1	14.1	33.4	52.4
PBR 2	19.7	48.4	31.9
PBR 3	14.3	49.0	36.7
PBR 6	18.2	55.7	26.5
PBR 7	31.9	49.7	18.3
STR 1	13.5	34.8	51.6
STR 2	84.7	12.7	1.6
STR 3	11.5	39.7	48.9
STR 4	18.6	56.4	25.0
STR 5	11.7	50.8	37.5

As seen in Table 4.22, the algal oil predominantly contained unsaturated and polyunsaturated fatty acids in keeping with other well known observations (Belarbi *et al.*, 2000; Guschina & Harwood, 2006; Stansell *et al.*, 2012). Oils rich in polyunsaturated fatty acids are generally considered to be unsatisfactory for making biodiesel of the desired characteristics (Knothe, 2011; Stansell *et al.*, 2012), but can be hydrogenated and deoxygenated to make conventional diesel, gasoline and kerosene (Chisti, 2012).

4.5.2 The alga MGA-1-NZ

4.5.2.1 Concentrations of elements in MGA-1-NZ total lipid extract

The concentrations of various elements in the crude oil of MGA-1-NZ are presented in Table 4.23.

Table 4.23 Concentrations of elements in crude oil of MGA-1-NZ

Element	Concentration (mg g^{-1} oil)	Method used	Detection limit
	MGA-1-NZ in 2 L bottle		(mg g^{-1})
Calcium, Ca	2.10	ICP-OES	0.0002
Copper, Cu	25	ICP-MS	0.005×10^{-4}
Iron, Fe	250	ICP-OES	0.1×10^{-4}
Magnesium, Mg	8.00	ICP-OES	0.0002
Phosphorus, P	3.10	ICP-OES	0.001
Sodium, Na	0.97	ICP-OES	0.005

4.5.2.2 Fractionation of MGA-1-NZ total lipid extract

The total lipids from MGA-1-NZ grown in 2 L Duran bottles were separated into neutral lipid and the other oils. The neutral lipids constituted 40.6% (w/w) of the total lipids.

4.5.2.3 Fatty acid profiles of MGA-1-NZ total lipid extract

The total lipids extracted from MGA-1-NZ biomass from 2 L bottles and the 10 L Corning stirred photobioreactor (Section 3.7) were analyzed as explained above (Section 4.5.1.3).

The fatty acid profiles are summarized in Table 4.24. Using the data of Table 4.24, the proportions of saturated, unsaturated and polyunsaturated fatty acids in the oil samples could be determined and are shown in Table 4.25.

From Table 4.25, the alga MGA-1-NZ was generally rich in polyunsaturated fatty acids, but unlike *C. vulgaris* (Table 4.22) tended to have more saturated fatty acids compared with the monounsaturated fatty acids. The method of biomass production (i.e. 2 L bottle or 10 L Corning stirred bioreactor) did not have a large effect on the composition of the lipids (Table 4.25).

Table 4.24 Fatty acid profiles of MGA-1-NZ total lipids

Fatty acid	Concentration (g/100 g oil)		
	2 L bottle	BR 1*	BR 3*
C6:0 Caproic	ND	ND	ND
C8:0 Caprylic	ND	ND	ND
C10:0 Capric	ND	ND	0.05
C11:0 Undecanoic	ND	ND	ND
C12:0 Lauric	ND	0.02	0.17
C13:0 Tridecanoic	ND	ND	ND
C14:0 Myristic	0.04	0.03	0.26
C14:1-cis9 Myristoleic	ND	ND	ND
C15:1-cis10 Pentadecenoic	ND	ND	ND
C16:0 Palmitic	0.29	0.42	3.96
C16:1-cis9 Palmetoleic	0.05	0.02	0.29
C17:0 Margaric	ND	0.01	0.04
C17:1-cis10 Heptadecenoic	ND	ND	ND
C18:0 Stearic	ND	0.01	0.09
C18:1-tran9 Elaidic	ND	ND	ND
C18:1-tran11 Vaccenic	ND	ND	ND
C18:1-cis9 Oleic	0.02	0.05	0.65
C18:1-cis11 Vaccenic	ND	0.01	1.09

Table 4.24 Fatty acid profiles of MGA-1-NZ total lipids (Cont.)

Fatty acid	Concentration (g/100 g oil)		
	2 L bottle	BR 1*	BR 3*
C18:2-tran9,12 Linolelaidic	ND	ND	ND
C18:2-cis9,12 Linoleic	0.52	0.49	5.38
C20:0 Arachidic	ND	ND	ND
C18:3n6-cis6,9,12 γ-Linolenic	ND	ND	ND
C20:1-cis11 Eicosenoic	ND	ND	ND
C18:3-cis9,12,15 Linolenic	0.45	0.18	2.27
C21:0 Heneicosanoic	ND	ND	ND
C20:2-cis11,14 Eicosadienoic	ND	ND	ND
C22:0 Behenic	ND	ND	ND
C20:3n6-cis8,11,14 Eicosatrienoic	ND	ND	ND
C22:1-cis13 Erucic	ND	ND	ND
C20:3n6-cis11,14,17 Eicosatrienoic	ND	ND	ND
C20:4n6-cis5,8,11,14 Arachidonic	ND	ND	ND
C23:0 Tricosanoic	ND	ND	0.01
C22:2-cis13,16 Docosadienoic	ND	ND	ND
C24:0 Lignoceric	ND	0.01	0.04
C20:5n3-cis5,8,11,14,17 Epa	ND	ND	ND
C24:1-cis15 Nervonic	ND	ND	ND
C22:5-cis7,10,13,16,19 DPA	ND	ND	ND
C22:6n3-cis4,7,10,13,16,19 DHA	ND	ND	ND
Percent total fatty acids	1.37	1.25	14.30

* 10 L Corning stirred photobioreactor.

ND – not detected.

Table 4.25 Proportions of the various classes of fatty acids in lipids of MGA-1-NZ

Run	Fatty acid class as percent of total fatty acid present (%)		
	Saturated	Monounsaturated	Polyunsaturated
2 L bottle	24.1	5.1	70.8
BR 1*	40.0	6.4	53.6
BR 3*	32.3	14.2	53.5

* 10 L Corning stirred photobioreactor.

4.6 Comparison of the lipid productivity of *C. vulgaris*

The lipid productivity of *C. vulgaris* in Duran bottles, tubular photobioreactors and stirred-tank bioreactors are compared in Table 4.26. The table also provides some literature data that had been obtained in freshwater media.

Table 4.26 The lipid productivity of *C. vulgaris* in Duran bottles, tubular photobioreactors and stirred-tank bioreactors

Sample from	Lipid productivity ($mg\ L^{-1}d^{-1}$)
1 L Duran bottle (freshwater)	18.3
(seawater)	37.10
2 L Duran bottle (freshwater)	4.80±0.00
(seawater)	11.43±0.13
PBR 1	15.08±0.00
PBR 2	2.63±0.00
PBR 3	4.87±0.01
PBR 4	0.32±0.00
PBR 5	2.37±0.01
PBR 6	8.04±0.00
PBR 7	13.62±0.02
PBR 8	7.03±0.00
PBR 10	7.02±0.00
PBR 11	3.00±0.00
PBR 12	0.68±0.00
PBR 13	0.56±0.00
PBR 15	0.44±0.00
STR 1	23.46±0.29
STR 2	42.24±0.25
STR 3	12.27±0.41

Table 4.26 The lipid productivity of *C. vulgaris* in Duran bottles, tubular photobioreactors and stirred-tank bioreactors (Cont.)

Sample from	Lipid productivity ($mg\ L^{-1}d^{-1}$)
STR 4	32.71±0.39
STR 5 (Day 38)	27.16±0.03
STR 6 (Day 29)	16.63±0.34
STR 7 at SS1	13.31±0.50
STR 8 at SS1	10.13±0.19
SS2	3.71±0.08
STR 9 at SS1	11.69±0.15
STR 10	19.07±0.02
STR 11 at SS11	5.43±0.02
SS12	14.75±0.23
SS13	18.29±0.62
SS14	19.01±0.40
STR 11 at SS21	8.40±0.54
SS22	15.71±0.54
SS23	21.28±0.10
SS24	27.78±0.45
STR 12 at SS11	5.75±0.24
SS12	20.06±0.42
SS13	7.75±0.02
SS14	19.62±1.56

Table 4.26 The lipid productivity of *C. vulgaris* in Duran bottles, tubular photobioreactors and stirred-tank bioreactors (Cont.)

Sample from	Lipid productivity ($mg\ L^{-1}d^{-1}$)
STR 12 at SS21	5.43±0.38
SS22	10.27±0.39
SS23	16.88±0.63
SS24	16.51±0.43
Scragg *et al*. (2002)[a]	11.20
Scragg *et al*. (2002)[b]	13.90
Liang *et al.* (2009)[c]	4.00
Lee *et al.* (2010)[d]	11.10
Potvin *et al.* (2011)[e]	32.00

[a] Grown in tubular photobioreactor in nutrient sufficient freshwater media

[b] Grown in tubular photobioreactor in nitrogen limited freshwater media

[c] Grown in 1 L bottle with freshwater medium

[d] Grown in 9 L jar with freshwater medium

[e] Grown in tubular photobioreactor with freshwater medium

The biomass samples being compared in Table 4.26 were produced under different sets of previously mentioned conditions. Therefore, the purpose of the table is simply to compare the maximum lipid productivities attainable, with some of the published data. An extensive review of lipid productivity of many microalgae suggests a productivity of 26-28

mg $L^{-1}d^{-1}$ for freshwater *C. vulgaris* in nutrient replete conditions (Griffiths & Harrison, 2009). For freshwater *C. vulgaris* grown in a tubular photobioreactor, Potvin *et al*. (2011) reported a lipid productivity of 32 mg $L^{-1}d^{-1}$. This appears to be one of the highest values reported. Under suitable conditions, a similar level of productivity is attainable in seawater, as shown by a productivity of nearly 33 mg $L^{-1}d^{-1}$ for the run STR 4 (Table 4.26). A much higher lipid productivity of >42 mg $L^{-1}d^{-1}$ was consistently attainable (run STR 2, Table 4.26) under suitable conditions. This appears to be one of the highest values attained for *C. vulgaris*. A majority (>57%) of the productivity data measured in this work (Table 4.26) exceeded the maximum productivity of 13.9 mg $L^{-1}d^{-1}$ reported for freshwater *C. vulgaris* in a tubular photobioreactor under nitrogen limiting conditions (Scragg *et al.*, 2002). For microalgae that have been grown in seawater, the oil productivity has mainly ranged from 17 to 77 mg $L^{-1}d^{-1}$ in nutrient replete media (Griffiths & Harrison, 2009).

Chapter 5

Summary and Conclusions

5.1 Summary

This work focused on characterization of production of crude oil (total lipids) by the microalga *C. vulgaris* in full strength seawater media. A screening of several microalgae that were readily accessible in New Zealand led to the choice of *C. vulgaris* as the focus of this study as this alga had a high oil productivity in full strength seawater. An ability to thrive and produce oil in a seawater environment was an important selection criterion because any future production of fuel oils using algae cannot use freshwater that is generally in short supply worldwide and has other important uses. Municipal wastewater has a limited supply and therefore cannot be used to produce any substantial quantity of microalgae, as has been demonstrated by earlier analyses (Chisti, 2012).

C. vulgaris is normally a freshwater alga and has only been studied as such (Illman *et al.*, 2000; Scragg *et al.*, 2002; Liang *et al.*, 2009; Bhola *et al.*, 2011; Potvin *et al.*, 2011; Hempel *et al.*, 2012; Mujtaba *et al.*, 2012). No prior extensive characterization of this alga in full strength marine media existed. Hence, the need for this study. *C. vulgaris* had other important advantages in being safe and edible by humans and domestic animals (Becker, 1994). In freshwater media, *C. vulgaris* was known to be one of the fastest growing microalgae that thrives in warm (25-30 °C) tropical waters. An ability to thrive in relatively warm waters is important in an oil producing alga because it allows it to be grown in tropical regions that have high levels of irradiance throughout the calendar year and therefore

potentially allow year-round production of the oil. Tropical shallow waters also generally tend to be warm (25-30 °C).

In small (1 L) culture bottles in a seawater based media at 25-27 °C, *C. vulgaris* was shown to have a relatively high oil productivity of 37.1 mg $L^{-1}d^{-1}$. Also, the calorific value (i.e. the total energy content) of the algal biomass was high at >25 kJ g^{-1}. An alga with a high calorific value is useful for fuel production even if some of the calorific value of the biomass is due to nonoil products such as carbohydrates. This is because after the oil has been extracted, the residual biomass still contains a significant amount of biochemical energy that can be recovered by processes such as anaerobic digestion to combustible biogas (Nyns & Naveau, 1982; Samson & Le Duy, 1982; Sánchez Hernández & Travieso Córdoba, 1993; Chisti, 2008; Vergara-Fernández *et al.*, 2008; Ras *et al.*, 2011; Zamalloa *et al.*, 2011). This additional energy can be used in operations involved in growing the biomass and extraction of the oil.

In freshwater media, others have achieved an oil productivity of 32 mg $L^{-1}d^{-1}$ using *C. vulgaris* (Potvin *et al.*, 2011). This oil productivity was for a biomass concentration of 7.7 g L^{-1} and therefore, the biomass specific productivity of the oil must have been quite low. In freshwater media, an oil content of 21% was attained by Bhola *et al*. (2011) but the biomass had an exceedingly low calorific value of only 17.4 kJ g^{-1} (Bhola *et al.*, 2011). One report suggests a lipid productivity of 88.5 mg $L^{-1}d^{-1}$ for freshwater *C. vulgaris* (Hempel *et al.*, 2012). In freshwater media, nitrogen deprivation at late stages of culture has enhanced the oil content and calorific value of algal biomass (Illman *et al.*, 2000; Scragg *et al.*, 2002; Griffiths & Harrison, 2009). In studies with *C. vulgaris* in freshwater media, the calorific value of the biomass could be raised to 23 kJ g^{-1} through nitrogen starvation (Illman *et al.*, 2000), but this is comparable to the value attained in the present study without nitrogen

starvation in a marine medium. Without nitrogen starvation, the calorific value of *C. vulgaris* was 18 kJ g^{-1} (Illman *et al.*, 2000).

As pointed out in Section 4.3.1, the algal biomass was grown to a high concentration in seawater with the above mentioned reasonably high productivities of lipids and a high calorific value, but using a relatively low phosphate level in the medium. This assured a complete consumption of phosphate and demonstrated that a good oil productivity could be achieved without an excessive consumption of phosphorus. This is important for large-scale production of algal oils for fuel, as phosphorus is a nonrenewable resource and its global supply is limited (Cordell *et al.*, 2009; Gilbert, 2009).

The effect of day-night cycling on *C. vulgaris* in seawater was characterized in comparison with continuous illumination. Day-night cycling reduced biomass productivity to 68% of the productivity under continuous illumination. Similarly, the oil productivity was reduced to 69% of the continuous illumination productivity. This productivity reduction would occur in any alga, as a 12 h/12 h night-day cycle reduces the supply of light by 50% compared with 24 h illumination. The latter is unfortunately not possible if the freely available sunlight is to be used for producing algal fuel oils. Significantly, day-night cycling did not affect the oil content of the algal biomass in comparison with continuous illumination (Section 4.12). Furthermore, day-night cycling had barely any impact on the calorific value of the biomass which was within 8% of the calorific value obtained for continuous illumination (Section 4.12).

Self-consumptive biomass loss kinetics of *C. vulgaris* were characterized in a seawater medium. All algae are known to loose biomass in the dark as starch is consumed by respiration to satisfy the metabolic energy demand, but the kinetics of loss appear not to have been characterized for any alga. The self-consumptive loss was found to be first-order in the concentration of the biomass. The rate of biomass loss was highest at 25 °C. As the dark

period in practice will never exceed 12 h, a maximum of ~3% of the biomass attained at the end of the previous light period may be lost during the night by *C. vulgaris* cultures. In the subsequent light period this loss will be recovered and additional biomass will be produced. This will result in net growth until either light or some nutrient becomes limiting.

Highly controlled batch and continuous cultures of *C. vulgaris* in marine media were carried out in tubular photobioreactors to characterize the behaviour of the culture under various conditions. The maximum oil productivity attained in these cultures in continuous light was low at 15 mg $L^{-1}d^{-1}$. This value is only 50% of the value that was consistently attained for the same alga in continuously illuminated culture bottles. The main reason for the low lipid productivity in the tubular photobioreactor was the cyclic biomass loss from the culture broth as a consequence of foaming that could not be prevented despite multiple attempts and modification of the operational strategies. Although, certain *Chlorella* strains have been previously successfully grown in tubular photobioreactors (Scragg *et al.*, 2002; de Morais & Costa, 2007; Ortiz *et al.*, 2010; Potvin *et al.*, 2011), the media used were based on freshwater in all cases. In seawater based media, an extremely high concentration of salt (>35 g L^{-1}) severely reduces bubble coalescence (Chisti, 1989). Small bubbles (1-2 mm) produced by turbulence-associated break up of larger bubbles accumulate in the culture broth to form a fine gas-liquid emulsion and froth. Cells attach to bubbles and are carried out into the headspace of the reactor by the froth. Also, the presence of many small bubbles in the broth adversely affects light penetration and therefore cell growth. Although the oil productivity in tubular photobioreactor was low, the calorific value of the biomass was sufficiently high in most cases. For example, of the 13 calorific values shown in Table 4.7, a vast majority (>80%) exceeded the value of 18 kJ g^{-1} reported for *C. vulgaris* produced in freshwater media under nutrient replete conditions (Illman *et al.*, 2000) and a value of 17.4 kJ g^{-1} reported by Bhola *et al*. (2011) for freshwater growth. In nitrogen limited freshwater

media the calorific value of *C. vulgaris* biomass was increased to 23 kJ g^{-1} in studies of Illman *et al*. (2000). In the marine media used in this study, the calorific value of the biomass grown in the tubular bioreactor generally exceeded 23 kJ g^{-1} in nutrient sufficient conditions, for example, in the runs PBR 1-3 (Table 4.7) and runs PBR 5-6 (Table 4.3). Notwithstanding the low biomass and oil productivities, a steady state operation of continuous cultures in the tubular photobioreactor was shown to be possible.

Compared with the tubular photobioreactor cultures, the studies in the stirred-tank bioreactors were far more promising. In these studies, depending on the operational conditions, high values of lipid in biomass and high calorific value of the biomasss were commonly attained. For example, the lipid contents in the biomass were >20% in >31% of the 35 measurements (Table 4.10) and >30% in several cases (Table 4.10). In view of the data in Table 4.10, *C. vulgaris* is quite capable of attaining a lipid level of >50% in the biomass. The calorific value of the biomass exceeded 25 kJ g^{-1} in >40% of the 34 measurements (Table 4.10). Calorific values of ≥27 kJ g^{-1} were attained in several cases in Table 4.10. Depending on the conditions, the lipid productivity was >15 mg $L^{-1}d^{-1}$ in 55% of the 27 cases in Table 4.12.

Nitrogen starvation was shown to be able to enhance the lipid content in the biomass by at least 3.3-fold relative to nonstarved conditions. In steady state continuous cultures in stirred-tank bioreactors, existence of an optimum dilution rate for maximizing the productivity of the biomass and lipids was demonstrated. The optimal dilution rate depended on the level of irradiance. The reasons behind the variation of productivity with dilution rate were explained.

Some work was done on the unknown marine microalga MGA-1-NZ as it had initially appeared promising for oil production. For example, the oil contents of the biomass exceeded 20% in >33% of the 12 measurements in Table 4.15 and the calorific value

exceeded 25 kJ g^{-1} in >58% of 12 measurements (Table 4.15). The maximum lipid productivity of the alga was about 23 mg $L^{-1}d^{-1}$ (Table 4.17).

Further work on MGA-1-NZ was discontinued in favor of *C. vulgaris* as the latter was superior on terms of oil content in the biomass, the calorific value of the biomass and the lipid productivity, specially in nitrogen depleted conditions. *C. vulgaris* crude oil generally had a high proportion (e.g. >45% in >58% of the 12 measurements shown in Table 4.19) of neutral lipids, but a high proportion of the fatty acids in the oil were polyunsaturated fatty acids. These are generally considered to be poorly suited for direct conversion to biodiesel. The presence of a good proportion of the saturated and monounsaturated fatty acids in many of oil samples (Table 4.22) and the data reported by others for freshwater grown *C. vulgaris* (Yeh & Chang, 2011; Mallick *et al.*, 2012; Ördög *et al.*, 2013), suggest that the culture conditions can be potentially modified to favor the production of saturated and monounsaturated fatty acids instead of the polyunsaturates.

Relatively high concentrations of certain elements (Ca, Cu, Fe, Mg, N, P, Na, S) were found in the crude oil of *C. vulgaris*. These elements have the potential to interfere with certain chemical catalytic processes that would be required to convert the crude oil to diesel, gasoline and kerosene. Future studies should develop oil extraction or pretreatment methods that either extract a cleaner crude oil or wash away the unwanted elements as much as possible.

5.2 Conclusions

1. Of the freshwater microalgae screened, only *C. vulgaris*, or some strains of it, can grow in full strength seawater nearly as well as in freshwater.

2. In growth on seawater media, *C. vulgaris* is capable of attaining lipid productivities that are comparable to what is attainable by this alga in freshwater media. The lipid content in the biomass of marine growth of *C. vulgaris* can be commonly >30% (w/w), but has the potential to be raised to >50% (w/w).
3. In marine media, nitrogen starvation of *C. vulgaris* enhances the lipid content in the biomass by at least 3.3-fold relative to the nonstarved conditions.
4. In marine media, *C. vulgaris* biomass can be made to achieve exceptionally high calorific values of >25 kJ g^{-1}, but the metabolic potential of the alga is such that biomass with a calorific value of >27 kJ g^{-1} can be produced.
5. Like other microalgae, seawater grown *C. vulgaris* consumed itself in the dark, but the loss in biomass during a 12-h night is not likely to exceed ~3% of the biomass attained at the end of the previous light period. The biomass loss kinetics tend to be of first-order in the concentration of the biomass.
6. *C. vulgaris* can be grown readily both in batch and steady-state continuous cultures in marine media, but appears to be easier to grow in relatively quiescent stirred-tank photobioreactor rather than in the highly turbulent tubular photobioreactors.
7. The crude oil of *C. vulgaris* grown in marine media generally has a low proportion of triglycerides. The triglycerides present in the oil are fairly rich in polyunsaturated fatty acids but also contain substantial amounts of saturated and monounsaturated fatty acids.
8. Methods will need to be developed to remove the high levels of elements such as Ca, Cu, Fe, Mg, N, P, Na, and S from the crude algal oil to allow it to be processed via chemical catalysis to usable fuels such as diesel, gasoline and kerosene.

In view of the low amount of fatty acids in the crude *C. vulgaris* oil, it is unlikely to be an economic source of biodiesel.

References

Acién Fernández, F. G., Sevilla, J. M. F., Perez, J. A. S., Grima, E. M., & Chisti, Y. (2001). Airlift-driven external-loop tubular photobioreactors for outdoor production of microalgae: assessment of design and performance. *Chemical Engineering Science, 56*, 2721-2732.

Acién, F. G., Fernández, J. M., Magán, J. J., & Molina, E. (2012). Production cost of a real microalgae production plant and strategies to reduce it. *Biotechnology Advances, 30*, 1344-1353.

Affenzeller, M. J., Darehshouri, A., Andosch, A., Lutz, C., & Lutz-Meindl, U. (2009). Salt stress-induced cell death in the unicellular green alga *Micrasterias denticulata*. *Journal of Experimental Botany, 60*, 939-954.

Alonso, D. L., Belarbi, E.-H., Fernández-Sevilla, J. M., Rodriguez-Ruiz, J., & Grima, E. M. (2000). Acyl lipid composition variation related to culture age and nitrogen concentration in continuous culture of the microalga *Phaeodactylum tricornutum*. *Phytochemistry, 54*, 461-471.

Alyabyev, A. J., Loseva, N. L., L. Kh, G., Andreyeva, I. N., Rachimova, G. G., Tribunskih, V. I., Ponomareva, A. A., & Kemp, R. B. (2007). The effect of changes in salinity on the energy yielding processes of *Chlorella vulgaris* and *Dunaliella maritima* cells. *Thermochimica Acta, 458*, 65-70.

Anderson, R. A. (Ed.). (2005). *Algal culturing techniques*. Burlington, MA: Elsevier.

Araujo, G. S., Matos, L. J. B. L., Fernandes, J. O., Cartaxo, S. J. M., Gonçalves, L. R. B., Fernandes, F. A. N., & Farias, W. R. L. (2013). Extraction of lipids from microalgae by ultrasound application: Prospection of the optimal extraction method. *Ultrasonics Sonochemistry, 20*, 95-98.

Araújo, O. Q. F., Gobbi, C. N., Chaloub, R. M., & Coelho, M. A. Z. (2008). Assessment of the impact of salinity and irradiance on the combined carbon dioxide sequestration and carotenoids production by *Dunaliella salina*: A mathematical model. *Biotechnology and Bioengineering, 102*, 425-435.

Atkin, O. K., Edwards, E. J., & Loveys, B. R. (2000). Response of root respiration to changes in temperature and its relevance to global warming. *New Phytologist, 147*, 141-154.

Avron, M. (1986). The osmotic components of halotolerant algae. *Trends in Biochemical Sciences, 11*, 5-6.

Banerjee, A., Sharma, R., Chisti, Y., & Banerjee, U. C. (2002). *Botryococcus braunii*: A renewable source of hydrocarbons and other chemicals. *Critical Reviews in Biotechnology, 22*, 245-279.

Banković-Ilić, I. B., Stamenković, O. S., & Veljković, V. B. (2012). Biodiesel production from non-edible plant oils. *Renewable and Sustainable Energy Reviews, 16*, 3621-3647.

Baum, S. D., Haqq-Misra, J. D., & Karmosky, C. (2012). Climate change: Evidence of human causes and arguments for emissions reduction. *Science and Engineering Ethics, 18*, 393-410.

Becker, E. W. (1994). *Microalgae: Biotechnology and microbiology*. Cambridge: Cambridge University Press.

Belarbi, E. H., Molina, E., & Chisti, Y. (2000). A process for high yield and scalable recovery of high purity eicosapentaenoic acid esters from microalgae and fish oil. *Enzyme and Microbial Technology, 26*, 516-529.

Bergmann, P., Ripplinger, P., Beyer, L., & Trösch, W. (2013). Disposable flat panel airlift photobioreactors. *Chemie Ingenieur Technik, 85*, 202-205.

Bertozzini, E., Galluzzi, L., Penna, A., & Magnani, M. (2011). Application of the standard addition method for the absolute quantification of neutral lipids in microalgae using Nile red *Journal of Microbiological Methods, 87*, 17-23.

Bhola, V., Desikan, R., Santosh, S. K., Subburamu, K., Sanniyasi, E., & Bux, F. (2011). Effects of parameters affecting biomass yield and thermal behaviour of *Chlorella vulgaris*. *Journal of Bioscience and Bioengineering, 111*, 377-382.

Bisson, M. A., & Kirst, G. O. (1995). Osmotic acclimation and turgor pressure regulation in algae. *Naturwissenschaften, 82*, 461-471.

Bligh, E. G., & Dyer, W. J. (1959). A rapid method of total lipid extraction and purification. *Canadian Journal of Biochemistry and Physiology*(8), 911-917.

Bolton, J. R., & Hall, D. O. (1991). The maximum efficiency of photosynthesis. *Photochemistry and Photobiology, 53*, 545-548.

Borowitzka, M. A. (1995). Microalgae as sources of pharmaceuticals and other biologically-active compounds. *Journal of Applied Phycology, 7*, 3-15.

Borowitzka, M. A. (2005). Culturing microalgae in outdoor ponds. In I. R. A. Anderson (Ed.), *Algal culturing techniques* (pp. 205-218). New York: Elsevier.

Borugadda, V. B., & Goud, V. V. (2012). Biodiesel production from renewable feedstocks:Status and opportunities. *Renewable and Sustainable Energy Reviews, 16*, 4763-4784.

Boussiba, S., Vonshank, A., Cohen, Z., Avissar, Y., & Richmond, A. (1987). Lipid and biomass production by the halotolerant microalga *Nannochloropsis salina*. *Biomass, 12*, 37-47.

Breuer, G., Lamers, P. P., Martens, D. E., Draaisma, R. B., & Wijffels, R. H. (2012). The impact of nitrogen starvation on the dynamics of triacylglycerol accumulation in nine microalgae strains. *Bioresource Technology, 124*, 217-226.

Bumbak, F., Cook, S., Zachleder, V., Hauser, S., & Kovar, K. (2011). Best practices in heterotrophic high-cell-density microalgal processes: achievements, potential and possible limitations. *Applied Microbiology and Biotechnology, 91*, 31-46.

Camacho Rubio, F., Camacho, F. G., Sevilla, J. M. F., Chisti, Y., & Grima, E. M. (2003). A mechanistic model of photosynthesis in microalgae. *Biotechnology and Bioengineering, 81*, 459-473.

Campenni', L., Nobre, B. P., Santos, C. A., Oliveira, A. C., Aires-Barros, M. R., Palavra, A. M. F., & Gouveia, L. (2013). Carotenoid and lipid production by the autotrophic microalga *Chlorella protothecoides* under nutritional, salinity, and luminosity stress conditions. *Applied Microbiology and Biotechnology, 97*, 1383-1393.

Cappuccino, J. G., & Natalie, S. (2011). *Microbiology: A laboratory manual* (9th ed.). USA: Pearson Education, Inc.

Cardozo, K. H. M., Guaratini, T., Barros, M. P., Falcão, V. R., Tonon, A. P., Lopes, N. P., Campos, S., Torres, M. A., Souza, A. O., Colepicolo, P., & Pinto, E. (2007). Metabolites from algae with economical impact. *Comparative Biochemistry and Physiology C – Toxicology & Pharmacology, 146*, 60-78.

Carvalho, A. P., & Malcata, F. X. (2005). Optimization of ω-3 fatty acid production by microalgae: crossover effect of CO_2 and light intensity under batch and continuous cultivation modes. *Marine Biotechnology, 7*, 381-388.

Carvalho, A. P., Meireles, L. A., & Malcata, F. X. (2006). Microalgal reactors: A review of enclosed system designs and performances. *Biotechnology Progress, 22*, 1490-1506.

Cembella, A. D., Antia, N. J., & Harrison, P. J. (1984). The utilization of inorganic and organic phosphorus compounds as nutrients by eukaryotic microalgae: A multidisciplinary perspective : Part 2. *Critical Reviews in Microbiology, 11*, 13-81.

Chase, M. W., Soltis, D. E., Olmstead, R. G., Morgan, D., Lee, D. H., Mishler, B. D., Duvall, M. R., Price, R. A., Hills, H. G., Qiu, Y.-L., Kron, K. A., Retting, J. H., Conti, E., Palmer, J. D., Manhart, J. R., Sytsma, K. J., Michael, H. J., Kress, W. J., Karol, K. G., Clark, W. D., Hedren, M., Gaut, B. S., Jansen, R. K., Kim, K.-J., Wimpee, C. F., Smith, J. F., Furnier, G. R., Strauss, S. H., Xiang, Q.-Y., Plunkett, G. M., Soltis, P. S., Swensen, S. M., Williams, S. E., Gadek, P. A., Quinn, C. J., Eguiarte, L. E., Golenberg, E., Gerald H. Learn, J., Graham, S. W., Barrett, S. C. H., Dayanandan, S., & Albert, V. A. (1993). Phylogenetics of seed plants: An analysis of nucleotide sequences from the plastid gene *rbc*L[1]. *Annals of the Missouri Botanic Garden, 80*, 528-580.

Chen, F., & Johns, M. R. (1991). Effect of C/N ratio and aeration on the fatty acid composition of heterotrophic *Chlorella sorokiniana. Journal of Applied Phycology, 3*, 203-209.

Chen, H.-W., Yang, T.-S., Chen, M.-J., Chang, Y.-C., Lin, C.-Y., Wang, E. I.-C., Ho, C.-L., Huang, K.-M., Yu, C.-C., Yang, F.-L., Wu, S.-H., Lu, Y.-C., & Chao, L. K.-P. (2012). Application of power plant flue gas in a photobioreactor to grow *Spirulina* algae, and a bioactivity analysis of the algal water-soluble polysaccharides. *Bioresource Technology, 120*, 256-263.

Chen, W., Zhang, C., Song, L., Sommerfeld, M., & Hu, Q. (2009). A high throughput Nile red method for quantitative measurement of neutral lipids in microalgae. *Journal of Microbiological Methods, 77*, 41-47.

Chi, Z., O'Fallon, J. V., & Chen, S. (2011). Bicarbonate produced from carbon capture for algae culture. *Trends in Biotechnology, 29*, 537-541.

Chinnasamy, S., Ramakrishnan, B., Bhatnagar, A., & Das, K. C. (2009). Biomass production potential of a wastewater alga *Chlorella vulgaris* ARC 1 under elevated levels of CO_2 and temperature. *International Journal of Molecular Sciences, 10*, 518-532.

Chisti, Y. (1989). *Airlift bioreactors*. London: Elsevier.

Chisti, Y. (1999). Shear sensitivity. In M. C. Flickinger & S. W. Drew (Eds.), *Encyclopedia of bioprocess technology: Fermentation, biocatalysis, and bioseparation* (Vol. 5, pp. 2379-2406). New York: Wiley.

Chisti, Y. (2006). Microalgae as sustainable cell factories. *Environmental Engineering and Management Journal, 5*, 261-275.

Chisti, Y. (2007). Biodiesel from microalgae. *Biotechnology Advances, 25*, 294-306.

Chisti, Y. (2008). Biodiesel from microalgae beats bioethanol. *Trends in Biotechnology, 26*, 126-131.

Chisti, Y. (2010). Fuels from microalgae. *Biofuels, 1*, 233-235.

Chisti, Y. (2010*b*). Shear sensitivity. In M. C. Flickinger (Ed.), *Encyclopedia of industrial biotechnology, bioprocess, bioseparation, and cell technology* (Vol. 7, pp. 4360-4398). New York: Wiley.

Chisti, Y. (2012). Raceways-based production of algal crude oil. In C. Posten & C. Walter (Eds.), *Microalgal biotechnology: Potential and production* (pp. 113-146). Berlin: de Gruyter.

Chisti, Y., & Yan, J. (2011). Algal biofuels – A status report. *Applied Energy, 88*, 3277-3279.

Cho, S. H., Ji, S.-C., Hur, S. B., Bae, J., Park, I.-S., & Song, Y.-C. (2007). Optimum temperature and salinity conditions for growth of green algae *Chlorella ellipsoidea* and *Nannochloris oculata*. *Fisheries Science, 73*, 1050-1056.

Christenson, L., & Sims, R. (2011). Production and harvesting of microalgae for wastewater treatment, biofuels, and bioproducts. *Biotechnology Advances, 29*, 686-702.

Ciniglia, C., Yoon, H. S., Pollio, A., Pinto, G., & Bhattacharya, D. (2004). Hidden biodiversity of the extremophilic Cyanidiales red algae. *Molecular Ecology, 13*, 1827-1838.

Converti, A., Casazza, A. A., Ortiz, E. Y., Perego, P., & Borghi, M. D. (2009). Effect of temperature and nitrogen concentration on the growth and lipid content of *Nannochloropsis oculata* and *Chlorella vulgaris* for biodiesel production. *Chemical Engineering and Processing, 48*, 1146-1151.

Cooney, M., Young, G., & Nagle, N. (2009). Extraction of bio-oils from microalgae. *Separation & Purification Reviews, 38*, 291-325.

Cooney, M. J., Young, G., & Pate, R. (2011). Bio-oil from photosynthetic microalgae: Case study. *Bioresource Technology, 102*, 166-177.

Cordell, D., Drangert, J.-O., & White, S. (2009). The story of phosphorus: Global food security and food for thought. *Global Environmental Change, 19*, 292-305.

Courchesne, N. M. D., Parisien, A., Wang, B., & Lan, C. Q. (2009). Enhancement of lipid production using biochemical, genetic and transcription factor engineering approaches. *Journal of Biotechnology, 141*, 31-41.

Csavina, J. L., Stuart, B. J., Riefler, R. G., & Vis, M. L. (2011). Growth optimization of algae for biodiesel production. *Journal of Applied Microbiology, 111*, 312-318.

de Boer, K., Moheimani, N. R., Borowitzka, M. A., & Bahri, P. A. (2012). Extraction and conversion pathways for microalgae to biodiesel: a review focused on energy consumption. *Journal of Applied Phycology, 24*, 1681-1698.

de Morais, M. G., & Costa, J. A. V. (2007). Carbon dioxide fixation by *Chlorella kessleri*, *C. vulgaris*, *Scenedesmus obliquus* and *Spirulina* sp. cultivated in flasks and vertical tubular photobioreactors. *Biotechnology Letters, 29*, 1349-1352.

Debska, D., Potvin, G., Lan, C., & Zhang, Z. (2010). Effects of medium composition on the growth of *Chlorella vulgaris* during photobioreactor batch cultivations. *Journal of Biobased Materials and Bioenergy, 4*, 68-72.

Del Campo, J. A., García-González, M., & Guerrero, M. G. (2007). Outdoor cultivation of microalgae for carotenoid production: current state and perspectives. *Applied Microbiology and Biotechnology, 74*, 1163-1174.

Dempster, T. A., & Sommerfeld, M. R. (1998). Effects of environmental conditions on growth and lipid accumulation in *Nitzschia communis* (Bacillariophyceae). *Journal of Phycology, 34*, 712-721.

Dismukes, G. C., Carrieri, D., Bennette, N., Ananyev, G. M., & Posewitz, M. C. (2008). Aquatic phototrophs: efficient alternatives to land-based crops for biofuels. *Current Option in Biotechnology, 19*, 235-240.

Doan, T.-T. Y., & Obbard, J. P. (2011). Improved Nile red staining of *Nannochloropsis* sp. *Journal of Applied Phycology, 23*, 895-901.

Dodd, J. C. (1986). Elements of pond design and construction. In A. Richmond (Ed.), *CRC handbook of microalgal mass culture* (pp. 265-283). Boca Raton, FL: CRC Press.

Donoghue, M. J., Olmstead, R. G., Smith, J. F., & Palmer, J. D. (1992). Phylogenetic relationships of Dipsacales based on *rbc*L sequences. *Annals of the Missouri Botanic Garden, 79*, 333-345.

Doran, P. M. (1995). *Bioprocess engineering principles*. London: Academic Press Limited.

Duerr, E. O., Molnar, A., & Sato, V. (1998). Cultured microalgae as aquaculture feeds. *Journal of Marine Biotechnology, 6*, 65-70.

Eixler, S., Selig, U., & Karsten, U. (2005). Extraction and detection methods for polyphosphate storage in autotrophic planktonic organisms. *Hydrobiologia, 533*, 135-143.

Elsey, D., Jameson, D., Raleigh, B., & Cooney, M. J. (2007). Fluorescent measurement of microalgal neutral lipids. *Journal of Microbiological Methods, 68*, 639-642.

Feng, Y., Li, C., & Zhang, D. (2011). Lipid production of *Chlorella vulgaris* cultured in artificial wastewater medium. *Bioresource Technology, 102*, 101-105.

Fernández, I., Acién, F. G., Fernández, J. M., Guzmán, J. L., Magán, J. J., & Berenguel, M. (2012). Dynamic model of microalgal production in tubular photobioreactors. *Bioresource Technology, 126*, 172-181.

Ferroni, L., Baldisserotto, C., Pantaleoni, L., Billi, P., Fasulo, M. P., & Pancaldi, S. (2007). High salinity alters chloroplast morpho-physiology in a freshwater *Kirchneriella* species (Selenastraceae) from Ethiopian Lake Awasa. *American Journal of Botany, 94*, 1972-1983.

Franco-Lara, E., Havel, J., Peterat, F., & Weuster-Botz, D. (2006). Model-supported optimization of phototrophic growth in a stirred-tank photobioreactor. *Biotechnology and Bioengineering, 95*, 1177-1187.

Fu, W., Gudmundssona, O., Feist, A. M., Herjolfssona, G., Brynjolfssona, S., & Palsson, B. Ø. (2012). Maximizing biomass productivity and cell density of *Chlorella vulgaris* by using light-emitting diode-based photobioreactor. *Journal of Biotechnology, 161*, 242-249.

Gallardo Rodríguez, J. J., Mirón, A. S., Camacho, F. G., García, M. C. C., Belarbi, E. H., Chisti, Y., & Grima, E. M. (2009). Causes of shear sensitivity of the toxic dinoflagellate *Protoceratium reticulatum*. *Biotechnology Progress, 25*, 792-800.

Gallardo Rodríguez, J. J., Mirón, A. S., Camacho, F. G., García, M. C. C., Belarbi, E. H., Chisti, Y., & Grima, E. M. (2011). Carboxymethyl cellulose and Pluronic F68 protect the dinoflagellate *Protoceratium reticulatum* against shear-associated damage. *Bioprocess and Biosystems Engineering, 34*, 3-12.

García Camacho, F., Grima, E. M., Mirón, A. S., Pascual, V. G., & Chisti, Y. (2001). Carboxymethyl cellulose protects algal cells against hydrodynamic stress. *Enzyme and Microbial Technology, 29*, 602-610.

García Camacho, F., Rodríguez, J. G., Mirón, A. S., García, M. C. C., Belarbi, E. H., Chisti, Y., & Grima, E. M. (2007). Biotechnological significance of toxic marine dinoflagellates. *Biotechnology Advances, 25*, 176-194.

García Camacho, F., Rodríguez, J. J. G., Mirón, A. S., Belarbi, E. H., Chisti, Y., & Grima, E. M. (2011). Photobioreactor scale-up for a shear-sensitive dinoflagellate microalga. *Process Biochemistry, 46*, 936-944.

Geider, R. J., & Roche, J. L. (2002). Redfield revisited: variability of C:N:P in marine microalgae and its biochemical basis. *European Journal of Phycology, 37*, 1-17.

Giannelli, L., Scoma, A., & Torzillo, G. (2009). Interplay between light intensity, chlorophyll concentration and culture mixing on the hydrogen production in sulfur-deprived *Chlamydomonas reinhardtii* cultures grown in laboratory photobioreactors. *Biotechnology and Bioengineering, 104*, 76-90.

Gielly, L., & Taberlet, P. (1994). The use of chloroplast DNA to resolve plant phylogenies: Noncoding versus *rbc*L sequences. *Molecular Biology and Evolution, 11*, 769-777.

Gilbert, N. (2009). The disappearing nutrient. *Nature, 461*, 716-718.

Gleick, P. H. (1998). Water in crisis: Paths to sustainable water use. *Ecological Applications, 8*, 571-579.

Goldman, J. C. (1979). Outdoor algal mass cultures-II. Photosynthetic yield limitations. *Water Research, 13*, 119-136.

Goldman, J. C., & Carpenter, E. J. (1974). A kinetic approach to the effect of temperature on algal growth. *Limnology and Oceanography, 19*, 756-766.

Gómez, P. I., Barriga, A., Cifuentes, A. S., & González, M. A. (2003). Effect of salinity on the quantity and quality of carotenoids accumulated by *Dunaliella salina* (strain CONC-007) and *Dunaliella bardawil* (strain ATCC 30861) Chlorophyta. *Biological Research, 36*, 185-192.

González, J. A., & Calbó, J. (2002). Modelled and measured ratio of PAR to global radiation under cloudless skies. *Agricultural and Forest Meteorology, 110*, 319-325.

González López, C. V., García, M. d. C. C., Fernández, F. G. A., Bustos, C. S., Chisti, Y., & Sevilla, J. M. F. (2010). Protein measurements of microalgal and cyanobacterial biomass. *Bioresource Technology, 101*, 7587-7591.

Gordon, J. M., & Polle, J. E. W. (2007). Ultrahigh bioproductivity from algae. *Applied Microbiology and Biotechnology, 76*, 969-975.

Greenwell, H. C., Laurens, L. M. L., Shields, R. J., Lovitt, R. W., & Flynn, K. J. (2010). Placing microalgae on the biofuels priority list: a review of the technological challenges. *Journal of the Royal Society Interface, 7*, 703-726.

Griffiths, M. J., & Harrison, S. T. L. (2009). Lipid productivity as a key characteristic for choosing algal species for biodiesel production. *Journal of Applied Phycology, 21*, 493-507.

Griffiths, M. J., van Hille, R. P., & Harrison, S. T. L. (2012). Lipid productivity, settling potential and fatty acid profile of 11 microalgal species grown under nitrogen replete and limited conditions. *Journal of Applied Phycology, 24*, 989-1001.

Grobbelaar, J. U. (2004). Algal nutrition. In A. Richmond (Ed.), *Handbook of microalgal culture: Biotechnology and applied phycology* (pp. 97-115). Oxford: Blackwell.

Gu, N., Lin, Q., Li, G., Tan, Y., Huang, L., & Lin, J. (2012). Effect of salinity on growth, biochemical composition, and lipid productivity of *Nannochloropsis oculata* CS 179. *Engineering in Life Science, 12*, 631-637.

Guedes, A. C., Amaro, H. M., & Malcata, F. X. (2011). Microalgae as sources of carotenoids. *Marine Drugs, 9*, 625-644.

Guerin, M., Huntley, M. E., & Olaizola, M. (2003). *Haematococcus* astaxanthin: applications for human health and nutrition. *Trends in Biotechnology, 21*, 210-216.

Guschina, I. A., & Harwood, J. L. (2006). Lipids and lipid metabolism in eukaryotic algae. *Progress in Lipid Research, 45*, 160-186.

Gustavs, L., Eggert, A., Michalik, D., & Karsten, U. (2010). Physiological and biochemical responses of green microalgae from different habitats to osmotic and matric stress. *Protoplasma, 243*, 3-14.

Hach. (2009). Nitrate, HR, Cadmium reduction method 8039, 1st edition. Retrieved 9th 2009, from Hach Company.

Haik, Y., Selim, M. Y. E., & Abdulrehman, T. (2010). *Combustion of raw algae oil and its methyl ester in a diesel engine.* Paper presented at the ASME 10th Biennial Conference on Engineering Systems Design and Analysis

Haik, Y., Selim, M. Y. E., & Abdulrehman, T. (2011). Combustion of algae oil methyl ester in an indirect injection diesel engine. *Energy, 36*, 1827-1835.

Hakanson, L., & Stenstrom-Khalili, M. I. (2009). Uncertainties in data and spurious correlations related to the Redfield ratio. *International Review of Hydrobiology, 94*(3), 338-351.

Halim, R., Danquah, M. K., & Webley, P. A. (2012). Extraction of oil from microalgae for biodiesel production: A review. *Biotechnology Advances, 30*, 709-732.

Hall, C. A. S., & Benemann, J. R. (2011). Oil from algae? *BioScience, 62*, 741-742.

Hanagata, N., Takeuchi, T., Fukuju, T., Barnes, C. J., & Karube, I. (1992). Tolerance of microalgae to high CO_2 and high temperature. *Phytochemistry, 31*, 3345-3348.

Harwood, J. L., & Guschina, I. A. (2009). The versatility of algae and their lipid metabolism. *Biochimie, 91*, 679-684.

He, Y.-Y., & Häder, D.-P. (2002). Reactive oxygen species and UV-B: effect on cyanobacteria. *Photochemical and Photobiological Sciences, 1*, 729-736.

Hemaiswarya, S., Raja, R., Kumar, R. R., Ganesan, V., & Anbazhagan, C. (2011). Microalgae: a sustainable feed source for aquaculture. *World Journal of Microbiology and Biotechnology, 27*, 1737-1746.

Hempel, N., Petrick, I., & Behrendt, F. (2012). Biomass productivity and productivity of fatty acids and amino acids of microalgae strains as key characteristics of suitability for biodiesel production. *Journal of Applied Phycology, 24*, 1407-1418.

Henley, W. J. (1993). Measurement and interpretation of photosynthetic light-response curves in algae in the context of photoinhibition and diel changes. *Journal of Phycology, 29*, 729-739.

Heredia-Arroyo, T., Wei, W., Ruan, R., & Hu, B. (2011). Mixotrophic cultivation of *Chlorella vulgaris* and its potential application for the oil accumulation from non-sugar materials. *Biomass and Bioenergy, 35*, 2245-2253.

Hernández, J.-P., de-Bashan, L. E., & Bashan, Y. (2006). Starvation enhances phosphorus removal from wastewater by the microalga *Chlorella* spp. co-immobilized with *Azospirillum brasilense*. *Enzyme and Microbial Technology, 38*, 190-198.

Herrera-Valencia, V. A., Contreras-Pool, P. Y., López-Adrián, S. J., Peraza-Echeverría, S., & Barahona-Pérez, L. F. (2011). The green microalga *Chlorella saccharophila* as a suitable source of oil for biodiesel production. *Current Microbiology, 63*, 151-157.

Hsiao, S. I. C. (1988). Spatial and seasonal variations in primary production of sea ice microalgae and phytoplankton in Frobisher Bay, Arctic Canada. *Marine Ecology - Progress Series, 44*, 275-285.

Hu, Q., Kurano, N., Kawachi, M., Iwasaki, I., & Miyachi, S. (1998). Ultrahigh-cell-density culture of a marine green alga *Chlorococcum littorale* in a flat-plate photobioreactor. *Applied Microbiology and Biotechnology, 49*, 655-662.

Hu, Q., Sommerfeld, M., Jarvis, E., Ghorardi, M., Posewitz, M., Seibert, M., & Darzins, A. (2008). Microalgal triacyglycerols as feedstocks for biofuel production: perspectives and advances. *The Plant Journal, 54*, 621-639.

Huang, G., Chen, F., Wei, D., Zhang, X., & Chen, G. (2010). Biodiesel production by microalgal biotechnology. *Applied Energy, 87*, 38-46.

Huang, G., Chen, G., & Chen, F. (2009). Rapid screening method for lipid production in alga based on Nile red fluorescence. *Biomass and Bioenergy, 33*, 1386-1392.

Huang, Y.-m., & Rorrer, G. L. (2003). Cultivation of microplantlets derived from the marine red alga *Agardhiella subulata* in a stirred tank photobioreactor. *Biotechnology Progress, 19*, 418-427.

Hulatt, C. J., Lakaniemi, A.-M., Puhakka, J. A., & Thomas, D. N. (2012). Energy demands of nitrogen supply in mass cultivation of two commercially important microalgal species, *Chlorella vulgaris* and *Dunaliella tertiolecta*. *Bioenergy Reserve, 5*, 669-684.

Illman, A. M., Scragg, A. H., & Shales, S. (2000). Increase in Chlorella strains calorific values when grown in low nitrogen medium. *Enzyme and Microbial Technology, 27*, 631-635.

Jacob-Lopes, E., Scoparo, C. H. G., Lacerda, L. M. C. F., & Franco, T. T. (2009). Effect of light cycles (night/day) on CO_2 fixation and biomass production by microalgae in photobioreactors. *Chemical Engineering and Processing, 48*, 306-310.

James, G. O., Hocart, C. H., Hillier, W., Price, G. D., & Djordjevic, M. A. (2013). Temperature modulation of fatty acid profiles for biofuel production in nitrogen deprived *Chlamydomonas reinhardtii*. *Bioresource Technology, 127*, 441-447.

Janssen, M., Kuijpers, T. C., Veldhoen, B., Ternbach, M. B., Tramper, J., Mur, L. R., & Wijffels, R. H. (1999). Specific growth rate of *Chlamydomonas reinhardtii* and *Chlorella sorokiniana* under medium duration light/dark cycles: 13–87 s. *Journal of Biotechnology, 70*, 323-333.

Janssen, M., Tramper, J., Mur, L. R., & Wijffels, R. H. (2003). Enclosed outdoor photobioreactors: light regime, photosynthetic efficiency, scale-up, and future prospects. *Biotechnology and Bioengineering, 81*, 193-210.

John, E. H., & Flynn, K. J. (2000). Modelling phosphate transport and assimilation in microalgae; how much complexity is warranted? *Ecological Modelling, 125*, 145-157.

Jones, C. S., & Mayfield, S. P. (2012). Algae biofuels: versatility for the future of bioenergy. *Current Opinion in Biotechnology, 23*, 346-351.

Kanda, H., Li, P., Ikehara, T., & Yasumoto-Hirose, M. (2012). Lipids extracted from several species of natural blue–green microalgae by dimethyl ether: Extraction yield and properties. *Fuel, 95*, 88-92.

Kates, M. (1986). *Techniques of lipidology: Isolation, analysis and identification of lipids* (2nd revised ed.). Amsterdam: Elsevier.

Kay, R. A. (1991). Microalgae as food and supplement. *Critical Reviews in Food Science and Nutrition, 30*, 555-573.

Kessler, E. (1974). Physiologische und biochemische Beitrage zur Taxonomie der Gattung *Chlorella*. *Archives of Microbiology, 100*, 51-56.

Khalil, Z. I., Asker, M. M. S., El-Sayed, S., & Kobbia, I. A. (2010). Effect of pH on growth and biochemical rsponses of *Dunaliella bardawil* and *Chlorella ellipsoidea*. *World Journal of Microbiology and Biotechnology, 26*, 1225-1231.

Khozin-Goldberg, I., & Cohen, Z. (2011). Unraveling algal lipid metabolism: Recent advances in gene identification. *Biochimie, 93*, 91-100.

Knothe, G. (2011). A technical evaluation of biodiesel from vegetable oils vs. algae. Will algae-derived biodiesel perform? *Green Chemistry, 13*, 3048-3065.

Kojima, E., & Lin, B. (2004). Effect of partial shading on photoproduction of hydrogen by *Chlorella*. *Journal of Bioscience and Bioengineering, 97*, 317-321.

Kong, W.-B., Hua, S.-F., Cao, H., Muc, Y.-W., Yang, H., Song, H., & Xia, C.-G. (2012). Optimization of mixotrophic medium components for biomass production and biochemical composition biosynthesis by *Chlorella vulgaris* using response surface methodology. *Journal of the Taiwan Institute of Chemical Engineers, 43*, 360-367.

Kong, W.-B., Song, H., Cao, Y., Yang, H., Hua, S., & Xia, C. (2011). The characteristics of biomass production, lipid accumulation and chlorophyll biosynthesis of *Chlorella vulgaris* under mixotrophic cultivation. *African Journal of Biotechnology, 10*(55), 11620-11630.

Krause, G. H., & Weis, E. (1991). Chlorophyll fluorescence and photosynthesis: The basics. *Annual Review of Plant Physiology and Plant Molecular Biology, 42*, 313-349.

Ladas, N. P., & Papageorgiou, G. C. (2000). The salinity tolerance of freshwater cyanobacterium *Synechococcus* sp. PCC 7942 is determined by its ability for osmotic adjustment and presence of osmolyte sucrose. *Photosynthetica, 38*, 343-348.

Lam, M. K., & Lee, K. T. (2012). Potential of using organic fertilizer to cultivate *Chlorella vulgaris* for biodiesel production. *Applied Energy, 94*, 303-308.

Lee, C.-G., & Palsson, B. O. (1996). Photoacclimation of *Chlorella vulgaris* to red light from light emitting diodes leads to autospore release following each cellular division. *Biotechnology Progress, 12*, 249-256.

Li, J., Xu, N. S., & Su, W. W. (2003). Online estimation of stirred-tank microalgal photobioreactor cultures based on dissolved oxygen measurement. *Biochemical Engineering Journal, 14*, 51-65.

Li, X., Přibyl, P., Bišová, K., Kawano, S., Cepák, V., Zachleder, V., Čížková, M., Brányiková, I., & Vítova, M. (2013). The microalga *Parachlorella kessler*i—A novel highly efficient lipid producer. *Biotechnology and Bioengineering, 110*, 97-107.

Li, Y., Horsman, M., Wu, N., Lan, C. Q., & Dubois-Calero, N. (2008). Biocatalysts and bioreactor design. *Biotechnology Progress, 24*, 815-820.

Liang, K., Zhang, Q., Gu, M., & Cong, W. (2013). Effect of phosphorus on lipid accumulation in freshwater microalga *Chlorella* sp. *Journal of Applied Phycology, 25*, 311-318.

Liang, Y., Sarkany, N., & Cui, Y. (2009). Biomass and lipid productivities of *Chlorella vulgaris* under autotrophic, heterotrophic and mixotrophic growth conditions. *Biotechnology Letters, 31*, 1043-1049.

Liu, Z.-Y., Wang, G.-C., & Zhou, B.-C. (2008). Effect of iron on growth and lipid accumulation in *Chlorella vulgaris*. *Bioresource Technology, 99*, 4717-4722.

Lorenz, R. T., & Cysewski, G. R. (2000). Commercial potential for *Haematococcus* microalgae as a natural source of astaxanthin. *Trends in Biotechnology, 18*, 160-167.

Lü, J., Sheahanb, C., & Fu, P. (2011). Metabolic engineering of algae for fourth generation biofuels production. *Energy & Environmental Science, 4*, 2451-2466.

Lynn, S. G., Kilham, S. S., Kreeger, D. A., & Interlandi, S. J. (2000). Effect of nutrient availability on the biochemical and elemental stoichiometry in the freshwater diatom *Stephanodiscus minutulus* (Bacillariophyceae). *Journal of Phycology, 36*, 510-522.

Mallick, N., Mandal, S., Singh, A. K., Bishai, M., & Dash, A. (2012). Green microalga *Chlorella vulgaris* as a potential feedstock for biodiesel. *Journal of Chemical Technology and Biotechnology, 87*, 137-145.

Markager, S., Jesperson, A.-M., Madsen, T. V., Berdalet, E., & Weisburd, R. (1992). Diel changes in dark respiration in a plankton community. *Hydrobiologia, 238*, 119-130.

Martínez, L., Morán, A., & García, A. I. (2012). Effect of light on *Synechocystis* sp and modelling of its growth rate as a response to average irradiance. *Journal of Applied Phycology, 24*, 125-134.

Mata, T. M., Martins, A. A., & Caetano, N. S. (2010). Microalgae for biodiesel production and other applications: A review. *Renewable and Sustainable Energy Reviews, 14*, 217-232.

Matthijs, H. C. P., Balke, H., Hes, U. M. V., Kroon, B. M. A., Mur, L. R., & Binot, R. A. (1996). Application of light-emitting diodes in bioreactors: flashing light effects and energy economy in algal culture (*Chlorella pyrenoidosa*). *Biotechnology and Bioengineering, 50*, 98-107.

Maxwell, D. P., Falk, S., & Huner, N. P. A. (1995). Photosystem II excitation pressure and development of resistance to photoinhibition. *Plant Physiology, 107*, 687-694.

Maxwell, K., & Johnson, G. N. (2000). Chlorophyll fluorescence-a practical guide. *Journal of Experimental Botany, 51*, 659-668.

Mayo, A. W. (1997). Effects of temperature and pH on the kinetic growth of unialga *Chlorella vulgaris* cultures containing bacteria. *Water Environment Research, 69*, 64-72.

Mazzuca Sobczuk, T., Camacho, F. G., Grima, E. M., & Chisti, Y. (2006). Effects of agitation on the microalgae *Phaeodactylum tricornutum* and *Porphyridium cruentum*. *Bioprocess and Biosystems Engineering, 28*, 243-250.

Mazzuca Sobczuk, T., & Chisti, Y. (2010). Potential fuel oils from the microalga *Choricystis minor*. *Journal of Chemical Technology and Biotechnology, 85*, 100-108.

Mercer, P., & Armenta, R. E. (2011). Developments in oil extraction from microalgae. *European Journal of Lipid Science and Technology, 113*, 539-547.

Mi-Kyung, K., & Smith, R. E. H. (2001). Effect of ionic copper toxicity on the growth of green alga, *Selenastrum capricornutum*. *Journal of Microbiol Biotechnology, 11*, 211-216.

Miron, A. S., Garcia, M.-C. C., Camacho, F. G., Grima, E. M., & Chisti, Y. (2002). Growth and biochemical characterization of microalgal biomass produced in bubble column and airlift photobioreactors: studies in fed-batch culture. *Enzyme and Microbial Technology, 31*, 1015-1023.

Miyachi, S., Kanai, R., Mihara, S., Miyachi, S., & Aoki, S. (1964). Metabolic roles of inorganic polyphosphates in *Chlorella* cells. *Biochimica et Biophysica Acta, 93*, 625-634.

Miyachi, S., & Miyachi, S. (1961). Modes of formation of phosphate compounds and their turnover in *Chlorella* cells during the process of life cycle as studied by the technique of synchronous culture. *Plant & Cell Physiology, 2*, 415-424.

Miyachi, S., & Tamiya, H. (1961). Distribution and turnover of phosphate compounds in growing *Chlorella* cells. *Plant & Cell Physiology, 2*, 405-414.

Molina, E., Fernández, J., Acién, F. G., & Chisti, Y. (2001). Tubular photobioreator design for algal cultures. *Journal of Biotechnology, 92*, 113-131.

Molina Grima, E., Belarbi, E.-H., Fernandez, F. G. A., Medina, A. R., & Chisti, Y. (2003). Recovery of microalgal biomass and metabolites: process options and economics. *Biotechnology advances, 20*, 491-515.

Molina Grima, E., Fernández, F. G. A., Camacho, F. G., & Chisti, Y. (1999). Photobioreactors: light regime, mass transfer, and scaleup. *Journal of Biotechnology, 70*, 231-247.

Molina Grima, E., Fernández, F. G. A., Camacho, F. G., Rubio, F. C., & Chisti, Y. (2000). Scale-up of tubular photobioreactors. *Journal of Applied Phycology, 12*, 355-368.

Molina Grima, E., Sanchez Perez, J. A., Garciá Camacho, F., Fernandez Sevilla, J. M., & Acien Fernandez, F. G. (1996). Productivity analysis of outdoor chemostat culture in tubular air-lift photobioreactors. *Journal of Applied Phycology, 8*, 369-380.

Moreno, J., Vargas, M. Á., Rodŕiguez, H., Rivas, J., & Guerrero, M. G. (2003). Outdoor cultivation of a nitrogen-fixing marine cyanobacterium, *Anabaena* sp. ATCC 33047. *Biomolecular Engineering, 20*, 191-197.

Morison, J. I. L., Gallouët, E., Lawson, T., Cornic, G., Herbin, R., & Baker, N. R. (2005). Lateral diffusion of CO_2 in leaves is not sufficient to support photosynthesis. *Plant Physiology, 139*, 254-266.

Mudili, J. (2007). *Introductory practical microbiology*. UK: Alpha Science International Ltd.

Mujtaba, G., Choi, W., Lee, C.-G., & Lee, K. (2012). Lipid production by *Chlorella vulgaris* after a shift from nutrient-rich to nitrogen starvation conditions. *Bioresource Technology, 123*, 279-283.

Najafabady, N., Rasoul-Amini, S., & Ghasemi, Y. (2010). Production of biodiesel by a naturally isolated strain of *Chlorella vulgaris* in bubble-column photobioreactor. *Special Abstracts /Journal of Biotechnology, 150S*, S1-S576.

Nakamura, Y., & Miyachi, S. (1982). Effect of temperature on starch degradation in *Chlorella vulgaris* 11H cells. *Plant and Cell Physiology, 23*, 333-341.

Nichols, B. W. (1965). Light induced changes in the lipids of *Chlorella vulgaris*. *Biochimica et Biophysica Acta, 106*, 274-279.

Nielsen, S. L., Enríquez, S., Duarte, C. M., & Sand-Jensen, K. (1996). Scaling maximum growth rates across photosynthetic organisms. *Functional Ecology, 10*, 167-175.

Novis, P. (2007). Extremophilic algae: a selection from New Zealand, Antarctica, and North America. *New Zealand Journal of Botany, 45*, 294-294.

Nyns, E. J., & Naveau, H. P. (1982). Methane production by anaerobic digestion of algae. Contract No 406-78-1/ES B, Final Report. Brussels: Directorate-General for Research, Science and Education, Commission of the European Communities *http://bookshop.europa.eu/en/methane-production-by-anaerobic-digestion-of-algae-pbCDNA07685/*

Ogbonna, J. C., Yada, H., Masui, H., & Tanaka, H. (1996). Novel internally illuminated stirred tank photobioreactor for large-scale cultivation of photosynthetic cells. *Journal of Fermentation and Bioengineering, 82*, 61-67.

Ördög, V., Stirk, W. A., Bálint, P., Lovász, C., Pulz, O., & van Staden, J. (2013). Lipid productivity and fatty acid composition in *Chlorella* and *Scenepdesmus* strains grown in nitrogen-stressed conditions. *Journal of Applied Phycology, 25*, 233-243.

Ortiz, E., Casazza, A., Aliakbarian, B., Perego, P., Converti, A., & Carvalho, J. C. (2010). Growth and lipid composition of *Chlorella vulgaris* cultivated in a tubular photobioreactor fed with CO_2-enriched air. *Journal of Biotechnology, 150*, 184-184.

Oukarroum, A., Perreault, F., & Popovic, P. (2012). Interactive effects of temperature and copper on photosystem II photochemistry in *Chlorella vulgaris*. *Journal of Photochemistry and Photobiology B – Biology, 110*, 9-14.

Papazi, A., Makridis, P., Divanach, P., & Kotzabasis, K. (2008). Bioenergetic changes in the microalgal photosynthetic apparatus by extremely high CO_2 concentrations induce an intense biomass production. *Physiologia Plantarum, 132*, 338-349.

Parkhurst, D. F. (1986). Internal leaf-structure: a three-dimensional perspective. In T. J. Givnish (Ed.), *On the economy of plant form and function* (pp. 215-250). Cambridge: Cambridge University Press.

Pate, R., Klise, G., & Wu, B. (2011). Resource demand implications for US algae biofuels production scale-up. *Applied Energy, 88*, 3377-3388.

Piorreck, M., Baasch, K.-H., & Pohl, P. (1984). Biomass production, total protein, chlorophylls, lipids and fatty acids of freshwater green and blue-green algae under different nitrogen regimes. *Phytochemistry, 23*, 207-216.

Polynov, V. A., Matorin, D. N., Vavilin, D. V., & Venediktov, P. S. (1993). Effect of low copper concentrations on photosystem-II photoinhibition in *Chlorella vulgaris*. *Russian Journal of Plant Physiology, 40*, 651-655.

Poorter, H., Werf, A. v. d., Owen K, A., & Lambers, H. (1991). Respiratory energy requirements of roots vary with the potential growth rate of a plant spedes. *Physiologia Plantarum, 83*, 469-475.

Post, A. F. (1993). Ammonia enhanced dark respiration in *Chlorella vulgaris* is related to collapse of a transmembrane pH gradient. *FEMS Microbiology Letters, 113*, 9-13.

Posten, C., & Walter, C. (Eds.). (2012). *Microalgal biotechnology: Integration and economy*. Berlin: de Gruyter.

Potvin, G., Debska, D., Lan, C., & Zhang, Z. S. (2011). Effect of operating conditions on the photobioreactor cultivation of *Chlorella vulgaris*. *Journal of Biobased Materials and Bioenergy, 5*, 319-323.

Powles, S. B. (1984). Photoinhibition of photosynthesis induced by visible light. *Annual Review of Plant Physiology, 35*, 15-44.

Přibyl, P., Cepák, V., & Zachleder, V. (2012). Production of lipids in 10 strains of *Chlorella* and *Parachlorella*, and enhanced lipid productivity in *Chlorella vulgaris*. *Applied Microbiology and Biotechnology, 94*, 549-561.

Pruvost, J., Legrand, J., & Legentilhomme, P. (2002). Simulation of microalgae growth in limiting light conditions: flow effect. *AIChE Journal, 48*, 1109-1120.

Pulz, O. (2001). Photobioreactors: production systems for phototrophic microorganisms. *Applied Microbiology and Biotechnology, 57*, 287-293.

Qin, S., Lin, H., & Jiang, P. (2012). Advances in genetic engineering of marine algae. *Biotechnology Advances, 30*, 1602-1613.

Quinn, J. C., Turner, C. W., & Bradley, T. H. (2012). Scale-Up of flat plate photobioreactors considering diffuse and direct light characteristics. *Biotechnology and Bioengineering, 109*, 363-370.

Radakovits, R., Eduafo, P. M., & Posewitz, M. C. (2011). Genetic engineering of fatty acid chain length in *Phaeodactylum tricornutum*. *Metabolic Engineering, 13*, 89-95.

Radakovits, R., Jinkerson, R. E., Darzins, A., & Posewitz, M. C. (2010). Genetic engineering of algae for enhanced biofuel production. *Eukaryotic Cell, 9*, 486-501.

Raja, R., Hemaiswarya, S., Kumar, N. A., Sridhar, S., & Rengasamy, R. (2008). A perspective on the biotechnological potential of microalgae. *Critical Reviews in Microbiology, 34*, 77-88.

Rao, A. R., Dayananda, C., Sarada, R., Shamala, T. R., & Ravishankar, G. A. (2007). Effect of salinity on growth of green alga *Botryococcus braunii* and its constituents. *Bioresource Technology, 98*, 560-564.

Raposo, M. F. d. J., de Morais, R. M. S. C., & de Morais, A. M. M. B. (2013). Bioactivity and applications of sulphated polysaccharides from marine microalgae. *Marine Drugs, 11*, 233-252.

Ras, M., Lardon, L., Bruno, S., Bernet, N., & Steyer, J.-P. (2011). Experimental study on a coupled process of production and anaerobic digestion of *Chlorella vulgaris*. *Bioresource Technology, 102*, 200-206.

Rasoul-Amini, S., Montazeri-Najafabady, N., Mobasher, M. A., Hoseini-Alhashemi, S., & Ghasemi, Y. (2011). *Chlorella* sp.: A new strain with highly saturated fatty acids for biodiesel production in bubble-column photobioreactor. *Applied Energy, 88*, 3354-3356.

Ratchford, I. A. J., & Fallowfield, H. J. (2003). The effect of light:dark cycles of medium frequency on photosynthesis by *Chlorella vulgaris* and the implications for waste stabilisation pond design and performance. *Water Science and Technology, 48*, 69-74.

Ratchford, l. A. J., & Fallowfield, H. J. (1992). Performance of a flat-plate, airlift reactor for the growth of high biomass algal cultures. *Journal of Applied Phycology, 4*, 1-9.

Rathinasabapathi, B. (2000). Metabolic engineering for stress tolerance: Installing osmoprotectant synthesis pathways. *Annals of Botany, 86*, 709-716.

Raven, J. A., & Geider, R. J. (1988). Temperature and algal growth. *New Phytologist, 10*, 441-461.

Reitan, K. I., Rainuzzo, J. R., & Olsen, Y. (1994). Effect of nutrient limitation on fatty acid and lipid content of marine microalgae. *Journal of Phycology, 30*, 972-979.

Renaud, S. M., Thinh, L.-V., Lambrinidis, G., & Parry, D. L. (2002). Effect of temperature on growth, chemical composition and fatty acid compposition of tropical Australian microalgae grown in batch cultures. *Aquaculture, 211*, 195-214.

Richmond, A. (2004). Biological principles of mass cultivation. In A. Richmond (Ed.), *Handbook of microalgal culture: Biotechnology and applied phycology* (pp. 125-177). Oxford: Blackwell Science.

Rittmann, B. E. (2008). Opportunities for renewable bioenergy using microorganisms. *Biotechnology and Bioengineering, 100*, 203-212.

Rodolfi, L., Zittelli, G. C., Bassi, N., Padovani, G., Biondi, N., Bonini, G., & Tredici, M. R. (2009). Microalgae for oil: strain selection, induction of lipid synthesis and outdoor mass cultivation in a low-cost photobioreactor. *Biotechnology and Bioengineering, 102*, 100-112.

Rosenberg, J. N., Oyler, G. A., Wilkinson, L., & Betenbaugh, M. J. (2008). A green light for engineered algae: redirecting metabolism to fuel a biotechnology revolution. *Current Opinion in Biotechnology, 19*, 430-436.

Samson, R., & Le Duy, A. (1982). Biogas production from anaerobic digestion of *Spirulina maxima* algal biomass. *Biotechnology and Bioengineering, 24*, 1919-1924.

Sánchez Hernández, E. P., & Travieso Córdoba, L. (1993). Anaerobic digestion of *Chlorella vulgaris* for energy production. *Resources, Conservation and Recycling, 9*, 127-132.

Sánchez Mirón, A., Camacho, F. G., Gomez, A. C., Grima, E. M., & Chisti, Y. (2000). Bubble-column and airlift photobioreactors for algal culture. *AIChE Journal, 46*, 1872-1887.

Sánchez Mirón, A., Cerón Garci´a, M. C., Garci´a Camacho, F., Molina Grima, E., & Chisti, Y. (2002). Growth and biochemical characterization of microalgal biomass produced

in bubble column and airlift photobioreactors: studies in fed-batch culture. *Enzyme and Microbial Technology, 31*, 1015-1023.

Sánchez Mirón, A., Garcia, M. C. C., Gomez, A. C., Camacho, F. G., Grima, E. M., & Chisti, Y. (2003). Shear stress tolerance and biochemical characterization of *Phaeodactylum tricornutum* in quasi steady-state continuous culture in outdoor photobioreactors. *Biochemical Engineering Journal, 16*, 287-297.

Sánchez Mirón, A., Gomez, A. C., Camacho, F. G., Grima, E. M., & Chisti, Y. (1999). Comparative evaluation of compact photobioreactors for large-scale monoculture of microalgae. *Journal of Biotechnology, 70*, 249-270.

Sánchez, S., Martínez, M.-E., & Espinola, F. (2000). Biomass production and biochemical variability of the marine microalga *Isochrysis galbana* in relation to culture medium. *Biochemical Engineering Journal, 6*, 13-18.

Sasi, D., Mitra, P., Vigueras, A., & Hill, G. A. (2011). Growth kinetics and lipid production using *Chlorella vulgaris* in a circulating loop photobioreactor. *Journal of Chemical Technology and Biotechnology, 86*, 875-880.

Scarsella, M., Belotti, G., Filippis, P. D., & Bravi, M. (2010). *Study on the optimal growing conditions of Chlorella vulgaris in bubble column photobioreactors.* Paper presented at the 2nd International Conference on Industrial Biotechnology, Padua, Italy.

Schenk, P. M., Thomas-Hall, S. R., Stephens, E., Marx, U. C., Mussgnug, J. H., Posten, C., Kruse, O., & Hankamer, B. (2008). Second generation biofuels: high-efficiency microalgae for biodiesel production. *Bioenergy Reserve, 1*, 20-43.

Scragg, A. H., Illman, A. M., Carden, A., & Shales, S. W. (2002). Growth of microalgae with increased calorific values in a tubular bioreactor. *Biomass and Bioenergy, 23*, 67-73.

Sheehan, J., Dunahay, T., Benemann, J., & Roessler, P. (1998). *A look back at the U.S. Department of Energy's aquatic species program—biodiesel from algae*. Colorado: National Renewable Energy Laboratory.

Sheng, J., Vannela, R., & Rittmann, B. E. (2011). Evaluation of methods to extract and quantify lipids from *Synechocystis* PCC 6803. *Bioresource Technology, 102*, 1697-1703.

Shi, X., Wu, Z., & Chen, F. (2006). Kinetic modeling of lutein production by heterotrophic *Chlorella* at various pH and temperatures. *Molecular Nutrition and Food Research, 50*, 763-768.

Shuler, M. L., & Kargi, F. (2002). *Bioprocess engineering basic concepts*. USA: Prentice Hall.

Sierra, E., Acién, F. G., Fernández, J. M., García, J. L., González, C., & Molina, E. (2008). Characterization of a flat plate photobioreactor for the production of microalgae. *Chemical Engineering Journal, 138*, 136-147.

Sirisansaneeyakul, S., Singhasuwan, S., Choorit, W., Phoopat, N., Garcia, J. L., & Chisti, Y. (2011). Photoautotrophic production of lipids by some *Chlorella* strains. *Marine Biotechnology, 13*, 928-941.

Slegers, P. M., Wijffels, R. H., van Straten, G., & van Boxtel, A. J. B. (2011). Design scenarios for flat panel photobioreactors. *Applied Energy, 88*, 3342-3353.

Snow, A. A., & Smith, V. H. (2012). Genetically engineering algae for biofuels: A key role for ecologists. *BioScience, 62*, 765-768.

Sompech, K., Chisti, Y., & Srinophakun, T. (2012). Design of raceway ponds for producing microalgae. *Biofuels, 3*, 387-397.

Spolaore, P., Joannis-Cassan, C., Duran, E., & Isambert, A. (2006). Review: commercial applications of microalgae. *Journal of Bioscience and Bioengineering, 101*, 87-96.

Stal, L. J., & Moezelaar, R. (1997). Fermentation in cyanobacteria. *FEMS Microbiology Reviews, 21*, 179-211.

Stansell, G. R., Gray, V. M., & Sym, S. D. (2012). Microalgal fatty acid composition: implications for biodiesel quality. *Journal of Applied Phycology, 24*, 791-801.

Stephenson, A. L., Dennis, J. S., Howe, C. J., Scott, S. A., & Smith, A. G. (2010). Influence of nitrogen-limitation regime in the production by *Chlorella vulgaris* of lipids for biodiesel feedstocks. *Biofuels, 1*, 47-58.

Stephenson, P. G., Moore, C. M., Terry, M. J., Zubkov, M. V., & Bibby, T. S. (2011). Improving photosynthesis for algal biofuels: toward a green revolution. *Trends in Biotechnology, 29*, 615-623.

Strickland, J. D. H., & Parsons, T. R. (1972). Determination of reactive phosphorus. In J. D. H. Strickland & T. R. Parsons (Eds.), *A Practical Handbook of Seawater Analysis* (pp. 49-56). Bulletin 167: Fisheries Research Board of Canada.

Su, C.-H., Fu, C.-C., Chang, Y.-C., Nair, G. R., Ye, J.-L., Chu, I.-M., & Wu, W.-T. (2008). Simultaneous estimation of chlorophyll a and lipid contents in microalgae by three-color analysis. *Biotechnology and Bioengineering, 99*, 1034-1039.

Szabó, I., Bergantino, E., & Giacometti, G. M. (2005). Light and oxygenic photosynthesis: energy dissipation as a protection mechanism against photo-oxidation. *EMBO Reports, 6*, 629-634.

Tabernero, A., Valle, E. M. M. d., & Galán, M. A. (2012). Evaluating the industrial potential of biodiesel from a microalgae heterotrophic culture: Scale-up and economics. *Biochemical Engineering Journal, 63*, 104-115.

Takagi, M., & Yoshida, T. (2006). Effect of salt concentration on intracellular accumulation of lipids and triacylglyceride in marine microalgae Dunaliella cells. *Journal of Bioscience and Bioengineering, 101*, 223-226.

Tang, H., Abunasser, N., Garcia, M. E. D., Chen, M., Ng, K. Y. S., & Salley, S. O. (2011a). Potential of microalgae oil from *Dunaliella tertiolecta* as a feedstock for biodiesel. *Applied Energy, 88*, 3324-3330.

Tang, H., Chen, M., Garcia, M. E. D., Abunasser, N., Ng, K. Y. S., & Salley, S. O. (2011b). Culture of microalgae *Chlorella minutissima* for biodiesel feedstock production. *Biotechnology and Bioengineering, 108*, 2280-2287.

Tennessen, D. J., Bula, R. J., & Sharkey, T. D. (1995). Efficiency of photosynthesis in continuous and pulsed light emitting diode irradiation. *Photosynthesis Research, 44*, 261-269.

Tennessen, D. J., Singsaas, E. L., & Sharkeyl, T. D. (1994). Light-emitting diodes as a light source for photosynthesis research. *Photosynthesis Research, 39*, 85-92.

Terry, K. L., & Raymond, L. P. (1985). System design for the autotrophic production of microalgae. *Enzyme and Microbial Technology, 7*, 474-487.

Trecidi, M. R. (1999). Bioreactors, Photo. In M. C. Flickinger & S. W. Drew (Eds.), *Encyclopedia of bioprocess technology: Fermentation, biocatalysis and bioseparation* (Vol. 1, pp. 395-419). New York: Wiley.

Tsukahara, K., & Sawayama, S. (2005). Liquid fuel production using microalgae. *Journal of the Japan Petroleum Institute, 48*(5), 251-259.

Uduman, N., Qi, Y., Danquah, M. K., Forde, G. M., & Hoadley, A. (2010). Dewatering of microalgal cultures: A major bottleneck to algae-based fuels. *Journal of Renewable and Sustainable Energy 2*, article 012701.

Ugwu, C. U., & Aoyagi, H. (2008). Influence of shading inclined tubular photobioreactor surfaces on biomass productivity of *C. sorokiniana*. *Photosynthetica, 46*, 283-285.

Ugwu, C. U., Aoyagi, H., & Uchiyama, H. (2007). Influence of irradiance, dissolved oxygen concentration, and temperature on the growth of *Chlorella sorokiniana*. *Photosynthetica, 45*, 309-311.

Ugwu, C. U., Ogbonna, J. C., & Tanaka, H. (2005). Light/dark cyclic movement of algal culture (*Synechocystis aquatilis*) in outdoor inclined tubular photobioreactor equipped with static mixers for efficient production of biomass. *Biotechnology Letters, 27*, 75-78.

Van Den Hende, S., Vervaeren, H., & Boon, N. (2012). Flue gas compounds and microalgae: (Bio-)chemical interactions leading to biotechnological opportunities. *Biotechnology Advances, 30*, 1405-1424.

Vasudevan, P. T., & Briggs, M. (2008). Biodiesel production—current state of the art and challenges. *Journal of Industrial Microbiology and Biotechnology, 35*, 421-430.

Vasumathi, K. K., Premalatha, M., & Subramanian, P. (2012). Parameters influencing the design of photobioreactor for the growth of microalgae. *Renewable and Sustainable Energy Reviews, 16*, 5443-5450.

Vergara-Fernández, A., Vargas, G., Alarcón, N., & Velasco, A. (2008). Evaluation of marine algae as a source of biogas in a two-stage anaerobic reactor system. *Biomass and Bioenergy, 32*, 338-344.

Wang, C.-Y., Fu, C.-C., & Liu, Y.-C. (2007). Effects of using light-emitting diodes on the cultivation of *Spirulina platensis*. *Biochemical Engineering Journal, 37*, 21-25.

Weber, T. S., & Deutsch, C. (2010). Ocean nutrient ratios governed by plankton biogeography. *Nature, 467*, 550-554.

Weyer, K. M., Bush, D. R., Darzins, A., & Willson, B. D. (2010). Theoretical maximum algal oil production. *Bioenergy Reserve, 3*, 204-213.

Wijffels, R. H., & Barbosa, M. J. (2010). An outlook on microalgal biofuels. *Science, 329*, 796-799.

Williams, P. J. l. B. (2007). Biofuel: microalgae cut the social and ecological costs. *Nature, 450*, 478-478.

Wongluang, P., Chisti, Y., & Srinophakun, T. (2013). Optimal hydrodynamic design of tubular photobioreactors. *Journal of Chemical Technology and Biotechnology, 88*, 55-61.

Xin, L., Hong-ying, H., Ke, G., & Ying-xue, S. (2010). Effects of different nitrogen and phosphorus concentrations on the growth, nutrient uptake, and lipid accumulation of a freshwater microalga *Scenedesmus* sp. *Bioresource Technology, 101*, 5494-5500.

Xin, L., Hong-ying, H., & Yu-ping, Z. (2011). Growth and lipid accumulation properties of a freshwater microalga *Scenedesmus* sp. under different cultivation temperature. *Bioresource Technology, 102*, 3098-3102.

Yamaberi, K., Takagi, M., & Yoshida, T. (1998). Nitrogen depletion for intracellular triglyceride accumulation to enhance liquefaction yield of marine microalgal cells into a fuel oil. *Journal of Marine Biotechnology, 6*, 44-48.

Yeh, K.-L., & Chang, J.-S. (2011). Nitrogen starvation strategies and photobioreactor design for enhancing lipid production of a newly isolated microalga *Chlorella vulgaris* ESP-31: Implications for biofuels. *Biotechnology Journal, 6*, 1358-1366.

Yeh, K.-L., & Chang, J.-S. (2012). Effects of cultivation conditions and media composition on cell growth and lipid productivity of indigenous microalga *Chlorella vulgaris* ESP-31. *Bioresource Technology, 105*, 120-127.

Yokota, T., Hizume, M., Ohtake, T., & Takahashi, K. (1994). A new growth kinetic-model for photo-autotrophic microalgae culture. *Journal of Chemical Engineering of Japan, 27*, 399-403.

Yun, Y.-S., & Park, J. M. (2003). Kinetic modeling of the light-dependent photosynthetic activity of the green microalga *Chlorella vulgaris*. *Biotechnology and Bioengineering, 83*, 303-311.

Zamalloa, C., Vulsteke, E., Albrecht, J., & Verstraete, W. (2011). The techno-economic potential of renewable energy through the anaerobic digestion of microalgae. *Bioresource Technology, 102*, 1149-1158.

Zhu, C. J., Lee, Y. K., & Chao, T. M. (1997). Effects of temperature and growth phase on lipid and biochemical composition of *Isochrysis galbana* TK1. *Journal of Applied Phycology, 9*, 451-457.

Zhu, X. G., Long, S. P., & Ort, D. R. (2008). What is the maximum efficiency with which photosynthesis can convert solar energy into biomass? *Current Opinion in Biotechnology, 19*, 153-159.

Appendix 1

Standard deviation calculations

The standard deviation calculations for the various data were as per: http://www.ecs.umass.edu/cee/reckhow/course/572/572bk23/572BK23.html

Thus, standard deviation (s_1, s_2) for addition or subtraction of two numbers (x_1, x_2) was calculated as follows:

$$(x_1 \pm s_1)+(x_2 \pm s_2)=(x_1 + x_2)\pm\sqrt{s_1^2 + s_2^2}$$
$$(x_1 \pm s_1)-(x_2 \pm s_2)=(x_1 - x_2)\pm\sqrt{s_1^2 + s_2^2}$$

Standard deviation (s_1, s_2) for two numbers (x_1, x_2) when multiplied or divided by a constant was calculated as follows:

$$n(x \pm s)=nx \pm ns$$

Standard deviation (s_1, s_2) for multiplication or division of two numbers (x_1, x_2) was calculated as follows:

$$(x_1 \pm s_1)(x_2 \pm s_2)=(x_1 \times x_2)\pm(x_1 \times x_2)\sqrt{\left(\frac{s_1}{x_1}\right)^2+\left(\frac{s_2}{x_2}\right)^2}$$

$$\frac{(x_1 \pm s_1)}{(x_2 \pm s_2)}=\frac{x_1}{x_2}\pm\left(\frac{x_1}{x_2}\right)\sqrt{\left(\frac{s_1}{x_1}\right)^2+\left(\frac{s_2}{x_2}\right)^2}$$

Appendix 2

Experimental data

Data for calibration curve for Figure 3.17

Absorbance 680 nm	Dried biomass concentration (g L^{-1})
0	0±0
0.099	0.020±0.001
0.212	0.039±0
0.310	0.057±0.003
0.412	0.078±0.003
0.482	0.094±0
0.593	0.113±0.003

Data for calibration curve for Figure 3.18

Absorbance 680 nm	Dried biomass concentration (g L^{-1})
0	0±0
0.106	0.036±0.002
0.221	0.071±0.001
0.318	0.106±0.004
0.408	0.143±0.003
0.505	0.174±0.002
0.608	0.221±0.003

Data for calibration curve for Figure 3.19

Absorbance 680 nm	Dried biomass concentration (g L^{-1})
0	0±0
0.101	0.013±0
0.196	0.026±0.001
0.298	0.040±0
0.381	0.051±0
0.492	0.065±0.003
0.585	0.076±0.001

Data for calibration curve for Figure 3.20

Absorbance 680 nm	Dried biomass concentration (g L^{-1})
0	0±0
0.086	0.030±0.003
0.200	0.059±0.008
0.293	0.089±0.001
0.391	0.117±0.001
0.473	0.145±0.003
0.586	0.175±0

Data for calibration curve for Figure 3.21

Absorbance 680 nm	Dried biomass concentration (g L^{-1})
0	0±0
0.099	0.020±0
0.197	0.038±0.001
0.305	0.054±0
0.377	0.075±0
0.491	0.094±0.004
0.576	0.106±0

Data for calibration curve for Figure 3.22

Absorbance 680 nm	Dried biomass concentration (g L^{-1})
0	0±0
0.101	0.064±0
0.199	0.124±0
0.300	0.186±0.001
0.400	0.242±0.003
0.493	0.312±0.001
0.595	0.372±0

Data for calibration curve for Figure 3.23

Absorbance 680 nm	Dried biomass concentration (g L^{-1})
0	0±0
0.097	0.014±0
0.195	0.027±0.001
0.301	0.040±0
0.402	0.054±0.003
0.506	0.079±0.003
0.562	0.083±0

Data for light profile for Figure 3.24

% Light intensity setting	Light intensity (μmol $m^{-2}s^{-1}$)
0	14.3
10	171.1
20	360.7
30	555.4
40	742.1
50	912.4
60	1081.6
70	1229.9
80	1348.1
90	1460.8
100	1536.5

Data for light profile for Figure 3.25

% Light intensity setting	Light intensity (μmol $m^{-2}s^{-1}$)
0	12.7
10	104.2
20	200.3
30	322.0
40	453.7
50	596.2
60	764.7
70	969.8
80	1213.7
90	1428.9
100	1421.2

Data for light profile for Figure 3.26

% Light intensity setting	Light intensity (μmol $m^{-2}s^{-1}$)
0	22.1
10	66.7
20	137.6
30	230.0
40	336.1
50	462.2
60	599.6
70	731.1
80	861.9
90	993.2
100	1123.2

Data for nitrate calibration curve for Figure 3.27

Nitrate concentration (mg L^{-1})	Absorbance 525 nm
0	0
1.38	0.001
2.20	0.003
4.40	0.008
11.00	0.026
22.00	0.051

Data for nitrate calibration curve for Figure 3.28

Nitrate concentration (mg L^{-1})	Absorbance 525 nm
0	0±0
1.38	0.002±0
2.20	0.004±0
4.40	0.007±0.001
5.50	0.008±0.001
11.00	0.019±0.001
22.00	0.037±0.001

Data for phosphate calibration curve for Figure 3.29

Phosphate concentration (mg L^{-1})	Absorbance 525 nm
0	0±0
0.0699	0.016±0.001
0.1397	0.031±0.002
0.2096	0.047±0.002
0.2794	0.063±0.002
0.3439	0.079±0.002

Data for the biomass concentration (g L^{-1}) profile for Figure 4.1

Time (d)	Freshwater	Freshwater:seawater (1:1 by vol.)	Seawater
0	0.034	0.022	0.026
1	0.060	0.035	0.030
3	0.325	0.129	0.164
5	0.743	0.427	0.707
7	1.144	0.728	1.285
10	1.493	0.828	1.696
12	1.813	1.086	1.884
14	2.110	1.305	2.149
16	2.368	1.469	2.313
18	2.469	1.563	2.524
20	2.674	1.759	2.626
22	2.819	1.946	2.915
24	2.985	2.048	2.887
26	3.111	2.251	2.858
29	3.500	2.470	3.179
31	3.663	2.537	3.354
33	4.000	2.878	3.694
35	3.930	2.800	3.488

Data for the biomass concentration (g L^{-1}) profile for Figure 4.2

Time (d)	Freshwater	Freshwater:seawater (1:1 by vol.)	Seawater
0	0.020	0.012	0.022
1	0.046	0.018	0.026
3	0.233	0.021	0.011
5	0.528	0.010	0.032
7	0.952	0.004	0.018
10	1.346	0.028	0.030
12	1.455	0.006	0.028
14	1.703	0.008	0.016
16	2.045	0.016	0.023
18	2.293	0.016	0.027
20	2.398	0.014	0.027
22	2.784	0.016	0.029
24	2.961	0.016	0.030
26	3.053	0.014	0.028
29	3.474	0.016	0.020
31	3.590	0.017	0.027
33	3.964	0.015	0.032
35	4.225	-	-
37	5.075	-	-

Data for the biomass concentration (g L^{-1}) profile for Figure 4.3

Time (d)	Freshwater	Freshwater:seawater (1:1 by vol.)	Seawater
0	0.038	0.038	0.045
1	0.094	0.051	0.065
3	0.330	0.060	0.138
5	0.600	0.178	0.205
7	0.923	0.217	0.325
10	1.224	0.272	0.345
12	1.435	0.272	0.410
14	1.645	0.288	0.451
16	1.880	0.287	0.501
18	2.177	0.302	0.511
20	2.424	0.333	0.555
22	2.733	0.430	0.637
24	2.968	0.312	0.644
26	3.055	0.309	0.670
29	3.537	0.372	0.710
31	3.847	0.348	0.753
33	4.477	-	0.803
35	4.600	-	0.793
37	5.169	-	0.747

Data for the biomass concentration (g L^{-1}) profile for Figure 4.4

Time (d)	Freshwater	Freshwater:seawater (1:1 by vol.)	Seawater
0	0.017	0.004	0.011
3	0.120	0.025	0.029
5	0.204	0.037	0.033
7	0.422	0.052	0.058
9	0.735	0.073	0.094
11	1.176	0.138	0.146
13	1.584	0.200	0.211
15	2.062	0.306	0.277
17	2.171	0.313	0.333
19	2.055	0.359	0.363
22	2.032	0.489	0.400
24	-	0.622	0.441
26	-	0.644	0.493
28	-	0.648	0.497
30	-	-	0.518

Data for lipid content for lipid productivity in Table 4.1

Sample	Biomass (mg)	Total lipid (%)
Chlorella vulgaris (freshwater)	1000	15.2
Choricystis minor (freshwater)	1000	33.3
Neochloris sp. (freshwater)	1000	23.1
Pseudococcomixa simplex (freshwater)	1000	18.1
Chlorella vulgaris (freshwater:seawater)(1:1 by vol.)	1000	26.6
Neochloris sp. (freshwater:seawater)(1:1 by vol.)	500	39.8
Pseudococcomixa simplex (freshwater:seawater)(1:1 by vol.)	500	39.9
Chlorella vulgaris (seawater)	1000	33.4
Neochloris sp. (seawater)	500	34.1
Pseudococcomixa simplex (seawater)	500	41.4

Data for the biomass concentration (g L^{-1}) profile for Figure 4.5

Time (d)	Freshwater	Freshwater:seawater (1:1 by vol.)	Seawater
0	0.212	0.208	0.285
1	0.330	0.341	0.396
2	0.484	0.498	0.551
3	0.654	0.618	0.675
4	0.793	0.792	0.780
6	1.125	1.154	1.039
8	1.277	1.385	1.211
10	1.449	1.648	1.365
12	1.575	1.893	1.531
14	1.752	1.996	1.748
16	1.861	2.151	1.948
18	1.918	2.332	1.926
20	2.026	2.418	2.063
22	2.112	2.777	2.126
24	2.135	2.730	2.206
26	2.272	2.848	2.347
28	2.294	2.887	2.433
30	2.482	3.252	2.621
32	2.497	3.057	2.550
34	2.638	3.466	2.769
36	2.654	3.271	2.707

Data for the biomass concentration (g L^{-1}) profile for Figure 4.6

Time (d)	Freshwater	Seawater
0	0.294	0.146
1	0.406	0.057
2	0.512	0.192
4	0.629	0.212
6	1.047	0.226
8	1.114	0.142
10	1.260	0.103
13	1.649	0.162
14	1.687	0.171
17	1.709	0.161
19	1.860	0.176
21	1.931	0.178
23	1.995	0.167
26	2.045	0.165
28	2.119	0.148
31	2.274	0.138
33	2.327	0.118
35	2.247	0.057
38	2.374	0.139

Data for the biomass concentration (g L^{-1}) profile for Figure 4.7

Time (d)	Freshwater	Seawater
0	0.330	0.174
1	0.382	0.154
2	0.428	0.232
4	0.535	0.288
6	0.557	0.374
8	0.783	0.465
10	0.996	0.587
13	1.273	0.770
14	1.343	0.786
17	1.565	0.806
19	1.685	0.883
21	1.862	0.929
23	1.989	1.148
26	2.103	0.982
28	2.388	1.020
31	2.511	1.064
33	2.560	1.153
35	2.560	1.210
38	2.647	1.071

Data for the biomass concentration (g L^{-1}) profile for Figure 4.8

Time (d)	Freshwater	Seawater
0	0.088	0.109
1	0.108	0.071
2	0.116	0.111
4	0.393	0.140
6	0.526	0.384
8	0.752	0.499
10	0.601	0.570
13	0.977	0.584
14	1.052	0.620
17	0.965	0.620
19	1.258	0.657
21	0.926	0.634
23	1.377	0.613
26	0.997	0.630
28	1.306	0.599
31	1.147	0.599
33	1.250	0.564
35	1.270	-
38	1.365	-

Data for the biomass concentration (g L^{-1}) profile for Figure 4.9

Time (d)	Freshwater	Freshwater:seawater (1:1 by vol.)	Seawater
0	0.420	0.346	0.357
1	0.577	0.477	0.424
2	0.826	0.686	0.553
3	1.083	0.886	0.673
4	1.289	1.058	0.753
5	1.420	1.307	0.880
7	1.888	1.850	1.323
9	2.275	2.187	1.342
11	2.655	2.692	1.504
13	2.768	3.241	1.728
15	3.142	3.578	1.841
17	3.242	3.965	1.965
19	3.554	4.326	2.084
21	4.028	4.663	2.265
23	4.290	4.832	2.433
25	4.152	5.019	2.477
27	4.389	5.262	2.477
29	4.576	5.805	2.851
30	4.676	5.954	2.826
32	4.589	5.936	2.789

Data for lipid content analysis for Table 4.2

Sample	NO.	Biomass (mg)	Total lipid (%)	Average total lipid (%)
Chlorella vulgaris (Freshwater)	1	1000	7.1±0.0	-
Choricystis minor (Freshwater)	1	1000	29.1±0.0	-
Neochloris sp. (Freshwater)	1	1000	14.9	
	2	1000	14.8	14.9±0.1
Pseudococcomixa simplex (Freshwater)	1	500	15.2	-
Scenedesmus sp. (Freshwater)	1	1000	6.1	
	2	1000	6.3	6.2±0.2
Chlorella vulgaris (Freshwater:seawater)(1:1 by vol.)	1	1000	16.5	
	2	1000	15.9	16.2±0.4
Scenedesmus sp. (Freshwater:seawater)(1:1 by vol.))	1	1000	10.0	
	2	1000	11.83	10.9±1.2
Chlorella vulgaris (Seawater)	1	1000	15.5	
	2	1000	15.8	15.6±0.2
Neochloris sp. (Seawater)	1	1000	19.1	
	2	1000	12.1	19.0±0.2
Pseudococcomixa simplex (Seawater)	1	500	15.7	
	2	500	15.2	13.9±2.5
Scenedesmus sp. (Seawater)	1	1000	16.5	
	2	1000	15.5	15.9±0.9

Data for the biomass concentration (g L^{-1}) profile for Figure 4.10

Time (h)	24/0	12/12
0	0.281	0.264
24	0.389	0.378
36	0.454	0.378
48	0.515	0.454
60	0.572	0.433
72	0.625	0.511
84	0.677	0.507
96	0.738	0.563
108	0.799	0.578
120	0.829	0.604
132	0.929	0.614
144	0.986	0.677
156	1.051	0.671
168	1.085	0.723
180	1.173	0.723
192	1.211	0.799
204	1.275	0.795
216	1.340	0.875
228	1.401	0.860
240	1.457	0.944
252	1.502	0.936
264	1.565	1.031

Data for the biomass concentration (g L^{-1}) profile for Figure 4.10 (Cont.)

Time (h)	24/0	12/12
276	1.571	0.990
288	1.634	1.066
300	1.697	1.066
312	1.743	1.127
324	1.760	1.112
336	1.811	1.222
348	1.845	1.218
360	1.880	1.256
372	1.908	1.253
384	1.954	1.306
396	1.954	1.306
408	2.023	1.352
420	2.046	1.356
432	2.086	1.401
444	2.109	1.401
456	2.160	1.462
468	2.189	1.474
480	2.189	1.502
492	2.240	1.554
504	2.269	1.565
516	2.261	1.565
528	2.332	1.605

Data for the biomass concentration (g L^{-1}) profile for Figure 4.10 (Cont.)

Time (h)	24/0	12/12
540	2.332	1.605
552	2.332	1.640
564	2.386	1.702
576	2.433	1.680
588	2.652	1.680
600	2.433	1.720
612	2.535	1.720
624	2.402	1.754
636	2.433	1.720
648	2.535	1.743
660	2.519	1.828
672	2.613	1.794
684	2.605	1.777
696	2.613	1.903
708	2.660	1.823
720	2.636	1.903
732	2.722	1.903
744	2.707	1.908
756	2.691	1.920
768	2.746	1.931

Data for lipid content for lipid productivity in Table 4.4

Sample	NO.	Biomass (mg)	Total lipid (%)	Average total lipid (%)
24/0	1	1000	14.6	
	2	1000	14.8	14.7±0.1
12/12	1	1000	14.6	
	2	1000	15.3	15.0±0.5

Data for the culture profile for Figure 4.13 (PBR 1)

Culture conditions were: Temperature = 24.7±0.9 °C; pH = 6.5±0.2; dissolved oxygen concentration = 7.0±0.6 ppm; culture circulation rate = 105.8±6.6 L min^{-1}

Time (d)	Biomass concentration (g L^{-1})	Nitrate concentration (mg L^{-1})	Phosphate concentration (mg L^{-1})
0	0.102	1133.0±42.2	15.1±0
1	0.151	1133.0±0	12.8±0.2
2	0.245	1103.2±84.3	9.7±0.2
3	0.335	1133.0±0	5.0±0.1
4	0.422	1103.2±0	0.9±0
6	0.739	983.9±84.3	0.2±0.1
7	0.980	969.0±21.1	0.1±0
8	1.388	864.6±84.3	0.1±0
9	2.055	775.2±42.2	0.1±0
10	1.991	715.6±42.2	0.1±0
11	1.800	-	-
12	2.313	745.4±42.2	0.1±0
13	3.545	-	-
14	3.747	596.3±21.1	0.1±0
15	4.127	-	-
16	3.687	626.1±21.1	0.1±0

Table Data for the culture profile for Figure 4.13 (PBR 1) (Cont.)

Culture conditions were: Temperature = 24.7±0.9 °C; pH = 6.5±0.2; dissolved oxygen concentration = 7.0±0.6 ppm; culture circulation rate = 105.8±6.6 L min^{-1}

Time (d)	Biomass concentration (g L^{-1})	Nitrate concentration (mg L^{-1})	Phosphate concentration (mg L^{-1})
17	3.628	-	-
18	2.593	536.7±0	0.1±0
19	4.545	-	-
20	2.889	477.0±21.1	0.1±0

Data for the culture profile for Figure 4.19 (PBR 3)

Culture conditions were: Temperature = 22.4±0.7 °C; pH = 6.6±0.1; dissolved oxygen concentration = 6.8±0.2 ppm; 1st culture circulation rate = 97.0±10.2 L min^{-1}, 2nd culture circulation rate = 45.2±8.3

Time (d)	Biomass concentration (g L^{-1})	Nitrate concentration (mg L^{-1})	Phosphate concentration (mg L^{-1})
0	0.076	1088.3±105.4	15.2±0.3
1	0.080	1043.5±0.0	13.8±0.0
2	0.136	1058.4±63.2	13.4±0.2
4	0.152	1088.3±63.2	11.6±3.1
5	0.152	1028.6±105.4	10.4±0.3
6	0.160	983.9±126.5	9.54±0.1
7	0.135	998.8±105.4	8.8±0.5
8	0.148	1013.7±0.0	8.2±0.1
9	0.209	954.1±126.5	7.5±0.1
10	0.165	954.1±168.7	6.9±0.3
11	0.261	954.1±84.3	6.1±0.1
12	0.338	998.8±21.1	5.3±0.1
13	0.302	954.1±0.0	4.4±0.0
14	0.274	983.9±84.3	3.4±0.1
15	0.480	983.9±84.3	2.5±0.0
16	0.551	864.6±84.3	1.3±0.0
17	0.598	849.7±63.2	0.5±0.0
18	0.626	805.0±42.2	0.1±0.0
19	0.672	849.7±21.1	0.0±0.0

Data for the culture profile for Figure 4.19 (PBR 3) (Cont.)

Culture conditions were: Temperature = 22.4±0.7 °C; pH = 6.6±0.1; dissolved oxygen concentration = 6.8±0.2 ppm; 1st culture circulation rate = 97.0±10.2 L min^{-1}, 2nd culture circulation rate = 45.2±8.3

Time (d)	Biomass concentration (g L^{-1})	Nitrate concentration (mg L^{-1})	Phosphate concentration (mg L^{-1})
20	0.658	805.0±42.2	0.0±0.0
21	0.675	849.7±21.1	0.0±0.0
22	0.730	730.5±21.1	0.0±0.0
23	0.733	685.7±0.0	0.0±0.0
24	0.655	730.5±105.4	0.0±0.0
25	0.640	655.9±84.3	0.0±0.0
26	0.629	685.7±0.0	0.0±0.0
27	0.672	596.3±42.2	0.0±0.0
28	1.661	611.2±63.2	0.0±0.0
29	2.165	596.3±84.3	0.0±0.0
30	2.113	655.9±42.2	0.0±0.0
31	0.745	596.3±0.0	0.0±0.0
32	1.614	730.5±105.4	0.0±0.0
33	1.991	655.9±84.3	0.0±0.0
34	1.504	685.7±0.0	0.0±0.0
35	1.643	596.3±42.2	0.0±0.0
36	1.069	-	-
37	0.652	551.6±21.1	0.0±0.0

Data for the culture profile for Figure 4.19 (PBR 3) (Cont.)

Culture conditions were: Temperature = 22.4±0.7 °C; pH = 6.6±0.1; dissolved oxygen concentration = 6.8±0.2 ppm; 1st culture circulation rate = 97.0±10.2 L min^{-1}, 2nd culture circulation rate = 45.2±8.3

Time (d)	Biomass concentration (g L^{-1})	Nitrate concentration (mg L^{-1})	Phosphate concentration (mg L^{-1})
39	0.594	-	-
40	0.843	-	-
41	0.588	566.5±42.2	0.0±0.0
43	0.809	-	-
45	0.484	536.7±42.2	0.0±0.0
47	0.571	551.6±21.1	0.0±0.0
49	0.548	-	-

Data for the culture profile for Figure 4.20 (PBR 6)

Culture conditions were: Temperature = 25.5±0.9 °C; pH = 6.4±0.1; dissolved oxygen concentration = 5.5±1.3 ppm; culture circulation rate = 104.7±7.8 L min^{-1}

Time (d)	Biomass concentration (g L^{-1})	Nitrate concentration (mg L^{-1})	Phosphate concentration (mg L^{-1})
0	0.202	655.9±0.0	15.7±0.3
1	0.300	611.2±63.2	13.9±0.3
3	0.560	566.5±0.0	7.3±0.2
4	0.690	551.6±63.2	4.4±0.2
5	0.829	551.6±63.2	1.6±0.0
6	0.893	499.5±10.5	0.2±0.0
7	1.087	469.6±52.7	0.2±0.0
8	1.029	424.9±10.5	0.1±0.0
9	1.319	372.7±0.0	0.1±0.0
9.1	0.809	380.1±52.7	0.1±0.0
10	0.983	357.8±42.2	0.1±0.0
11	1.169	350.3±31.6	0.0±0.0
12	1.256	320.5±10.5	0.0±0.0
13	0.930	320.5±10.5	0.0±0.0
14	1.487	313.1±63.2	0.0±0.0
15	1.412	298.2±0.0	0.0±0.0
16	1.475	305.6±31.6	0.0±0.0
17	1.626	313.1±21.1	0.0±0.0
18	1.313	298.2±21.1	0.0±0.0

Data for the culture profile for Figure 4.20 (PBR 6) (Cont.)

Culture conditions were: Temperature = 25.5±0.9 °C; pH = 6.4±0.1; dissolved oxygen concentration = 5.5±1.3 ppm; culture circulation rate = 104.7±7.8 L min^{-1}

Time (d)	Biomass concentration (g L^{-1})	Nitrate concentration (mg L^{-1})	Phosphate concentration (mg L^{-1})
19	1.371	283.2±21.1	0.0±0.0
20	1.313	298.2±0.0	0.0±0.0
21	1.539	298.2±42.2	0.0±0.0
22	1.354	238.5±21.1	0.0±0.0
22.1	0.872	223.6±0.0	0.0±0.0
23	1.006	238.5±21.1	0.0±0.0
24	1.209	223.6±0.0	0.0±0.0
25	1.185	201.3±31.6	0.0±0.0
26	1.104	205.8±4.2	0.0±0.0
27	1.174	205.7±4.2	0.0±0.0
28	1.267	180.4±6.3	0.0±0.0
29	1.151	172.9±8.4	0.0±0.0
30	0.953	171.4±6.3	0.0±0.0
31	0.896	172.9±0.0	0.0±0.0
32	1.035	178.9±0.0	0.0±0.0
33	0.982	178.9±0.0	0.0±0.0
35	1.162	180.4±14.8	0.0±0.0
36.1	0.756	180.4±2.1	0.0±0.0
37	0.861	177.4±10.5	0.0±0.0

Data for the culture profile for Figure 4.20 (PBR 6) (Cont.)

Culture conditions were: Temperature = 25.5±0.9 °C; pH = 6.4±0.1; dissolved oxygen concentration = 5.5±1.3 ppm; culture circulation rate = 104.7±7.8 L min^{-1}

Time (d)	Biomass concentration (g L^{-1})	Nitrate concentration (mg L^{-1})	Phosphate concentration (mg L^{-1})
39	0.942	178.9±0.0	0.0±0.0
41	1.087	161.0±12.6	0.0±0.0
43	0.971	167.0±0.0	0.0±0.0
45	0.965	174.4±14.8	0.0±0.0
47	0.942	165.5±6.3	0.2±0.2
50	0.791	190.8±4.2	0.0±0.0
50.1	0.669	184.9±12.6	0.0±0.0
51	0.774	187.8±8.4	0.0±0.0
52	1.301	-	-
53	0.861	181.9±12.6	0.0±0.0
55	0.774	184.9±0.0	0.0±0.0
57	0.832	183.4±14.8	0.0±0.0
58	0.953	-	-
60	1.064	177.4±2.1	0.0±0.0
62	0.930	187.8±0.0	0.0±0.0
64	0.803	184.9±8.4	0.0±0.0

Data for the culture profile for Figure 4.21 (PBR 8)

Culture conditions were: Temperature = 25.3±0.8 °C; pH = 6.4±0.2; dissolved oxygen concentration = 7.1±3.9 ppm; culture circulation rate = 102.1±6.1 L min^{-1}

Time (d)	Biomass concentration (g L^{-1})	Nitrate concentration (mg L^{-1})	Phosphate concentration (mg L^{-1})
0	0.209	1073.3±42.2	16.3±0.3
1	0.280	1073.3±0.0	14.8±0.2
2	0.367	1028.6±21.1	13.8±0.2
2.1	0.160	998.8±21.1	10.7±0.0
4	0.626	864.6±42.2	3.8±0.1
5	0.699	864.6±126.5	0.3±0.0
6	0.809	864.6±0.0	0.1±0.0
7	0.844	864.6±0.0	0.1±0.0
8	0.850	805.0±84.3	0.1±0.0
9	0.745	834.8±84.3	0.0±0.0
10	0.902	864.6±42.2	0.0±0.0
11	1.018	864.6±42.2	0.0±0.0
13	0.885	879.5±21.1	0.0±0.0
15	0.832	864.6±42.2	0.0±0.0
17	0.803	805.0±42.2	0.0±0.0
19	0.838	790.1±63.2	0.0±0.0

Data for the culture profile for Figure 4.21 (PBR 8) (Cont.)

Culture conditions were: Temperature = 25.3±0.8 °C; pH = 6.4±0.2; dissolved oxygen concentration = 7.1±3.9 ppm; culture circulation rate = 102.1±6.1 L min^{-1}

Time (d)	Biomass concentration (g L^{-1})	Nitrate concentration (mg L^{-1})	Phosphate concentration (mg L^{-1})
20	1.528	-	-
21	0.814	700.7±63.2	0.1±0.0
22	1.475	-	-
23	0.791	641.0±105.4	0.1±0.0
24	1.023	-	-
25	0.640	670.8±63.2	0.1±0.0
26	0.640	-	-
27	0.675	626.1±0.0	1.1±0.0
28	0.635	-	-
29	0.594	641.0±105.4	0.1±0.0
29.1	0.385	402.5±21.1	0.1±0.0
30	0.353	387.6±42.2	0.1±0.0
32	0.516	387.6±42.2	0.1±0.0
33	0.455	-	-
34	0.333	-	-
35	0.333	417.4±84.3	2.2±0.0

Data for the culture profile for Figure 4.21 (PBR 8) (Cont.)

Culture conditions were: Temperature = 25.3±0.8 °C; pH = 6.4±0.2; dissolved oxygen concentration = 7.1±3.9 ppm; culture circulation rate = 102.1±6.1 L min^{-1}

Time (d)	Biomass concentration (g L^{-1})	Nitrate concentration (mg L^{-1})	Phosphate concentration (mg L^{-1})
36	0.240	387.6±84.3	3.8±0.0
37	0.191	290.7±31.6	4.8±0.0
38	0.116	260.9±10.5	6.0±0.0
39	0.072	-	-
40	0.043	-	-
41	0.028	-	-
41	0.023	-	-

Data for the culture profile for Figure 4.14 and 4.22 (PBR 9)

Culture conditions were: Temperature = 23.8±1.1 °C; pH = 6.6±0.1; dissolved oxygen concentration = 12.9±1.1 ppm; culture circulation rate = 104.4±7.1 L min^{-1}

Time (d)	Biomass concentration (g L^{-1})	Nitrate concentration (mg L^{-1})	Phosphate concentration (mg L^{-1})
0	0.248	536.7±0.0	15.7±0.3
1	0.239	506.9±0.0	13.3±0.0
2	0.305	506.9±84.3	10.4±0.2
3	0.400	506.9±0.0	7.4±0.2
3.1	0.353	447.2±42.2	6.5±0.0
4	0.415	447.2±0.0	3.0±0.2
5	0.487	357.8±0.0	0.0±0.0
6	0.571	357.8±42.2	0.0±0.0
7	0.740	350.3±10.5	0.1±0.0
8	0.606	328.0±21.1	0.1±0.0
9	0.771	328.0±21.1	0.1±0.0
10	0.754	290.7±52.7	0.1±0.0
11	0.754	268.3±42.2	0.0±0.0
12	0.792	-	-
13	0.792	246.0±10.5	0.0±0.0
13.1	0.754	-	-
14	0.681	208.7±0.0	0.0±0.0
15	0.675	-	-
16	0.597	-	-

Data for the culture profile for Figure 4.14 and 4.22 (PBR 9) (Cont.)

Culture conditions were: Temperature = 23.8±1.1 °C; pH = 6.6±0.1; dissolved oxygen concentration = 12.9±1.1 ppm; culture circulation rate = 104.4±7.1 L min^{-1}

Time (d)	Biomass concentration (g L^{-1})	Nitrate concentration (mg L^{-1})	Phosphate concentration (mg L^{-1})
17	0.553	126.7±10.5	0.0±0.0
18	0.629	-	-
19	0.565	111.8±10.5	0.0±0.0
20	0.487	-	-
21	0.432	-	-
22	0.458	67.1±10.5	0.0±0.0
23	0.437	-	-
24	0.353	-	-
25	0.330	59.6±21.1	0.0±0.0
26	0.310	-	-
27	0.310	-	-
28	0.307	52.2±10.5	0.0±0.0
29	0.316	-	-
30	0.316	-	-
31	0.307	1.8±0.8	0.0±0.0
32	0.316	-	-
33	0.330	1.2±0.8	0.0±0.0
34	0.333	-	-
35	0.336	1.8±0.0	0.0±0.0

Data for the culture profile for Figure 4.14 and 4.22 (PBR 9) (Cont.)

Culture conditions were: Temperature = 23.8±1.1 °C; pH = 6.6±0.1; dissolved oxygen concentration = 12.9±1.1 ppm; culture circulation rate = 104.4±7.1 L min^{-1}

Time (d)	Biomass concentration (g L^{-1})	Nitrate concentration (mg L^{-1})	Phosphate concentration (mg L^{-1})
36	0.345	-	-
37	0.339	-	-
38	0.313	3.3±0.4	0.0±0.0
39	0.284	-	-
40	0.261	3.3±1.3	0.0±0.0
41	0.232	-	-
42	0.246	3.6±0.0	0.1±0.0
44	0.162	3.6±1.7	0.5±0.0
45	0.145	-	-
46	0.139	2.4±0.8	1.0±0.0
47	0.142	-	-
48	0.150	-	-
49	0.136	-	-
50	0.275	-	-
50.1	0.226	-	-
52	0.246	-	-
53	0.272	-	-
55	0.313	-	-
56	0.345	-	-

Data for the culture profile for Figure 4.14 and 4.22 (PBR 9) (Cont.)

Culture conditions were: Temperature = 23.8±1.1 °C; pH = 6.6±0.1; dissolved oxygen concentration = 12.9±1.1 ppm; culture circulation rate = 104.4±7.1 L min^{-1}

Time (d)	Biomass concentration (g L^{-1})	Nitrate concentration (mg L^{-1})	Phosphate concentration (mg L^{-1})
57	0.350	-	-
58	0.368	-	-
59	0.374	-	-
60	0.359	-	-
61	0.359	-	-
62	0.426	-	-
63	0.350	-	-
65	0.353	-	-
66	0.342	-	-

Data for the culture profile for Figure 4.17 (PBR 10)

Culture conditions were: Temperature = 24.5±2.5 °C; pH = 6.6±0.1; dissolved oxygen concentration = 11.8±1.7 ppm; culture circulation rate = 118.0±24.8 L min^{-1}

Time (d)	Biomass concentration (g L^{-1})	Nitrate concentration (mg L^{-1})	Phosphate concentration (mg L^{-1})
0	0.207	1371.5±0.0	19.5±0.3
1	0.247	1386.4±21.1	16.8±0.2
2	0.277	1356.6±21.1	13.1±0.0
4	0.429	1341.7±42.2	5.8±0.2
5	0.516	1252.2±84.3	3.6±0.2
6	0.542	1192.6±42.2	3.1±0.0
8	0.597	1192.6±0.0	1.6±0.1
9	0.592	1237.3±21.1	1.5±0.0
10	0.592	1192.6±0.0	1.4±0.2
12	0.557	1013.7±84.3	1.4±0.2
13	0.571	-	-
14	0.537	819.9±21.1	0.0±0.0
15	0.522	-	-
16	0.507	805.0±42.2	0.0±0.0
18	0.487	745.4±42.2	0.0±0.0
19	0.481	-	-
20	0.469	730.5±63.5	0.0±0.0

Data for the culture profile for Figure 4.15 (PBR 13)

Culture conditions were: Temperature = 20.5±1.1 °C; pH = 6.4±0.2; dissolved oxygen concentration = 10.3±2.3 ppm; culture circulation rate = 103.8±5.3 L min^{-1}

Time (d)	Biomass concentration (g L^{-1})	Nitrate concentration (mg L^{-1})	Phosphate concentration (mg L^{-1})
0	0.107	290.7±10.5	16.6±0.2
1	0.159	216.2±52.7	14.4±0.2
2	0.201	208.7±0.0	10.5±0.2
4	0.253	208.7±0.0	5.0±0.2
5	0.277	149.1±21.1	3.4±0.0
6	0.293	169.9±25.3	2.3±0.1
8	0.334	138.6±35.8	0.1±0.0
10	0.368	113.3±0.0	0.0±0.0
12	0.393	116.3±8.4	0.0±0.0
14	0.354	134.2±0.0	0.0±0.0
16	0.366	111.8±6.3	0.0±0.0
18	0.371	95.4±4.2	0.0±0.0
20	0.389	102.9±6.3	0.0±0.0
22	0.385	93.9±14.8	0.0±0.0
24	0.390	86.5±8.4	0.0±0.0
26	0.404	53.7±0.0	0.0±0.0
28	0.416	56.6±0.0	0.0±0.0
30	0.423	59.6±0.0	0.0±0.0
32	0.430	50.7±25.3	0.0±0.0

Data for the culture profile for Figure 4.15 (PBR 13) (Cont.)

Culture conditions were: Temperature = 20.5±1.1 °C; pH = 6.4±0.2; dissolved oxygen concentration = 10.3±2.3 ppm; culture circulation rate = 103.8±5.3 L min^{-1}

Time (d)	Biomass concentration (g L^{-1})	Nitrate concentration (mg L^{-1})	Phosphate concentration (mg L^{-1})
34	0.432	44.7±0.0	0.0±0.0
36	0.430	43.2±2.1	0.0±0.0
39	0.430	40.3±2.1	0.0±0.0
41	0.432	40.3±2.1	0.0±0.0
41.1	0.414	41.7±4.2	0.8±0.0
43	0.406	37.3±6.3	0.0±0.0
46	0.407	38.8±4.2	0.1±0.0
48	0.403	38.8±0.0	0.0±0.0
50	0.394	41.7±4.2	0.1±0.0
52	0.387	38.8±4.2	0.1±0.0
54	0.384	44.7±0.0	0.1±0.0
55	0.379	-	-
55.1	0.349	41.7±4.2	0.9±0.0
56	0.355	38.8±0.0	0.4±0.0
58	0.353	38.8±0.0	0.2±0.0
60	0.349	37.3±2.1	0.2±0.0
62	0.349	37.3±2.1	0.2±0.0
64	0.337	40.3±6.3	0.2±0.0
66	0.335	41.7±8.4	0.8±0.0

Data for the culture profile for Figure 4.15 (PBR 13) (Cont.)

Culture conditions were: Temperature = 20.5±1.1 °C; pH = 6.4±0.2; dissolved oxygen concentration = 10.3±2.3 ppm; culture circulation rate = 103.8±5.3 L min^{-1}

Time (d)	Biomass concentration (g L^{-1})	Nitrate concentration (mg L^{-1})	Phosphate concentration (mg L^{-1})
68	0.339	34.3±6.3	1.7±0.0
68.1	0.306	29.8±4.2	2.2±0.1
70	0.303	22.4±10.5	1.9±0.2
72	0.301	11.9±4.2	1.8±0.2
74	0.307	23.9±4.2	1.5±0.0
76	0.294	14.9±0.0	1.4±0.0
78	0.298	22.4±14.8	1.2±0.0
80	0.298	22.4±2.1	1.1±0.0
82	0.336	20.9±0.0	0.9±0.0
85	0.317	29.8±0.0	0.8±0.0

Data for the culture profile for Figure 4.18 (PBR 14)

Culture conditions were: Temperature = 19.7±2.3 °C; pH = 6.6±0.1; dissolved oxygen concentration = 7.6±3.4 ppm; culture circulation rate = 79.9±6.0 L min^{-1}

Time (d)	Biomass concentration (g L^{-1})	Nitrate concentration (mg L^{-1})	Phosphate concentration (mg L^{-1})
0	0.140	235.5±0.0	16.1±0.2
1	0.182	205.7±0.0	14.0±0.2
2	0.205	199.8±8.4	10.2±0.5
4	0.273	149.1±12.6	3.3±0.5
6	0.307	143.1±4.2	0.2±0.0
8	0.305	119.3±0.0	0.1±0.0
10	0.300	126.7±52.7	0.2±0.0
12	0.301	122.2±8.4	0.2±0.0
14	0.288	132.7±23.2	0.5±0.0
16	0.265	123.7±27.4	0.9±0.0
18	0.285	96.9±14.8	1.2±0.0
20	0.273	147.6±35.8	1.2±0.0
22	0.273	135.7±10.5	1.3±0.0
24	0.275	144.6±6.3	1.3±0.0
26	0.257	156.5±14.8	1.3±0.0
28	0.257	122.2±4.2	1.2±0.0
32	0.257	131.2±8.4	1.2±0.0

Data for the culture profile for Figure 4.18 (PBR 14) (Cont.)

Culture conditions were: Temperature = 19.7±2.3 °C; pH = 6.6±0.1; dissolved oxygen concentration = 7.6±3.4 ppm; culture circulation rate = 79.9±6.0 L min^{-1}

Time (d)	Biomass concentration (g L^{-1})	Nitrate concentration (mg L^{-1})	Phosphate concentration (mg L^{-1})
45	0.286	143.1±0.0	1.5±0.0
49	0.270	158.5±4.2	1.4±0.0
53	0.294	152.1±0.0	1.5±0.0
57	0.282	164.0±12.6	1.5±0.2
61	0.281	183.4±10.5	1.6±0.0
65	0.293	167.0±4.2	1.6±0.0
69	0.290	161.0±4.2	1.6±0.0

Data for lipid content analysis for Table 4.7

Sample	NO.	Biomass (mg)	Total lipid (%)	Average total lipid (%)
PBR 1	1	1000	8.5	
	2	1000	8.5	8.5±0.0
PBR 2	1	1000	7.7	
	2	1000	7.9	7.8±0.1
PBR 3	1	19000	10.5	
	2	19000	10.1	10.3±0.3
PBR 4	1	11000	10.9	
	2	11000	11.0	10.9±0.1
PBR 5	1	10500	6.1	
	2	10500	6.5	6.3±0.3
PBR 6	1	1000	9.6	
	2	1000	9.6	9.6±0.1
PBR 7	1	6000	12.4	
	2	6000	12.1	12.3±0.2
PBR 8	1	7000	10.7	
	2	7000	10.7	10.7±0.0
PBR 10	1	1000	14.4	
	2	1000	14.4	14.4±0.0

Data for lipid content analysis for Table 4.7 (Cont.)

Sample	NO.	Biomass (mg)	Total lipid (%)	Average total lipid (%)
PBR 11	1	1000	10.0	
	2	1000	9.8	9.9±0.2
PBR 12	1	1000	4.1	
	2	1000	4.2	4.2±0.0
PBR 13	1	1000	6.3	
	2	1000	6.1	6.2±0.2
PBR 15	1	1000	1.6	
	2	1000	2.2	1.9±0.4

Data for the culture profile for Figure 4.23 (STR 1)

Culture conditions were: Temperature = 25.0±0.0 °C; pH = 7.0±0.2; dissolved oxygen concentration = 133.4±9.6% of air saturation

Time (d)	Biomass concentration (g L^{-1})	Nitrate concentration (mg L^{-1})	Phosphate concentration (mg L^{-1})
0	0.214	1073.3±0.0	10.7±0.2
1	0.322	1043.5±42.2	8.2±0.2
2	0.568	909.4±105.4	0.4±0.1
3	0.922	909.4±63.2	0.1±0.1
4	1.267	879.5±105.4	0.1±0.0
5	1.655	745.4±84.3	0.1±0.1
7	2.171	626.1±42.2	0.1±0.0
9	2.644	491.9±63.2	0.1±0.0
11	2.852	387.6±42.2	0.1±0.0
13	3.131	283.2±63.2	0.1±0.0
15	3.192	223.6±0.0	0.1±0.0
18	3.470	164.0±0.0	0.0±0.0
20	3.450	201.3±10.5	0.0±0.0
22	3.676	-	-
24	3.699	-	-
26	3.581		-
28	3.973	141.6±10.5	0.1±0.0

Data for the culture profile for Figure 4.23 (STR 1) (Cont.)

Culture conditions were: Temperature = 25.0±0.0 °C; pH = 7.0±0.2; dissolved oxygen concentration = 133.4±9.6% of air saturation

Time (d)	Biomass concentration (g L^{-1})	Nitrate concentration (mg L^{-1})	Phosphate concentration (mg L^{-1})
30	4.009	-	-
32	3.236	119.3±42.2	0.0±0.0

Data for the culture profile for Figure 4.24 (STR 2)

Culture conditions were: Temperature = 25.0±0.0 °C; pH = 7.0±0.1; dissolved oxygen concentration = 136.4±7.1% of air saturation

Time (d)	Biomass concentration (g L^{-1})	Nitrate concentration (mg L^{-1})	Phosphate concentration (mg L^{-1})
0	1.573	342.9±21.1	1.1±0.0
1	1.389	298.2±42.2	0.8±0.2
2	1.516	193.8±21.1	0.8±0.2
3	1.650	149.1±42.2	0.3±0.0
4	1.841	59.6±0.0	0.3±0.0
5	1.986	29.8±0.0	0.1±0.0
7	2.421	23.9±0.0	0.1±0.0
9	2.751	32.8±4.2	0.1±0.0
11	2.812	23.9±8.4	0.1±0.0
13	2.986	29.8±0.0	0.1±0.0
15	3.169	29.8±0.0	0.1±0.0
17	3.334	17.9±1.7	0.1±0.0
19	3.635	15.5±0.0	0.1±0.0
20	3.486	-	-
21	3.517	17.3±0.8	0.1±0.0
22	3.072	-	-
23	3.340	18.5±0.8	-

Data for the culture profile for Figure 4.24 (STR2) (Cont.)

Culture conditions were: Temperature = 25.0±0.0 °C; pH = 7.0±0.1; dissolved oxygen concentration = 136.4±7.1% of air saturation

Time (d)	Biomass concentration (g L^{-1})	Nitrate concentration (mg L^{-1})	Phosphate concentration (mg L^{-1})
24	3.492	-	-
25	3.492	16.4±0.4	0.1±0.0
26	3.407	-	-
27	3.413	-	-
28	3.456	-	-
29	3.547	15.5±0.8	0.1±0.0
30	3.578	-	-
31	3.657	-	-
32	3.578	18.5±0.8	0.1±0.0
33	3.535	-	-
34	3.717	-	-
36	4.146	18.2±0.4	0.1±0.0

Data for the culture profile for Figure 4.25 (STR 4)

Culture conditions were: Temperature = 24.5±1.5 °C; pH = 6.6±0.1; dissolved oxygen concentration = 124.4±6.1% of air saturation

Time (d)	Biomass concentration (g L^{-1})	Nitrate concentration (mg L^{-1})	Phosphate concentration (mg L^{-1})
0	0.021	700.7±21.1	15.9±0.5
1	0.030	685.7±63.2	15.5±0.3
2	0.050	648.5±52.7	13.7±0.3
3	0.088	618.7±31.6	11.8±0.3
4	0.146	633.6±31.6	8.8±0.0
5	0.267	573.9±10.5	2.3±0.2
6	0.437	484.5±52.7	0.3±0.0
7	0.606	380.1±31.6	0.0±0.0
8	0.763	298.2±0.0	0.0±0.0
9	0.998	260.9±10.5	0.0±0.0
10	1.215	164.0±21.1	0.0±0.0
11	1.378	111.8±10.5	0.0±0.0
12	1.563	67.1±10.5	0.0±0.0
13	1.726	11.9±0.0	0.0±0.0
14	1.720	11.9±4.2	0.0±0.0
15	1.905	9.8±1.3	0.0±0.0
16	2.033	10.4±0.4	0.0±0.0

Data for the culture profile for Figure 4.25 (STR 4) (Cont.)

Culture conditions were: Temperature = 24.5±1.5 °C; pH = 6.6±0.1; dissolved oxygen concentration = 124.4±6.1% of air saturation

Time (d)	Biomass concentration (g L^{-1})	Nitrate concentration (mg L^{-1})	Phosphate concentration (mg L^{-1})
17	2.102	-	-
18	2.189	9.8±1.3	0.0±0.0
19	2.198	-	-
20	2.233	10.1±0.8	0.0±0.0
21	2.242	-	-
22	2.346	10.7±0.0	0.0±0.0
23	2.372	-	-
24	2.285	-	-
25	2.537	10.1±0.0	0.0±0.0
27	2.424	-	-
29	2.563	10.1±0.8	0.0±0.0
31	2.676	9.8±0.4	0.0±0.0
33	2.772	-	-
35	2.624	-	-
37	2.807	9.5±0.8	0.0±0.0
39	3.042	-	-
41	2.859	12.5±0.8	0.0±0.0

Data for the culture profile for Figure 4.25 (STR 4) (Cont.)

Culture conditions were: Temperature = 24.5±1.5 °C; pH = 6.6±0.1; dissolved oxygen concentration = 124.4±6.1% of air saturation

Time (d)	Biomass concentration (g L^{-1})	Nitrate concentration (mg L^{-1})	Phosphate concentration (mg L^{-1})
44	2.903	11.9±1.7	0.0±0.0
46	2.842	-	
48	2.920	11.6±0.4	0.0±0.0
51	3.111	9.2±0.4	0.0±0.0
53	3.163	-	
55	3.390	11.6±0.4	0.0±0.0
59	3.363	10.7±2.5	0.0±0.0

Data for the culture profile for Figure 4.26 (STR 5)

Culture conditions were: Temperature = 24.6±1.3 °C; pH = 6.7±0.3; dissolved oxygen concentration = 124.4±10.0% of air saturation

Time (d)	Biomass concentration (g L^{-1})	Nitrate concentration (mg L^{-1})	Phosphate concentration (mg L^{-1})
0	0.243	581.4±0.0	15.3±0.6
1	0.308	544.1±10.5	10.5±0.3
2	0.612	439.8±10.5	0.2±0.3
3	0.720	387.6±42.2	0.2±0.0
4	0.899	320.5±10.5	0.2±0.0
5	1.238	260.9±10.5	0.1±0.2
6	1.523	186.3±10.5	0.0±0.0
7	1.783	134.2±21.1	0.0±0.0
8	1.963	74.5±0.0	0.0±0.0
9	2.128	44.7±21.1	0.0±0.0
10	2.372	44.7±0.0	0.0±0.0
11	2.337	-	-
12	2.415	38.8±4.2	0.0±0.0
13	2.450	-	-
14	2.642	34.3±2.1	0.0±0.0
15	2.937	-	-
16	3.016	11.0±0.4	0.0±0.0

Data for the culture profile for Figure 4.26 (STR 5) (Cont.)

Culture conditions were: Temperature = 24.6±1.3 °C; pH = 6.7±0.3; dissolved oxygen concentration = 124.4±10.0% of air saturation

Time (d)	Biomass concentration (g L^{-1})	Nitrate concentration (mg L^{-1})	Phosphate concentration (mg L^{-1})
17	3.016	-	-
18	3.024	-	-
19	3.033	11.3±0.8	0.0±0.0
20	3.163	-	-
21	3.103	11.6±0.4	0.0±0.0
22	3.216	-	-
23	2.972	12.2±1.3	0.0±0.0
23.1	2.102	8.9±0.8	0.0±0.0
24	2.268	-	-
25	2.372	9.2±0.4	0.0±0.0
26	2.337	-	-
27	2.459	8.6±0.4	0.0±0.0
28	2.398	-	-
29	2.415	-	-
30	2.250	-	-
31	2.476	8.1±0.4	0.0±0.0
33	2.650	7.8±0.8	0.0±0.0

Data for the culture profile for Figure 4.26 (STR 5) (Cont.)

Culture conditions were: Temperature = 24.6±1.3 °C; pH = 6.7±0.3; dissolved oxygen concentration = 124.4±10.0% of air saturation

Time (d)	Biomass concentration (g L^{-1})	Nitrate concentration (mg L^{-1})	Phosphate concentration (mg L^{-1})
35	2.650	8.1±0.4	0.0±0.0
37	2.729	8.1±0.4	0.0±0.0
38	-	-	-
38.1	2.381	-	-
41	2.181	-	-
60	2.198	7.8±0.0	0.0±0.0

Data for the culture profile for Figure 4.27 (STR 6)

Culture conditions were: Temperature = 24.7±1.1 °C; pH = 6.7±0.2; dissolved oxygen concentration = 112.6±9.7% of air saturation

Time (d)	Biomass concentration (g L^{-1})	Nitrate concentration (mg L^{-1})	Phosphate concentration (mg L^{-1})
0	0.248	529.2±10.5	14.4±0.3
1	0.333	491.9±21.1	11.0±0.6
2	0.467	417.4±42.2	2.1±0.3
3	0.702	328.0±21.1	0.1±0.0
5	1.105	216.2±10.5	0.0±0.0
6	1.325	171.4±10.5	0.0±0.0
7	1.389	141.6±31.6	0.0±0.0
8	1.749	59.6±8.4	0.0±0.0
9	1.969	34.3±2.1	0.0±0.0
10	2.102	20.9±8.4	0.0±0.0
11	2.233	14.9±0.0	0.0±0.0
12	2.329	14.9±0.0	0.0±0.0
14	2.502	14.9±0.0	0.0±0.0
16	2.294	14.9±0.0	0.0±0.0
18	2.633	14.9±0.8	0.0±0.0
20	2.963	14.9±0.8	0.0±0.0
21	2.955	-	-

Data for the culture profile for Figure 4.27 (STR 6) (Cont.)

Culture conditions were: Temperature = 24.7±1.1 °C; pH = 6.7±0.2; dissolved oxygen concentration = 112.6±9.7% of air saturation

Time (d)	Biomass concentration (g L^{-1})	Nitrate concentration (mg L^{-1})	Phosphate concentration (mg L^{-1})
22	3.076	13.7±0.0	0.0±0.0
23	3.146	12.8±1.3	0.0±0.0
24	3.137	13.1±0.8	0.0±0.0
25	3.146	13.1±0.0	0.0±0.0
26	3.129	12.2±2.1	0.0±0.0
27	3.207	12.5±0.0	0.0±0.0
28	3.250	13.1±1.7	0.0±0.0
29	3.459	11.6±1.3	0.0±0.0
29.1	2.311	12.2±0.4	0.0±0.0
30	2.294	11.0±0.4	0.0±0.0
31	2.268	11.9±0.0	0.0±0.0
31.1	1.624	11.9±1.7	0.0±0.0
33	1.650	-	-
33.1	1.207	6.9±0.4	0.0±0.0
35	1.180	-	-
35.1	0.772	6.0±0.0	0.0±0.0
37	0.873	6.3±2.1	0.0±0.0

Data for the culture profile for Figure 4.27 (STR 6) (Cont.)

Culture conditions were: Temperature = 24.7±1.1 °C; pH = 6.7±0.2; dissolved oxygen concentration = 112.6±9.7% of air saturation

Time (d)	Biomass concentration (g L^{-1})	Nitrate concentration (mg L^{-1})	Phosphate concentration (mg L^{-1})
37.1	0.601	5.4±0.0	0.0±0.0
39	0.624	6.0±0.0	0.0±0.0
39.1	0.380	6.6±0.0	0.0±0.0
40	0.427	-	-
42	0.433	-	-

Data for the culture profile for Figure 4.29 (STR 7)

Culture conditions were: Temperature = 25.0±0.0 °C; pH = 6.6±0.1; dissolved oxygen concentration = 209.6±9.8% of air saturation

Time (d)	Biomass concentration (g L^{-1})	Nitrate concentration (mg L^{-1})	Phosphate concentration (mg L^{-1})
0	0.221	402.5±21.1	15.9±0.0
1	0.322	402.5±63.2	10.7±0.3
2	0.520	342.9±21.1	0.1±0.0
3	0.725	253.4±21.1	0.0±0.0
4	0.943	171.4±10.5	0.0±0.0
5	1.250	134.2±0.0	0.0±0.0
6	1.537	126.7±10.5	0.0±0.0
7	1.737	74.5±0.0	0.0±0.0
8	1.859	52.2±2.1	0.0±0.0
9	2.015	14.9±8.4	0.0±0.0
10	2.189	8.9±0.0	0.0±0.0
11	2.285	8.9±0.0	0.0±0.0
12	2.381	8.9±0.8	0.0±0.0
13	2.450	-	-
14	2.546	8.6±0.4	0.0±0.0
15	2.668	-	-
16	2.642	8.6±0.4	0.0±0.0

Data for the culture profile for Figure 4.29 (STR 7) (Cont.)

Culture conditions were: Temperature = 25.0±0.0 °C; pH = 6.6±0.1; dissolved oxygen concentration = 209.6±9.8% of air saturation

Time (d)	Biomass concentration (g L^{-1})	Nitrate concentration (mg L^{-1})	Phosphate concentration (mg L^{-1})
18	2.807	8.6±0.4	0.0±0.0
20	2.998	9.8±2.1	0.0±0.0
20.1	2.529	-	-
21	2.537	8.3±0.0	0.0±0.0
24	2.789	8.3±0.0	0.0±0.0
26	2.833	8.9±0.8	0.0±0.0
28	2.789	-	-
29	2.415	8.9±0.8	0.0±0.0
29.1	2.242	-	-
30	2.128	-	-
31	2.094	8.6±0.4	0.0±0.0
32	1.833	8.3±0.0	0.0±0.0
33	1.615	7.8±0.8	0.0±0.0
34	1.433	8.3±0.0	0.0±0.0
35	1.267	7.2±0.8	0.0±0.0
36	1.137	6.9±0.4	0.0±0.0
37	1.059	5.7±0.4	0.0±0.0

Data for the culture profile for Figure 4.29 (STR 7) (Cont.)

Culture conditions were: Temperature = 25.0±0.0 °C; pH = 6.6±0.1; dissolved oxygen concentration = 209.6±9.8% of air saturation

Time (d)	Biomass concentration (g L^{-1})	Nitrate concentration (mg L^{-1})	Phosphate concentration (mg L^{-1})
38	0.885	5.4±0.8	0.0±0.0
39	0.798	5.4±0.0	0.0±0.0
40	0.728	5.4±0.0	0.0±0.0
41	0.670	6.0±0.8	0.0±0.0
42	0.653	6.0±0.8	0.0±0.0
43	0.647	-	-
44	0.647	-	-
45	0.606	5.4±0.8	0.0±0.0
46	0.577	-	-
47	0.537	6.6±0.0	0.0±0.0
48	0.520	-	-
49	0.728	5.7±0.4	0.0±0.0
51	0.676	6.6±0.0	0.0±0.0
52	0.659	-	-
53	0.647	5.7±1.3	0.0±0.0

Data for the culture profile for Figure 4.30 (STR 8)

Culture conditions were: Temperature = 24.8±0.8 °C; pH = 6.7±0.1; dissolved oxygen concentration = 148.9±27.5% of air saturation

Time (d)	Biomass concentration (g L^{-1})	Nitrate concentration (mg L^{-1})	Phosphate concentration (mg L^{-1})
0	0.309	1192.6±42.2	14.2±0.2
1	0.388	1192.6±42.2	10.4±0.2
2	0.588	1162.8±84.3	0.2±0.1
4	1.156	894.5±0.0	0.0±0.0
5	1.325	864.6±0.0	0.0±0.0
6	1.470	864.6±0.0	0.0±0.0
8	1.643	805.0±42.2	0.0±0.0
9	1.754	790.1±21.1	0.0±0.0
10	1.800	790.1±21.1	0.0±0.0
12	1.904	655.9±0.0	0.0±0.0
13	1.968	-	-
14	2.038	253.4±63.2	0.0±0.0
15	2.229	-	-
16	2.191	268.3±21.1	0.0±0.0
18	2.270	268.3±0.0	0.0±0.0
19	2.339	-	-
20	2.348	283.2±0.0	0.0±0.0
22	2.426	246.0±10.5	0.0±0.0
27	2.600	95.4±0.0	0.0±0.0
27.1	1.870	95.4±0.0	0.0±0.0

Data for the culture profile for Figure 4.30 (STR 8) (Cont.)

Culture conditions were: Temperature = 24.8±0.8 °C; pH = 6.7±0.1; dissolved oxygen concentration = 148.9±27.5% of air saturation

Time (d)	Biomass concentration (g L^{-1})	Nitrate concentration (mg L^{-1})	Phosphate concentration (mg L^{-1})
28	1.974	-	-
29	2.009	-	-
30	2.000	95.4±4.2	0.0±0.0
31	1.739	83.5±4.2	0.0±0.0
32	1.452	117.8±10.5	0.0±0.0
33	1.330	123.7±10.5	0.0±0.0
34	1.174	164.0±0.0	0.0±0.0
35	1.026	161.0±0.0	0.0±0.0
36	0.896	268.3±21.1	0.0±0.0
37	0.835	335.4±52.7	0.0±0.0
38	0.756	357.8±0.0	0.0±0.0
39	0.722	342.9±0.0	0.0±0.0
40	0.722	350.3±31.6	0.0±0.0
41	0.713	447.2±0.0	0.0±0.0
42	0.669	529.2±10.5	0.0±0.0
43	0.669	626.1±21.1	0.0±0.0
44	0.643	715.6±42.2	0.0±0.0
46	0.582	715.6±0.0	0.0±0.0
48	0.600	655.9±42.2	0.0±0.0
49	0.669	-	-

Data for the culture profile for Figure 4.30 (STR 8) (Cont.)

Culture conditions were: Temperature = 24.8±0.8 °C; pH = 6.7±0.1; dissolved oxygen concentration = 148.9±27.5% of air saturation

Time (d)	Biomass concentration (g L^{-1})	Nitrate concentration (mg L^{-1})	Phosphate concentration (mg L^{-1})
50	0.643	641.0±63.2	0.0±0.0
51	0.643	-	-
52	0.678	670.8±21.1	0.0±0.0
53	0.678	-	-
54	0.635	655.9±42.2	0.0±0.0
55	0.722	581.4±63.2	0.0±0.0
56	0.748	566.5±0.0	0.0±0.0
57	0.739	551.6±21.1	0.0±0.0
58	0.782	521.8±21.1	0.0±0.0
59	0.852	357.8±0.0	0.0±0.0
60	0.896	387.6±0.0	0.0±0.0
61	0.878	469.6±73.8	0.0±0.0
62	0.930	514.3±52.7	0.0±0.0
63	0.869	-	-
64	0.965	462.1±21.1	0.0±0.0
65	0.948	-	-
66	0.939	499.4±52.7	0.0±0.0
68	0.913	536.7±84.3	0.0±0.0
69	0.904	-	-
70	0.887	499.4±31.6	0.0±0.0

Data for the culture profile for Figure 4.30 (STR 8) (Cont.)

Culture conditions were: Temperature = 24.8±0.8 °C; pH = 6.7±0.1; dissolved oxygen concentration = 148.9±27.5% of air saturation

Time (d)	Biomass concentration (g L^{-1})	Nitrate concentration (mg L^{-1})	Phosphate concentration (mg L^{-1})
71	0.904	-	-
73	0.869	-	-
74	0.843	469.6±31.6	0.0±0.0
76	0.826	447.2±0.0	0.0±0.0
78	0.765	469.6±31.6	0.0±0.0
80	0.730	469.6±10.5	0.0±0.0
83	0.713	603.8±52.7	0.0±0.0
86	0.635	633.6±31.6	0.0±0.0

Data for the culture profile for Figure 4.31 (STR 9)

Culture conditions were: Temperature = 25.0±0.3 °C; pH = 6.6±0.2

Time (d)	Biomass concentration (g L^{-1})	Nitrate concentration (mg L^{-1})	Phosphate concentration (mg L^{-1})
0	0.206	998.8±63.2	14.8±0.3
1	0.287	790.1±21.1	9.4±0.0
2	0.443	760.3±21.1	0.2±0.1
3	0.568	670.8±21.1	0.1±0.0
4	0.710	626.1±42.2	0.0±0.0
5	0.875	596.3±126.5	0.0±0.0
6	1.046	506.9±84.3	0.0±0.0
7	1.301	506.9±0.0	0.0±0.0
8	1.417	506.9±0.0	0.0±0.0
9	1.533	447.2±21.1	0.0±0.0
10	1.730	387.6±63.2	0.0±0.0
18	2.391	119.3±0.0	0.0±0.0
19	2.470	107.3±4.2	0.0±0.0
20	2.504	102.9±6.3	-
22	2.574	101.4±4.2	0.0±0.0
24	2.757	96.9±10.5	-
26	2.835	92.4±8.4	0.0±0.0

Data for the culture profile for Figure 4.31 (STR 9) (Cont.)

Culture conditions were: Temperature = 25.0±0.3 °C; pH = 6.6±0.2

Time (d)	Biomass concentration (g L^{-1})	Nitrate concentration (mg L^{-1})	Phosphate concentration (mg L^{-1})
28	2.922	93.9±10.5	0.0±0.0
31	3.079	83.5±0.0	0.0±0.0
34	3.148	83.5±8.4	-
36	3.226	85.0±2.1	0.0±0.0
38	3.392	88.0±6.3	0.0±0.0
41	3.348	77.5±8.4	0.0±0.0
42	3.200	208.7±21.1	-
43	2.783	186.3±10.5	0.0±0.0
44	2.739	268.3±21.1	-
45	2.626	275.8±52.7	-
46	2.331	342.9±21.1	0.0±0.0
47	2.270	357.8±42.2	0.0±0.0
48	2.122	380.1±52.7	0.0±0.0
49	2.061	387.6±84.3	0.0±0.0
50	1.922	402.5±21.2	0.0±0.0
51	1.800	447.2±42.2	0.0±0.0
52	1.661	521.8±105.4	0.0±0.0

Data for the culture profile for Figure 4.31 (STR 9) (Cont.)

Culture conditions were: Temperature = 25.0±0.3 °C; pH = 6.6±0.2

Time (d)	Biomass concentration (g L^{-1})	Nitrate concentration (mg L^{-1})	Phosphate concentration (mg L^{-1})
53	1.652	626.1±42.2	0.0±0.0
54	1.548	566.5±42.2	0.0±0.0
55	1.452	-	-
56	1.400	611.2±63.2	0.0±0.0
58	1.226	670.8±105.4	0.0±0.0
59	1.226	-	-
60	1.165	685.7±84.3	0.0±0.0
61	1.174	-	-
62	1.069	536.7±0.0	0.0±0.0
63	1.087	-	-
64	1.069	566.5±42.2	0.0±0.0
65	1.061	-	-
66	0.991	596.3±42.2	0.0±0.0
68	1.009	596.3±84.3	0.0±0.0
69	0.939	-	-
70	0.956	-	-
71	0.956	626.1±42.2	0.0±0.0

Data for the culture profile for Figure 4.31 (STR 9) (Cont.)

Culture conditions were: Temperature = 25.0±0.3 °C; pH = 6.6±0.2

Time (d)	Biomass concentration (g L^{-1})	Nitrate concentration (mg L^{-1})	Phosphate concentration (mg L^{-1})
72	0.991	-	-
73	0.904	-	-
75	0.956	596.3±42.2	0.0±0.0
77	0.956	-	-
79	0.956	-	-
81	0.930	581.4±21.1	0.0±0.0
83	0.948	-	-
85	0.922	566.5±42.2	0.0±0.0
86	0.922	-	-
88	0.922	551.6±21.1	0.0±0.0
91	0.948	-	-
93	0.948	596.3±84.3	0.0±0.0
96	0.956	-	-
98	0.982	581.4±63.2	0.0±0.0

Data for the culture profile for Figure 4.28 (STR 10)

Culture conditions were: Temperature = 24.8±0.7 °C; pH = 6.9±0.3; dissolved oxygen concentration = 161.5±21.5% of air saturation

Time (d)	Biomass concentration (g L^{-1})	Nitrate concentration (mg L^{-1})	Phosphate concentration (mg L^{-1})
0	0.116	849.7±21.1	15.0±1.0
1	0.179	760.3±105.4	13.3±0.2
2	0.269	730.5±147.6	6.0±0.0
3	0.366	745.4±0.0	1.1±0.0
4	0.480	715.6±0.0	0.0±0.0
5	0.551	715.6±0.0	0.0±0.0
6	0.661	685.7±0.0	0.0±0.0
7	0.753	745.4±42.2	0.0±0.0
8	0.864	715.6±0.0	0.0±0.0
9	0.962	715.6±0.0	0.0±0.0
10	1.058	521.8±21.1	0.0±0.0
12	1.267	506.9±0.0	0.0±0.0
14	1.429	432.3±0.0	0.0±0.0
16	1.603	387.6±42.2	-
18	1.704	342.9±21.1	0.0±0.0
20	1.800	283.2±21.1	-
22	1.861	222.1±6.3	0.0±0.0

Data for the culture profile for Figure 4.28 (STR 10) (Cont.)

Culture conditions were: Temperature = 24.8±0.7 °C; pH = 6.9±0.3; dissolved oxygen concentration = 161.5±21.5% of air saturation

Time (d)	Biomass concentration (g L^{-1})	Nitrate concentration (mg L^{-1})	Phosphate concentration (mg L^{-1})
23	1.835	219.1±14.8	0.0±0.0
25	1.930	189.3±31.6	0.0±0.0
28	2.183	190.8±4.2	-
30	2.226	158.0±33.7	0.0±0.0
33	2.452	152.1±4.2	0.0±0.0
35	2.452	152.1±0.0	0.0±0.0

Data for the culture profile for Figure 4.32 (STR 11)

Culture conditions were: Temperature = 25.0±0.0 °C; pH = 7.2±5.0; dissolved oxygen concentration = 128.9±11.7% of air saturation

Time (d)	Biomass concentration (g L^{-1})	Nitrate concentration (mg L^{-1})	Phosphate concentration (mg L^{-1})
0	0.196	954.1±42.2	13.9±0.1
1	0.303	894.5±0.0	13.2±0.0
2	0.501	879.5±63.2	0.5±0.0
3	0.722	864.6±42.2	0.1±0.0
4	0.829	775.2±84.3	0.1±0.0
5	1.046	685.7±0.0	0.1±0.0
6	1.336	566.5±84.3	0.1±0.0
7	1.522	566.5±84.3	0.1±0.0
8	1.701	551.6±147.6	0.1±0.0
9	1.875	506.9±84.3	0.1±0.0
10	1.910	506.9±126.5	0.1±0.0
11	2.000	387.6±84.3	0.1±0.0
13	2.183	335.4±10.5	0.0±0.0
15	2.365	335.4±31.6	0.0±0.0
17	2.409	365.2±10.5	0.0±0.0
19	2.478	305.6±52.7	0.0±0.0
21	2.687	342.9±21.1	0.0±0.0
23	2.705	328.0±0.0	0.0±0.0
25	2.809	229.6±42.2	0.0±0.0
27	2.887	234.0±10.5	0.0±0.0

Data for the culture profile for Figure 4.32 (STR 11) (Cont.)

Culture conditions were: Temperature = 25.0±0.0 °C; pH = 7.2±5.0; dissolved oxygen concentration = 128.9±11.7% of air saturation

Time (d)	Biomass concentration (g L^{-1})	Nitrate concentration (mg L^{-1})	Phosphate concentration (mg L^{-1})
29	2.905	216.2±2.1	0.0±0.0
31	2.992	205.7±8.4	0.0±0.0
33	2.939	208.7±0.0	0.0±0.0
35	2.983	253.4±0.0	0.0±0.0
36	2.878	372.7±21.1	0.0±0.0
37	2.731	342.9±21.1	0.0±0.0
39	2.591	328.0±0.0	0.0±0.0
41	2.470	350.3±52.7	0.0±0.0
43	2.348	350.3±10.5	0.0±0.0
45	2.261	335.4±31.6	0.0±0.0
47	2.157	342.9±84.3	0.0±0.0
49	2.035	328.0±42.2	0.0±0.0
51	1.939	328.0±21.1	0.0±0.0
53	1.878	335.4±137.0	0.0±0.0
55	1.757	417.4±42.2	0.0±0.0
57	1.600	283.2±63.2	0.0±0.0
59	1.522	298.2±84.3	0.0±0.0
61	1.400	313.1±105.4	0.0±0.0
63	1.322	253.4±21.1	0.0±0.0
65	1.148	402.5±21.1	0.0±0.0

Data for the culture profile for Figure 4.32 (STR 11) (Cont.)

Culture conditions were: Temperature = 25.0±0.0 °C; pH = 7.2±5.0; dissolved oxygen concentration = 128.9±11.7% of air saturation

Time (d)	Biomass concentration (g L^{-1})	Nitrate concentration (mg L^{-1})	Phosphate concentration (mg L^{-1})
67	1.087	313.1±21.1	0.0±0.0
69	0.974	387.6±0.0	0.0±0.0
71	0.948	342.9±21.1	0.0±0.0
73	0.861	298.2±0.0	0.0±0.0
75	0.774	387.6±42.2	0.0±0.0
77	0.765	402.5±63.2	0.0±0.0
79	0.756	447.2±42.2	0.1±0.0
81	0.678	641.0±21.1	0.0±0.0
83	0.713	581.4±21.1	0.0±0.0
85	0.704	715.6±126.5	0.0±0.0
87	0.713	670.8±63.2	0.0±0.0
89	0.739	700.7±21.1	0.0±0.0
91	0.739	655.9±42.2	0.0±0.0
93	0.730	551.6±21.1	0.0±0.0
95	0.774	581.4±21.1	0.0±0.0
97	0.835	700.7±147.6	0.0±0.0
99	0.809	685.7±84.3	0.0±0.0
101	0.826	685.7±84.3	0.0±0.0
103	0.869	626.1±0.0	0.0±0.0
105	0.878	626.1±42.2	0.0±0.0

Data for the culture profile for Figure 4.32 (STR 11) (Cont.)

Culture conditions were: Temperature = 25.0±0.0 °C; pH = 7.2±5.0; dissolved oxygen concentration = 128.9±11.7% of air saturation

Time (d)	Biomass concentration (g L^{-1})	Nitrate concentration (mg L^{-1})	Phosphate concentration (mg L^{-1})
107	0.869	626.1±84.3	0.0±0.0
109	0.887	596.3±4.2	0.0±0.0
111	0.869	596.3±4.2	0.0±0.0
113	0.939	447.2±4.2	0.0±0.0
116	0.930	447.2±84.3	0.0±0.0
118	0.948	611.2±21.1	0.0±0.0
120	0.869	566.5±42.2	0.0±0.0
121	0.861	641.0±63.2	0.0±0.0
123	0.791	566.5±42.2	0.0±0.0
125	0.713	566.5±0.0	0.0±0.0
127	0.713	506.9±84.3	0.0±0.0
129	0.852	611.2±63.2	0.0±0.0
131	0.939	551.6±21.1	0.0±0.0
133	0.817	626.1±42.2	0.0±0.0
135	0.765	581.4±63.2	0.0±0.0
137	1.017	506.9±0.0	0.0±0.0
139	0.878	655.9±0.0	0.0±0.0
141	0.785	536.7±0.0	0.0±0.0
143	0.710	685.7±0.0	0.0±0.0
145	0.675	655.9±210.8	0.0±0.0

Data for the culture profile for Figure 4.32 (STR 11) (Cont.)

Culture conditions were: Temperature = 25.0±0.0 °C; pH = 7.2±5.0; dissolved oxygen concentration = 128.9±11.7% of air saturation

Time (d)	Biomass concentration (g L^{-1})	Nitrate concentration (mg L^{-1})	Phosphate concentration (mg L^{-1})
147	0.751	745.4±42.2	0.0±0.0
149	0.716	805.0±0.0	0.0±0.0
151	0.751	715.6±42.2	0.0±0.0
153	0.774	626.1±42.2	0.0±0.0
155	0.739	805.0±42.2	0.0±0.0
157	0.727	834.8±0.0	0.0±0.0
159	0.733	834.8±0.0	0.0±0.0
161	0.617	983.9±0.0	0.0±0.0
163	0.507	894.5±84.3	0.0±0.0
165	0.420	834.8±210.8	0.0±0.0
167	0.423	805.0±42.2	0.0±0.0
169	0.414	834.8±84.3	0.0±0.0
171	0.403	611.2±21.1	0.0±0.0
173	0.406	700.7±63.2	0.0±0.0
175	0.400	685.7±126.5	0.0±0.0
177	0.414	596.3±42.2	0.0±0.0
179	0.553	491.9±21.1	0.0±0.0
181	0.727	462.1±105.4	0.0±0.0
183	0.777	477.0±42.2	0.0±0.0
185	0.832	521.8±21.1	0.1±0.0

Data for the culture profile for Figure 4.32 (STR 11) (Cont.)

Culture conditions were: Temperature = 25.0±0.0 °C; pH = 7.2±5.0; dissolved oxygen concentration = 128.9±11.7% of air saturation

Time (d)	Biomass concentration (g L^{-1})	Nitrate concentration (mg L^{-1})	Phosphate concentration (mg L^{-1})
187	0.835	626.1±210.8	0.1±0.0
189	1.154	760.3±21.1	0.1±0.0
191	1.011	491.9±147.6	0.0±0.0
193	1.081	506.9±0.0	0.0±0.0
195	0.925	491.9±147.6	0.0±0.0
197	0.884	596.3±42.2	0.0±0.0
210	0.762	581.4±21.1	0.0±0.0
212	0.762	536.7±84.3	0.0±0.0
214	0.814	491.9±147.6	0.0±0.0
216	0.872	521.8±21.1	0.0±0.0
218	0.872	521.8±105.4	0.0±0.0
220	0.901	402.5±21.1	0.0±0.0
222	0.901	506.9±84.3	0.0±0.0
224	0.872	641.0±21.1	0.0±0.0
226	0.896	536.7±0.0	0.0±0.0
228	0.849	715.6±42.2	0.0±0.0
230	0.872	298.2±42.2	0.0±0.0
232	0.884	521.8±147.6	0.0±0.0
234	0.872	506.9±42.2	0.0±0.0
236	0.791	670.8±21.1	0.0±0.0

Data for the culture profile for Figure 4.32 (STR 11) (Cont.)

Culture conditions were: Temperature = 25.0±0.0 °C; pH = 7.2±5.0; dissolved oxygen concentration = 128.9±11.7% of air saturation

Time (d)	Biomass concentration (g L^{-1})	Nitrate concentration (mg L^{-1})	Phosphate concentration (mg L^{-1})
238	0.756	790.1±21.1	0.0±0.0
240	0.756	700.7±21.1	0.0±0.0
242	0.901	536.7±0.0	0.0±0.0
244	0.774	641.0±63.2	0.0±0.0
246	0.756	670.8±21.1	0.0±0.0
248	0.797	596.3±42.2	0.0±0.0
250	0.820	641.0±105.4	0.0±0.0
252	0.809	834.8±0.0	0.0±0.0
254	0.849	909.4±21.1	0.0±0.0
256	0.791	849.7±63.2	0.0±0.0
258	0.809	626.1±0.0	0.0±0.0
260	0.988	521.8±21.1	0.0±0.0
262	1.180	641.0±21.1	0.0±0.0
264	1.313	670.8±21.1	0.0±0.0
266	1.145	596.3±0.0	0.0±0.0
268	1.069	581.4±21.1	0.0±0.0
270	1.052	670.8±63.2	0.0±0.0
272	1.093	566.5±0.0	0.0±0.0
274	1.087	745.4±0.0	0.1±0.0
276	1.069	685.7±0.0	0.1±0.0

Data for the culture profile for Figure 4.32 (STR 11) (Cont.)

Culture conditions were: Temperature = 25.0±0.0 °C; pH = 7.2±5.0; dissolved oxygen concentration = 128.9±11.7% of air saturation

Time (d)	Biomass concentration (g L^{-1})	Nitrate concentration (mg L^{-1})	Phosphate concentration (mg L^{-1})
278	1.058	715.6±0.0	0.0±0.0
280	1.040	670.8±63.2	0.0±0.0
282	1.064	626.1±126.5	0.1±0.0
284	0.878	775.2±0.0	0.0±0.0
286	0.809	685.7±0.0	0.0±0.0
288	0.901	715.6±42.2	0.0±0.0
290	0.820	805.0±84.3	0.0±0.0
292	0.826	790.1±63.2	0.0±0.0
294	0.843	805.0±0.0	0.0±0.0
296	0.849	760.3±21.1	0.0±0.0
298	0.809	894.5±0.0	0.0±0.0
300	0.756	834.8±42.2	0.0±0.0
302	0.635	819.9±63.2	0.0±0.0
304	0.571	819.9±21.1	0.0±0.0
306	0.577	805.0±0.0	0.0±0.0
308	0.577	834.8±42.2	0.0±0.0
310	0.577	879.5±21.1	0.0±0.0

Data for the culture profile for Figure 4.33 (STR 12)

Culture conditions were: Temperature = 25.0±0.0 °C; pH = 6.9±0.3; dissolved oxygen concentration = 161.3±122.8% of air saturation

Time (d)	Biomass concentration (g L^{-1})	Nitrate concentration (mg L^{-1})	Phosphate concentration (mg L^{-1})
0	0.156	939.2±63.2	14.0±0.5
1	0.329	834.8±42.2	9.3±0.0
2	0.503	775.2±0.0	0.1±0.0
3	0.675	685.7±0.0	0.1±0.0
4	0.881	655.9±0.0	0.0±0.0
5	1.188	685.7±0.0	0.0±0.0
6	1.499	641.0±21.1	0.0±0.0
7	1.754	536.7±0.0	0.0±0.0
8	1.951	521.8±21.1	0.0±0.0
9	2.044	491.9±63.2	0.0±0.0
10	2.104	491.9±21.1	0.0±0.0
12	2.313	402.5±21.1	0.0±0.0
14	2.444	313.1±63.2	0.0±0.0
16	2.574	305.6±31.6	0.0±0.0
18	2.713	283.2±63.2	0.0±0.0
20	2.922	275.8±31.6	0.0±0.0
22	2.974	268.3±21.1	0.0±0.0
24	3.079	231.1±31.6	0.0±0.0
26	3.122	231.1±31.6	0.0±0.0
28	3.139	216.2±31.6	0.0±0.0

Data for the culture profile for Figure 4.33 (STR 12) (Cont.)

Culture conditions were: Temperature = 25.0±0.0 °C; pH = 6.9±0.3; dissolved oxygen concentration = 161.3±122.8% of air saturation

Time (d)	Biomass concentration (g L^{-1})	Nitrate concentration (mg L^{-1})	Phosphate concentration (mg L^{-1})
30	3.165	216.2±31.6	0.0±0.0
32	3.165	208.7±42.2	0.0±0.0
34	3.183	141.6±52.7	0.1±0.0
35	3.035	178.9±63.2	0.0±0.0
36	2.983	268.3±21.1	0.0±0.0
38	2.722	335.4±10.5	0.0±0.0
40	2.574	305.6±10.5	0.2±0.0
42	2.357	268.3±21.1	0.0±0.0
44	2.209	305.6±31.6	0.0±0.0
46	2.157	283.2±63.2	0.0±0.0
48	2.026	283.2±21.1	0.0±0.0
50	1.913	275.8±31.6	0.0±0.0
52	1.817	246.0±31.6	0.0±0.0
54	1.722	410.0±10.5	0.0±0.0
56	1.557	447.0±84.3	0.0±0.0
58	1.478	432.3±63.2	0.0±0.0
60	1.374	447.2±42.2	0.0±0.0
62	1.217	387.6±42.2	0.0±0.0
64	1.139	506.9±84.3	0.0±0.0
66	1.104	700.7±63.2	0.0±0.0

Data for the culture profile for Figure 4.33 (STR 12) (Cont.)

Culture conditions were: Temperature = 25.0±0.0 °C; pH = 6.9±0.3; dissolved oxygen concentration = 161.3±122.8% of air saturation

Time (d)	Biomass concentration (g L^{-1})	Nitrate concentration (mg L^{-1})	Phosphate concentration (mg L^{-1})
68	1.000	655.9±84.3	0.0±0.0
70	1.026	685.7±0.0	0.0±0.0
72	1.009	715.6±0.0	0.0±0.0
74	0.991	655.9±0.0	0.0±0.0
76	0.956	715.6±0.0	0.0±0.0
78	0.939	685.7±0.0	0.0±0.0
80	0.939	715.6±0.0	0.1±0.0
82	0.930	566.5±0.0	0.0±0.0
84	0.991	566.5±0.0	0.0±0.0
86	0.930	685.7±126.5	0.0±0.0
88	0.982	760.3±21.1	0.0±0.0
90	0.861	939.2±21.1	0.0±0.0
92	0.843	879.5±105.4	0.0±0.0
94	0.809	760.3±63.2	0.0±0.0
96	0.835	700.7±21.1	0.0±0.0
98	0.809	730.5±147.6	0.0±0.0
100	0.809	700.7±63.2	0.0±0.0
102	0.800	506.9±42.2	0.0±0.0
104	0.861	536.7±42.2	0.0±0.0
106	0.869	655.9±168.7	0.0±0.0

Data for the culture profile for Figure 4.33 (STR 12) (Cont.)

Culture conditions were: Temperature = 25.0±0.0 °C; pH = 6.9±0.3; dissolved oxygen concentration = 161.3±122.8% of air saturation

Time (d)	Biomass concentration (g L^{-1})	Nitrate concentration (mg L^{-1})	Phosphate concentration (mg L^{-1})
108	0.896	715.6±84.3	0.0±0.0
110	0.896	954.1±84.3	0.0±0.0
112	0.896	834.8±84.3	0.0±0.0
115	0.887	834.8±0.0	0.0±0.0
117	0.896	715.6±84.3	0.0±0.0
119	0.887	685.7±42.2	0.0±0.0
120	0.896	655.9±42.2	0.0±0.0
122	0.887	626.1±0.0	0.0±0.0
124	0.809	581.4±63.2	0.0±0.0
126	0.782	626.1±0.0	0.0±0.0
128	0.722	760.3±21.1	0.0±0.0
130	0.661	775.2±0.0	0.0±0.0
132	0.626	964.6±0.0	0.0±0.0
134	0.600	805.0±84.3	0.0±0.0
136	0.626	775.2±0.0	0.0±0.0
138	0.574	670.8±21.1	0.0±0.0
140	0.820	775.2±0.0	0.0±0.0
142	0.669	834.8±84.3	0.0±0.0
144	0.542	819.9±21.1	0.0±0.0
146	0.490	805.0±42.2	0.0±0.0

Data for the culture profile for Figure 4.33 (STR 12) (Cont.)

Culture conditions were: Temperature = 25.0±0.0 °C; pH = 6.9±0.3; dissolved oxygen concentration = 161.3±122.8% of air saturation

Time (d)	Biomass concentration (g L^{-1})	Nitrate concentration (mg L^{-1})	Phosphate concentration (mg L^{-1})
148	0.420	864.6±42.2	0.0±0.0
150	0.356	864.6±0.0	0.0±0.0
152	0.356	849.7±147.6	0.0±0.0
154	0.316	1043.5±0.0	0.0±0.0
156	0.287	983.9±42.2	0.0±0.0
158	0.304	536.7±84.3	0.0±0.0
160	0.281	581.4±63.2	0.2±0.0
162	0.264	730.5±147.6	0.1±0.0
164	0.136	685.7±168.7	0.4±0.0
166	0.089	477.0±42.2	0.5±0.0
168	0.070	402.5±105.4	0.8±0.0
170	0.056	730.5±21.1	1.0±0.0
172	0.055	864.6±84.3	1.0±0.0
174	0.058	864.6±84.3	1.4±0.0
176	0.056	611.2±105.4	1.4±0.0
178	0.056	864.6±126.5	1.7±0.0
180	0.220	864.6±168.7	0.0±0.0
182	0.278	1311.9±42.2	0.7±0.0
184	0.356	1162.8±0.0	1.8±0.0
186	0.368	1088.3±21.1	1.0±0.0

Data for the culture profile for Figure 4.33 (STR 12) (Cont.)

Culture conditions were: Temperature = 25.0±0.0 °C; pH = 6.9±0.3; dissolved oxygen concentration = 161.3±122.8% of air saturation

Time (d)	Biomass concentration (g L^{-1})	Nitrate concentration (mg L^{-1})	Phosphate concentration (mg L^{-1})
188	0.446	1255.2±0.0	1.3±0.0
190	0.394	864.6±84.3	1.4±0.0
192	0.377	775.2±42.2	1.2±0.0
194	0.379	879.5±105.4	1.3±0.0
196	0.371	879.5±21.1	1.0±0.0
209	1.017	655.9±0.0	0.2±0.0
211	1.040	670.8±21.1	0.1±0.0
213	0.953	566.5±42.2	0.0±0.0
215	0.913	730.5±21.1	0.0±0.0
217	0.919	715.6±168.7	0.0±0.0
219	0.843	745.4±42.2	0.0±0.0
221	0.867	805.0±84.3	0.0±0.0
223	0.826	790.1±105.4	0.0±0.0
225	0.838	834.8±126.5	0.1±0.0
227	0.756	909.4±63.2	0.1±0.0
229	0.745	730.5±21.1	0.0±0.0
231	0.646	708.1±10.5	0.0±0.0
233	0.681	715.6±210.8	0.0±0.0
235	0.611	805.0±0.0	0.0±0.0
237	0.582	745.4±42.2	0.0±0.0

Data for the culture profile for Figure 4.33 (STR 12) (Cont.)

Culture conditions were: Temperature = 25.0±0.0 °C; pH = 6.9±0.3; dissolved oxygen concentration = 161.3±122.8% of air saturation

Time (d)	Biomass concentration (g L^{-1})	Nitrate concentration (mg L^{-1})	Phosphate concentration (mg L^{-1})
239	0.606	819.9±147.6	0.0±0.0
241	0.617	760.3±21.1	0.0±0.0
243	0.617	775.2±0.0	0.0±0.0
245	0.617	715.6±42.2	0.0±0.0
247	0.629	775.2±84.3	0.0±0.0
249	0.716	626.1±0.0	0.0±0.0
251	0.704	745.4±84.3	0.0±0.0
253	0.756	790.1±21.1	0.0±0.0
255	0.727	809.9±21.1	0.0±0.0
257	0.710	805.0±253.0	0.0±0.0
259	0.704	730.5±147.6	0.0±0.0
261	0.727	670.8±21.1	0.0±0.0
263	0.658	790.1±147.6	0.0±0.0
265	0.635	700.7±105.4	0.0±0.0
267	0.565	685.7±84.3	0.0±0.0
269	0.577	655.9±0.0	0.0±0.0
271	0.536	879.5±21.1	0.0±0.0
273	0.519	864.6±0.0	0.0±0.0
275	0.530	864.6±0.0	0.0±0.0
277	0.536	894.5±0.0	0.0±0.0

Data for the culture profile for Figure 4.33 (STR 12) (Cont.)

Culture conditions were: Temperature = 25.0±0.0 °C; pH = 6.9±0.3; dissolved oxygen concentration = 161.3±122.8% of air saturation

Time (d)	Biomass concentration (g L^{-1})	Nitrate concentration (mg L^{-1})	Phosphate concentration (mg L^{-1})
279	0.542	864.6±0.0	0.1±0.0
281	0.530	894.5±0.0	0.4±0.0
283	0.507	894.5±0.0	0.4±0.0
285	0.501	834.8±0.0	1.3±0.0
287	0.507	939.2±21.1	0.8±0.0
289	0.501	939.2±189.7	0.8±0.0
291	0.495	894.5±42.2	0.5±0.0
293	0.501	1028.6±105.4	1.0±0.0
295	0.490	954.1±84.3	1.6±0.0
297	0.490	1013.7±0.0	1.2±0.0
299	0.408	1028.6±105.4	2.8±0.0
301	0.316	954.1±84.3	3.5±0.0
303	0.339	954.1±42.2	3.1±0.0
305	0.304	954.1±0.0	3.4±0.0
307	0.281	924.3±84.3	3.9±0.0
309	0.281	924.3±0.0	4.0±0.0
311	0.258	924.3±42.2	4.0±0.0

Data for lipid content analysis for Table 4.10

Sample	NO.	Biomass (mg)	Total lipid (%)	Average total lipid (%)
STR 1	1	1000	17.3	
	2	1000	17.6	17.5±0.2
STR 2	1	1000	58.9	
	2	1000	59.3	59.1±0.3
STR 3	1	19000	26.3	
	2	19000	27.6	26.9±0.9
STR 4	1	11000	53.9	
	2	11000	53.0	53.4±0.6
STR 5 (Day 23)	1	10500	21.0	
	2	10500	22.6	21.8±1.1
STR 5 (Day 38)	1	1000	48.2	
	2	1000	48.3	48.3±0.1
STR 5 (Day 60)	1	6000	47.8	
	2	6000	20.3	49.0±1.8
STR 6 (Day 29)	1	7000	15.2	
	2	7000	14.8	15.0±0.3
STR 6 (Day 31)	1	1000	17.0	
	2	1000	16.8	16.9±0.2

Data for lipid content analysis for Table 4.10 (Cont.)

Sample	NO.	Biomass (mg)	Total lipid (%)	Average total lipid (%)
STR 6 (Day 33)	1	1000	19.3	
	2	1000	18.1	18.7±0.9
STR 6 (Day 35)	1	1000	24.0	
	2	1000	31.6	27.8±5.3
STR 6 (Day 37)	1	19000	28.2	
	2	19000	27.3	27.8±0.6
STR 6 (Day 39)	1	11000	35.6	
	2	11000	34.6	35.1±0.7
STR 6 (Day 42)	1	10500	37.8	
	2	10500	37.3	37.5±0.4
STR 7 (SS1)	1	1000	11.9	
	2	1000	12.6	
	3	1000	11.7	12.1±0.5
STR 8 (SS1)	1	1000	7.0	
	2	1000	7.2	7.1±0.1
STR 8 (SS2)	1	1000	5.1	
	2	1000	5.0	5.1±0.1
STR 9 (SS1)	1	1000	15.7	
	2	1000	15.5	15.6±0.2

Data for lipid content analysis for Table 4.10 (Cont.)

Sample	NO.	Biomass (mg)	Total lipid (%)	Average total lipid (%)
STR 10	1	1000	20.1	
	2	1000	20.1	20.1±0.0
STR 11 (SS11)	1	1000	9.5	
	2	1000	9.5	9.5±0.0
STR 11 (SS12)	1	19000	10.3	
	2	19000	10.5	10.4±0.2
STR 11 (SS13)	1	11000	11.6	
	2	11000	11.1	11.4±0.4
STR 11 (SS14)	1	10500	13.5	
	2	10500	13.9	13.7±0.3
STR 11 (SS21)	1	1000	12.6	
	2	1000	11.5	12.1±0.8
STR 11 (SS22)	1	6000	9.7	
	2	6000	9.2	9.4±0.3
STR 11 (SS23)	1	7000	11.7	
	2	7000	11.6	11.6±0.1
STR 11 (SS24)	1	1000	14.2	
	2	1000	13.9	14.1±0.2

Data for lipid content analysis for Table 4.10 (Cont.)

Sample	NO.	Biomass (mg)	Total lipid (%)	Average total lipid (%)
STR 12 (SS11)	1	1000	7.3	
	2	1000	7.8	7.6±0.3
STR 12 (SS12)	1	19000	14.1	
	2	19000	14.6	14.4±0.3
STR 12 (SS13)	1	11000	11.8	
	2	11000	11.7	11.7±0.0
STR 12 (SS14)	1	10500	14.1	
	2	10500	15.8	14.9±1.2
STR 12 (SS21)	1	1000	9.0	
	2	1000	10.0	9.5±0.7
STR 12 (SS22)	1	6000	11.8	
	2	6000	12.5	12.1±0.5
STR 12 (SS23)	1	7000	15.1	
	2	7000	15.9	15.5±0.6
STR 12 (SS24)	1	1000	18.0	
	2	1000	17.4	17.7±0.5

Data for the culture profile for Figure 4.36

Time (d)	Biomass concentration (g L^{-1})	Nitrate concentration (mg L^{-1})	Phosphate concentration (mg L^{-1})
0	0.174	1133.0±0.0	7.7±0.3
1	0.284	1088.3±21.1	0.6±0.2
2	0.417	1013.7±0.0	0.2±0.0
4	0.724	1013.7±0.0	0.2±0.0
5	0.806	1028.6±21.1	0.1±0.0
6	0.935	969.0±63.2	0.1±0.0
7	1.072	924.3±0.0	0.1±0.0
8	1.232	894.5±42.2	0.1±0.0
10	1.350	849.7±21.1	0.1±0.0
11	1.438	849.7±21.1	0.1±0.0
12	1.526	805.0±84.3	0.1±0.0
13	1.591	805.0±84.3	0.1±0.0
14	1.587	805.0±0.0	0.1±0.0
15	1.741	760.3±21.1	0.1±0.0
16	1.693	730.5±63.2	0.1±0.0
17	1.819	745.4±0.0	0.1±0.0
18	1.795	745.4±0.0	0.1±0.0
19	1.933	715.6±0.0	0.1±0.0

Data for the culture profile for Figure 4.36 (Cont.)

Time (d)	Biomass concentration (g L^{-1})	Nitrate concentration (mg L^{-1})	Phosphate concentration (mg L^{-1})
20	1.975	-	-
21	2.149	715.6±0.0	0.1±0.0
22	2.191	-	-
23	2.173	-	-
24	2.467	715.6±84.3	0.0±0.0
25	2.504	-	-
26	2.533	-	-
27	2.735	715.6±84.3	0.0±0.0
28	2.713	-	-
29	2.720	655.9±0.0	0.0±0.0

Data for the culture profile for Figure 4.37 (BR 1)

Culture conditions were: Temperature = 24.6±1.2 °C; pH = 6.6±0.4

Time (d)	Biomass concentration (g L^{-1})	Nitrate concentration (mg L^{-1})	Phosphate concentration (mg L^{-1})
0	0.091	1192.6±42.2	13.9±0.3
1	0.148	1192.6±0.0	2.1±0.1
2	0.234	1103.2±84.3	0.1±0.0
3	0.347	1073.3±0.0	0.1±0.0
4	0.443	1043.5±0.0	0.0±0.0
5	0.543	1013.7±0.0	0.0±0.0
6	0.636	1013.7±0.0	0.0±0.0
7	0.721	1013.7±84.3	0.0±0.0
8	0.771	969.0±21.1	0.0±0.0
9	0.838	969.0±63.2	0.0±0.0
10	0.897	924.3±0.0	0.0±0.0
11	0.946	-	-
12	0.990	730.5±21.1	0.0±0.0
13	1.040	-	-
14	1.078	700.7±21.1	0.0±0.0
15	1.122	-	-
16	1.215	700.7±21.1	0.0±0.0

Data for the culture profile for Figure 4.37 (BR 1) (Cont.)

Culture conditions were: Temperature = 24.6±1.2 °C; pH = 6.6±0.4

Time (d)	Biomass concentration (g L^{-1})	Nitrate concentration (mg L^{-1})	Phosphate concentration (mg L^{-1})
17	1.141	-	-
18	1.237	730.5±21.1	0.0±0.0
19	1.185	-	-
20	1.237	655.9±0.0	0.0±0.0
21	1.215	-	-
22	1.202	655.9±84.3	0.0±0.0
23	1.149	-	-
24	1.246	581.4±21.1	0.0±0.0
26	1.176	551.6±21.1	0.0±0.0
28	1.206	551.6±21.1	0.0±0.0
30	1.215	551.6±21.1	0.0±0.0
34	1.202	536.7±42.2	0.0±0.0
34.1	0.934	506.9±42.2	0.0±0.0
50	0.472	410.0±10.5	0.0±0.0
50.1	0.417	380.1±10.5	0.0±0.0
53	0.417	223.6±21.1	0.0±0.0

Data for the culture profile for Figure 4.38 (BR 2)

Culture conditions were: Temperature = 25.0±0.0 °C; pH = 6.7±0.4

Time (d)	Biomass concentration (g L^{-1})	Nitrate concentration (mg L^{-1})	Phosphate concentration (mg L^{-1})
0	0.100	226.6±8.4	12.4±0.0
1	0.182	202.7±8.4	0.1±0.0
2	0.285	187.8±4.2	0.1±0.0
3	0.413	107.3±16.9	0.0±0.0
4	0.538	44.7±4.2	0.0±0.0
5	0.657	32.8±4.2	0.0±0.0
6	0.712	13.4±2.1	0.0±0.0
7	0.791	12.8±3.0	0.0±0.0
8	0.920	12.2±3.8	0.0±0.0
9	1.003	12.2±3.0	0.0±0.0
10	1.012	12.2±14.6	0.0±0.0
12	1.113	11.3±2.5	0.0±0.0
14	1.082	12.5±0.8	0.0±0.0
15	1.097	12.8±0.4	0.0±0.0
16	1.110	12.5±0.8	0.0±0.0
18	1.141	13.7±0.0	0.0±0.0
20	1.101	10.7±0.0	0.0±0.0
22	1.053	10.7±0.0	0.0±0.0
24	1.101	10.1±0.0	0.0±0.0
26	1.106	11.3±0.0	0.0±0.0

Data for the culture profile for Figure 4.38 (BR 2) (Cont.)

Culture conditions were: Temperature = 25.0±0.0 °C; pH = 6.7±0.4

Time (d)	Biomass concentration (g L^{-1})	Nitrate concentration (mg L^{-1})	Phosphate concentration (mg L^{-1})
28	1.079	11.3±0.0	0.0±0.0
32	1.044	11.3±0.0	0.0±0.0
34	1.031	9.5±0.8	0.0±0.0
34.1	0.763	5.4±0.0	0.0±0.0
36	0.970	6.3±0.4	0.0±0.0
36.1	0.553	3.6±0.0	0.0±0.0
38	0.583	4.2±0.0	0.0±0.0
38.1	0.373	3.6±0.0	0.0±0.0
40	0.364	3.3±0.4	0.0±0.0
40.1	0.272	2.7±0.4	0.0±0.0
42	0.270	0.0±0.0	0.0±0.0
42.1	0.142	0.0±0.0	0.0±0.0
45	0.159	0.0±0.0	0.0±0.0
45.1	0.070	0.0±0.0	0.0±0.0
48	0.067	0.0±0.0	0.0±0.0

Data for the culture profile for Figure 4.39(BR 3)

Culture conditions were: Temperature = 25.0±0.1 °C; pH = 6.8±0.2

Time (d)	Biomass concentration (g L^{-1})	Nitrate concentration (mg L^{-1})	Phosphate concentration (mg L^{-1})
0	0.098	257.9±4.7	12.9±0.2
1	0.181	219.1±13.5	2.5±0.0
2	0.302	174.4±19.9	0.1±0.0
3	0.439	132.7±2.1	0.1±0.0
4	0.561	74.5±6.7	0.0±0.0
5	0.658	21.6±3.0	0.0±0.0
6	0.737	17.1±3.6	0.0±0.0
7	0.822	10.6±0.8	0.0±0.0
9	0.916	9.8±1.3	0.0±0.0
10	1.034	9.5±0.4	0.0±0.0
11	1.065	-	-
12	1.071	9.4±0.2	0.0±0.0
13	1.080	-	-
14	1.097	7.8±0.4	0.0±0.0
16	1.110	7.8±0.4	0.0±0.0
17	1.103	-	-
18	1.097	7.6±0.2	0.0±0.0
20	1.095	7.5±0.4	0.0±0.0
21	1.097	7.3±0.5	0.0±0.0

Data for lipid content analysis for Table 4.15

Sample	NO.	Biomass (mg)	Total lipid (%)	Average total lipid (%)
2 L	1	7000	23.4	
	2	7000	24.5	24.0±0.7
BR 1 (Day 34)	1	1000	24.5	
	2	1000	23.5	24.0±0.7
BR 1 (Day 50)	1	1000	6.2	
	2	1000	6.2	6.2±0.0
BR 1 (Day 65)	1	6000	13.3	
	2	6000	13.7	13.5±0.3
BR 2 (Day 34)	1	1000	28.1	
	2	1000	20.7	24.4±5.2
BR 2 (Day 36)	1	500	12.7	
	2	500	12.2	12.5±0.4
BR 2 (Day 38)	1	500	11.2	
	2	500	11.5	11.4±0.3
BR 2 (Day 40)	1	500	16.8	
	2	500	17.1	16.9±0.2
BR 2 (Day 42)	1	500	15.2	
	2	500	14.4	14.8±0.5

Data for lipid content analysis for Table 4.15 (Cont.)

Sample	NO.	Biomass (mg)	Total lipid (%)	Ave total lipid (%)
BR 2 (Day 45)	1	500	22.5	
	2	500	17.5	19.8±3.8
BR 2 (Day 48)	1	1000	15.8	
	2	1000	11.6	13.7±3.0
BR 3	1	14000	34.2	
	2	14000	33.1	33.6±0.7